

GEOPHYSICAL INVESTIGATIONS AT LOS NARANJOS HONDURAS:
INSIGHTS INTO EARLY MESOAMERICAN CULTURE

A Dissertation

Presented to the Faculty of the Graduate School

of Cornell University

in Partial Fulfillment of the Requirements for the Degree of

Doctor of Philosophy

by

Tiffany Forbes Tchakirides

May 2010

© 2010 Tiffany Forbes Tchakirides

GEOPHYSICAL INVESTIGATIONS AT LOS NARANJOS, HONDURAS:
INSIGHTS INTO EARLY MESOAMERICAN CULTURE

Tiffany Forbes Tchakirides, Ph. D.

Cornell University 2010

This dissertation discusses the results of three-dimensional ground-penetrating radar (GPR) data and magnetometry data conducted at the archaeological site of Los Naranjos, Honduras during the summer of 2003 and spring of 2007. The goals of these surveys were to augment limited archaeological excavations of a joint Cornell University – University of California, Berkeley field program and to non-invasively image the subsurface in three dimensions to identify potential archaeological and geological features that may relate to specific occupations of the site. Non-invasive geophysical methods are particularly attractive at sites like Los Naranjos, as the Instituto Hondureño de Antropología e Historia (IHAI) designated a portion of the site as the Parque Eco-Arqueológico Los Naranjos to be preserved and protected from future extensive excavations.

Closely-spaced GPR profiles that resulted in three-dimensional grids of data, individual GPR transects, and grids of magnetometry data were acquired within a region of Los Naranjos approximately 1 hectare in size, adjacent to Structure IV, a large earthen platform mound located within the Principal Group. Extensive velocity analyses performed on the six common mid-point (CMP) profiles collected at Los Naranjos provided accurate time to depth conversions of GPR data. Three-dimensional migration corrected GPR reflection profiles so that they accurately represent the subsurface and increased the resolution of features.

Ground-penetrating radar delineated Quaternary stratigraphy at depths ranging from 2 to 6 meters in almost all areas of the site and proved effective at identifying buried geological features such as basins, complex layering, strata onlaps, unconformities, and possible volcanic marker horizons and faults. Archaeological features such as a presumed buried structure and potential buried sculpture were also imaged by GPR. The GPR results have also been useful at distinguishing between natural and anthropogenic features exposed at the site as well as probing the interior of a portion of Structure IV. Correlation with magnetometry data helped distinguish between different lithologic materials and artifact compositions. The GPR results obtained at Los Naranjos demonstrate considerable potential for this technology in delineating both geological and anthropogenic structures. Most importantly, GPR and magnetometry have proven especially effective for probing this protected site in a non-invasive and non-destructive manner.

BIOGRAPHICAL SKETCH

Tiffany Forbes Tchakirides is the youngest of three children born to Nelson and Barbara Tchakirides. She debuted in the booming metropolis of Seymour, Connecticut in the late summer of 1977 and has been dreaming of an Ivy League education almost since the very beginning. While her fourth grade classmates were drawing straws to see who would be King of the Four-Square game at recess, Tiffany was busy mapping out her future that was sure to involve education at Harvard University and Harvard Law School, before becoming one of the most successful lawyers this country had ever known. She maintained this dream steadfastly until high school, when a class trip to Pompeii, Italy in 1994 opened her eyes to the possibility that archaeology, not law, might be her future calling. Somehow the thought of finding a buried city of her own easily trumped the thoughts of years spent in a dark courtroom, bickering over the interpretation of one word of law.

After graduating from Seymour High School in 1995, she decided instead to attend Syracuse University (a non-Ivy League institution) where they had an extensive curriculum that allowed her to study anything from Anthropology to Zoology. She declared Anthropology as her major after her first archaeology course and had the opportunity to spend the following summer participating in an archaeological excavation in Elmina, Ghana, which was the site of the largest slave exportation from Africa. In many ways, that trip changed her life forever. Academically, she was sure there was a better way to do archaeology than by merely guessing where to place excavation units. She didn't know it at the time, but she was obviously destined to become a geophysicist, using ground-penetrating radar at archaeological sites, of course.

Tiffany's undergraduate Anthropology advisor, Christopher DeCorse, encouraged her to pursue coursework in Earth Science to satisfy her curiosity

regarding the processes affecting archaeological sites. A chance run-in with Professor Bryce Hand in the halls of Heroy set her on her way to double majoring in Earth Science, even though she initially only intended to take a course or two. Professor Hand's advice was simple: "If you are going to take one course in Earth Science, you might as well minor in Earth Science. If you are going to minor in Earth Science, you might as well major in Earth Science." Somehow it seemed as logical to her as it did to Professor Hand. Her involvement within the Department led Professor Hank Mullins to nominate her for a research assistant position with Professor Gene Domack at Hamilton College during the summer of 1999. While mapping the geology of Oneida Lake's eastern shore, she was introduced to ground-penetrating radar (GPR), a technique that would come to occupy a great deal of her time, energy, thoughts, and enthusiasm for the next decade. She quickly realized this was precisely the technique she desired to take the guesswork out of excavations.

Dreams of that Ivy League degree kept her working hard while an undergraduate, allowing her to become a member of Phi Beta Kappa, Golden Key, Phi Kappa Phi, and Phi Eta Sigma Honor Societies. She was also honored with a Remembrance Scholarship during her final year. This scholarship is in remembrance of the 35 SU students who perished aboard PanAm 103 over Lockerbie, Scotland on December 21, 1988; it is the highest distinction undergraduates can receive at SU. She graduated from Syracuse in December 1999, *summa cum laude*.

Much to the chagrin of her Earth Science professors (and her wallet), she decided to pursue her Master's degree in Anthropology, *not* Geology. Tiffany and her parents drove from Connecticut to Colorado in a rented Penske truck with just two seats. Three people, two seats. Thank Goodness they had the retro-fitted Anna LoPresti School cafeteria pea-green plastic chair. They arrived safely in Denver no worse for the wear, but her dad still wonders what happened to that chair. In the fall

of 2000, Tiffany entered the University of Denver (also not an Ivy League institution) to work with Professor Lawrence Conyers, who literally “wrote the book” on using GPR at archaeological sites. She gained valuable field experience during her time at DU and worked on more than 20 GPR projects in Mexico, China, and throughout the United States.

After obtaining her Master’s degree in June 2002, Tiffany took a two-year hiatus from higher education and worked as a GIS Technician at Integrated Mapping Services, compiling gas and utility services as part of the “Call Before You Dig” campaign at Northeast Utilities in Berlin, CT. Although she enjoyed having guilt-free time on evenings and weekends to do things other than study, she realized her talents would better serve her back in academia.

At the suggestion of Geoffrey Seltzer, one of her all-time favorite undergraduate professors, she applied to Cornell University (finally, an Ivy League institution) to work with Professor Larry Brown, a geophysicist, seismologist, and physicist, and a far cry from her decidedly *non-physicist* background. She was eager to become more technical and quantitative, and Cornell was the ideal place to develop into a card-carrying geophysicist. Tiffany has been a graduate student in the Department of Earth and Atmospheric Sciences since the fall of 2004.

Tiffany spent the summer of 2005 in Houston, Texas, where she interned with the New Detection Methods Team at Shell Oil. During this internship, she mastered the skill of using old methods to solve new problems, and she has been able to do similar things with her own dissertation research.

Tiffany’s time at Cornell has been generously funded through fellowships, teaching assistantships, and other forms of departmental and external support. She received a McMullen Fellowship her first year, an Eleanor Tatum Long Fellowship her third year, and a NASA Space Grant Graduate Fellowship during the fall semester

of her fifth year. Summer support was provided by departmental donations from Shell Oil as well as several of Larry Brown's NSF grants. Tiffany has been a TA for *Geophysical Field Methods, Earthquake!* (and its reincarnation: *Earthquake! and Other Natural Disasters*), *Introduction to Geological Sciences*, and *Introduction to the Earth and Life*. In May 2008, Tiffany received the *Bryan Isacks Excellence in Teaching Award* from the Department of Earth and Atmospheric Sciences.

By some twist of fate, Tiffany added delivery room experience to her résumé, even though she had absolutely nothing to do with the actual delivery. In January 2008, Tiffany became an aunt to Katherine Dana and Amelia Jean Gephart, the two most beautiful babies ever born. She is not sure why the twins arrived five and a half weeks early, but she can only surmise they arrived on her 'sister-sitting' watch while her brother-in-law was deployed in Iraq because they desperately wanted their *piggies* kissed. Fortunately, Auntie Tiffany was only too happy to oblige. Her life has not been the same since.

Tiffany is extremely relieved that the arduous task of writing a dissertation is finally behind her. After more than 14 years since her first day of orientation as an undergraduate, an Ivy League degree is imminent. Tiffany can now focus her efforts on packing up her belongings and moving to the great state of Texas. She has accepted a full-time position in the Marine Seismic Imaging Group at Shell Oil in Houston, Texas. Although she couldn't have predicted this career trajectory even several years ago, she is simply thrilled that things have all worked out so nicely in the end.

To Mom and Dad
Jennifer, Nelson, and Andrew
Katie and Amelia

ACKNOWLEDGMENTS

This dissertation would not have been possible without the joint Cornell University – University of California, Berkeley archaeological field program at Los Naranjos during the summers of 2003 and 2004. John Henderson and Rosemary Joyce co-directed the archaeological excavations for both summers. Larry Brown collected the majority of the GPR data, and he was assisted by William Perks, Joel Haenlein, and several Cornell undergraduates. Kira Blaisdell-Sloan, then a graduate student at Berkeley collected the magnetometry data. I thank Larry, John, and Rosemary for allowing me to participate in this research, for sharing their field data with me, and for helping me to integrate the geophysical and archaeological datasets. I appreciate the efforts of all of the fieldschool participants who collected the 2003 geophysical data and excavated during 2003 and 2004.

I would like to thank my Special Committee members: Larry Brown, John Henderson, and Michelle Goman. Their comments, suggestions, and guidance helped improve the quality of this dissertation immensely, and I am grateful for their involvement. Special thanks to my advisor, Larry Brown, for pushing me to succeed and for never once believing me when I told him “I can’t” do something. He afforded me the freedom to forge my own path and make my own mistakes, but he was always willing to help me over the hurdles or find a new direction after the many dead ends, false leads, and bad decisions. His unending enthusiasm, unfailing optimism in my abilities, fantastic pep talks, kindness, and genuine compassion helped bring this dissertation and Ph.D. to completion. I am extremely grateful to have known him and worked with him for the last five and a half years, and I’m looking forward to our continued interactions once I graduate.

Thank you also to John Henderson for taking an early interest in my research. John helped me to get better acquainted with Mesoamerican archaeology, he

successfully deciphered scruffy locus sheets for me, and he guided me through interpreting the geophysical data to determine their archaeological significance. Rosemary Joyce also provided useful commentary on the broader implications of my research and helped me to formulate ideas and clarify my thinking. I am grateful to both of them for their time and efforts.

This research was conducted under the auspices of the Instituto Hondureño de Antropología e Historia. I would like to thank its Director, Dr. Darío Euraque, for his support of my research and his interest in my participation in projects in Honduras. I have benefited from our conversations and have enjoyed the opportunity to utilize sophisticated geophysical methods in Honduras. Assistant Director, Lic. Eva Martinez, and the Representative of the IHAH North Region, Lic. Aldo Zelaya, went out of their ways to make my research project run smoothly, and I greatly appreciate all of their assistance, especially during the 2007 field season. Don Vito Veliz and the late Alberto Duron were also helpful and supportive of my research project in the earliest stages. Fieldwork during the spring of 2007 was accomplished with the help of Melissa Stephenson, Carlos Acosta, Rodolfo Mendoza, Luis Larios, and Narciso Lopez. The women at the *Casa de Huéspedes* in the *Zona de Americana* in La Lima graciously hosted me and all of my obscure and dirty equipment.

Professors and research associates in EAS made my time at Cornell more enjoyable and rewarding. I would especially like to thank Rick Allmendinger, Chris Andronicos, Kodjopa Attah, Larry Cathles, John Cisne, Bryan Isacks, Terry Jordan, Sue Kay, Bruce Monger, and Bill White. Muawia Barazangi deserves special note for awarding me his signature “C-” that officially indoctrinated me into the EAS Department. I was honored to receive my first C-, but I am still so proud to have received only one.

I appreciate the assistance provided by Ross Johnson and Mikhail Tchernychev (Geometrics, Inc.), Greg Johnston (Sensors and Software, Inc.), Dan Welch (GSSI), and Dr. Karl-Josef Sandmeier (Sandmeier Scientific Software). Their explanations and advice kept me moving forward, and I am grateful they were all so willing to answer the myriad of questions I posed related to their specific software and / or equipment.

I could not have made it through Cornell if it weren't for the incoming class of 2004 (to be known forever as the "First Years"): Gabriela Depine, Holly Moore, Rachel Shannon, Ursula Smith, and Katie Tamulonis. How fortunate I was to begin my Cornell experience in the company of such talented and wonderful individuals; how happy I was to spend my Cornell career with them; how grateful I am to call them friends. Special thanks to Ursula for allowing me to shamelessly steal all of her ideas for proper organization, file naming conventions, and note taking. I am also grateful for our late-night trips to Purity, our study sessions at Barnes and Noble, and our Saturday morning breakfasts at DeWitt Café.

The Snee graduate student community made it a pleasure to spend long hours each day plugging away in the lab or office. I am thankful for the friendship of Chen Chen (CC), Chen Chen (Female), Stephanie Devlin, Danielle Glasgow Wolf, Naomi Kirk-Lawlor, Mary Kosloski, Jack Loveless, Louise McGarry, Neil McGlashan, Jacob Moore, Peter Nester, Eliana Nossa, Christina (C-Pat) Patricola, Diego Quiros, Brian Ruskin, and Dave Wolf. Thanks also to Julie Hamblock for being the best neighbor ever.

Linda Hall, Nadine Porter, Elena Welch, and Clare Zuraw kept me abreast of all of the latest graduate school requirements, rules, and regulations. Carolyn Spohn performed administrative wonders with lightening speed. Jeanne Boodley-Buchanan 'designed' my old office / lab space so that it was more conducive to working. Steve

Gallow kept my laptop running in top shape, regardless of the things I did to accidentally sabotage it. He deserves special note for removing the ‘deeply infectious’ virus from my laptop about a week and a half before my defense. I am thankful to all of them for their assistance, but also for their encouragement and friendship.

I am indebted to Art Bloom, affectionately known as Uncle Art, and George Hade for improving the quality of my life. Their good-humored ribbing kept me honest, their stories kept me laughing, and their encouragement kept me working. Their concern for my well-being and that of my entire family has meant more to me than I can possibly say. Lunches with Art and afternoon chats with George were often the highlights of my time in Snee. I will miss them both so much once I leave, but “God willing” I will “See [them] Monday.”

Jeanne Lopiparo, Doris Maldonado, Lauren Morawski, Laura O’Rourke, and Esteban Gomez made my trip to Honduras in May – June 2007 an unbelievably memorable field experience. I will never forget all the fun, laughs, good times, and great food we shared. I never imagined living in a house on stilts, with cockroaches the size of Texas, could be so much fun.

Florencia Zapata cheerfully edited the Spanish translation of my first proposal to IHAH, and Eliana Nossa edited drafts of my Copán paper and presentation.

External funding for this research was generously provided by a Geological Society of America Research Grant, an American Association of Petroleum Geologists Grant-in-Aid, a Tinker Foundation / Cornell Latin American Studies Program Research Grant, numerous Cornell Graduate School Research Grants, a Hirsch Scholarship from the Archaeology Program at Cornell, and Barbara McBride Memorial Scholarships from the SEG Foundation Scholarship Program. I am extremely grateful to all of these organizations for supporting my research.

I am grateful to Shell Oil, especially their Marine Seismic Imaging Group, for offering me a full-time employment position. I would also like to thank Houston Brown and Peter Velez for taking a personal interest in my application and helping me navigate through the “Shell System.” Brian Ruskin, Holly Moore, Carol Lanier, and Karen Sheffield were also helpful, and I appreciate their assistance in the process.

I have been extremely fortunate to have the love and support of my wonderful family. My aunt, Helen Karaban, passed away prior to the completion of this dissertation, and I regret that she wasn’t able to see it all come to fruition. I often picture her reminding me to “Give ‘em hell, kid,” and it always makes me laugh. My parents, Nelson and Barbara, deserve an enormous amount of thanks for the countless sacrifices made so that I can selfishly pursue twelve years of higher education. Although they haven’t always understood what I’m doing or why I’m doing it, they’ve always believed in me and encouraged me, especially during those times when I was more than a little anxious to throw in the towel. My sister Jennifer Gephart, my brother Nelson, and my brother-in-law Andrew Gephart have supported and encouraged me and were always eager to remind me that there is life outside of graduate school. My beautiful twin nieces Katie and Amelia Gephart, who are just too perfect for words, have proven that the most important things in life have nothing to do with the number of grants received or publications amassed. There are no words to describe how much happiness and joy they bring to my life. My heart breaks to hear them cry, but their beautiful smiles warm my soul in an instant. I look forward to a lifetime of their hugs, kisses, and laughter.

Finally, I would like to thank Dr. Michael Dewar, a cardiovascular surgeon at Yale New Haven Hospital, for getting the *kinks* out of my dad so that he could see me become a Doctor.

TABLE OF CONTENTS

BIOGRAPHICAL SKETCH	iii
DEDICATION	vii
ACKNOWLEDGMENTS	viii
TABLE OF CONTENTS	xiii
LIST OF FIGURES	xix
LIST OF TABLES	xxv
INTRODUCTION	1
Chapter 1	4
Chapter 2	4
Chapter 3	5
Chapter 4	6
Chapter 5	7
Chapter 6	8
REFERENCES	9
CHAPTER 1: INTEGRATION, CORRELATION, AND INTERPRETATION OF GEOPHYSICAL AND ARCHAEOLOGICAL DATA AT LOS NARANJOS, HONDURAS	12
Abstract	12
Introduction	13
Study Site	14
Geophysical Data Collection	16
<i>Ground-penetrating Radar</i>	18

<i>GPR Grid 0</i>	18
<i>Structure IV</i>	20
<i>GPR Grids 2, 3, and 4</i>	21
<i>GPR Grids 10-12</i>	22
<i>Magnetometry</i>	23
<i>Correlation with GPR Data</i>	25
Conclusions	25
Acknowledgments	26
REFERENCES	27

CHAPTER 2: ESTIMATION OF DIFFRACTOR MORPHOLOGY FROM ANALYSIS OF AMPLITUDE AND TRAVEL TIME CURVATURE AT THE MAYA ARCHAEOLOGICAL SITE OF LOS NARANJOS, HONDURAS	30
Abstract	30
Introduction	31
Study Site	32
Geophysical Data Collection	35
<i>Grid 0</i>	38
Methodology	41
<i>Diffraction Picking</i>	42
<i>Velocity Analysis</i>	43
<i>Amplitude Analysis</i>	43
Conclusions	47
Acknowledgments	47
REFERENCES	48

CHAPTER 3: EFFECT OF REFLECTION PICKING CRITERIA ON <i>IN SITU</i>	
VELOCITY ESTIMATES FROM GROUND-PENETRATING RADAR COMMON	
MIDPOINT DATA	50
Abstract	50
Introduction	51
Velocity	53
<i>Time to Depth Conversions</i>	56
<i>Lithologic Discrimination</i>	56
<i>Discrimination of Clutter from Reflections</i>	57
<i>Quantifying Attenuation</i>	59
Velocity Estimation from CMP Surveys	61
Effect of Picking Position	62
Effect of Display Amplitude	68
Influence of Image Display	71
Effect of Offset (Range)	76
Effect of Picking Technique (Visual “Best Fit” Lines versus Formal Linear Regression)	84
Velocity Spectra / Semblance Analysis	86
Synthetic CMP Profiles	87
Effect on Depth and Interval Velocity Estimates	88
Conclusions	93
Acknowledgments	95
REFERENCES	96

CHAPTER 4: DISCRIMINATION OF BURIED ARTIFACTS AT LOS NARANJOS, HONDURAS USING THREE-DIMENSIONAL MIGRATION OF GROUND-PENETRATING RADAR (GPR) DATA AND MAGNETOMETRY

DATA	101
Abstract	101
Introduction	101
Platform Mounds and Sculpture	107
Geophysical Data Collection at Los Naranjos	110
Migration	114
Three-dimensional Migration	119
Discrimination of Diffractor Geometry	124
Correlation with Magnetometry	128
Conclusions	132
Acknowledgments	133
REFERENCES	134

CHAPTER 5: THREE-DIMENSIONAL GEOPHYSICAL IMAGING OF SUBSURFACE GEOLOGICAL AND ANTHROPOGENIC FEATURES AT LOS NARANJOS, HONDURAS WITH GROUND-PENETRATING RADAR AND MAGNETOMETRY

MAGNETOMETRY	147
Abstract	147
Introduction	148
Los Naranjos	150
Ground-penetrating Radar and Magnetometry	151
<i>Methods</i>	152
Results	153

<i>Faults</i>	153
<i>Minor Basins</i>	154
<i>Buried Sculpture?</i>	156
<i>Inside Structure IV</i>	159
Conclusions	161
Acknowledgments	161
REFERENCES	163

CHAPTER 6: IDENTIFYING ARCHAEOLOGICAL AND GEOLOGICAL
FEATURES IN THREE-DIMENSIONAL GROUND-PENETRATING RADAR
AND MAGNETOMETRY DATA FROM LOS NARANJOS, HONDURAS 171

Abstract	171
Introduction	172
Tectonic and Geologic Environment of Los Naranjos	176
Previous Geophysical Research in Mesoamerica	180
Previous Research at Los Naranjos	184
Ground-penetrating Radar	189
<i>Basic Principles</i>	189
<i>GPR Data Acquisition at Los Naranjos</i>	191
<i>Data Processing</i>	194
<i>Frequency Dependence</i>	197
<i>Velocity Estimation</i>	199
<i>Three-dimensional Migration</i>	201
Magnetometry	202
<i>Acquisition of Magnetic Data</i>	202
Geophysical Results	205

<i>Buried Sculpture?</i>	205
<i>Faulting and Paleoseismology</i>	207
<i>Small Depocenters</i>	209
<i>Inside Structure IV</i>	211
<i>Zone of Limited GPR Penetration</i>	213
<i>A Previously Unrecognized Buried Structure?</i>	216
<i>Natural Features versus Anthropogenic?</i>	222
<i>Volcanic Marker Horizon?</i>	226
<i>Stone-lined Path?</i>	230
Conclusions	232
Acknowledgments	233
REFERENCES	235

LIST OF FIGURES

Figure 1: Location of Los Naranjos, Honduras.	2
Figure 2: Location of all geophysical grids and archaeological excavations at Los Naranjos.	3
Figure 3: Location of Los Naranjos, Honduras.	15
Figure 4: Cultural features at Los Naranjos.	15
Figure 5: Site map of Los Naranjos and 2003 geophysical data collection.	17
Figure 6: Examples of GPR and magnetometry data from Grid 0.	19
Figure 7: GPR cross-sectional composite view across Structure IV.	21
Figure 8: Cross-sectional view from Grid 3, showing the lack of GPR penetration. ..	22
Figure 9: GPR cross-sectional view showing both structure and deep stratigraphy in grids to the west of Structure IV.	23
Figure 10: Correlation between magnetometry and GPR data from within the plaza.	24
Figure 11: Location of Los Naranjos, Honduras.	33
Figure 12: Location of Los Naranjos in relation to Lake Yojoa.	34
Figure 13: Cultural features of note at Los Naranjos.	35
Figure 14: Location of all 2003 geophysical data in relation to Structure IV.	36
Figure 15: Stone-lined ramp on west side of Structure IV.	37
Figure 16: Comparison of GPR and magnetometry data from Grid 0.	39
Figure 17: 3D view of the locations of all the 413 diffractions visually identified in Grid 0.	40
Figure 18: Vertical time slice showing the depth (in time) of the 413 diffractions in Grid 0.	41
Figure 19: Map view of the 413 diffractions in Grid 0.	42

Figure 20: Variation in apparent velocity due to changing radius of curvature of a source diffractor.	44
Figure 21: Variation in apparent amplitude of a diffractor with apex at 1 meter due to changes in diffractor curvature.	45
Figure 22: Theoretical relationship between apparent amplitude and velocity for diffractors of constant compositional contrast but with different radii.	46
Figure 23: Amplitude versus velocity for the 11 diffractors selected from Grid 0.	46
Figure 24: Location of the archaeological site of Los Naranjos on the northwestern shore of Lake Yojoa, within the present-day Department of Cortés, Honduras.	52
Figure 25: GPR data collection strategies.	54
Figure 26: Common mid-point schematic.	55
Figure 27: CMP PRO24 illustrating clutter and static shifts.	58
Figure 28: Wiggle trace images of the six CMP profiles collected at Los Naranjos.	60
Figure 29: Example velocity variations due to picking technique.	62
Figure 30: Example of an individual trace, indicating possible time zero picks.	63
Figure 31: Effect of picking position on direct airwave velocities in wiggle trace images.	65
Figure 32: Effect of picking position on direct ground wave velocities in wiggle trace images.	67
Figure 33: Four images of CMP PRO27 plotted using different gain functions.	69
Figure 34: Effect of amplitude on direct airwaves and ground waves.	70
Figure 35: Raster and wiggle trace image formats.	71
Figure 36: Effect of image display on direct airwaves.	72
Figure 37: Effect of image display on direct ground waves.	73
Figure 38: Effect of NMO stretch on three separate hyperbolae that were generated using a constant velocity of 0.060 m/ns.	75

Figure 39: Variations in velocity from simulated multiple picking positions on a single reflection.	75
Figure 40: Effect of offset on direct airwave velocities.	78
Figure 41: Effect of offset on direct ground wave velocities.	79
Figure 42: Effect of “wow” and attenuation with offset.	80
Figure 43: Effect of offset on direct airwave velocities in raster images.	82
Figure 44: Effect of offset on direct ground wave velocities in raster images.	83
Figure 45: Effect of picking technique on direct airwave velocities in wiggle trace images.	85
Figure 46: Effect of picking technique on direct ground wave velocities in wiggle trace images.	85
Figure 47: Velocity spectra for CMP PRO24.	86
Figure 48: Comparison of a synthetic CMP with CMP PRO24.	87
Figure 49: Interval velocities for CMP PRO24 based on all of the different picking strategies used in this paper.	91
Figure 50: Depth sections for CMP PRO24, showing the effect of slight variations in velocity on corresponding depths.	92
Figure 51: Location of Los Naranjos, on the northwestern shore of Lake Yojoa.	103
Figure 52: Principal Group of Los Naranjos.	104
Figure 53: Location of all geophysical grids at Los Naranjos in relation to Structure IV.	105
Figure 54: Olmec-style sculpture recovered previously at Los Naranjos.	110
Figure 55: Location of Operation 1 (Op 1) excavation units within GPR Grid 0.	113
Figure 56: Examples of GPR data collected at Los Naranjos.	113
Figure 57: The process of migration.	115

Figure 58: Comparison between the 250 MHz and 200 MHz data and corresponding frequency spectra.	118
Figure 59: Dip angle affected by aliasing.	120
Figure 60: Comparison of aperture width for 2D Kirchhoff migration.	122
Figure 61: Comparison of unmigrated, 2D migrated, and 3D migrated views of GPR profile Y = 48.0 m N, located within GPR Grid 0.	124
Figure 62: Envelope applied to a 3D migrated cross-sectional view from Grid 0. ...	125
Figure 63: Comparison of unmigrated, 2D migrated, and 3D migrated plan view GPR images of the high-amplitude feature at x = 67 m from a depth of 1.25 – 1.5 m.	127
Figure 64: Comparison of magnetometry data collected within Grid 0.	129
Figure 65: Comparison of basalt and sedimentary rock models with the actual magnetometry data collected over the high-amplitude feature generated in Grid 0.	131
Figure 66: Site map of a portion of the Principal Group at Los Naranjos, showing all geophysical data collected in relation to Structure IV.	149
Figure 67: “Pop-up” structure imaged within the plaza at Los Naranjos.	154
Figure 68: Small depocenters imaged by GPR.	155
Figure 69: Possible buried sculpture at Los Naranjos.	157
Figure 70: GPR cross-sectional view across Structure IV.	160
Figure 71: Location of Los Naranjos, on the northwestern shore of Lake Yojoa.	174
Figure 72: Principal Group of Los Naranjos.	175
Figure 73: Tectonic map of Central America.	177
Figure 74: Locations of all of the NEIC earthquakes from 1973-2009.	178
Figure 75: Locations of all of the 2009 earthquakes from the NEIC catalog.	179
Figure 76: Geologic map of Los Naranjos, Honduras and surrounding area.	180
Figure 77: Locations of the 24 geophysical surveys conducted at Mesoamerican archaeological sites discussed in text.	182

Figure 78: Olmec-style sculpture recovered previously at Los Naranjos.	184
Figure 79: Location of all geophysical grids at Los Naranjos in relation to Structure IV.	187
Figure 80: GPR data collection strategies.	190
Figure 81: Geophysical equipment used during the 2003 and 2007 field seasons. ...	192
Figure 82: Bi-directional GPR and magnetometry data collection scheme used in Grid 0.	194
Figure 83: Schematic of a wavelet with an “envelope.”	196
Figure 84: Comparison between the 250 MHz and 200 MHz antennae.	198
Figure 85: Wiggle trace images of the six CMP profiles collected at Los Naranjos.	200
Figure 86: The process of migration.	202
Figure 87: Map view of the 2003 horizontal gradient magnetometry data from Los Naranjos.	203
Figure 88: Comparison of the 2003 and 2007 magnetometry data collection.	204
Figure 89: Possible buried sculpture at Los Naranjos.	206
Figure 90: “Pop-up” structure imaged within the plaza at Los Naranjos.	208
Figure 91: Small depocenters imaged by GPR.	210
Figure 92: Composite of topographically corrected GPR cross-sectional views across Structure IV.	212
Figure 93: Limited GPR penetration in Grid 3 and comparison with an excavation wall profile.	214
Figure 94: A portion of unmigrated 400 MHz LINEY60 from GPR Grid 008.	215
Figure 95: Draping sediments and clusters of diffraction hyperbolae in an unmigrated GPR cross-sectional view from Grid 6.	217
Figure 96: Truncated sediments in GPR Grid 6.	217
Figure 97: Shallow dipping sediments in GPR Grid 6.	218

Figure 98: Cross-sectional view constructed perpendicular to GPR data collected within Grid 6.	218
Figure 99: Sub-horizontal layers in GPR Grid 6.	219
Figure 100: Possible buried structure in GPR Grid 6.	219
Figure 101: Horizontal gradient magnetometry data highlighting the buried structure imaged in Grid 6.	220
Figure 102: Horizontal gradient magnetometry profiles (transverse to direction of data collection) over the strong magnetic anomaly within Grid 6.	221
Figure 103: Domal reflection visible in GPR Grid 6.	221
Figure 104: Unmigrated GPR transect LINE1 across the “wall.”	223
Figure 105: Large basalt boulder, known informally as the Volkswagen.	225
Figure 106: Unmigrated GPR transect LINE2, east of the VW.	225
Figure 107: Unmigrated GPR transect LINE3, south of the VW.	226
Figure 108: Unmigrated LINEX480 showing the high-amplitude, sub-horizontal reflections generated in the southeastern corner of Grid 0.	227
Figure 109: High-amplitude reflections in the southeastern corner of GPR Grid 0 in relation to the excavations of Baudez and Becquelin.	228
Figure 110: Stratigraphic wall profiles from Baudez and Becquelin’s excavations on the northeastern slope of Structure IV.	229
Figure 111: Possible stone-lined path imaged in GPR Grid 0.	231
Figure 112: Map view of 3D migrated GPR Grid 0 data from a depth of 70 to 80 centimeters.	232

LIST OF TABLES

Table 1: Percent differences in velocities from simple picking error.	66
Table 2: Velocity estimates from the 100 MHz synthetic CMP profile.	88
Table 3: Mesoamerican time periods and associated date ranges.	107
Table 4: Mesoamerican time periods and associated date ranges.	186
Table 5: 2003 GPR data collection parameters.	193
Table 6: 2007 GPR data collection parameters.	194

INTRODUCTION

This dissertation developed out of an archaeological and geophysical field program at the site of Los Naranjos, Honduras (Figure 1) during the summer of 2003 that was co-sponsored by Cornell University and the University of California, Berkeley. Ground-penetrating radar (GPR) and magnetometry data were acquired in the vicinity of the excavations during this project (Figure 2). Beyond the obvious pedagogical objectives, an initial goal of the geophysical data collection was to test the efficacy of these techniques at the site, as they represented some of the first uses of geophysical methods in Honduras. It was also hoped that these datasets could provide useful information to help interpret partially excavated features or to pinpoint features of interest that could be targeted for excavation in the future. Additional Cornell – Berkeley archaeological excavations during the summer of 2004 (Figure 2) focused on locating Early Formative occupations and were not aimed at testing specific hypotheses about the geophysical data.

Analysis of the 2003 GPR data indicated an area of limited penetration to the west of Structure IV where both Early and Late Formative occupations were encountered during excavations. Additional, higher-frequency GPR data were then collected during the spring of 2007 (Figure 2) in hopes of providing higher resolution images of at least some of these occupations. Additional magnetometry data, with a closer transect spacing, were also acquired during this field season (Figure 2). All of the archaeological and geophysical data discussed in this dissertation were collected in an area approximately 1 hectare in size immediately surrounding Structure IV (Figure 2).

Although the entire suite of geophysical data includes GPR and magnetometry data, the main focus of this dissertation is on the GPR data. This is partially an artifact

of my personal bias, but it is also related to the usefulness of GPR over other geophysical techniques. Cross-sectional views, which are representations of subsurface stratigraphy, provide information that cannot be obtained from other methods.



Figure 1: Location of Los Naranjos, Honduras.

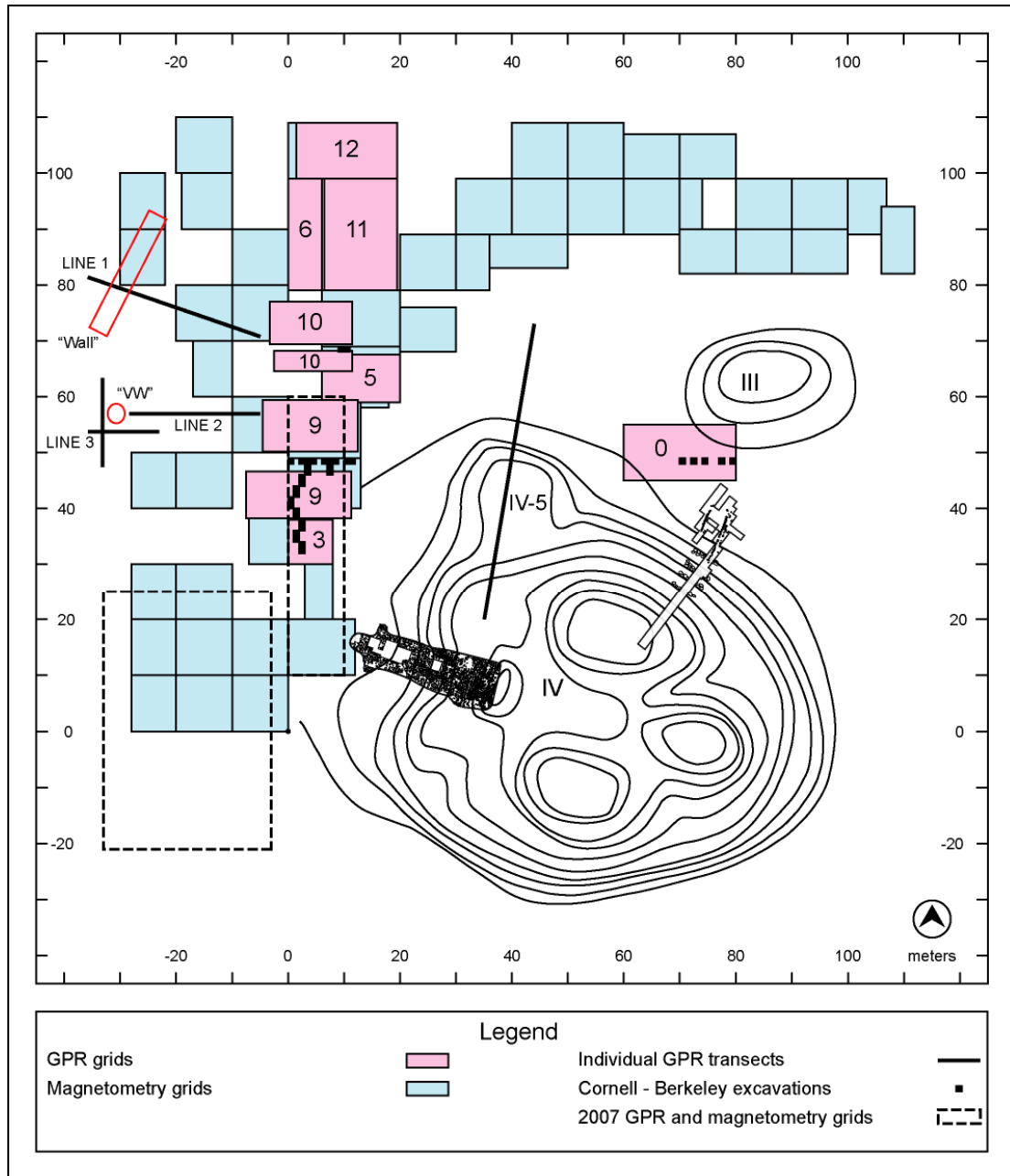


Figure 2: Location of all geophysical grids and archaeological excavations at Los Naranjos. All data were acquired in the immediate vicinity of Structure IV, a large earthen platform mound.

This dissertation is organized into six chapters that represent individual papers, and all chapters deal with some aspect of the geophysical data collected at Los Naranjos. Chapters 2, 3, and 4 are methodological, whereas Chapters 1, 5, and 6 focus

on the archaeological and geological interpretations of the data. Preliminary results of all of these chapters have been presented at national and international geological and archaeological conferences since the spring of 2005. These conferences include the Society of Exploration Geophysicists / American Geophysical Union Joint Meeting (Tchakirides *et al.*, 2005), the 11th International Conference on Ground-penetrating Radar (Tchakirides *et al.*, 2006a), the Symposium on the Application of Geophysics to Engineering and Environmental Problems Annual Meeting (Tchakirides *et al.*, 2006b), the American Geophysical Union Annual Meeting (Tchakirides *et al.*, 2006c), the Society for American Archaeology Annual Meetings (Tchakirides *et al.*, 2007; Tchakirides and Henderson, 2008), the Geological Society of America Annual Meeting (Tchakirides and Henderson, 2007), and the Three-dimensional Archaeology and Cultural Heritage Management Workshop in Honduras (Tchakirides and Brown, 2009).

Chapter 1

In Chapter 1, I present a brief introduction to some of the earliest interpretations of the geophysical data collected at Los Naranjos in 2003. Many of the original interpretations of these data are still valid, but my data processing and image-making abilities have obviously improved with time. Chapter 1 was published originally in the *Proceedings of the Symposium on the Application of Geophysics to Engineering and Environmental Problems*, April 2-6, 2006, Seattle, WA, p. 1400-1429.

Chapter 2

Chapter 2 represents an early attempt to discriminate between the numerous diffraction hyperbolae generated within GPR Grid 0 at Los Naranjos. Grid 0, located

just to the north of Structure IV (Figure 2), contains more than 400 individual diffraction hyperbolae in unmigrated GPR data. Initially, the coordinates of each were plotted in three-dimensions, but no specific features of interest were delineated by their spatial distribution. Therefore, we attempted to constrain the dimensions of the buried diffracting objects, and thus help discriminate natural from anthropogenic features, by analyzing variations in apparent velocity (from diffraction curvature) and peak amplitudes. The results indicated that amplitudes were too variable to be explained by geometry alone and must be related to different lithologies.

The analyses in this chapter were somewhat limited because we were dealing only with unmigrated data. It was entirely possible, therefore, that hyperbolae generated on multiple adjacent cross-sectional views stemmed only from one feature. From this study, it became apparent that something more sophisticated was needed to delineate specific features of interest, namely three-dimensional migration. In 2006, when this chapter was written, it was difficult for us to migrate GPR data using our seismic data processing programs, and our GPR programs did not yet include this as a viable option. Three-dimensional migration of the Grid 0 GPR data is addressed in greater detail in Chapter 4. Chapter 2 was published originally in the *Proceedings of the 11th International Conference on Ground-Penetrating Radar*, June 19-22, 2006, Columbus, Ohio, USA, p. 1-8.

Chapter 3

Common mid-point (CMP) data obtained using ground-penetrating radar provide *in situ* velocity estimates that can be used to discriminate lithology as well as convert images from time into depth domain. Initial analyses of the six CMP data from Los Naranjos produced inconsistent velocity estimates when calculated using different curve-fitting procedures (visual best-fit line versus formal regression

analyses). More quantitative analyses were carried out to evaluate the effect of reflection picking criteria as applied to the direct air and ground waves and reflections. We found that routine variations in velocity estimates translate into significant uncertainties in both interval velocity and depth estimates. These results indicate that a consistent picking criteria should be applied before velocities are used to identify either lithology or depth variations within a given survey grid. Chapter 3 is ready to be submitted to *Geophysics*.

Chapter 4

Migration has been a standard processing technique in the seismic industry since it was used to process the first seismic data collected in the early 1920s (Bednar, 2005; Neal, 2004; Sheriff and Geldart, 1995), but its use has not been as widespread in GPR projects (Hogan, 1988). Three-dimensional migration has proven critical to the interpretation of GPR results from Los Naranjos. In GPR Grid 0, numerous diffraction hyperbolae dominate the GPR cross-sections, ranging in depth from about 0.30 to 1.20 meters. Although these diffractions vary in amplitude, discriminating among them on the unmigrated imagery is problematic at best, as was shown in Chapter 2. Although 2D migration suggests differences in diffractor shape, only 3D migration provides the necessary detail to identify anomalous features.

Fundamentally, the goals of migration are to correct GPR reflection data so that they accurately represent the subsurface (Neal, 2004) and to increase the resolution of features in reflection profiles (Hogan, 1988). There are many techniques for implementing migration. Here we use a form of Kirchhoff summation, in which energy is summed along an appropriate diffraction hyperbola, thus focusing reflected energy at its apex (Hogan, 1988; Schneider, 1978). Diffractions collapse back to their respective point sources. We focus mainly on the use of migration in this paper as it is

applied to point source features because Grid 0 provides an excellent test case in which to demonstrate the effectiveness of collapsing the numerous diffraction hyperbolae. The most distinctive diffractor on the 3D migrated imagery corresponds with a prominent magnetic anomaly. The dimensions of this diffractor, as deduced from the 3D imagery, and its magnetic properties suggest that this feature may correspond to buried sculpture with a basaltic composition, rather than detrital rocks (limestone) or building blocks (sandstone) shed from nearby structures. We suggest that this feature marks a previously unrecognized sculpture similar to the distinctive Olmec-style columns and statuary that have been recovered at the surface of Los Naranjos. Chapter 4 is in preparation for *Archaeological Prospection*.

Chapter 5

Chapters 5 and 6 are intimately related, with Chapter 5 providing only a partial discussion of the 2003 and 2007 geophysical data collected at Los Naranjos. Chapter 5 developed into a separate chapter because of an invitation to present research on the use of three-dimensional methods at archaeological sites in Honduras. This international workshop, *Three-dimensional Archaeology and Cultural Heritage Management in Honduras*, was held at the Visitor's Center at the Copán Archaeological Park, in Copán, Honduras in April 2009 and was sponsored by the Instituto Hondureño de Antropología e Historia and the University of New Mexico.

The paper I presented was the only one to focus on geophysical methods and the only one to discuss 3D subsurface datasets. Since the original audience for this paper had no previous background in the methods or theory of geophysical techniques, the paper is more of an overview and is less technical than some of the other chapters in this dissertation. The main goals of this paper were to introduce the techniques of GPR and magnetometry, discuss the principal results, and provide an example of what

can be achieved through the use of non-invasive geophysical methods. This chapter was submitted to the Instituto Hondureño de Antropología e Historia for publication in a special edition of *Yaxkin* in December 2009. Due to coup-related activities since the spring of 2009, the exact date of publication is now unknown.

Chapter 6

Chapter 6 presents a comprehensive analysis of all aspects of the geophysical research at Los Naranjos, including both the 2003 and 2007 GPR and magnetometry data. All data have been processed and analyzed, making it possible to draw more extensive conclusions about the archeological significance. Key features revealed by the GPR data include a previously unrecognized buried structure, small depocenters (basins), buried sculpture (possibly Olmec in nature?), a stone-lined path, faults, and a possible volcanic marker horizon. The GPR results have also been useful at probing the interior of Structure IV as well as determining a geological origin for an exposed rock “wall” within the plaza and an anthropogenic origin for a large basalt boulder known as the “Volkswagen.” Correlation with magnetometry data helped identify a basaltic lithology for the buried sculpture and a highly magnetic material for the buried structure. The results obtained at Los Naranjos show considerable potential for this technology in defining geological setting and mapping buried anthropogenic structures. Most importantly, these geophysical methods have proven especially effective for probing this protected site in a non-invasive and non-destructive manner. Chapter 6 is in preparation for *Archaeological Prospection*.

REFERENCES

- Bednar, J.B. (2005). A brief history of seismic migration. *Geophysics*, 70(3): 3MJ-20MJ.
- Hogan, G. (1988). Migration of ground-penetrating radar data: A technique for locating subsurface targets, 59th Annual International Meeting of the Society of Exploration Geophysicists, pp. 345-347.
- Neal, A. (2004). Ground-penetrating radar and its use in sedimentology: principles, problems and progress. *Earth-Science Reviews*, 66(3-4): 261-330.
- Schneider, W.A. (1978). Integral Formulation for Migration in 2 and 3 Dimensions. *Geophysics*, 43(1): 49-76.
- Sheriff, R.E. and Geldart, L.P. (1995). *Exploration seismology*. Cambridge University Press, Cambridge; New York, xv, 592 pp.
- Tchakirides, T.F. and Brown, L.D. (2009). Three-dimensional Geophysical Imaging of Subsurface Geological and Anthropogenic Features at Los Naranjos, Honduras with Ground-penetrating Radar and Magnetic Gradiometry. Paper presented at the International Workshop: Arqueología 3D y la Gestión del Patrimonio Cultural en Honduras, Archaeological Park of Copán, Honduras, April 17-18, 2009.

- Tchakirides, T.F., Brown, L.D. and Henderson, J.S. (2005). GPR Experience at Mesoamerican Archaeological Sites in Honduras: Puerto Escondido and Copán, *Eos. Trans. AGU*, 86(18), Jt. Assem. Suppl., Abstract NS41A-03.
- Tchakirides, T.F., Brown, L.D. and Henderson, J.S. (2006a). Estimation of Diffractor Morphology from Analysis of Amplitude and Travel Time Curvature at the Maya Archaeological Site of Los Naranjos, Honduras., In *Proceedings of the 11th International Conference on Ground Penetrating Radar: June 19-22, Columbus, Ohio*, p. 1-8.
- Tchakirides, T.F., Brown, L.D., Henderson, J.S. and Blaisdell-Sloan, K. (2006b). Integration, Correlation, and Interpretation of Geophysical Data at Los Naranjos, Honduras, In *Proceedings of the Symposium on the Application of Geophysics to Engineering and Environmental Problems: April 2-6, 2006, Seattle, WA*, p. 1400-1429.
- Tchakirides, T.F., Brown, L.D., Henderson, J.S. and Joyce, R.A. (2006c). A Geophysical and Archaeological Analysis of Early Formative Paleoenvironments at Los Naranjos, Honduras. Paper presented at the American Geophysical Union Annual Meeting, San Francisco, CA, December 11-15, 2006.
- Tchakirides, T.F., Brown, L.D., Henderson, J.S. and Joyce, R.A. (2007). Understanding the Use of Space in Early Formative Honduras: A Geophysical and Archaeological Analysis of Los Naranjos, Honduras. Paper presented at

the Society for American Archaeology 72nd Annual Meeting, Austin, TX,
April 25-29, 2007.

Tchakirides, T.F. and Henderson, J.S. (2007). Exploring Formative Period Residential Structures at Puerto Escondido, Honduras Using Ground-Penetrating Radar and Magnetometry. Paper presented at the Geological Society of America Annual Meeting, Denver, CO, October 28-31, 2007.

Tchakirides, T.F. and Henderson, J.S. (2008). Identifying Anthropogenic Versus Geological Features in Geophysical Data: A Closer Look at Los Naranjos and Puerto Escondido, Honduras. Paper presented at the Society for American Archaeology 73rd Annual Meeting, Vancouver, British Columbia, CA, March 26-30, 2008.

CHAPTER 1

INTEGRATION, CORRELATION, AND INTERPRETATION OF GEOPHYSICAL AND ARCHAEOLOGICAL DATA AT LOS NARANJOS, HONDURAS*

Abstract

During the summer of 2003, ground-penetrating radar (GPR) and magnetometry surveys were conducted at the Maya archaeological site of Los Naranjos on the shore of Lake Yojoa in Central Honduras. Los Naranjos was occupied from the Early Formative to the Early Postclassic Periods and is of particular interest as Olmec-style artifacts have been recovered in situ at the site. GPR surveys were collected with 50, 100, 200, and 250 MHz antennae in both 2-D grids and linear profiles. Results of GPR, magnetometry, and resistivity surveys are being integrated with archaeological data to improve our understanding of the spatial relationships of partially excavated features as well as to target areas for future excavation. The surveys covered both apparent archeological and natural features, with GPR penetration in excess of 5 meters at 100 MHz. GPR proved especially effective in both delineating Quaternary stratigraphy and mapping localized buried features. Correlation between magnetic and resistivity anomalies and GPR-imaged features is highly variable, suggesting that a range of lithologies and artifact compositions are being imaged. Both types of data are essential guides for future archaeological excavations, with calibration boreholes and excavation test units planned for 2006.

* Published originally as: Tchakirides, T.F., Brown, L.D., Henderson, J.S., and Blaisdell-Sloan, K. (2006). Integration, Correlation, and Interpretation of Geophysical and Archaeological Data at Los Naranjos, Honduras. In Proceedings of the Symposium on the Application of Geophysics to Engineering and Environmental Problems: April 2-6, 2006, Seattle, WA, p. 1400-1429.

Introduction

Over the past few decades, geophysical methods have been integrated into traditional archaeological endeavors with a great deal of success, covering larger areas and penetrating deeper than many traditional excavations permit due to time and monetary constraints. By systematically collecting three-dimensional subsurface data over key portions of a site, calibrated by targeted excavations to establish both stratigraphic control and identification of likely artifacts, it is possible to reconstruct the topographic and geographic environment at different times of occupation and to map modifications to that configuration over time. Ground-penetrating radar (GPR) and magnetometry are two of the most widely used geophysical methods in archaeology (Kvamme, 2003).

Geophysical data were acquired at the early Maya site of Los Naranjos, Honduras during the summer of 2003. This project was undertaken in conjunction with an archaeological field school that was co-sponsored by the Department of Anthropology/Archaeology Program at Cornell University and the Department of Anthropology at the University of California, Berkeley. The excavations were led by Prof. Rosemary Joyce (Berkeley) and Prof. John Henderson (Cornell). During this fieldwork, GPR, magnetometry, and resistivity were integrated into archaeological endeavors for the purpose of obtaining three-dimensional coverage of the subsurface while excavating in areas dictated by preliminary analysis of the GPR data.

Although geophysical methods have proven to be effective in supporting archaeology in numerous locations, their application to studies in the Maya world has been limited to date. Some successful examples include reconstructing the topography of Cerén, El Salvador (Conyers, 1995), mapping Maya plazas at Ma'ax Na, Belize (Aitken and Stewart, 2004), and surveying several sites in the Yucatan region (Sauck,

1998), but no attempts have been made to apply these methodologies at Early Formative sites.

Study Site

Los Naranjos, Honduras (Figure 3) is situated on the current shoreline of Lake Yojoa, in the present-day Parque Arqueológico – Ecológico Los Naranjos, which is operated by the Instituto Hondureño de Antropología e Historia. This site is one of the earliest Maya settlements in Mesoamerica (Joyce and Henderson, 2002), with continuous occupation dating from the Early Formative to the Early Postclassic (1600 B.C. – A.D. 1200) (Joyce, 2004a). Numerous earthen platform mounds (Figure 4a), which are the “largest pre-Columbian structures in Honduras” (Joyce, 2004c, p. 10), comprise the site, some measuring up to 75 x 50 meters wide x 16 meters tall. Many of the platform mounds are clustered into groups, the largest of which, the Principal Group, has been the focus of previous excavations. These excavations have uncovered elaborate burials, complete with jade ornaments and Olmec-style artifacts located *in situ* at depth (Baudez and Becquelin, 1973; Joyce and Henderson, 2002). The size and extent of the early platforms, the early evidence of ranking represented by the burials, and the presence of Olmec-style artifacts from the deepest levels drastically differ from most other early Maya sites. Some scholars have suggested the platform mounds and associated ditches served as fortifications against enemies (Webster, 1976), but their significance has not yet been determined. Los Naranjos, therefore, offers an especially attractive opportunity to integrate geophysical methods with geological and archaeological studies to address key issues related to the emergence and evolution of social, economic, and political institutions that characterize Maya civilization.

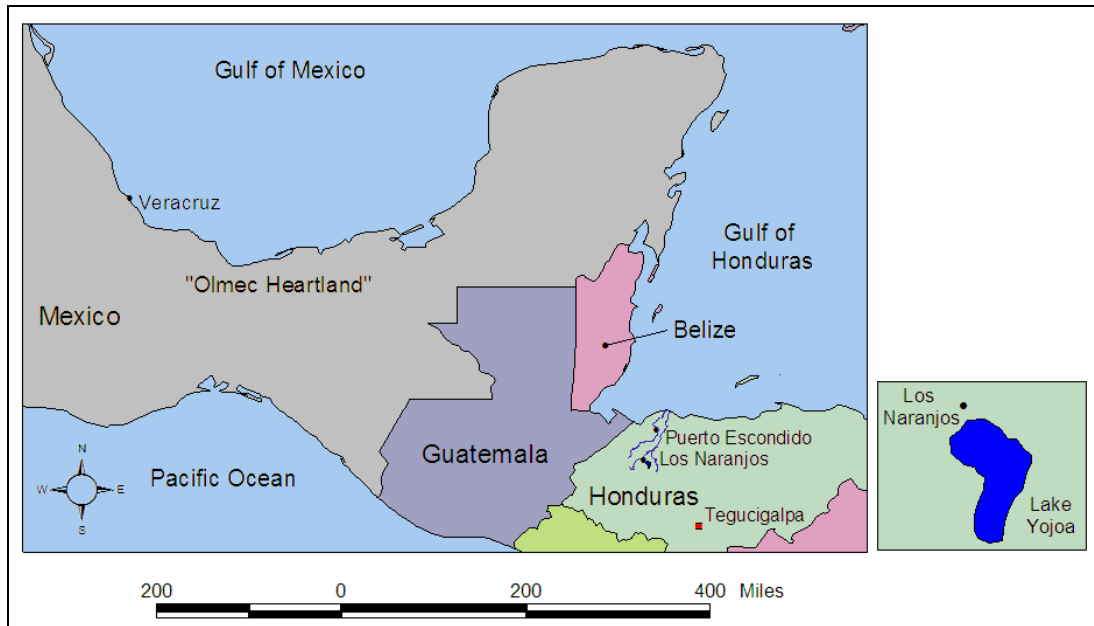


Figure 3: Location of Los Naranjos, Honduras. Note also the distance to Veracruz, Mexico in the “Olmec Heartland.”



Figure 4: Cultural features at Los Naranjos. (a) Stone ramp on west side of platform mound (Structure IV); (b) anthropomorphic Olmec-style statuette; (c) Plaza NW of Structure IV where additional statuary may be located. Much of the geophysical data discussed here were collected in this area.

In addition to the platform mounds, several basalt sculptures in Olmec style have been located dotting the landscape (Stone, 1934, p. 126) (Figure 4b). The original locations of these sculptures remain uncertain, but several were found in the vicinity of the Principal Group. Very little research has been undertaken on these figures, but since they are located in open spaces adjacent to pyramid mounds (Figure 4c), they are likely public monuments or displays. At the archaeological site of La

Venta, Mexico, Olmec sculptures are located in the open areas between mounds and are likely images of political leaders placed in relation to the platform mounds (Drucker *et al.*, 1959; Grove, 1999). They may have served a similar function at Los Naranjos. Five figures have been located to date; three are anthropomorphic, one has features of “transformation,” combining representations of fleshed and skeletal states, and one is a hybrid, having features of serpents, jaguars, and sharks.

The Olmec culture had a substantial impact on most of the later Mesoamerican civilizations, but large-scale monumental construction and sculptures are concentrated in the “Olmec Heartland” on the Gulf Coast of Mexico, near Veracruz (Figure 3). Los Naranjos and the nearby site of Puerto Escondido are the easternmost communities in which Olmec materials have been found, and the Olmec sculptures at Los Naranjos are also one of the largest clusters of Olmec sculpture outside of the Gulf Coast. Understanding Olmec occupation at Los Naranjos can potentially resolve the critical issue of the relationships among the Gulf Coast and the rest of Olmec Mesoamerica.

Geophysical Data Collection

During the summer of 2003, Prof. Larry Brown (Cornell) directed the collection of GPR, GPS, and resistivity data (Figure 5), during the joint Berkeley-Cornell field school. In addition, Kira Blaisdell-Sloan supervised the magnetometry surveys over much the same area. In addition to their pedagogic value, these surveys were also designed to test the effectiveness of these methods in delineating archaeologically significant features at the site. Results of the GPR surveys were especially encouraging, with penetration often in excess of 5 meters at 100 MHz (Lisman *et al.*, 2005; Tchakirides *et al.*, 2005). GPR data were collected with a Noggin 250 cart-mounted system (provided courtesy of GeoRad Surveys, Inc.), which is ideal for 3D surveys, and Cornell’s pulseEKKO 100 bistatic system (50, 100 and

250 MHz antennae), which provided deeper penetration profiles, additional 3D coverage, and high-quality common mid-point (CMP) data for *in situ* radar velocity estimation, which are essential for accurate depth estimation. Magnetometry data were collected using a Geometrics G-858 magnetometer, which is owned by the University of California. A limited amount of resistivity data was collected with Cornell's Bison Earth Resistivity Meter, Model 2350A; those results proved too insubstantial to be of use in this study, and therefore will not be discussed further.

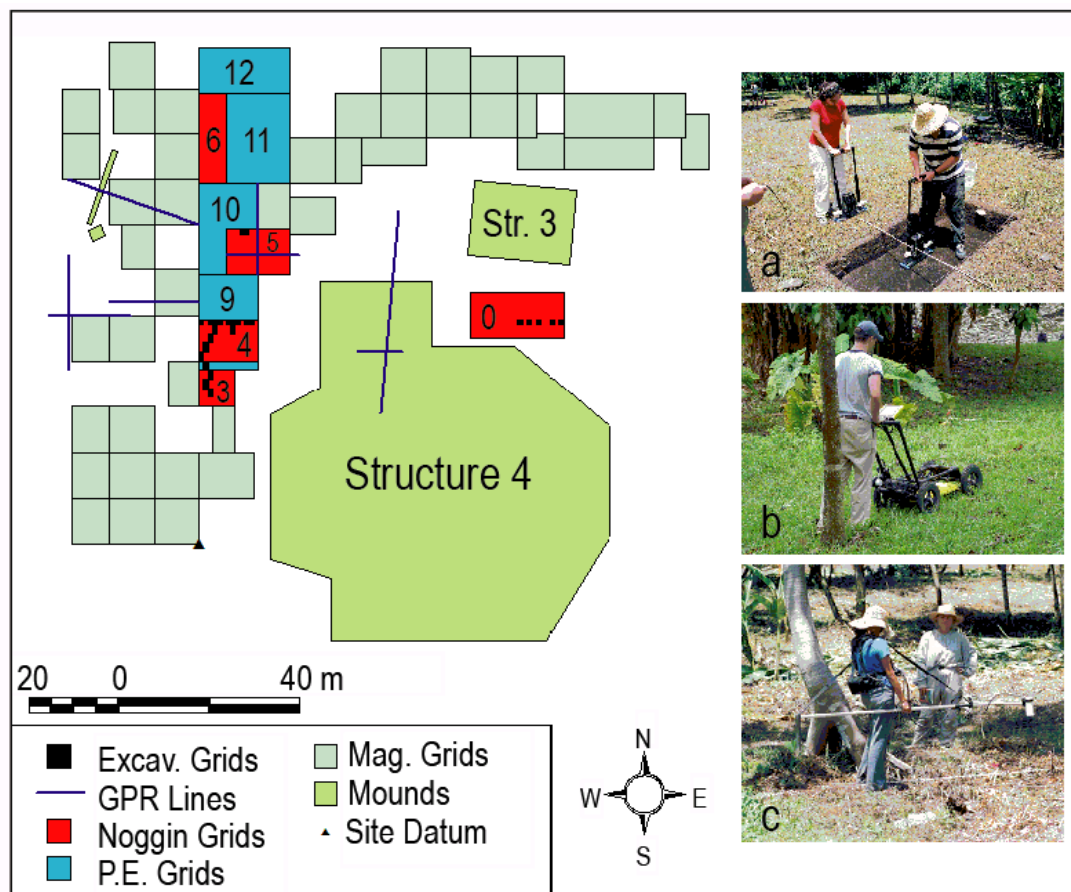


Figure 5: Site map of Los Naranjos and 2003 geophysical data collection. All geophysical data have been collected in the immediate vicinity of Structure IV. (a) GPR data collection with the pulseEKKO 100; (b) GPR data collection with the Noggin 250; (c) Magnetometry data collection with the Geometrics G-858. Numbers within grids refer to GPR grids.

Ground-penetrating Radar

GPR is a shallow geophysical method that transmits electromagnetic energy into the ground and receives reflections from subsurface features or interfaces back at the surface (Conyers, 2004). In this study, GPR data were acquired in linear profiles and 2-dimensional grids, using both the pulseEKKO and Noggin systems. The Noggin system failed due to heat problems during the surveying of Grid 6; thus all subsequent work was done with the pulseEKKO 100. All archaeological test units (Op 1 – Op 4) were surveyed with GPR prior to excavation (Figure 5) so as to target specific areas to excavate and to correlate all archaeological features with stratigraphic information in the GPR profiles. For grids collected with the pulseEKKO system (Grids 9, 10, 11, and 12), the transmitting and receiving antennae were spaced 1 meter apart, data were collected every 20 centimeters along a transect, and individual transects within each grid were spaced 50 centimeters apart. Transects were also spaced 50 centimeters apart within each Noggin grid (Grids 0, 2, 3, 4, 5, and 6). All GPR data were processed using the Sensors and Software suite of processing programs at Cornell.

GPR Grid 0

Grid 0, located immediately to the north of the base of Structure IV (Figure 5), with GPR penetration to a depth of about 2 meters at 250 MHz, provides an excellent example of the variety of subsurface features and structures seen at Los Naranjos. Diffraction hyperbolae are common beneath this grid (Figure 6) and range in depth from about 0.3 to 1.2 meters. The sources of these hyperbolae are unclear at the present time, but several possibilities come to mind. Many of them are likely due to buried rocks or perhaps building detritus from the construction or subsequent alteration of Structure IV. Archaeological excavations within this grid (Op 1)

encountered evidence of construction activity including packed surfaces and building debris (numerous stones and fragments of wattle and daub).

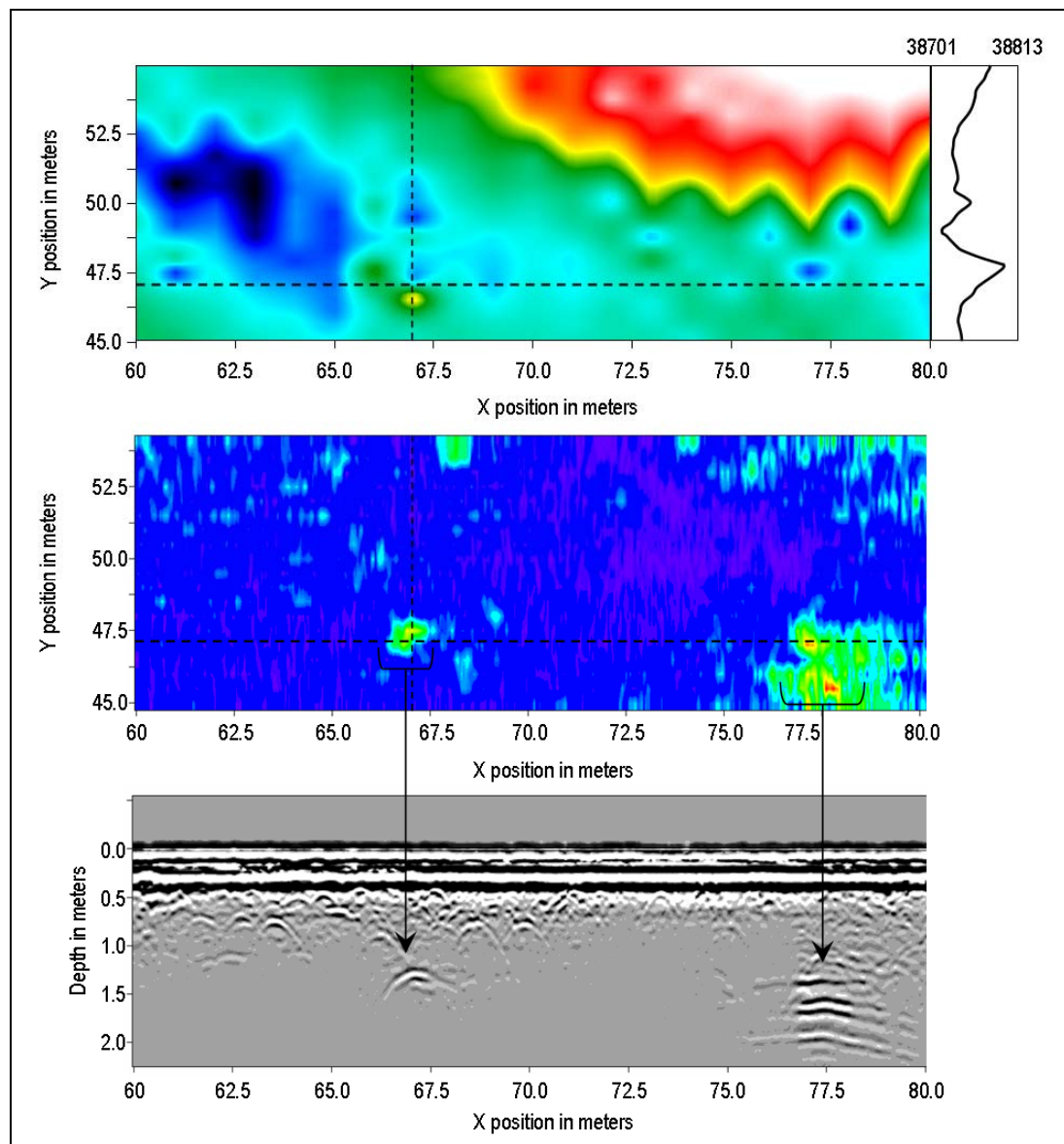


Figure 6: Examples of GPR and magnetometry data from Grid 0. (Top) Magnetometry data from Grid 0, located just north of Structure IV. On the right are the magnetometry results along the NS profile indicated by the dashed line. Numbers at the top of the profile are in units of nanoTesla. (Middle) Horizontal depth slice of GPR data from Grid 0, representing a depth of 1.2 to 1.3 meters. (Bottom) GPR section through Grid 0 along the EW dashed line, showing numerous diffractions that might be of archaeological significance. Also noted are the reflections corresponding to the amplitude anomalies (bright spots) in the horizontal slice map.

However, given the Olmec-style sculptures that have been previously found at Los Naranjos, it is certainly plausible that some of these hyperbolic reflections may mark such statuary still in the ground. As the area of Grid 0 is also located between Structures IV and III, it is possible that this area was used as a public space, where monumental sculptures were displayed.

GPR surveys in Grid 0 also delineated a domed bright spot located at about the 77.5 meter mark along the x-axis (Figure 6). At first, this high-amplitude anomaly appeared to be a large buried mound, either artificial or natural. On closer inspection, however, it appears that it is a natural geological feature, as it is part of the intact stratigraphy (Figure 6 bottom). If it is natural, it is intriguing that it is so strong in several of the cross-sectional views. Also of interest in this grid is a high-amplitude anomaly located at about 67.5 meters along the x-axis (Figure 6). In map view, this reflection is strongest in the depth slice from 1.2 – 1.3 meters. This small circular feature is significant in that it might represent a buried sculpture or monument, possibly Olmec in nature. Future research planned for 2006 is aimed at determining the genesis of these features.

Structure IV

GPR profiles across the flank of Structure IV, one of the main pyramid mounds within the Principal Group, raise equally interesting questions. As shown in Figure 7, the strong reflectivity from stratigraphy at the northern base of the structure is abruptly truncated as the survey moves onto the pyramid mound. It appears that conductive materials may have been used as fill, thereby preventing penetration of the GPR signal. Clay coating on the face of the pyramid mound would also produce a similar shielding effect, which might be characteristic of the pyramid mounds in general. Geophysical and archaeological surveys were specifically planned at the

perimeter of Structure IV, rather than on top of it, due to the complex nature of its stratigraphy, so no subsurface information exists at present. In any case, the experience indicates that even the lack of data is an important clue to construction technique/delineation of space. In spite of the more limited penetration, shallow structural variations are indicated on the top of the pyramid, though these may arise from the backfill of previous archaeological excavations conducted by Baudez and Becquelin in the 1960s.

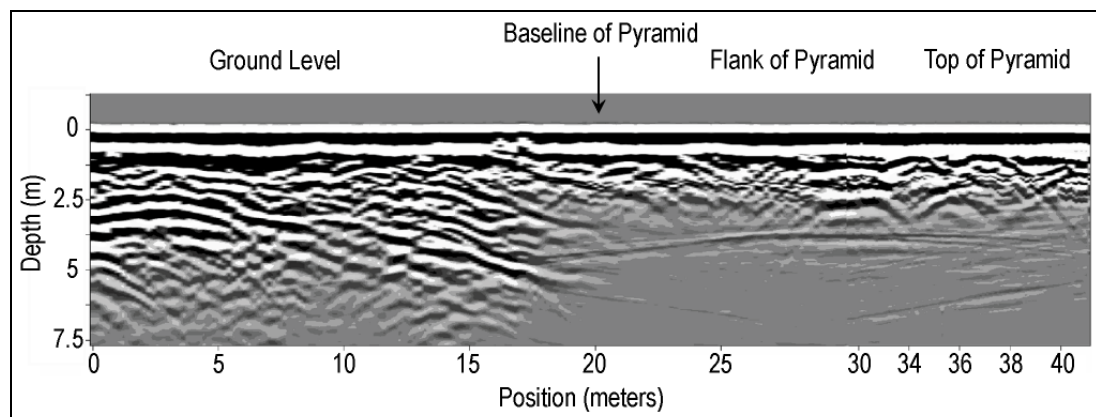


Figure 7: GPR cross-sectional composite view across Structure IV. Note the dramatic shielding effect on the pyramid itself and the high-frequency arcuate events below 2.5 meters on the pyramid. The high-frequency arcuate events below 2.5 meters on the pyramid top and flank are interpreted as backscatter (clutter) from the vegetation canopy.

GPR Grids 2, 3, and 4

Although the GPR method was successful at penetrating to depths in excess of 5 meters at several locations throughout the site, several of the grids contained materials exhibiting much poorer penetration, presumably due to more conductive materials (Figure 8). Data acquired in GPR Grids 2 and 3 (Figure 5), for example, show penetration to depths of less than 0.5 meters, and few features can be delineated. The lack of penetration within these grids was disappointing, as they were planned to

correlate directly with the archaeological excavations at Op 2 and Op 4 that were located within them. Subsequent archaeological excavations at Op 4 during the summer of 2003 unearthed thick lenses of uniform yellow clay, likely eroded from the west facing of Structure IV, and deeply buried burned clay floors associated with Early Formative occupation. Limited penetration may, therefore, be diagnostic of such habitation areas.

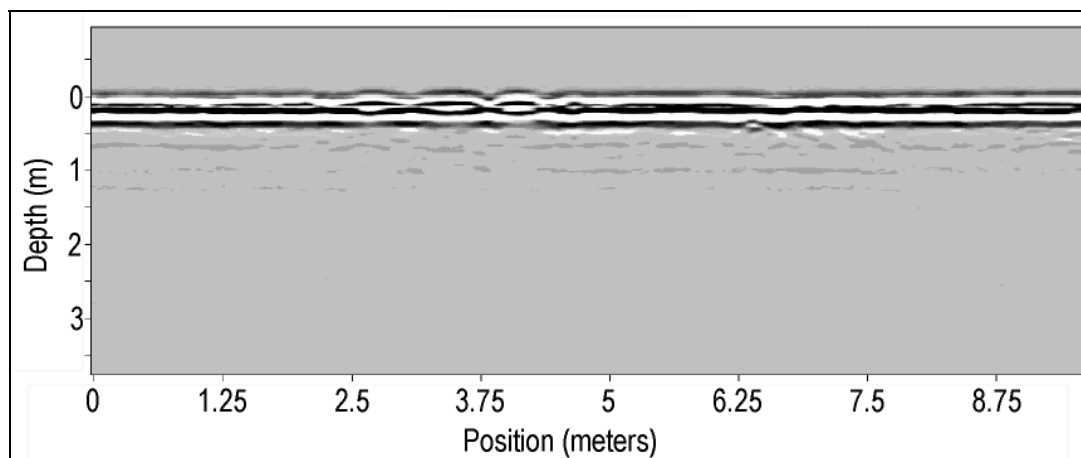


Figure 8: Cross-sectional view from Grid 3, showing the lack of GPR penetration. Subsequent excavations indicate that this area is characterized by packed clay floors associated with habitation.

GPR Grids 10-12

GPR Grids 10 – 12 were established in the main courtyard of the site, to the north/northwest of Structure IV (Figure 5). Data collected in this area are dominated by a SW to NE trending antiformal structure, with well-defined onlap of shallow strata on the NW flank, and indications of fault control on the SE flank (Figure 9). The antiform suggests a possible natural causeway between two of the major monumental structures at Los Naranjos. A key conclusion from surveys in this area was that previous identifications of natural versus anthropogenic structures were likely erroneous. A feature mapped as a “wall” by previous surface studies seems to be part

of a natural ridge of basement material. Likewise a large block (“the Volkswagen”) of volcanic rock, originally thought to be a simple outcrop, appears to be allochthonous given the undisrupted nature of adjacent stratigraphy on a GPR profile. Whether this large block was emplaced naturally by a landslide or flooding or was transported by inhabitants remains to be determined.

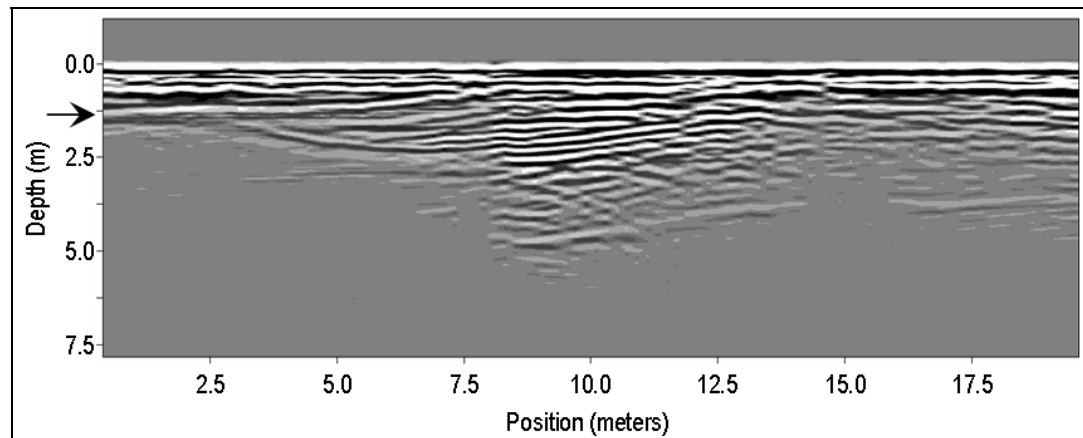


Figure 9: GPR cross-sectional view showing both structure and deep stratigraphy in grids to the west of Structure IV. Arrow indicates one of the more prominent unconformities.

Magnetometry

During the summer of 2003, more than 50 grids of magnetometry data were collected (Figure 5 and Figure 10). Almost all of the areas that were surveyed with GPR were also then surveyed with magnetometry to allow for direct correlation of the two data sets. For each grid, transects were spaced 1 meter apart and data points were collected every 2 meters along each transect. Data were processed using MagMap software and were then imported into Surfer and ArcGIS for analysis.

To take advantage of the large areal coverage of the magnetometry grids, all data were plotted on the same map to determine how the values ranged throughout the site. In order to do this, all data were imported into ArcGIS, and the color scales for

each grid were first normalized so that all grids were plotted to the same scale. Values between the grids ranged more than 7,500 nanoTesla, so slight variations within many of the grids were obliterated, as they all fell within the range of one of the colors within the scheme. Whereas a broad scale view of the site is possible with this mapping scheme, it is still necessary to refer to each corresponding subset to recognize smaller scale variations within each grid and to compare them to the corresponding GPR data (Figure 6).

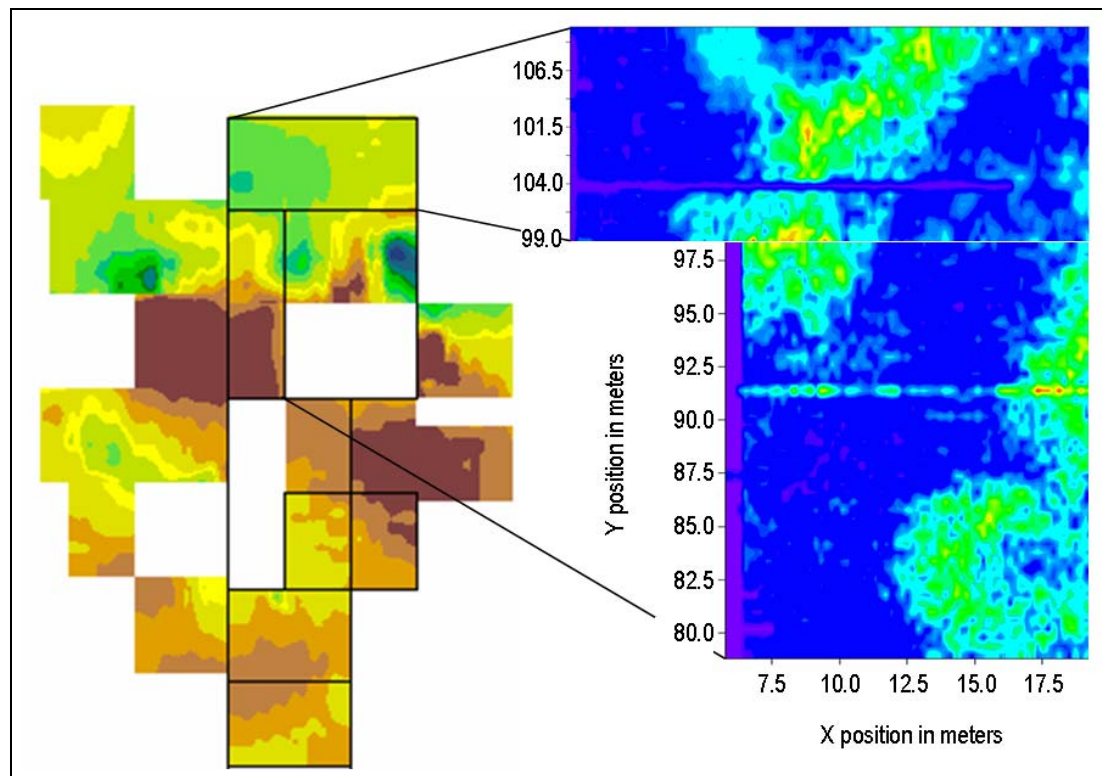


Figure 10: Correlation between magnetometry and GPR data from within the plaza. (Left) Magnetometry map of Los Naranjos, showing some of the magnetometry grids to the west of Structure IV. Black lines indicate outlines of GPR grids. (Right) Corresponding GPR data from Grids 11 and 12 show the antiformal structure that is also visible in the magnetometry data. The SE to NW trend of higher magnetic amplitudes in the magnetometry data has not yet been noted in the GPR data.

At a larger scale, however, it is possible to see that the SW to NE antiformal structure seen in GPR Grids 11 and 12 is also exhibited in the magnetometry grids that correspond to the same areas (Figure 10). In the magnetometry data, a general SE to NW trend to the data below GPR Grids 11 and 12 is also noticeable. This trend has not yet been noted in the GPR data.

Correlation with GPR Data

The magnetometry data contain strong anomalies associated with some of the buried features that are evident on the GPR sections, which we interpret as indicating the presence of volcanic materials, although whether natural (rocks) or formed (sculpture?) has yet to be determined (Figure 10). For several of the GPR and magnetometry grids, there was excellent correlation between the two datasets. Compare, for example, the magnetometry plot from Grid 0 with the corresponding GPR depth slice and section (Figure 6). Note that the strong circular anomaly located about 67 meters along the x-axis is similar in appearance and location to the high-amplitude reflection detected in the same location in the GPR horizontal slice. The correlation between these datasets suggests the anomaly is magnetic in nature, consistent with either volcanic rock (detritus) or sculpture from volcanic material.

Conclusions

GPR at Los Naranjos was successful at detailing stratigraphy to depths up to 5 meters. Pronounced variations in penetration, numerous diffractions, and material suspected to be clay facings all provide clues that may correlate with habitation areas and construction activity at the site. Correlation of the GPR and magnetometry data helps constrain the likely composition of buried features. The focus of future research is to use geophysics, particularly GPR and magnetometry, to reconstruct the

topographic and geographic environment at the time of occupation and to map modifications to that configuration over time. In addition, we plan to collect complementary geophysical data near and on Lake Yojoa and associated meander systems to build a broader view of the geological context of Los Naranjos. These surveys should help determine if a shift in the environment and/or ecology in the Lake Yojoa region led to the settlement of Los Naranjos.

Acknowledgments

The authors would like to express their appreciation to Juan Alberto Durón and his colleagues at the Instituto Hondureño de Antropología e Historia for their support during the collection of these data. Most of the data were collected by students participating in the 2003 Cornell-Berkeley archaeological field program; their effort and enthusiasm was critical to our success. The field program was directed by Profs. John Henderson (Cornell) and Rosemary Joyce (Berkeley). Special thanks to GeoRad, Inc., and its President, Mr. William Perks, for providing the Noggin for use at Los Naranjos. Mr. Perks also contributed generously of his time and expertise during the field work. Joel Haenlein directed the collection of much of the Noggin data. Photographs are by Dr. John Henderson and Dr. Larry Brown.

REFERENCES

- Aitken, J.A. and Stewart, R.R. (2004). Investigations using Ground Penetrating Radar (GPR) at a Maya Plaza Complex in Belize, Central America., In Proceedings of the Tenth International Conference on Ground-Penetrating Radar: June 21-24, Delft, The Netherlands., Evert Slob, Alex Yarovoy and Jan Rhebergen (editors). Delft University of Technology, The Netherlands and the Institute of Electrical and Electronics Engineers, Inc., Piscataway, New Jersey, pp. 447-450.
- Baudez, C.F. and Becquelin, P. (1973). Archéologie de Los Naranjos. Mission Archéologique et Ethnologique Française au Mexique, Mexico.
- Conyers, L.B. (1995). The use of ground-penetrating radar to map the buried structures and landscape of the Ceren Site, El Salvador. *Geoarchaeology: An International Journal*, 10(4): 275-299.
- Conyers, L.B. (2004). *Ground-Penetrating Radar for Archaeology. Geophysical Methods for Archaeology*. AltaMira Press, Walnut Creek, CA.
- Drucker, P., Heizer, R.F. and Squier, E.G. (1959). Excavations at La Venta, Tabasco, 1955. *Bulletin (Smithsonian Institution. Bureau of American Ethnology)*, no. 170. , Washington, D.C.
- Grove, D.C. (1999). Public Monuments and Sacred Mountains: Observations on Three Formative Period Social Landscapes. In: D.C. Grove and R.A. Joyce (Editors),

Social Patterns in Pre-Classic Mesoamerica. Dumbarton Oaks, Washington, DC, pp. 255-300.

Joyce, R.A. (2004a). Mesoamerica: A Working Model for Archaeology. In: J.A. Hendon and R.A. Joyce (Editors), *Mesoamerican Archaeology: Theory and Practice*. Blackwell Studies in Global Archaeology. Blackwell, Malden, MA, pp. 1-42.

Joyce, R.A. (2004b). Unprecedented Projects: The Birth of Mesoamerican Pyramids. *Expedition*, 46(2): 7-11.

Joyce, R.A. and Henderson, J.S. (2002). La arqueología del periodo Formativo en Honduras: nuevos datos sobre el «estilo olmeca» en la zona maya. *Mayab*, 15: 5-17.

Kvamme, K.L. (2003). Geophysical surveys as landscape archaeology. *American Antiquity*, 68(3): 435-457.

Lisman, T., Tchakirides, T.F., Brown, L.D. and Henderson, J.S. (2005). GPR Surveys at Los Naranjos, an Early Formative Mesoamerican Site in Central Honduras, *Eos. Trans. AGU*, 86(18), Jt. Assem. Suppl., Abstract NS41A-04.

Sauck, W.A. (1998). Long GPR Profiles for Geologic Reconnaissance and Mapping, *Proceedings of the Seventh International Conference on Ground-Penetrating Radar*, May 27-30, 1998., University of Kansas, Lawrence, Kansas, USA.

Radar Systems and Remote Sensing Laboratory, University of Kansas: 263-272.

Stone, D.Z. (1934). A new southernmost Maya city (Los Naranjos on Lake Yojoa, Honduras). *Maya Research*, 1(2): 125-128.

Tchakirides, T.F., Brown, L.D. and Henderson, J.S. (2005). GPR Experience at Mesoamerican Archaeological Sites in Honduras: Puerto Escondido and Copán, *Eos. Trans. AGU*, 86(18), Jt. Assem. Suppl., Abstract NS41A-03.

Webster, D. (1976). Lowland Maya Fortifications. *Proceedings of the American Philosophical Society*, 120(5): 361-371.

CHAPTER 2
ESTIMATION OF DIFFRACTOR MORPHOLOGY FROM ANALYSIS OF
AMPLITUDE AND TRAVEL TIME CURVATURE AT THE MAYA
ARCHAEOLOGICAL SITE OF LOS NARANJOS, HONDURAS*

Abstract

During the summer of 2003, ground-penetrating radar (GPR) data were acquired at the site of Los Naranjos on the shore of Lake Yojoa in Central Honduras. These surveys were undertaken in conjunction with magnetometry and limited archaeological excavations to understand this early Maya site. Los Naranjos was occupied from the Early Formative to the Early Postclassic Periods and is of particular interest as Olmec-style artifacts have been recovered *in situ* near one of the numerous large earthen platform mounds that comprise the site. GPR successfully penetrated to depths in excess of 5 meters at 100 MHz. Both natural and anthropogenic features were targeted by a number of 2D survey grids. One GPR grid located immediately north of the largest platform mound was characterized by numerous (more than 400) diffractions imaged at depths between 0.3 to 1.2 meters. Several of these correlate with pronounced magnetic anomalies within the same grid. In an attempt to constrain the dimensions of the buried diffracting objects, and thus help discriminate natural from anthropogenic features, variations in apparent velocity (from diffraction curvature) and peak amplitudes were analyzed. The observed variations do not follow the systematics expected if diffractor size were the dominant control on both velocity

* Published originally as: Tchakirides, T.F., Brown, L.D., & Henderson, J.S. (2006). Estimation of Diffractor Morphology from Analysis of Amplitude and Travel Time Curvature at the Maya Archaeological Site of Los Naranjos, Honduras., Proceedings of the 11th International Conference on Ground Penetrating Radar: June 19-22, Columbus, Ohio, p. 1-8.

and reflectivity. Proper evaluation of the utility of these measures awaits calibration by excavation scheduled for the future.

Introduction

The integration of geophysical methods into traditional archaeological endeavors over the past few decades has been met with great success, especially when employed from the outset of the survey and used in direct association with archaeological excavations. In this way, results of the geophysical surveys can be used to target specific areas to excavate, and the archaeological data can be used for calibration by establishing stratigraphic control and identification of likely artifacts. Ground-penetrating radar and magnetometry are two of the most widely used geophysical methods in archaeology (Kvamme, 2003), and both were used in this study.

During the summer of 2003, GPR and magnetometry data were acquired at the early Maya site of Los Naranjos, Honduras, as part of an archaeological field school that was co-sponsored by the Department of Anthropology at Cornell University and the Department of Anthropology at the University of California, Berkeley. Professors Rosemary Joyce (Berkeley) and John Henderson (Cornell) supervised the excavations, and Professor Larry Brown (Cornell) and Kira Blaisdell-Sloan (Berkeley) directed the collection of the GPR and magnetometry data, respectively. This geophysical work was carried out in advance of archaeological excavations to obtain detailed three-dimensional coverage of the subsurface that could be used to target specific areas of the site to excavate.

GPR data from a grid located immediately north of one of the largest platform mounds at the site (Structure IV) is dominated by diffraction hyperbolae that are of particular archaeological interest. Due to time constraints during fieldwork, most of

these diffractions could not be directly identified. Excavations in that area, however, did unearth evidence of building debris that could explain at least some of the diffractions. Since it is unlikely that all diffractions will be identified in future excavations, one objective of this analysis was to tease out constraints on the morphology (size) of these objects from analysis of diffraction amplitudes and travel time curvature.

Study Site

Los Naranjos, Honduras (Figure 11) is situated on the current shoreline of Lake Yojoa in Central Honduras, within the present-day Parque Arqueológico – Ecológico Los Naranjos (Figure 12). The Instituto Hondureño de Antropología e Historia operates the site, which represents one of the earliest Maya settlements in Mesoamerica (Joyce and Henderson, 2002), with continuous occupation dating from the Early Formative to the Early Postclassic (1600 B.C. – A.D. 1200) (Joyce, 2004a). Numerous earthen platform mounds, which are the “largest pre-Columbian structures in Honduras” (Joyce, 2004c) comprise the site, some measuring up to 75 x 50 meters wide x 16 meters tall.

Many of the platform mounds are clustered into groups, the largest of which, the Principal Group, has been the focus of previous excavations. These excavations have uncovered elaborate burials, complete with jade ornaments and Olmec-style artifacts located *in situ* at depth (Baudez and Becquelin, 1973; Joyce and Henderson, 2002). The size and extent of the early platforms, the early evidence of ranking represented by the burials, and the presence of Olmec-style artifacts from the deepest levels drastically differ from most other early Maya sites. Some scholars have suggested the platform mounds and associated ditches served as fortifications against enemies (Webster, 1976), but their significance has not yet been determined. Los

Naranjos, therefore, offers an especially attractive opportunity to integrate geophysical methods with geological and archaeological studies to address key issues related to the emergence and evolution of social, economic, and political institutions that characterize Maya civilization.



Figure 11: Location of Los Naranjos, Honduras. Note the distance to Veracruz, Mexico in the “Olmec Heartland.”

In addition to the platform mounds, several basalt sculptures in Olmec style have been located dotting the landscape (Stone, 1934) (Figure 13). The original locations of these sculptures remain uncertain, but several were found in the vicinity of the Principal Group. Very little research has been undertaken on these figures, but since they are located in open spaces adjacent to platform mounds, they are likely

public monuments or displays. At the archaeological site of La Venta, Mexico, Olmec sculptures are located in the open areas between mounds and are likely images of political leaders placed in relation to the platform mounds (Grove, 1999; Stone, 1934). They may have served a similar function at Los Naranjos. Five figures have been located to date; three are anthropomorphic, one has features of “transformation,” combining representations of fleshed and skeletal states, and one is a hybrid, having features of serpents, jaguars, and sharks.

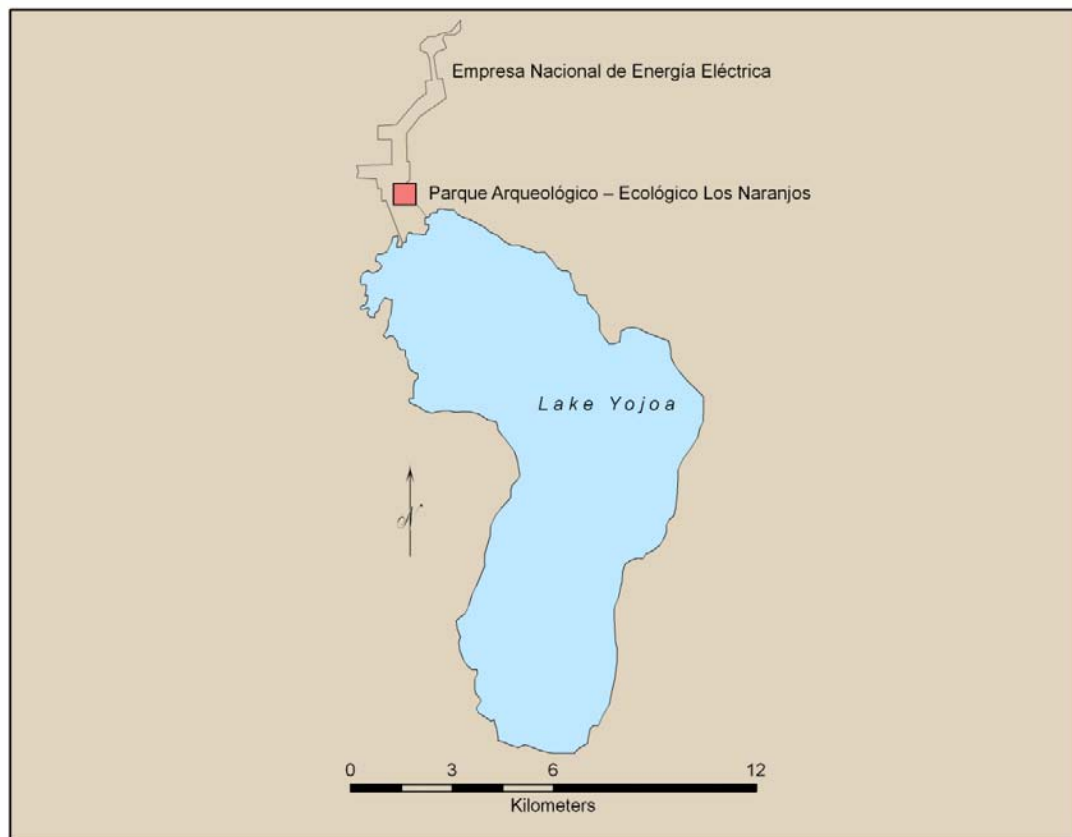


Figure 12: Location of Los Naranjos in relation to Lake Yojoa.

The Olmec culture had a substantial impact on most of the later Mesoamerican civilizations, but large-scale monumental construction and sculptures are concentrated in the “Olmec Heartland” on the Gulf Coast of Mexico, near Veracruz (Figure 11).

Los Naranjos and the nearby site of Puerto Escondido are the easternmost communities in which Olmec materials have been found, and the Olmec sculptures at Los Naranjos are also one of the largest clusters of Olmec sculpture outside of the Gulf Coast. Understanding Olmec occupation at Los Naranjos can potentially resolve the critical issue of the relationships among the Gulf Coast and the rest of Olmec Mesoamerica.



Figure 13: Cultural features of note at Los Naranjos. (a) Anthropomorphic Olmec-style statuary; (b) Plaza NW of Structure IV where additional statuary may be located.

Geophysical Data Collection

In addition to their pedagogic value, these surveys were also designed to test the effectiveness of these methods in delineating archaeologically significant features at the site. GPR data were collected with a Noggin 250 cart-mounted system (provided courtesy of GeoRad Surveys, Inc.), which is ideal for 3D surveys, and Cornell's pulseEKKO 100 bistatic system (50, 100 and 200 MHz antennae), which provided deeper penetration profiles, additional 3D coverage, and high-quality common mid-point (CMP) data for *in situ* radar velocity estimation, which are essential for accurate depth estimation (Figure 14). Magnetometry data were collected using a Geometrics G-858 magnetometer, which is owned by the University of California.

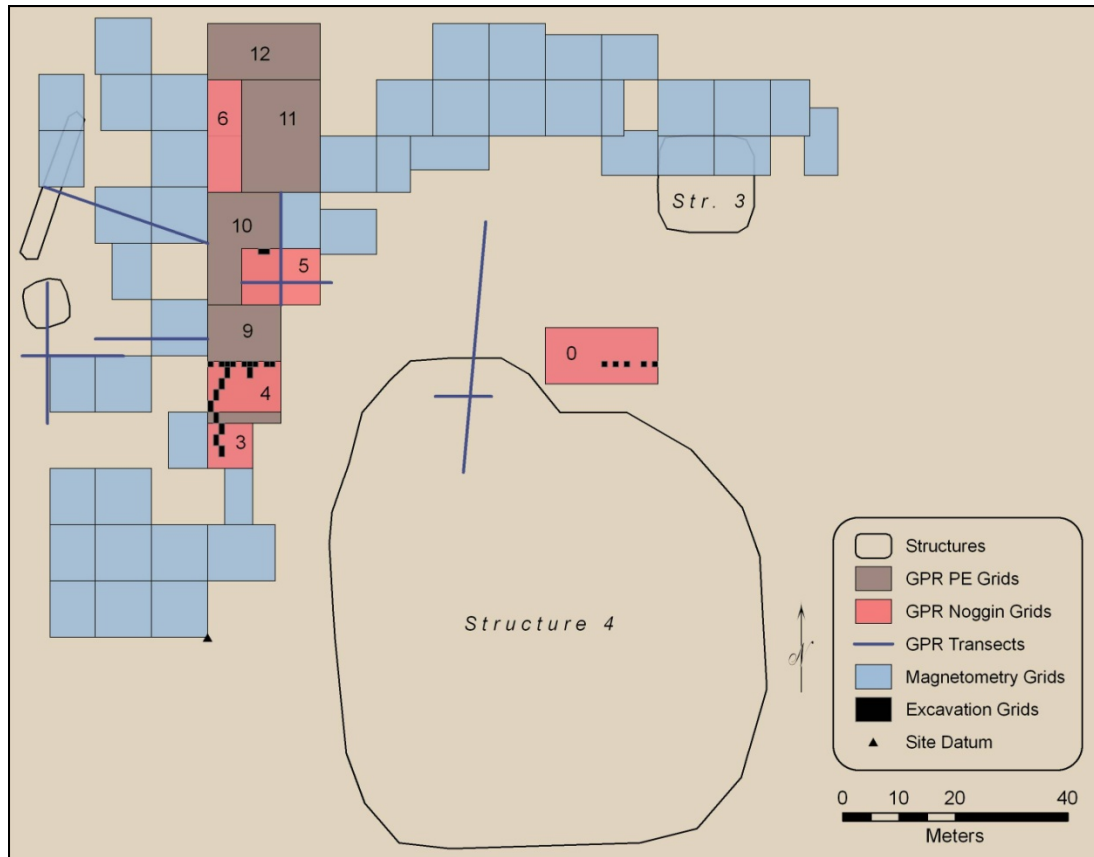


Figure 14: Location of all 2003 geophysical data in relation to Structure IV. (Left) GPR reflection profiling with the pulseEKKO 100; (Middle) GPR data collection with the Noggin 250; (Right) Magnetometry data collection with the Geometrics G-858. Numbers within grids refer to GPR grids.

In this study, GPR data were acquired in linear profiles and 2-dimensional grids, using both the pulseEKKO and Noggin systems. All archaeological test units (Op 1 – Op 4) were surveyed with GPR prior to excavation (Figure 14) so as to target specific areas to excavate and to correlate all archaeological features with stratigraphic

information in the GPR profiles. For grids collected with the pulseEKKO system (Grids 9, 10, 11, and 12), the transmitting and receiving antennae were spaced 1 meter apart, data were collected every 20 centimeters along a transect, and individual transects within each grid were spaced 50 centimeters apart. Transects were also spaced 50 centimeters apart within each Noggin grid (Grids 0, 2, 3, 4, 5, and 6). All GPR data were processed using the Sensors and Software suite of processing programs at Cornell.

These surveys covered both apparent archeological and natural features, and GPR proved especially effective in both delineating Quaternary stratigraphy and mapping localized buried features at numerous locations throughout the site (Tchakirides *et al.*, 2006b). One of the most interesting grids of data, Grid 0, located immediately to the north of Structure IV, one of the largest platform mounds at the site (Figure 15), is the focus of this paper.



Figure 15: Stone-lined ramp on west side of Structure IV. GPR Grid 0 is located to the north of this platform mound.

Grid 0

Grid 0 measures 20 x 10 meters. Surveys within this grid were undertaken to determine the possible use of space between Structures IV and III (Figure 14) and to learn as much as possible about the construction and use of Structure IV, without actually excavating within it. Platform mounds are rarely excavated because of their complex construction history and resulting stratigraphy, but much can be learned about them by studying the sediments that surround them.

Grid 0 was surveyed with the Noggin 250 and the magnetometer, with subsequent archaeological excavation to depths of about 0.5 m. GPR penetrated to a depth of about 2 meters at 250 MHz. Data from Grid 0 are dominated by a domed bright spot located at about the 77.5 meter mark along the x-axis (Figure 16). At first, this high amplitude anomaly appeared to be a large buried mound, either artificial or natural. Careful inspection, however, suggests that it is part of a continuous stratigraphic sequence that is simply less reflective away from the dome. The origin of the high amplitudes remains to be determined, and this structure is a prime candidate for excavation or coring in a future field season.

The most interesting features of the rest of the grid are the numerous diffractions. One in particular, a high-amplitude anomaly located at about 67.5 meters along the x-axis (Figure 16), stands out. In map view, this reflection is strongest in the depth slice from 1.2 – 1.3 meters. The prominence of this feature has made it a prime suspect for a piece of buried sculpture, possibly Olmec in nature. However, this speculation does not resolve the identity of all of the diffractions. It is hoped that at least some of these will be unearthed during future field excavations, but even if excavations are eventually implemented, it is not clear that one can uncover all of the diffraction sources within all of the GPR grids. We have, therefore, explored methods

that might help provide useful constraints on the nature of these objects from the GPR data alone, or in combination with the magnetometry data.

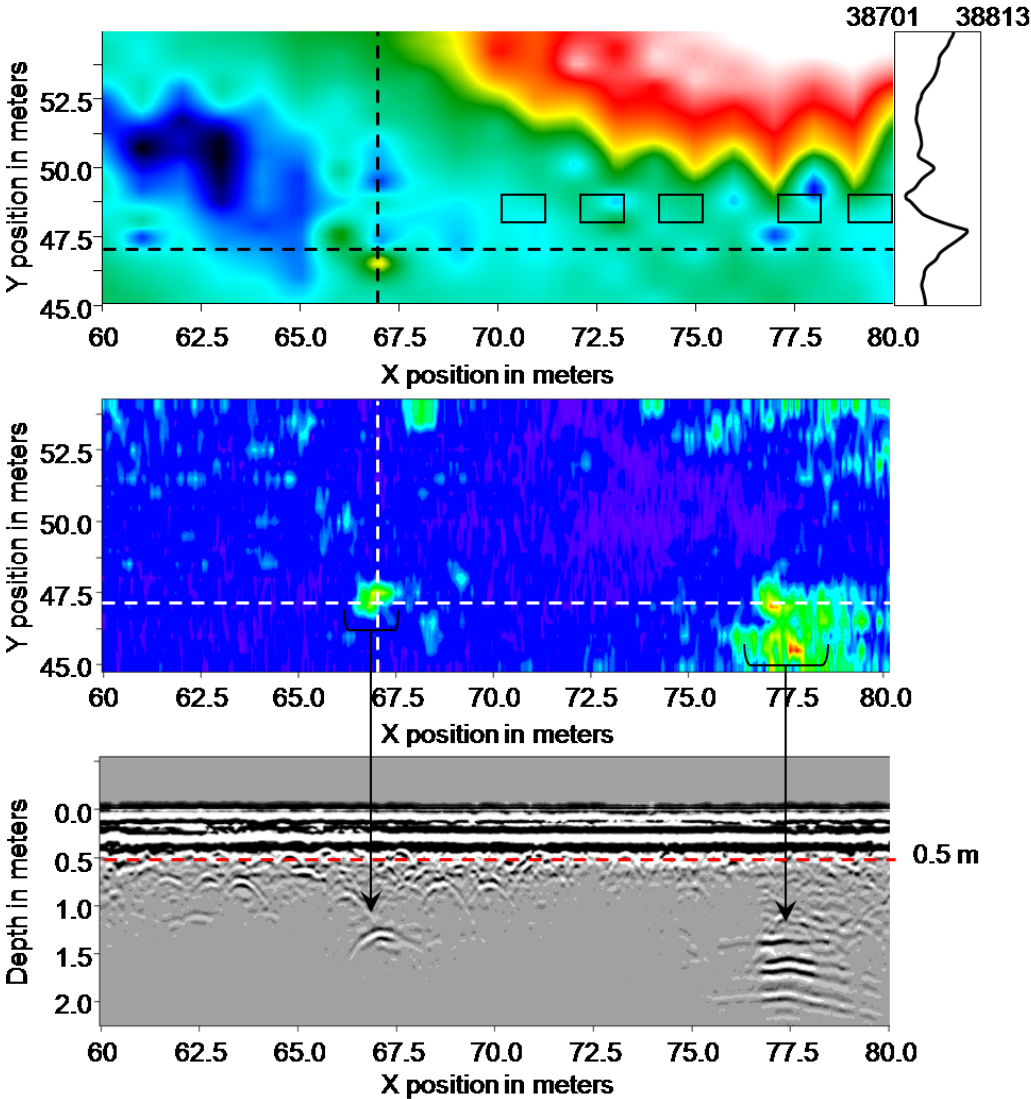


Figure 16: Comparison of GPR and magnetometry data from Grid 0. (Top) Magnetometry results over Grid 0. On the right are the magnetometry data along the NS profile indicated by the dashed line. Numbers at the top of the profile are in units of nanoTesla. Op 1 test units are noted. (Middle) Horizontal depth slice of GPR data from Grid 0, representing a depth of 1.2 to 1.3 meters. (Bottom) GPR section through Grid 0 along the EW dashed line, showing numerous diffractions that might be of archaeological significance. Also noted are the reflections corresponding to the amplitude anomalies (bright spots) in the horizontal slice map. Archaeological excavations within this grid went to a depth of about 0.5 meters, as denoted by the dashed line.

Grid 0 exhibits more than 400 diffraction hyperbolae, with apices ranging from 10 to 70 nanoseconds (about 0.3 to 1.2 meters) (Figure 17 and Figure 18). The sources of these hyperbolae are unclear at the present time, but several possibilities come to mind. Some, or perhaps many, are likely due to naturally accumulated rocks or building detritus from the construction or subsequent alteration of Structure IV. Archaeological excavations within this grid (Op 1) encountered evidence of construction activity, including packed surfaces and building debris (numerous stones and fragments of wattle and daub). However, given the Olmec-style sculptures that have been previously found at Los Naranjos, it is certainly plausible that some of these hyperbolic reflections may mark such statuary, or fragments thereof, still in the ground. If this area were used as a public space, monumental sculptures might likely have been displayed.

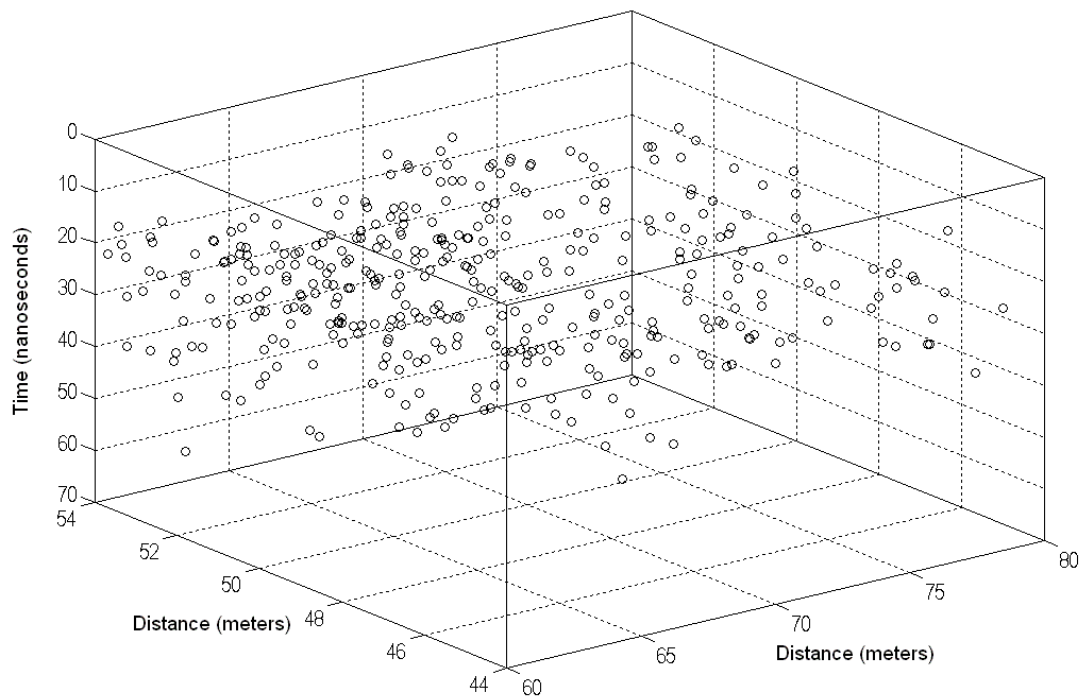


Figure 17: 3D view of the locations of all the 413 diffractions visually identified in Grid 0.

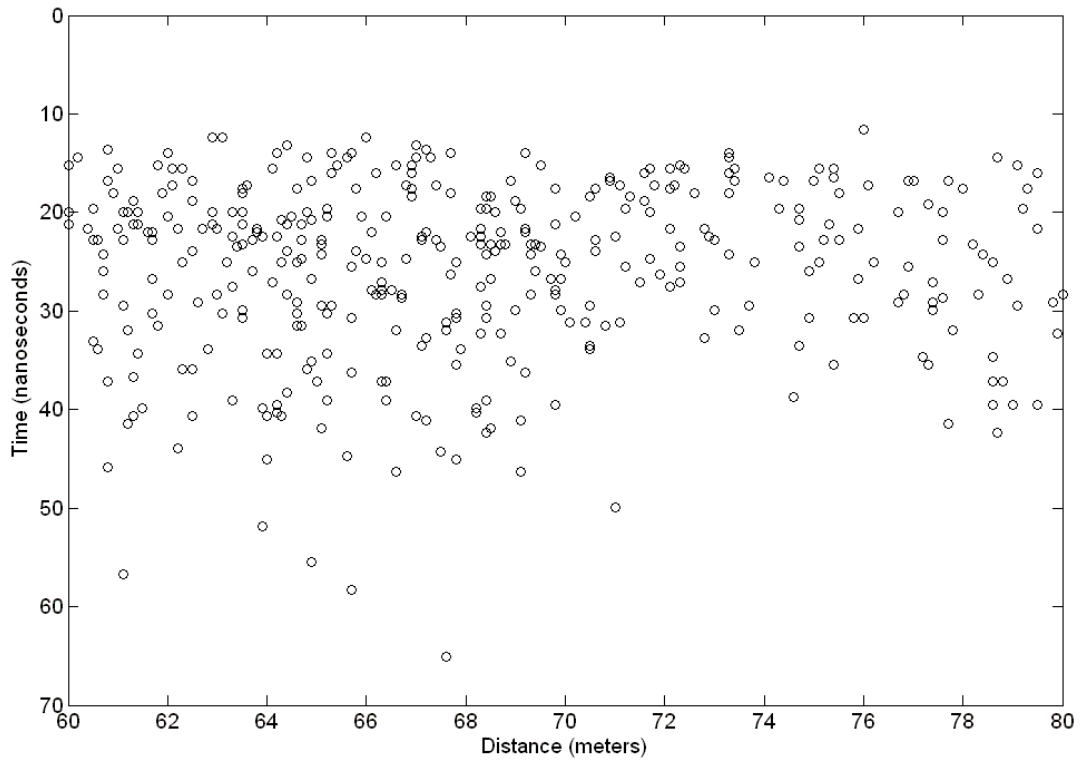


Figure 18: Vertical time slice showing the depths (in time) of the 413 diffractions in Grid 0.

Methodology

The obvious approach to focusing on the source of these diffractions would be 3D migration. It is not clear, however, that migration would be very effective in dealing with diffractions smaller than the usual Fresnel limits. Moreover, migration artifacts might well obscure some of the information containing the diffraction patterns. Here we attempt to exploit the expectation that both peak amplitude and travel time curvature of small body diffractions are expected to be dependent upon the body's morphology, specifically its size. Our analysis began with manual picking of diffraction curves within the grid along each survey line, recording the peak amplitudes for each diffraction, and then velocity estimation using the diffraction

travel times by assuming point sources. We then evaluated the systematics of the variations in amplitude and velocity for evidence of dependence on diffractor size.

Diffraction Picking

Diffraction picking was accomplished by visual inspection of all of the unmigrated vertical time slices from Grid 0. To identify a manageable subset for subsequent analysis, the locations of all were plotted in various spatial views (e.g. Figure 19). Obviously events tagged on adjacent lines are likely from the same 3D source. Given this expectation, inspection of Figure 19 reveals no immediately significant spatial clustering. Thus, the following analysis targeted eleven diffractions that seemed to be relatively well-defined and spatially diverse.

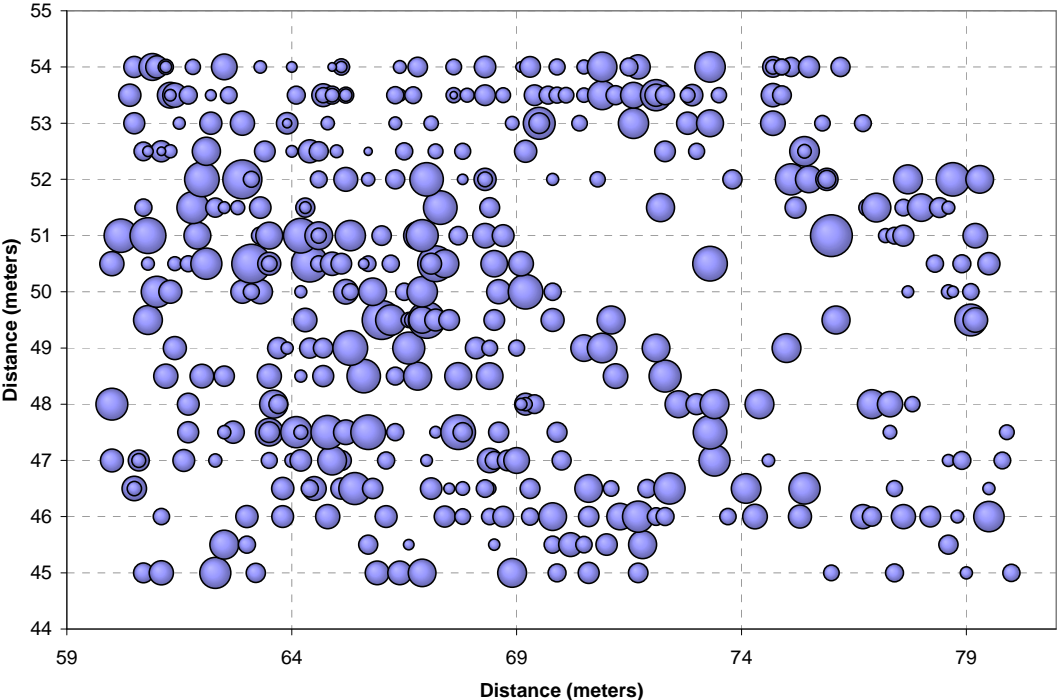


Figure 19: Map view of the 413 diffractions in Grid 0. Circle sizes are inversely scaled according to depth, with the larger circles representing diffractions at the shallowest depths.

Once these diffractions were selected, the apex and at least four additional points were digitized on each. Care was taken to select points across substantial aperture, so that a reasonably accurate representation of the diffraction shape (and resulting velocity) could be obtained.

Velocity Analysis

Two types of velocity analyses were performed on the GPR data from Los Naranjos. First, common mid-point (CMP) data that were collected with the pulseEKKO system were analyzed using the T^2-X^2 method (Reynolds, 1997). An average velocity of about 0.060 m/ns was characteristic of all of the CMPs. Similar velocity analyses were then performed on each of the 11 diffractions selected from Grid 0. The results obtained from these analyses were comparable, ranging from about 0.059 to 0.070 m/ns. The goal of this study was to determine if the variations in these estimates might be linked to diffractor size.

Figure 20 shows the variation in apparent velocity expected from T^2-X^2 analysis of diffractions from a source with apex at 1 m depth with varying radii of curvature. Here we have assumed a true ground velocity of 0.060 meters/nanosecond.

Amplitude Analysis

It is well-known that the amplitude of a reflection from a curved interface is dependent upon the curvature of the interface relative to curvature of the illuminating wavefront. Assuming the optical model applies in this case, we can compute the expected amplitude variations due to reflector (diffractor) curvature using the “brighten up” ratio:

$$\frac{A}{A_0} = \frac{1}{\left(1 - \frac{z}{R}\right)} \quad (1)$$

where A is the amplitude of reflection from the curved interface, z is the depth to the crest of the interface, and R is the radius of curvature of the interface (upwardly concave features having a negative radius of curvature). Figure 21 shows the expected variation in amplitude for a diffractor of variable radius, relative to a reference diffractor at 1 meter with a radius of 0.10 meter. Relatively significant variations in apparent velocity can be expected by reasonable variations in diffractor size.

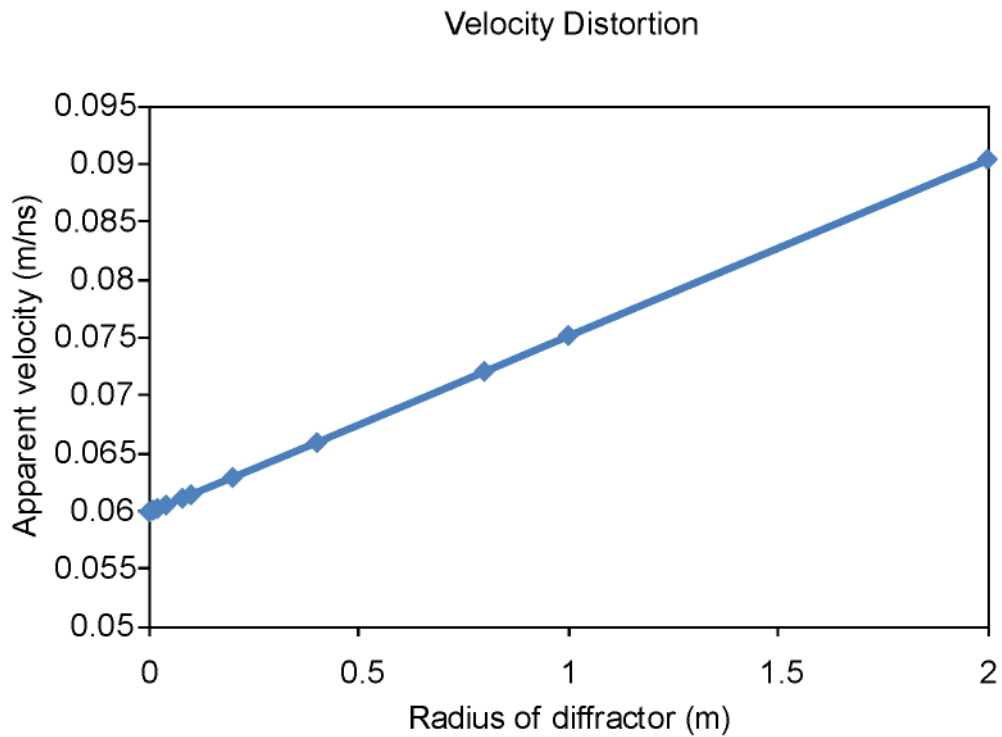


Figure 20: Variation in apparent velocity due to changing radius of curvature of a source diffractor.

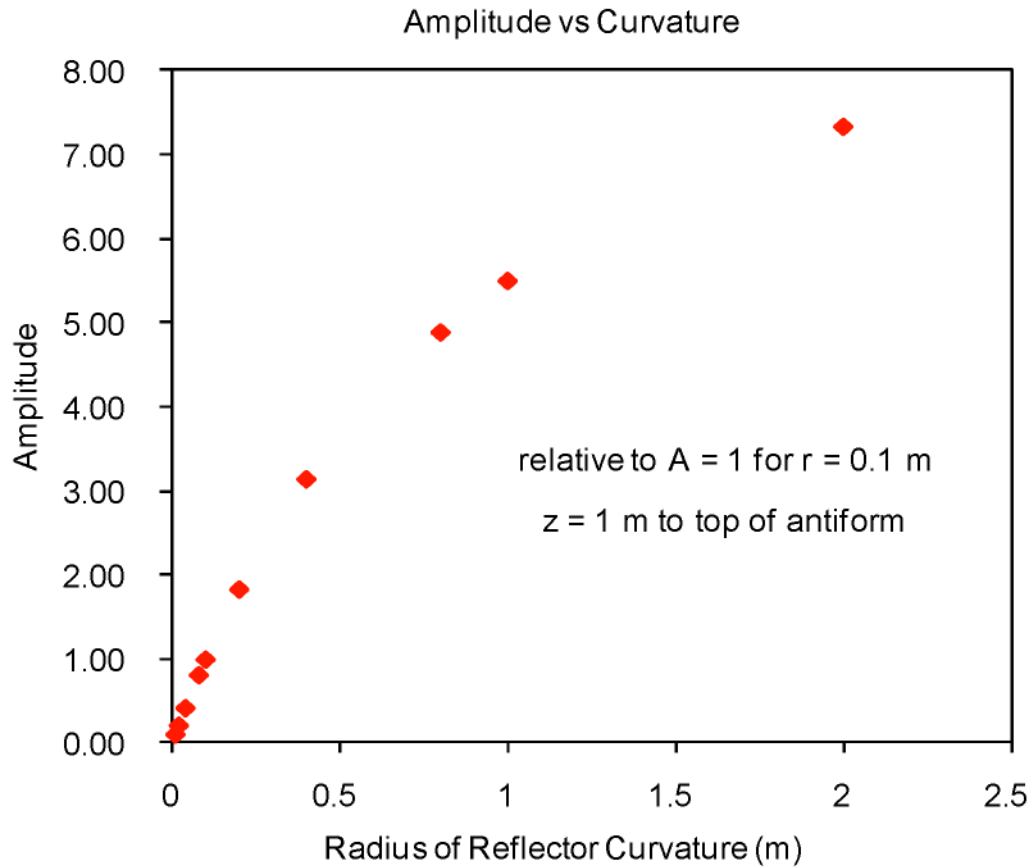


Figure 21: Variation in apparent amplitude of a diffractor with apex at 1 meter due to changes in diffractor curvature.

In Figure 22, we plot the theoretical relationship expected between apparent velocity and apparent peak amplitude if the diffractor size were the only relevant variable (e.g. all sources and intervening media were of constant lithology). The observed peak amplitudes for each of the 11 diffractions are shown in Figure 23. While the apparent velocities span a range comparable to that depicted in Figure 22, the amplitudes cover a much larger range, and there appears to be no distinguishable trend to the observed relationship that evokes that of Figure 22.

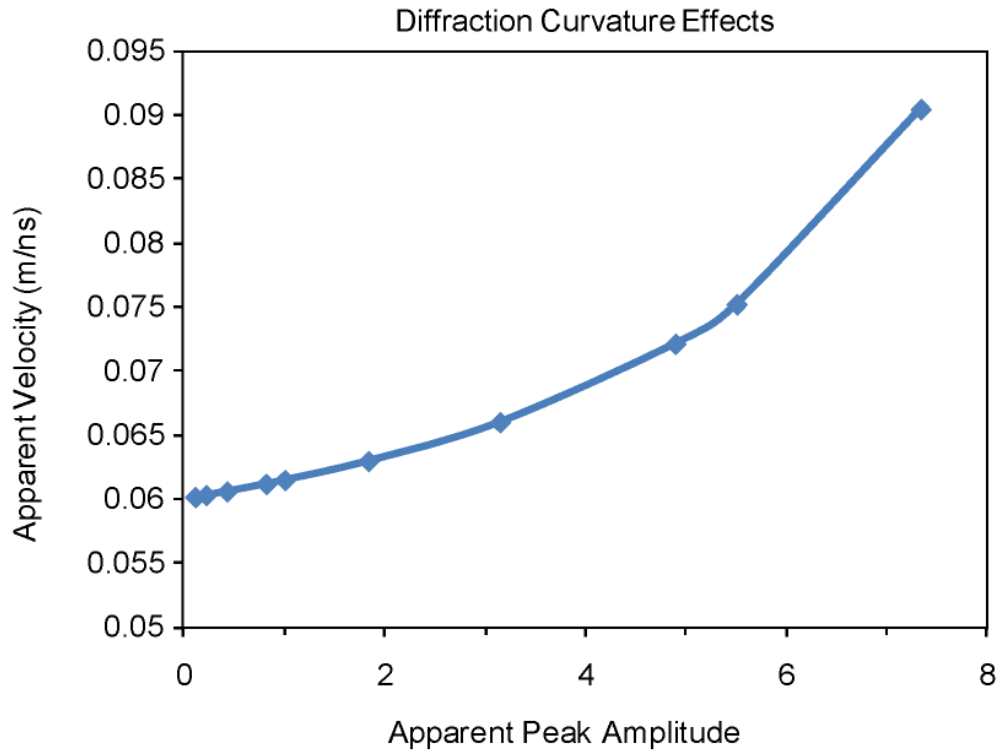


Figure 22: Theoretical relationship between apparent amplitude and velocity for diffractors of constant compositional contrast but with different radii.

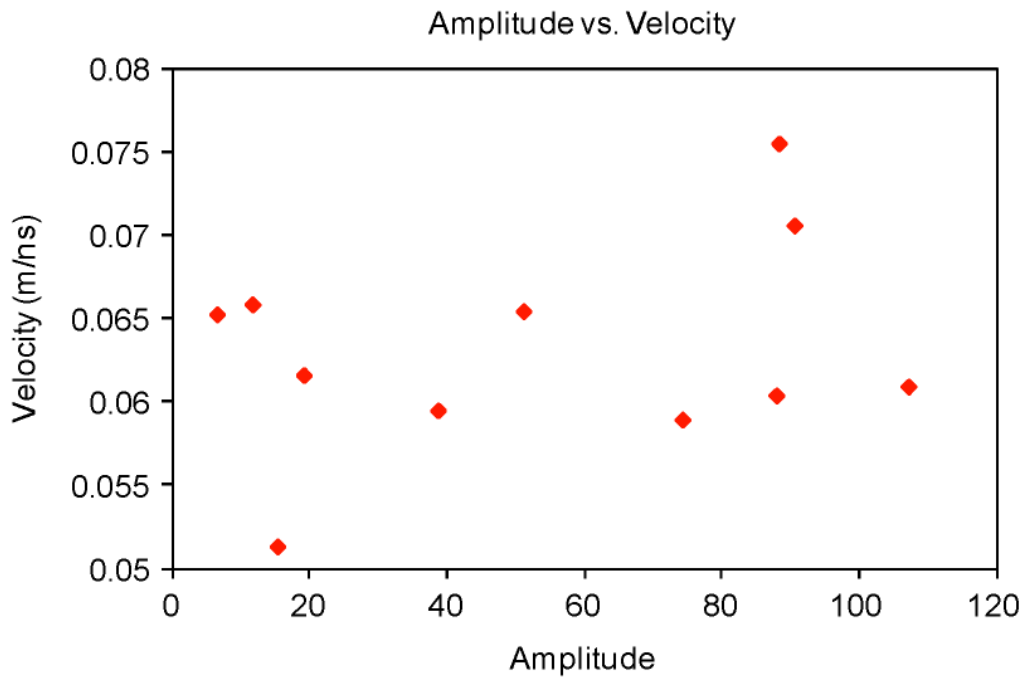


Figure 23: Amplitude versus velocity for the 11 diffractions selected from Grid 0. Spherical divergence correction normalized for reference at 25 nanoseconds.

Conclusions

Using GPR profiles to deduce details of buried targets that are small relative to the wavelengths of illumination is a particular challenge. Improved extraction of constraints on diffractor geometries and materials from GPR backscatter from such small objects is particularly relevant to archaeology. Here we have examined diffraction amplitudes and velocities from particularly well-defined datasets to evaluate whether careful analysis can provide such constraints. The results indicated the amplitudes are too variable to be explained by geometry alone. A complete test of this methodology at this site awaits excavations planned for the future, but the results of this study will help guide those excavations.

Acknowledgments

The authors would like to express their appreciation to Juan Alberto Durón and his colleagues at the Instituto Hondureño de Antropología e Historia for their support during the collection of these data. Most of the data were collected by students participating in the 2003 Cornell-Berkeley archaeological field program; their effort and enthusiasm was critical to our success. Special thanks to Kira Blaisdell-Sloan for directing the collection of the magnetometry data and to GeoRad, Inc., and its President, Mr. William Perks, for providing the Noggin for use. Mr. Perks also contributed generously of his time and expertise during the field work. Joel Haenlein directed the collection of much of the Noggin data.

REFERENCES

- Baudez, C.F. and Becquelin, P. (1973). *Archéologie de Los Naranjos*. Mission Archéologique et Ethnologique Française au Mexique, Mexico.
- Grove, D.C. (1999). Public Monuments and Sacred Mountains: Observations on Three Formative Period Social Landscapes. In: D.C. Grove and R.A. Joyce (Editors), *Social Patterns in Pre-Classic Mesoamerica*. Dumbarton Oaks, Washington, DC, pp. 255-300.
- Joyce, R.A. (2004a). Mesoamerica: A Working Model for Archaeology. In: J.A. Hendon and R.A. Joyce (Editors), *Mesoamerican Archaeology: Theory and Practice*. Blackwell Studies in Global Archaeology. Blackwell, Malden, MA, pp. 1-42.
- Joyce, R.A. (2004b). Unprecedented Projects: The Birth of Mesoamerican Pyramids. *Expedition*, 46(2): 7-11.
- Joyce, R.A. and Henderson, J.S. (2002). La arqueología del periodo Formativo en Honduras: nuevos datos sobre el «estilo olmeca» en la zona maya. *Mayab*, 15: 5-17.
- Kvamme, K.L. (2003). Geophysical surveys as landscape archaeology. *American Antiquity*, 68(3): 435-457.

Reynolds, J.M. (1997). *An Introduction to Applied and Environmental Geophysics*.
John Wiley & Sons, Chichester.

Stone, D.Z. (1934). A new southernmost Maya city (Los Naranjos on Lake Yojoa,
Honduras). *Maya Research*, 1(2): 125-128.

Tchakirides, T.F., Brown, L.D., Henderson, J.S. and Blaisdell-Sloan, K. (2006).
Integration, Correlation, and Interpretation of Geophysical Data at Los
Naranjos, Honduras, In *Proceedings of the Symposium on the Application of
Geophysics to Engineering and Environmental Problems: April 2-6, 2006*,
Seattle, WA, p. 1400-1429.

Webster, D. (1976). Lowland Maya Fortifications. *Proceedings of the American
Philosophical Society*, 120(5): 361-371.

CHAPTER 3
EFFECT OF REFLECTION PICKING CRITERIA ON *IN SITU* VELOCITY
ESTIMATES FROM GROUND-PENETRATING RADAR
COMMON MIDPOINT DATA

Abstract

Common midpoint (CMP) data obtained using ground-penetrating radar provide *in situ* velocity estimates that can be used to discriminate lithology as well as convert images from time into depth domain. Initial analyses of CMP data from the archaeological site of Los Naranjos, Honduras produced inconsistent velocity estimates when calculated using different curve fitting procedures (visual best-fit line versus formal regression analyses). More quantitative analyses were carried out to evaluate the effect of reflection picking criteria as applied to the direct air and ground waves and reflections. Factors considered include waveform pick-points, offset range, image display mode (i.e. raster versus wiggle trace), amplitude, and curve fitting procedure. Variation in average velocity estimates derived from different picking criteria were as large as 50 %, though most clustered within 10 – 20 %. These variations correspond to uncertainties in depth estimates in this case of as much as 35 centimeters. These variations are more pronounced when converted to interval velocities, which were found to range from -64 to +87 % of their mean value. These results indicate that a consistent picking criteria should be applied before velocities are used to identify either lithology or depth variations within a given survey grid. Best practice should focus on picking first-break points along individual traces in wiggle trace image display using linear regression analyses of picks from multiple traces, as these analyses produced the most consistent velocity estimates.

Introduction

Conventional ground-penetrating radar (GPR) profiles and common midpoint (CMP) recordings were acquired at the site of Los Naranjos, Honduras as part of an archaeological and geophysical field program aimed at understanding how Formative Period communities developed in relation to large earthen platform mound constructions. Los Naranjos, located on the northwestern shore of Lake Yojoa in central Honduras (Figure 24), is one of the earliest archaeological sites in Mesoamerica, with occupation beginning around 1100 B.C. (Baudez and Becquelin, 1973; Joyce, 2004b; Joyce, 2004c; Joyce and Henderson, 2002). A portion of the site is preserved by the Instituto Hondureño de Antropología e Historia (IHAH) as the Parque Arqueológico – Ecológico Los Naranjos. The Principal Group, partially located within this property, includes several of the largest earthen platform mounds as well as several low flat mounds, terraces, and open plaza areas. Almost all research undertaken at Los Naranjos has occurred within the Principal Group.

Six CMP profiles were included as part of the geophysical data collection at Los Naranjos to provide estimates of *in situ* GPR velocities. The CMP technique is a commonly used method for estimating subsurface velocities from both seismic and GPR data (Bristow and Jol, 2003; Sheriff and Geldart, 1995), and the estimates extracted are generally considered to be robust (Jol and Bristow, 2003). Any variation caused by display mode or limitations in screen resolution was thought to vary by 1 to 2 % at most (Annan and Davis, 1976). While conducting initial analyses of the CMP profiles from Los Naranjos, we noticed that velocities varied much more than 1 to 2 % depending on the particulars of the technique used to estimate velocity. For example, for CMP PRO 27 we obtained a ground wave velocity of 0.060 m/ns when visually fitting a line between 2 points, but we obtained an estimate of 0.055 m/ns with linear regression analyses using points picked from all the traces, a difference of 8.3 %. This

led us to perform a systematic study of several common picking strategies, display modes, and analytic techniques to evaluate the impact of these various “picking” criteria on the resulting velocity estimates.



Figure 24: Location of the archaeological site of Los Naranjos on the northwestern shore of Lake Yojoa, within the present-day Department of Cortés, Honduras.

We found that such routine variations in velocity estimates translate into significant uncertainties in both interval velocity and depth estimates. Jol and Bristow (2003) suggested that depths estimated from CMP velocity analyses are generally accurate to within 10-20 centimeters, whereas Annan and Davis (1976) thought it more likely that errors of about 1.5 meters resulted from CMP velocity analyses. Although these estimates may be adequate, and even tolerable, for sedimentological surveys that tend to extend 5 to 20 meters in total depth, they are much too coarse for archaeological studies where excavations may only extend to a meter or less. Careful and systematic analyses are needed to constrain these errors as best as possible.

Velocity

The two most common types of GPR data collection geometries are the common offset method and the common midpoint (CMP) method (Figure 25). In both of these survey modes, a radio signal is sent from the transmitting antenna (Tx) into the ground, where it reflects off buried discontinuities and is recorded back at the ground surface in the receiving antenna (Rx) (Daniels, 2004; Neal, 2004; Reynolds, 1997). For a given source-receiver offset, the direct airwave arrives at the receiving antenna first (Figure 26), as it travels through air at the speed approaching that of light in a vacuum, i.e. 3×10^8 m/s (Kearey *et al.*, 2002). The direct ground wave usually arrives next. This wave travels just below the ground surface from the transmitting to the receiving antenna and is significantly slower than the direct airwave. Reflections generated by subsurface discontinuities normally arrive after both the direct air and ground waves. All waves travel in the shortest path according to Fermat's principle of least time (Schuster, 1909; Sheriff and Geldart, 1995, p. 157).

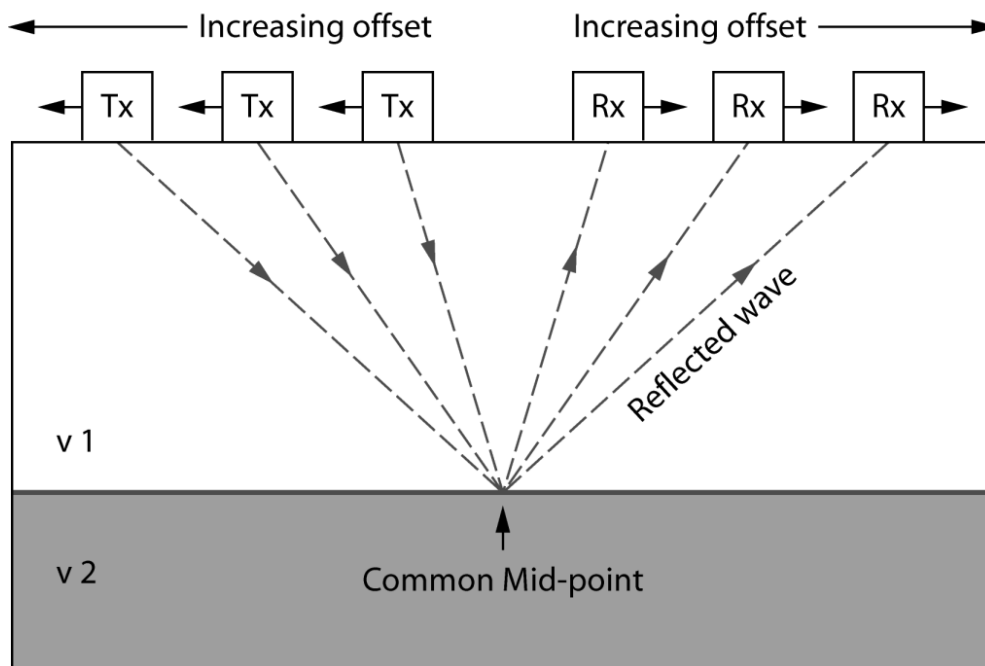
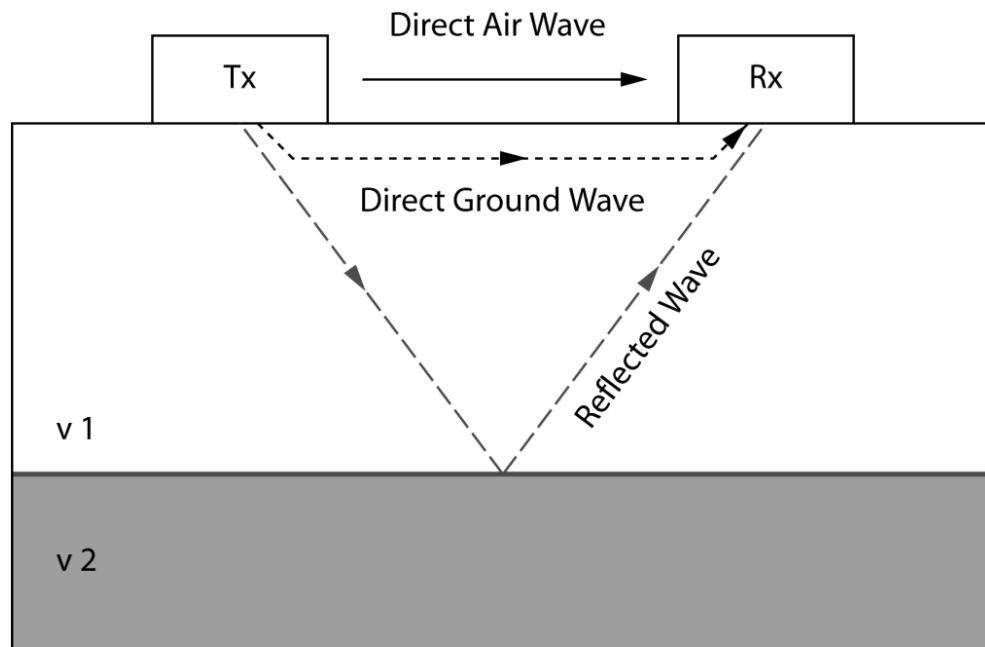


Figure 25: GPR data collection strategies. Top: Common offset method, showing the travel paths of the direct air and ground waves and the reflected wave generated by the surface of Layer 1 and Layer 2. $v_1 > v_2$. Bottom: Common midpoint (CMP) method, described in this study.

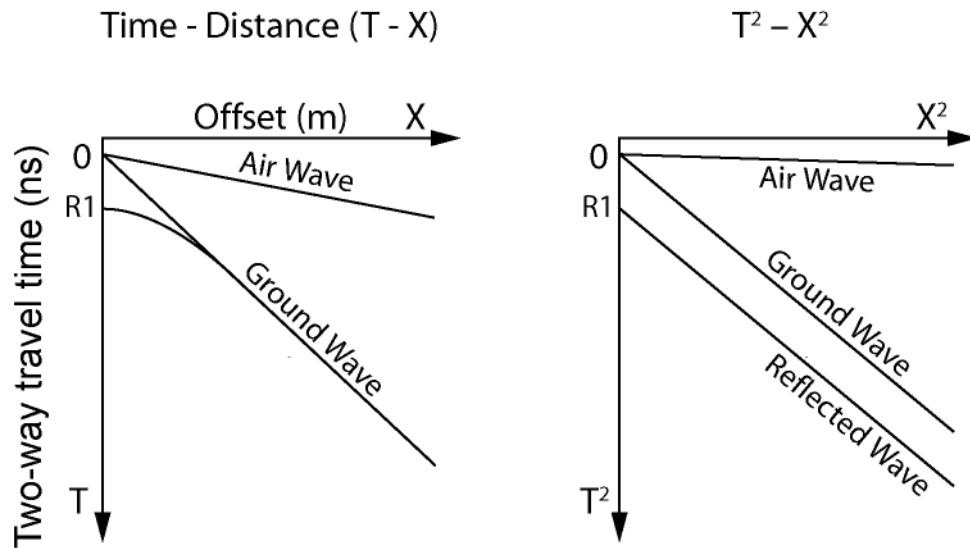


Figure 26: Common mid-point schematic. Left: Time-distance (T - X) plot, used to calculate velocities for the direct air and ground waves. Right: T^2 - X^2 plot, which is used to calculate reflection velocities.

In the CMP method, the transmitting and receiving antennae are moved apart from a fixed point (midpoint) at a set interval (Figure 25). For constant velocity media, the travel time for both the air and direct ground arrivals is a linear function of source-receiver offset, whereas reflected arrivals are hyperbolic functions of offset (Annan and Davis, 1976; Reynolds, 1997). Velocities for the direct arrivals are usually estimated from the travel time versus offset plots (Figure 26) by measuring the reciprocal of the resulting slope. Average velocity from the surface to a reflecting interface can be obtained either by fitting hyperbolic functions using trial velocities or plotting the square of the travel time versus the square of the offset (Figure 26), in which case the velocity is represented by the square root of the reciprocal of the slope (Reynolds, 1997).

Time to Depth Conversions

CMP profiles are useful for several reasons, but most importantly for providing *in situ* velocity estimates (Baker *et al.*, 2007) needed to convert observed travel times to depth (Reynolds, 1997). Reflection depths can be derived from velocity (v) and two-way travel time (t) via the relationship:

$$d = v_r \times \frac{t}{2} \quad (2)$$

The most appropriate velocity to use for such conversion is the reflection velocity, though the direct ground wave velocity is often an adequate proxy (Annan and Davis, 1976; Jol and Bristow, 2003) because the velocity of the first reflection represents the average velocity between the ground surface and the top of the first reflecting surface. Since the direct ground wave is generated within this same region, the direct ground wave velocity is usually very similar to the velocity of the first reflection.

Lithologic Discrimination

Common midpoint profiles also provide information regarding the dielectric properties of subsurface materials (Clough, 1976) because velocity is related to the dielectric constant (relative dielectric permittivity) of a material by the following equation:

$$v_r = \frac{c}{\sqrt{\mu_r \epsilon_r}} \quad (3)$$

where μ is the relative magnetic permittivity of the material (essentially 1 for all non-magnetic rocks), ϵ is relative dielectric constant of the material, and c is the speed of light in a vacuum (Daniels, 2004; Kearey *et al.*, 2002; Neal, 2004). Because of this relationship, CMP profiles can help constrain the types of subsurface materials through which radar waves are passing. Relative dielectric constants (ϵ_r) range between 1 in a vacuum or dry air and 81 in water (Annan, 2005; Reynolds, 1997) and

is frequency dependent above 100 MHz (Franks, 1972 p. 260). The dielectric constant for water represents the extreme value because water can be polarized more easily than any other material (Annan, 2005; Greaves *et al.*, 1996). Velocities in geological materials can range from 0.010 to 0.195 m/ns (Annan, 2005). Direct ground wave velocities identify the shallowest materials, whereas velocities of individual reflections identify the material between specific subsurface reflectors. Interval velocities, calculated from the Dix equation (Dix, 1952),

$$v_{\text{int}} = \left[\frac{(V_{RMS.n})^2 t_n - (V_{RMS.n-1})^2 t_{n-1}}{t_n - t_{n-1}} \right]^{\frac{1}{2}} \quad (4)$$

provide velocity estimates for the material between two defining reflectors. The root-mean-square (RMS) velocity (Al-Chalabi, 1974; Sheriff, 1976) is usually taken to be equivalent to the stacking velocity, which in turn is assumed to be equivalent to the velocity that best fits an hyperbola to the observed reflection travel times. These assumed equivalences are most valid in the limit as the source-receiver offset goes to zero (Al-Chalabi, 1974). Of course, appropriate corrections must be applied for dip (Sheriff, 1976), and the relationships break down for media with velocities that have rapid lateral variability (Al-Chalabi, 1974) (e.g. depth migration issues). While there is substantial overlap in the dielectric constant for various materials, such estimates clearly limit the permissible interpretation of subsurface GPR results.

Discrimination of Clutter from Reflections

Velocities obtained from CMP analyses are also useful to discriminate clutter from true subsurface reflections (Jol and Bristow, 2003). Clutter, or “airwave events” (Annan, 2005 p. 427), is systematic noise introduced into a radar section by reflections from objects that are located on the sides of or above the antennae, most often above

ground. These events can masquerade as reflections generated from subsurface features or layers (Daniels, 2004; Jol and Bristow, 2003). Clutter from above-ground sources can be identified in CMP profiles by its characteristic velocity, which will be that of the direct airwave velocity. This velocity is most often significantly faster than any velocity associated with a true subsurface reflection.

The most common source of clutter in GPR data from Los Naranjos is associated with the low tree canopy that covers much of the site. For example, in CMP PRO27, clutter is visible as nearly horizontal banding between the direct air and ground waves, at larger offsets (Figure 27). Clutter is often more obvious in CMP data, where it is usually manifest as hyperbolae that are asymptotic to the airwave. Without CMP control, clutter can easily go unrecognized in reflection sections and thus be misinterpreted as subsurface reflectivity.

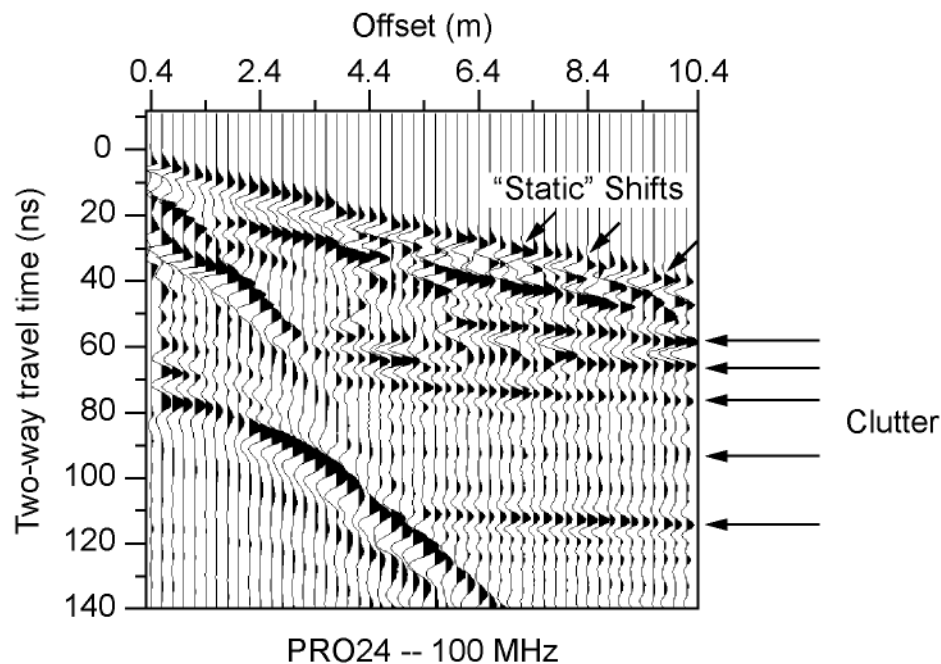


Figure 27: CMP PRO 24 illustrating clutter and static shifts. Clutter is evident as pronounced sub-horizontal banding that is asymptotic to the direct airwave. Small time shifts between traces, “statics,” also contribute to errors in velocity estimates.

In addition to clutter, CMP profiles also display small variations of travel time away from a straight line or hyperbola. Such time variations are usually referred to as “static” shifts in seismic processing (Sheriff and Geldart, 1995; Yilmaz, 2001). Such static shifts are evident in Figure 27. To lessen the adverse effects of such static shifts, great care was taken to avoid picking endpoints for best-fit lines on specific traces that seemed especially noisy. With linear regression analyses, whereby points along all traces were selected, the effect of static shifts is more pronounced on velocity estimates (see Figure 27 for examples of static shifts; see Figure 29 for their effect on velocity estimates).

Quantifying Attenuation

Common midpoint profiles can also be useful to recognize signal attenuation in the subsurface. For example, in the CMP profile LINE16, no reflections are visible (Figure 28), which could be interpreted to simply indicate uniform material in the subsurface. However, the relatively rapid truncation of the direct ground wave (at about 75 centimeters offset; 50 centimeters offset for profile PRO12) instead indicates high attenuation of the GPR signal at a very shallow depth. Thus the data cannot be used either to confirm or deny the presence of layering at depth. Signal attenuation has important implications for survey design (Jol and Bristow, 2003) in that it can help in selecting an adequate antennae separation and source frequency to mitigate attenuation. Furthermore, large time windows are not necessary in areas of high signal attenuation.

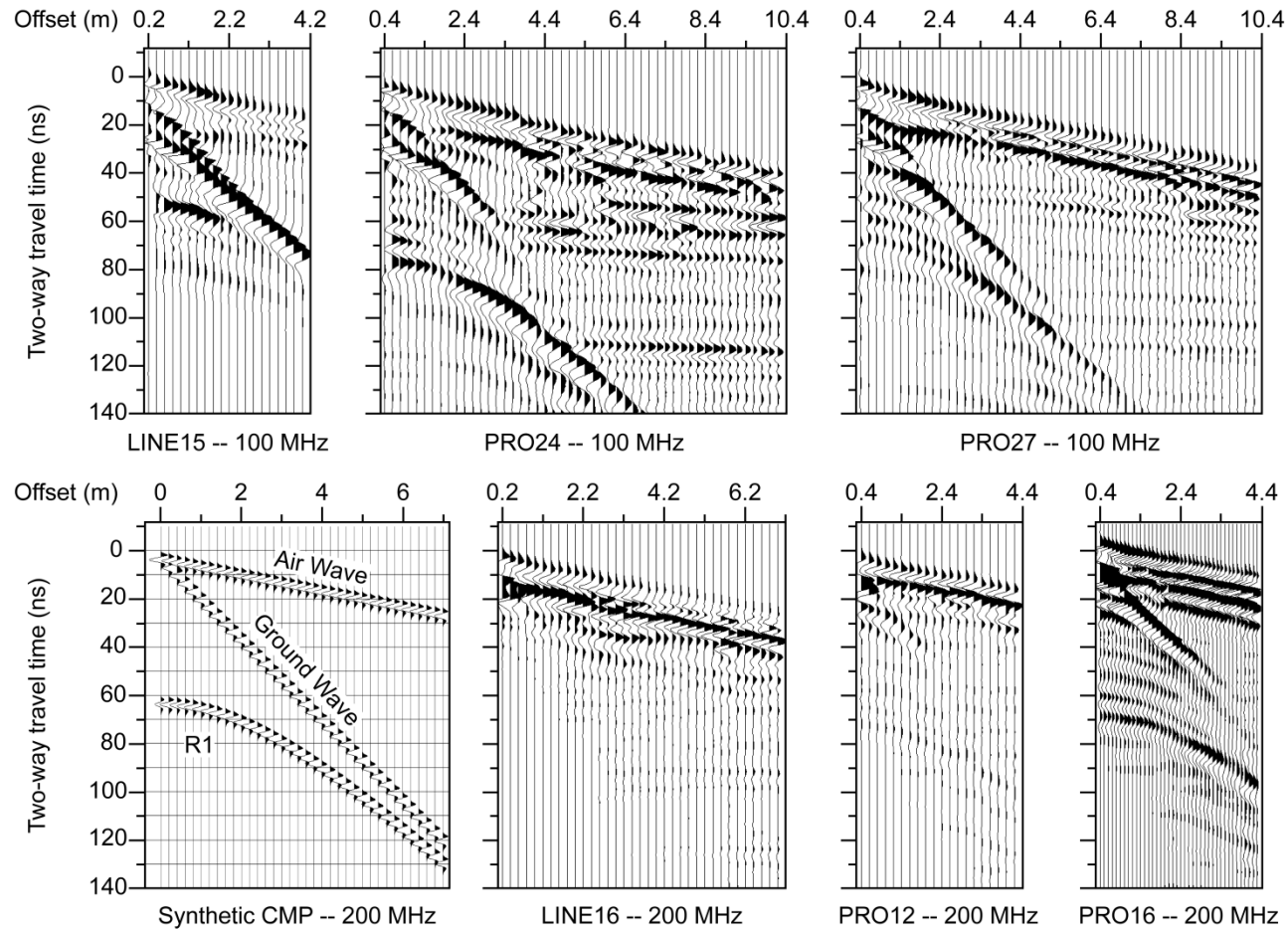


Figure 28: Wiggle trace images of the six CMP profiles collected at Los Naranjos. A synthetic CMP is shown in the bottom left, with direct air and ground waves, and one reflection. Vertical exaggeration = 2x.

Velocity Estimation from CMP Surveys

In this study, six common midpoint profiles (Annan and Davis, 1976; Greaves *et al.*, 1996) were acquired using a Sensors and Software PulseEKKO 100 system (Figure 28). Three CMP profiles were collected using the 100 MHz antennae, and three were collected using the 200 MHz antennae. All six show distinct direct airwaves. Clear reflection hyperbolae are visible on all profiles except CMP LINE16 (see above). At least four reflection hyperbolae are evident on the majority of CMP profiles, indicating at least four subsurface layers are present.

We use visual “best fit” lines and linear regression analyses (Figure 29) to compute velocities for the direct air and ground waves using both wiggle trace and raster image display format. Reflection velocities are calculated by performing T^2-X^2 analyses using the following equation (Yilmaz, 2001):

$$t_0^2 = t^2 + \frac{x^2}{v^2} \quad (5)$$

where v is the RMS velocity of the material located between the ground surface and the top of each reflector (Fisher *et al.*, 1992b). For horizontal layers with small changes in velocity, RMS velocities approximate stacking velocities. Note that the direct air and ground waves are non-hyperbolic in shape, thus do not generally add constructively during stacking (Fisher *et al.*, 1992a; Kearey *et al.*, 2002).

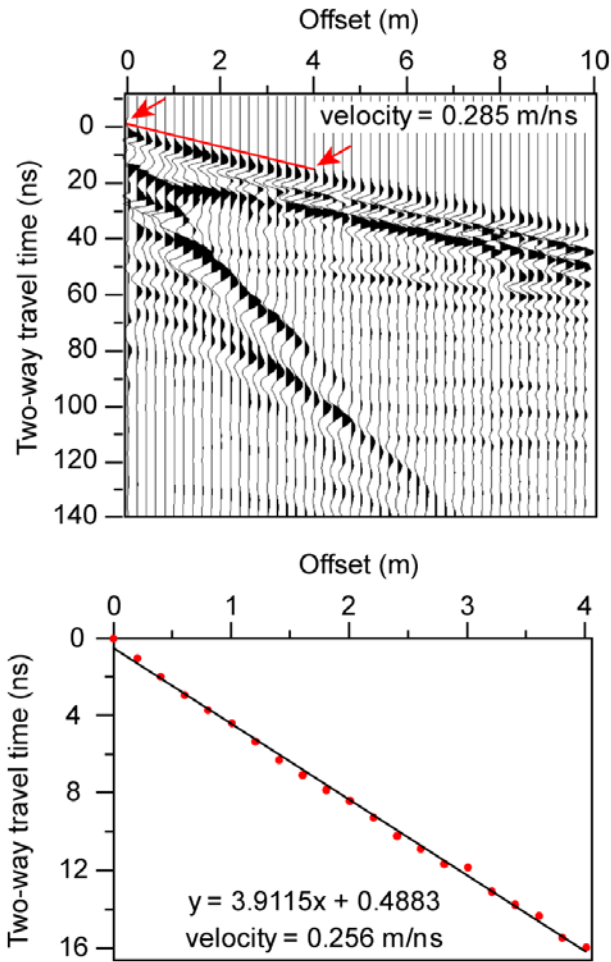


Figure 29: Example velocity variations due to picking technique. Top: Example of visually selected “best fit” line between two traces, indicated by arrows. Bottom: Linear regression analyses using visual picks of arrival times for all traces. Points were made by selecting first break positions at each trace along the direct airwave. Slight static shifts in individual traces account for some of the variation in velocity.

Effect of Picking Position

The first analysis of this study involved testing whether the specific picking position along each trace had an effect on the velocities calculated for the direct air and ground wave velocities. In a relevant study, Yelf (2004) surveyed numerous GPR practitioners to determine at which point along a trace they selected time zero. Although there was some general disagreement among these individuals, most selected one of five points along a trace (Figure 30): (1) first break point, (2) first

positive peak (maximum peak), (3) zero amplitude point, (4) mid-amplitude point, or (5) first negative peak (maximum trough). Picking position is important, not only for time zero, but also for accurate velocity estimates. To perform a similar analysis in this study, a best-fit line was manually created between two points along the first-break point of each trace (position 1), the maximum peak (position 2), and the maximum trough (position 5); velocities were calculated at each of these positions.

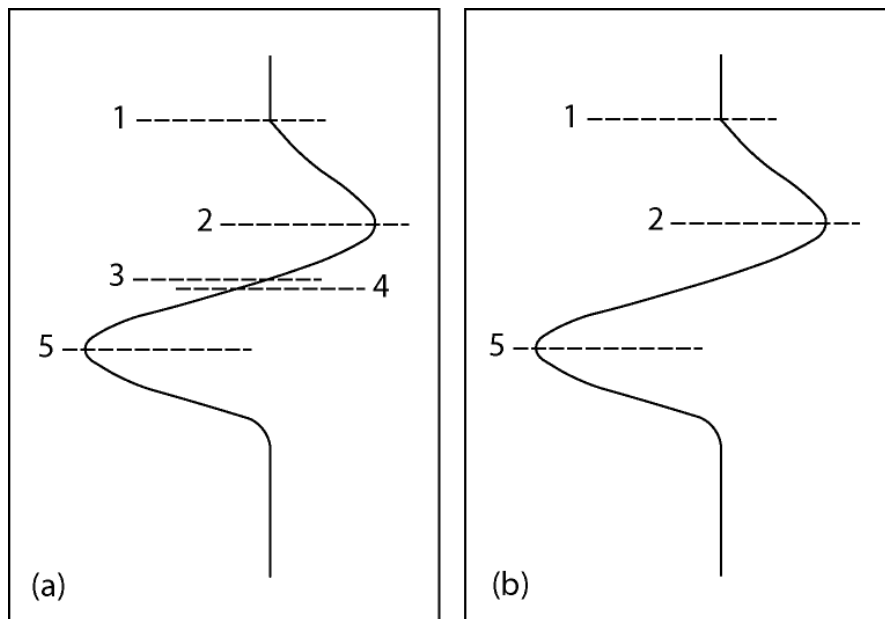


Figure 30: Example of an individual trace, indicating possible time zero picks. Example, based on a Yelf (2004) survey of numerous GPR practitioners. (b): Individual trace with picks used for velocity analyses in this study: position 1 = first break; position 2 = maximum peak; and position 5 = maximum trough.

Picking position had a significant effect on direct airwave velocities in wiggle trace images. Velocities calculated using visual line fits at the first break point were considerably faster than velocities calculated at either the maximum peak or the maximum trough (Figure 31), with all six CMP profiles producing the fastest first break velocities (position 1). Furthermore, the slowest velocities were calculated at the maximum trough position (position 5) in all six CMP profiles. These results

indicate (Figure 31 bottom) that average direct airwave velocities vary between 7 and 16% depending on picking position alone.

An additional airwave analysis on CMP PRO24 quantified the effect of simple “picking error” on velocity estimates. In this analysis, two traces were selected to define the endpoints of the direct airwave, and picks were made at position 1 using wiggle trace display mode with the same amplitude, scale, and zoom level for all iterations. Velocities were then calculated using linear regression. Even with this simple approach, the percent difference in velocity from basic “picking error” is almost 10 % (Table 1). Although picking error can be a contributing factor, it does not account for all of the variation noted above from picking position alone, suggesting that picking position does have a significant effect on direct airwave velocity estimates.

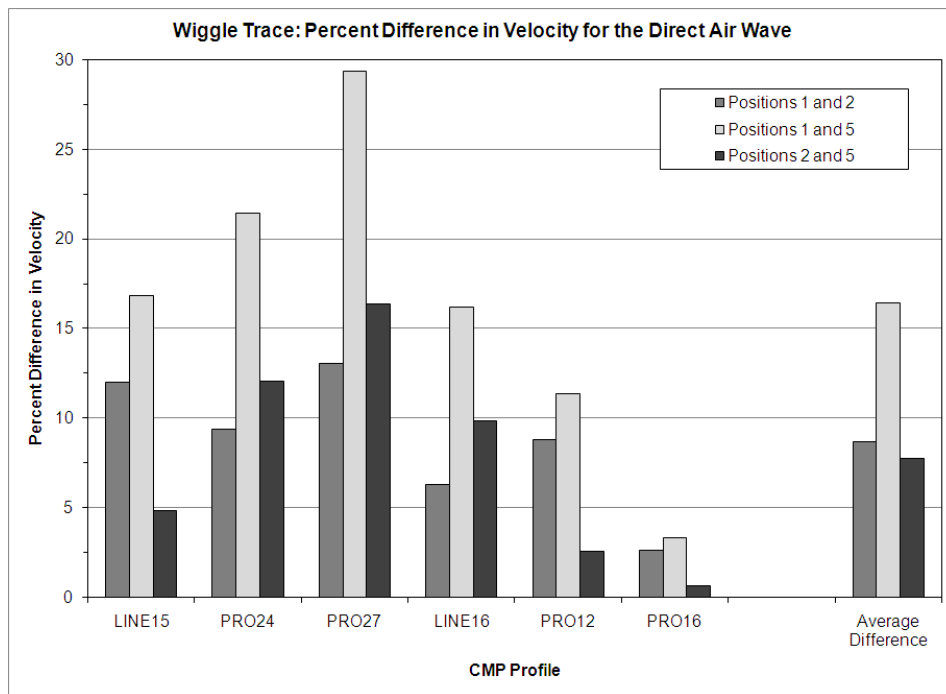
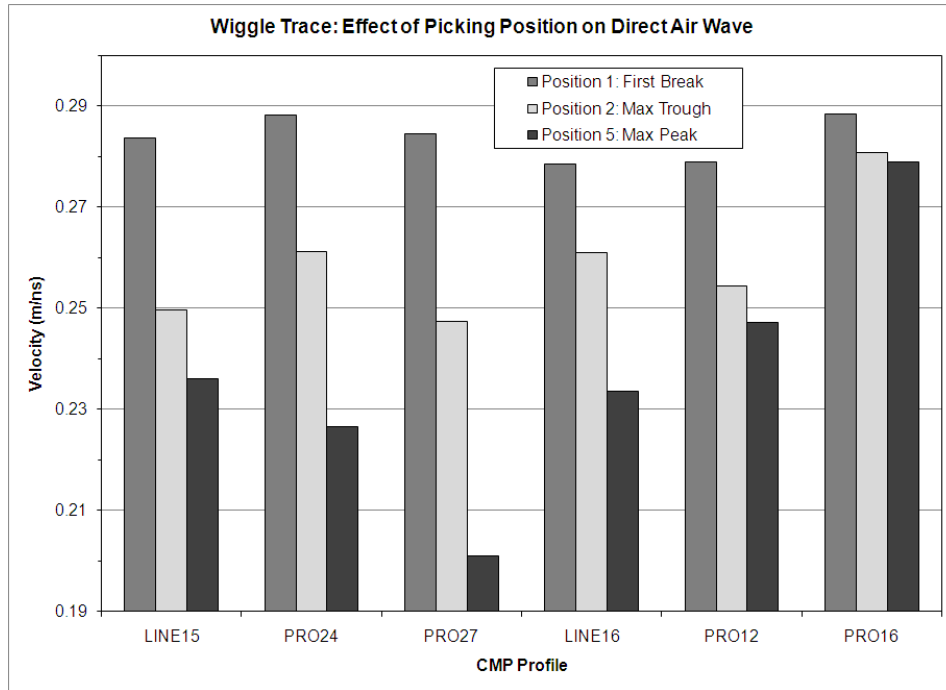


Figure 31: Effect of picking position on direct airwave velocities in wiggle trace images. Top: Plot of direct airwave velocities calculated at each position for each CMP profile. Bottom: Percent difference in airwave velocities depending on picking position, velocity using position 1 assumed as standard.

Table 1: Percent difference in velocities from simple picking error.

Trial Number	Velocity (m/ns)	Error (%)
1	0.2837	0.25
2	0.2749	-2.83
3	0.2891	2.18
4	0.2643	-6.57
5	0.2804	-0.92
6	0.2847	0.61
7	0.2891	2.18
8	0.2937	3.81
9	0.2891	2.18
10	0.2804	-0.91
Average	0.2829	

Velocities for the direct ground waves were likewise affected by picking position. Position 1 produced the fastest velocities in all six CMP profiles, and position 5 (maximum trough) produced the slowest velocities in all profiles (Figure 32). The variations in ground wave velocities are not nearly as dramatic as they are for the direct airwaves, generally being an order of magnitude smaller than the airwave velocity variations. The average difference in velocity between positions 1 and 5 is only 0.0038 m/ns, or between 3% and 9% (Figure 32).

These results clearly indicate that picking position is an important consideration for obtaining accurate velocities from direct air and ground waves. In an ideal situation, direct airwave velocities should be 0.30 m/ns. Four of the CMP profiles in this study had direct airwave velocities that were close to 0.30 m/ns using picking point1 but all six of the CMP profiles had position 5 velocities that were

significantly slower than the speed of light. Thus position 5 seems to produce the most suspect results, and we suggest it should be avoided in favor of position 1.

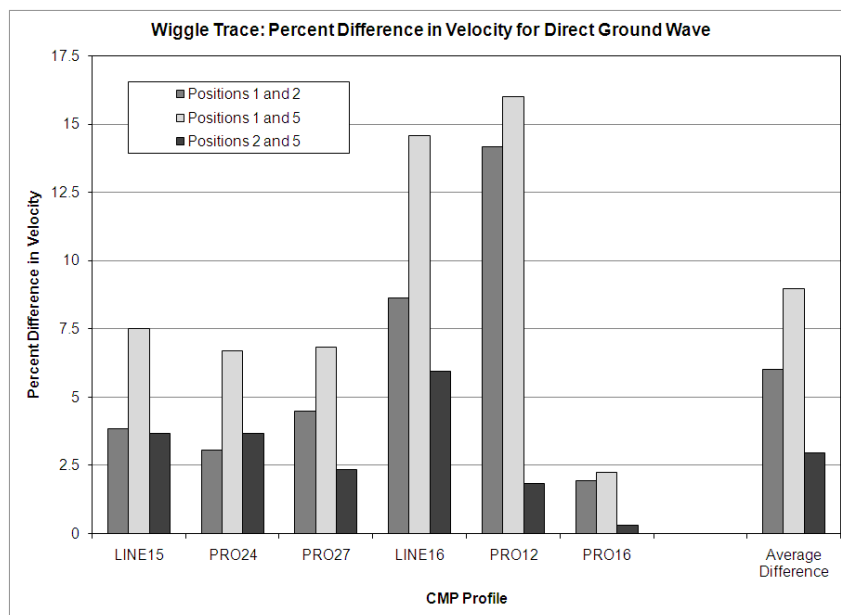
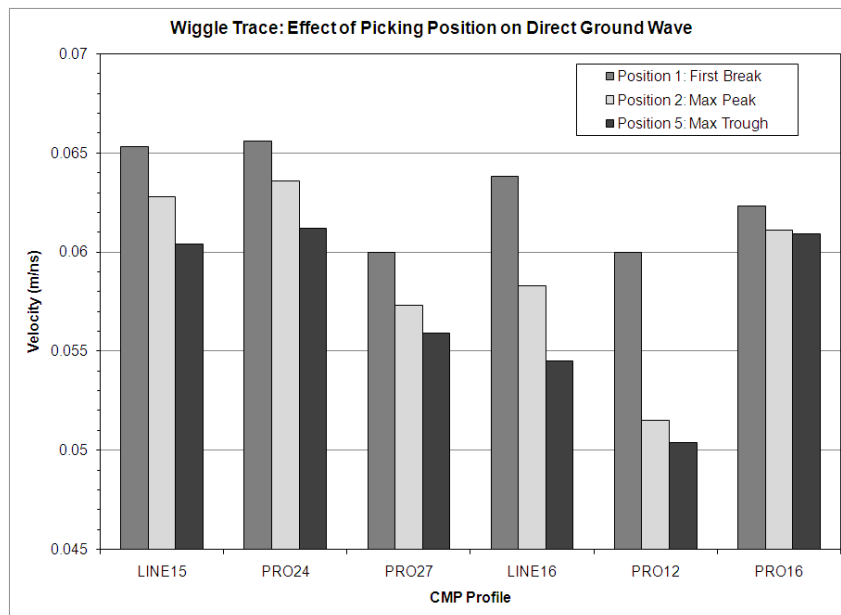


Figure 32: Effect of picking position on direct ground wave velocities in wiggle trace images. Top: Direct ground wave velocities calculated at each picking position for all six CMP profiles. Bottom: Percent difference in ground wave velocities depending on picking position.

The systematic differences noted from these analyses are consistent with frequency dependent signal absorption as the radar signal traverses greater distances between source and receiver in the ground. This differential attenuation results in variation of the waveform with offset, with the latter part of the signal (e.g. position 5) progressively delayed with respect to the initial portion of the signal (position 1) as a function of offset. If there were no signal attenuation, one would expect no change in the shape of the wavelet with depth and thus more uniform estimates regardless of picking point. However, inspection of the display in Figure 28 indicates that simple attenuation is not a complete explanation, in that there are distinct changes in apparent slope of even the initial part of the wavelet as a function of offset, a variation that may be due to the transition from near field to far field radiation (see below).

Effect of Display Amplitude

One CMP profile (PRO 27) was selected to determine if variations in display amplitude had any effect on estimation of the average velocities of either the direct air or ground waves using visual picking. Wiggle traces were scaled to increase the size of individual waveform deflections. Scale factors of 20, 50, and 100 (Figure 33) were applied. Individual picks were made for position 1. Position 1 was selected to avoid confusion due to clipping of traces at either the maximum peak or trough. Results indicate that amplitude variations have only negligible effects on velocities calculated for both the direct air and ground waves (Figure 34). Airwave velocities varied by 0.007 m/ns, and ground wave velocities varied by 0.003 m/ns, or 2% and 4%, respectively. Even though these results indicate that plot amplitudes are not a significant factor for determining position 1 velocities, a plotscale of 20 was used for all wiggle trace images in order to keep these analyses as standardized as possible.

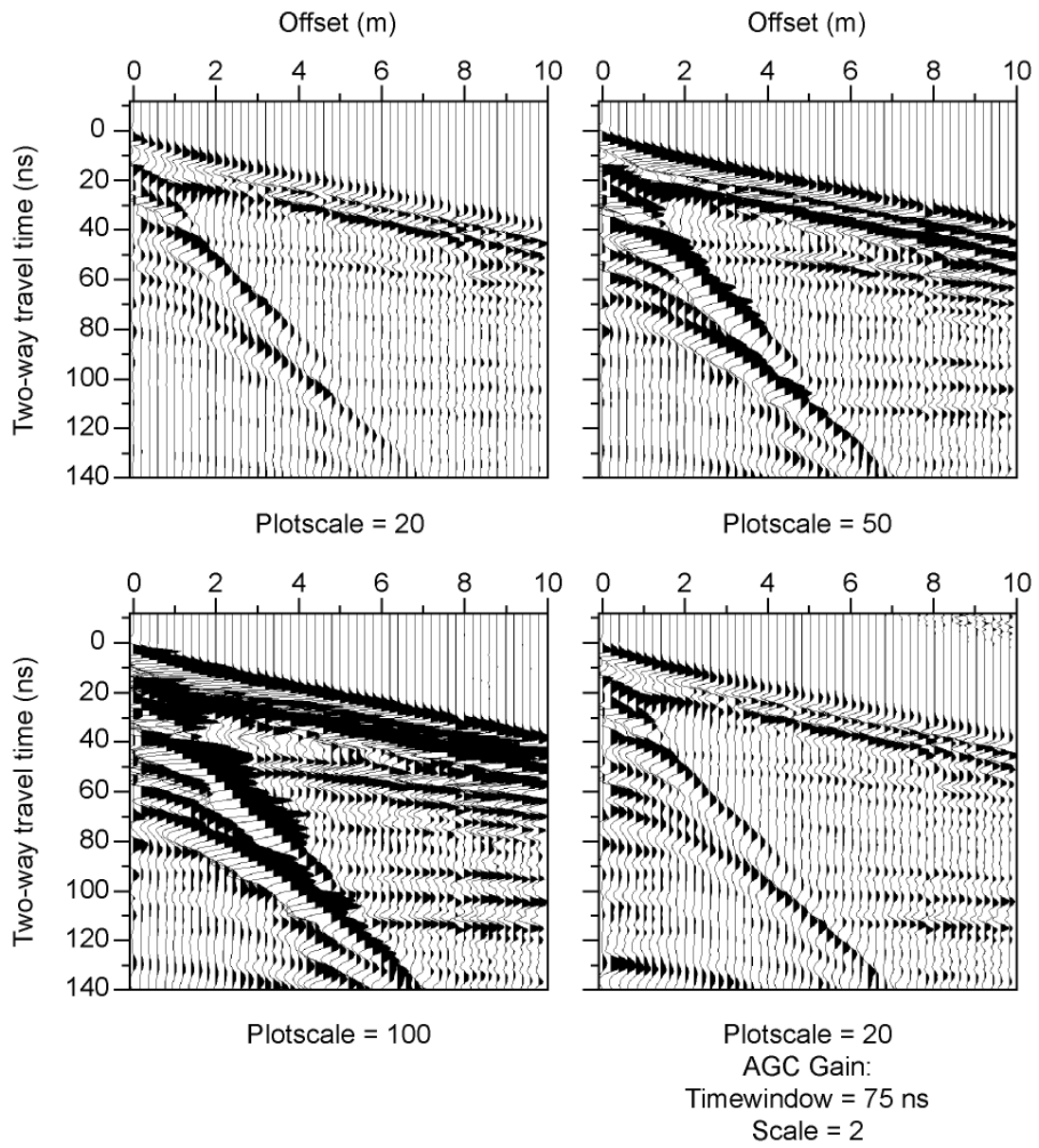


Figure 33: Four images of CMP PRO27 plotted using different gain functions.

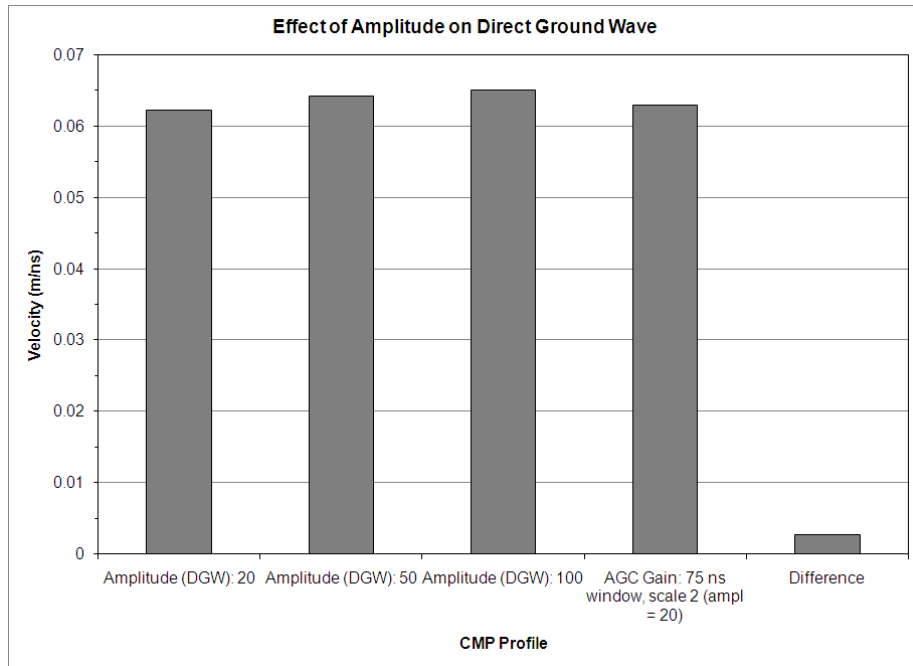
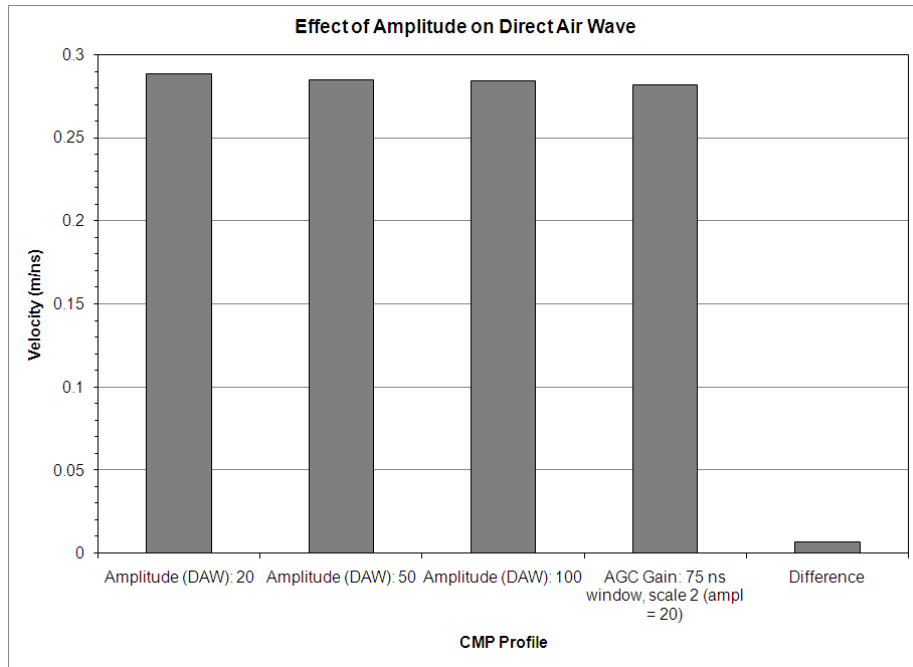


Figure 34: Effect of amplitude on direct airwaves and ground waves. Top: The effect of display amplitude on estimation of direct airwaves in wiggle trace mode, including the difference between the fastest and slowest velocities. Bottom: The effect of amplitude on the estimation of direct ground wave in wiggle trace mode, including the difference between the fastest and slowest velocities.

Influence of Image Display

In this analysis, velocities for the direct air and ground waves were calculated from picks made from wiggle trace versus raster displays (Figure 35) to determine if variations existed because of the display mode used. For wiggle trace images, the first break point, or position 1, of each wavelet was selected. For raster images, points along the top of the black waveform were selected for the direct airwaves and the top of the white waveform for the direct ground waves. These positions on the raster images were selected because they were the easiest to pick consistently.

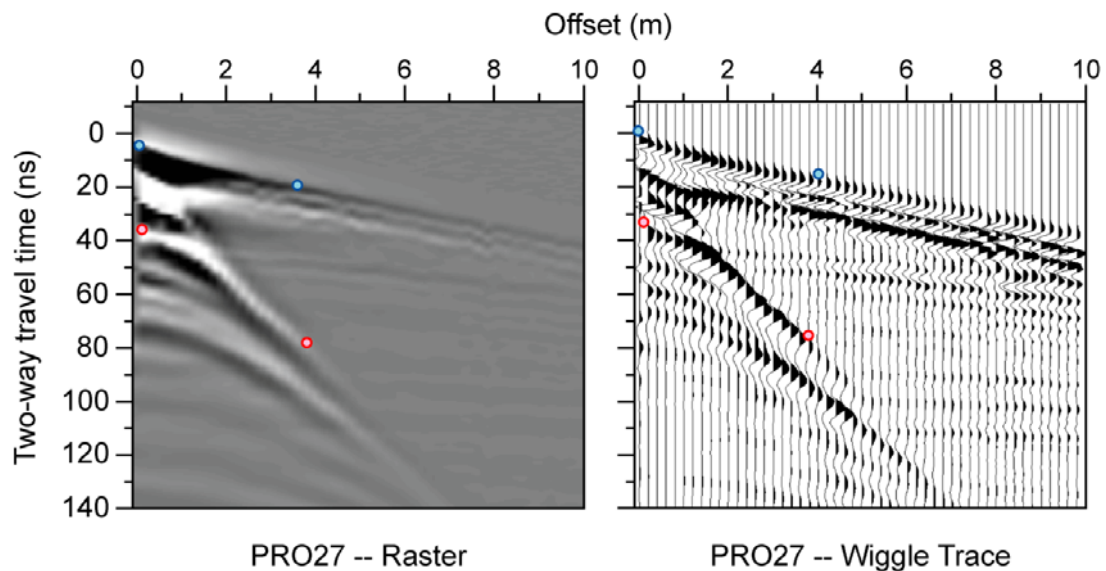


Figure 35: Raster and wiggle trace image formats. Picking is influenced by which display mode is used. Example picks are shown for the direct airwave and a reflection.

Image display appears to have a significant effect on the velocities calculated for the direct airwave. Velocities calculated in wiggle trace images are dramatically higher than velocities calculated in raster images in 5 of the six CMP profiles (Figure 36), with an average difference of more than 8%. Direct ground wave velocities

calculated in wiggle trace images are also higher than velocities calculated in raster images (Figure 37), but they only differ by about 2.6%.

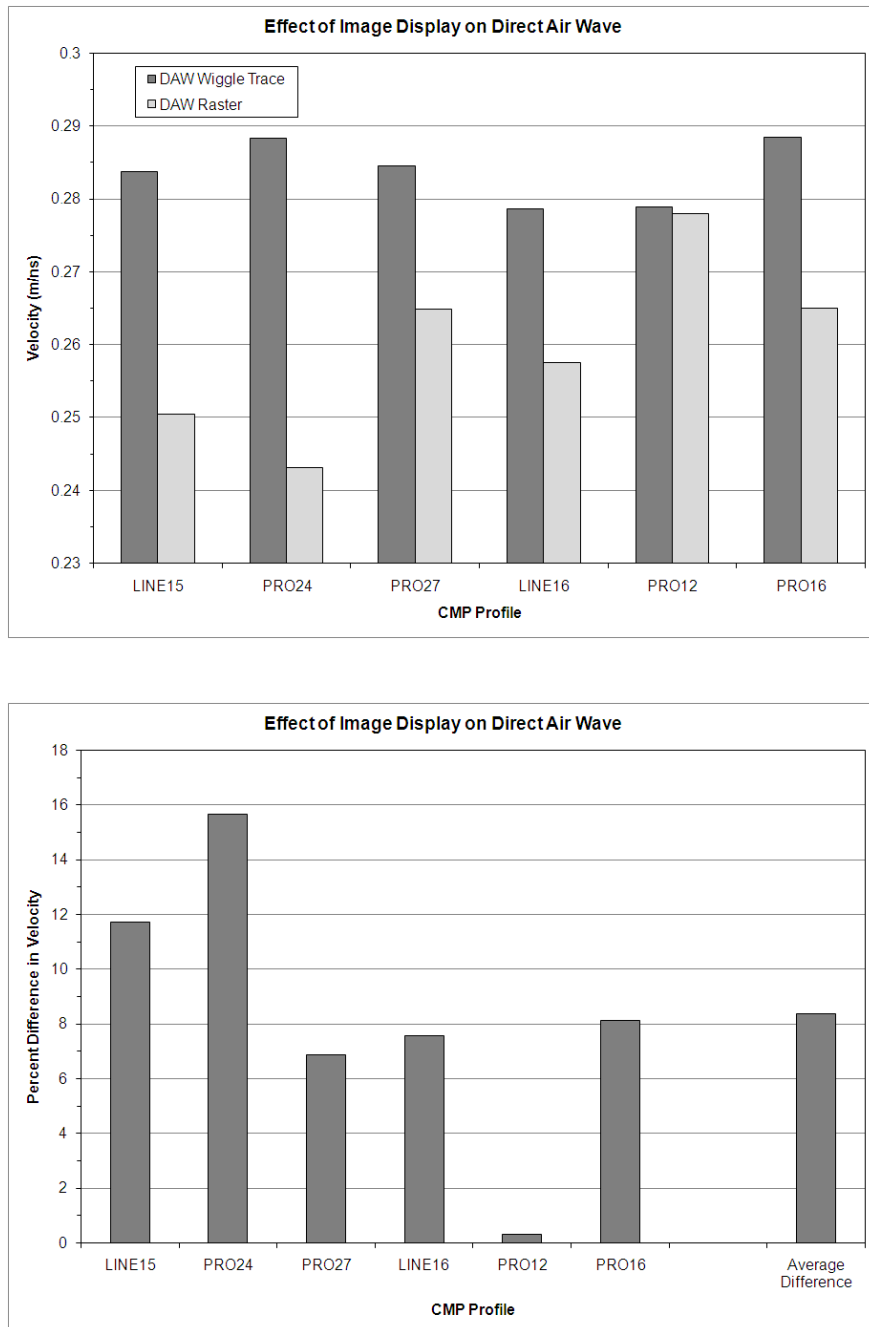


Figure 36: Effect of image display on direct airwaves. Top: The effect of image display on direct airwave velocities. Bottom: Percent difference in direct airwave velocities depending on image display.

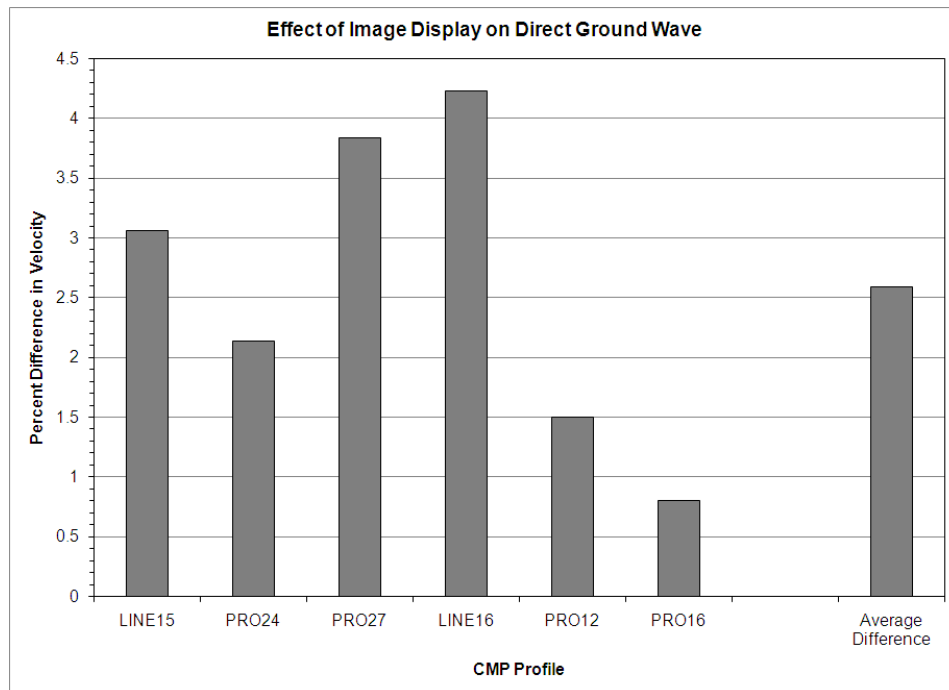
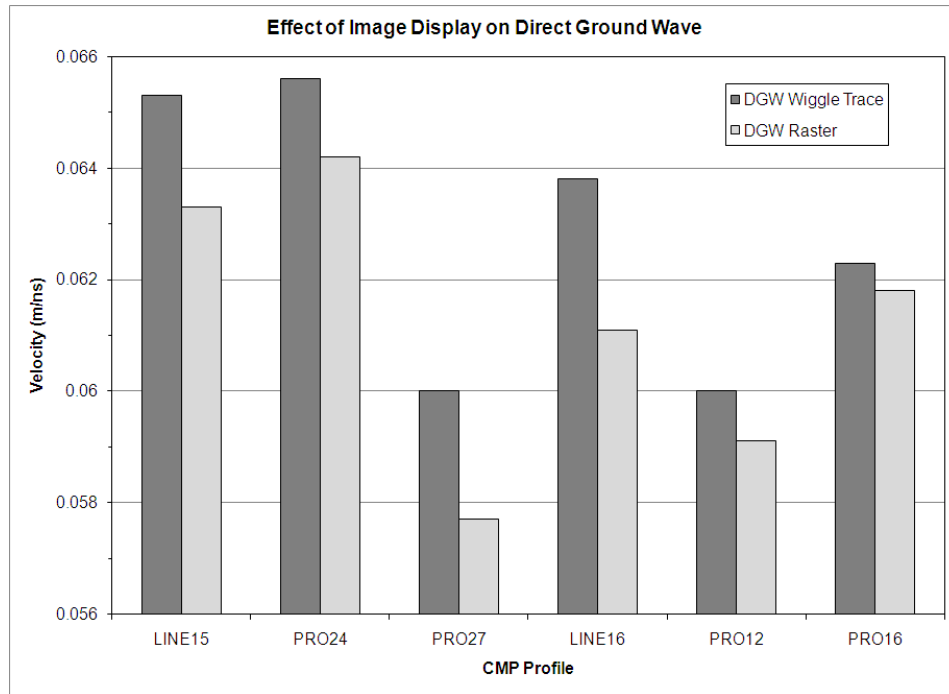


Figure 37: Effect of image display on direct ground waves. Top: The effect of image display on direct ground wave velocities. Bottom: Percent difference in direct ground wave velocities depending on image display.

Implicit in both the picking position (wiggle trace) and wiggle trace versus raster mode comparison is the issue of whether the variations are simply an expression of the effective displacement due to T_0 times implied. For example, it is clear that the first break positions on wiggle trace images are usually earlier than the “equivalent” tops of these reflectors as evident in raster images (Figure 35). This is similar to the NMO stretch effect (Yilmaz, 2001), which is related to the change in diffraction curvature and apparent T_0 time, even though the velocity has remained unchanged (Figure 38). In Figure 38, this effect is modeled using 3 separate hyperbolae that have the form

$$t = \frac{\sqrt{x^2 + 4h^2}}{v} \quad (6)$$

(where x is offset in meters, h is depth in meters, and v is velocity) with a constant velocity of 0.060 m/ns. In Figure 39, the topmost reflection in Figure 38 is redrawn, but with a constant time shift of 5 ns applied in the middle reflection, and a constant time shift of 10 ns was applied in the lower reflection. Even though each hyperbola is meant to represent a reflector for a velocity of 0.060 m/ns, analysis of the shifted hyperbolae yield estimates that differ by 5 % and 8.3 %, respectively.

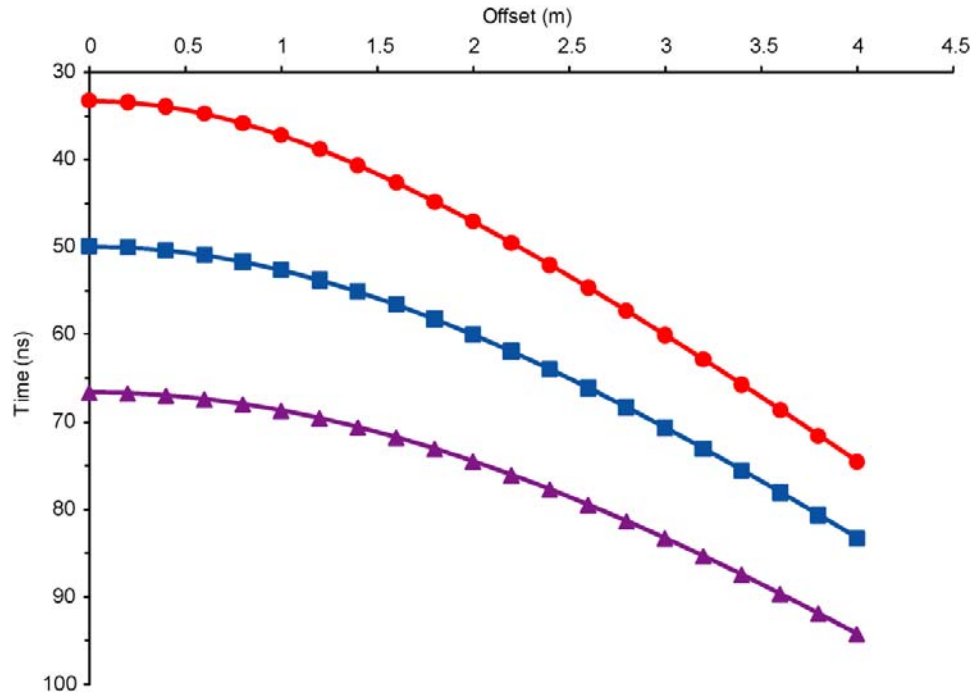


Figure 38: Effect of NMO stretch on three separate hyperbolae that were generated using a constant velocity of 0.060 m/ns.

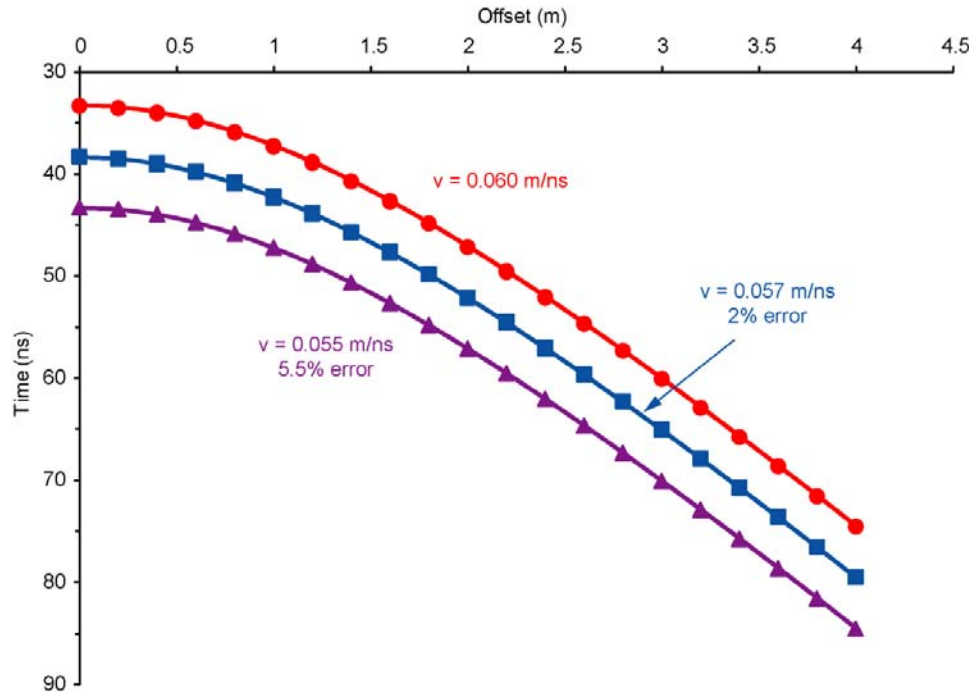


Figure 39: Variations in velocity from simulated multiple picking positions on a single reflection. Variations in velocity are due to a time shift of 5 ns and 10 ns, respectively.

Effect of Offset (Range)

Another analysis involved assessing the effect of offset on direct airwave and direct ground wave velocities in both wiggle trace and raster images. Prior to CMP analyses, some basic processing steps were performed on the data from Los Naranjos. The first step involved applying a time filter known as “dewow,” which is a high pass filter that removes signal saturation or low frequency “wow” from the GPR data (Gerlitz *et al.*, 1993; Sensors & Software Inc., 2003). Wow can be introduced because of the electrical properties of the ground (Jol and Bristow, 2003) or when the transmitting and receiving antennae are too close to one another (Sensors & Software Inc., 2003), which is why it most often occurs at near offsets in the CMP data. All profiles shown in this paper have been dewowed. This is a necessary step in all processing, but it is especially important here in order to view a representative wavelet. In seismology, it is well-known that offset plays an important role in obtaining adequate velocities. To resolve velocities sufficiently, both near and far offsets are needed to define a wavelet properly (Yilmaz, 2001). We decided, therefore, to demonstrate the effect of offset on the direct air and ground waves in this paper.

In this analysis, a best-fit line was created between two points along the first-break point (Figure 30) for each trace in wiggle trace images. For all CMP profiles, the offset boundary was set at one meter because the saturation is most obvious at offsets of one meter or less (near-offset), and less influential beyond 1 m (far offset). Far offset values were always picked between 1 and 4 meters, with 4 meters being the maximum offset, although some analyses did not extend as far as 4 meters. The maximum offset was set at 4 meters (for all analyses in this study) for two reasons. First, three of the six CMP profiles extend to about 4 meters, and we wanted to keep our analyses as consistent as possible between profiles. Second, a distinct change in

slope was noted at about 4 meters offset in the direct air and ground waves of several CMP profiles (note especially the direct airwave in CMP PRO 24). This change in slope is due most likely to attenuation of the signal at large offsets and fitting a line through these traces would bias the results, rendering comparisons inappropriate. Care was taken to choose endpoints that allowed for the most linear section between them; points with significant static shifts were not chosen, so that there was little bias introduced from the selection of endpoints.

In wiggle trace display, offset was a significant factor for direct airwave velocities (Figure 40). In all six CMP profiles, direct airwave velocities defined by near offset traces were significantly slower than the far offset and all offset velocities. On average, near offset velocities were as much as 0.040 m/ns, or almost 17%, slower than far offsets and almost 21% slower than all offsets. Far offset velocities and all offset velocities varied by less than 4%, with far offsets being slower than all offsets in all profiles (Figure 40). Using the “known” airwave velocity of 0.030 m/ns as a standard, the all offset picks were the most accurate in all profiles. This relationship is consistent with waveform changes that we expect, indicating that large spreads define the shape of the wavelet best.

Offset also had a significant effect on the velocity of the direct ground wave in wiggle trace images and was more pronounced than the direct airwave velocity variations. For all six CMP profiles, the near offset velocities were faster (not slower, as was the case with the direct airwaves) than both the far offset velocities and all offset velocities (Figure 41). Again, the far offset and all offset velocities were similar, with all of the far offset velocities being slightly slower than the all offset velocities. The effect of offset was especially pronounced in PRO27; the near offset velocity was more than 2.5 times faster than both the far offset and all offset velocities. Inspection of PRO27 indicates that the direct ground wave is hidden

behind the first reflection, making it difficult to pick consistently, thus most likely accounting for the large difference in velocity. On average, near offset velocities were almost 30% faster than far and all offset velocities.

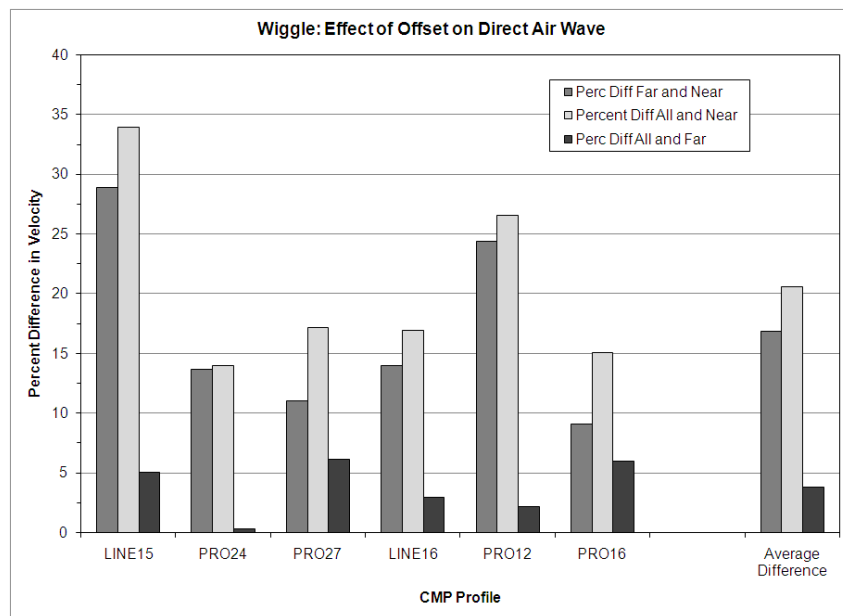
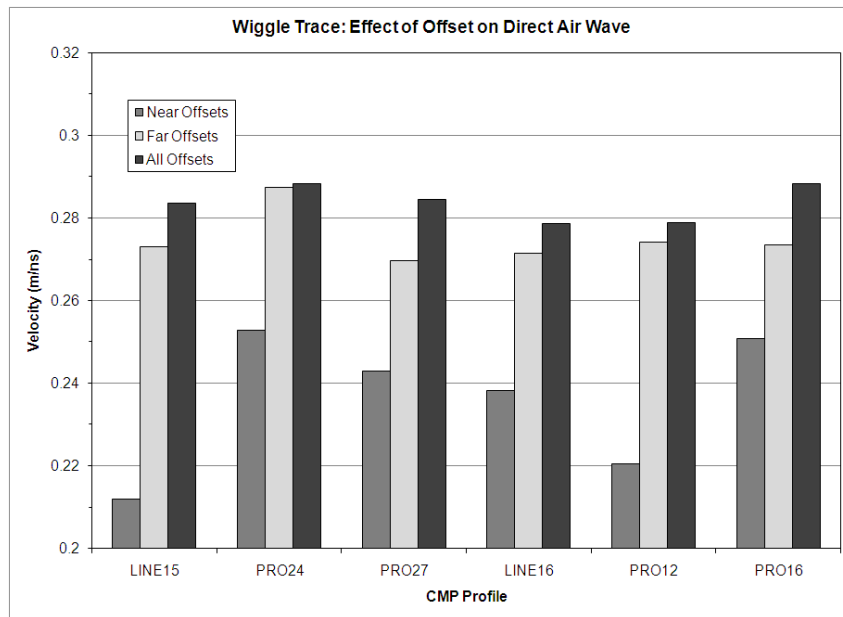


Figure 40: Effect of offset on direct airwave velocities. Top: Effect of offset on direct airwave velocities in wiggle trace images. Bottom: Percent difference in direct airwave velocities depending on offset in wiggle trace images.

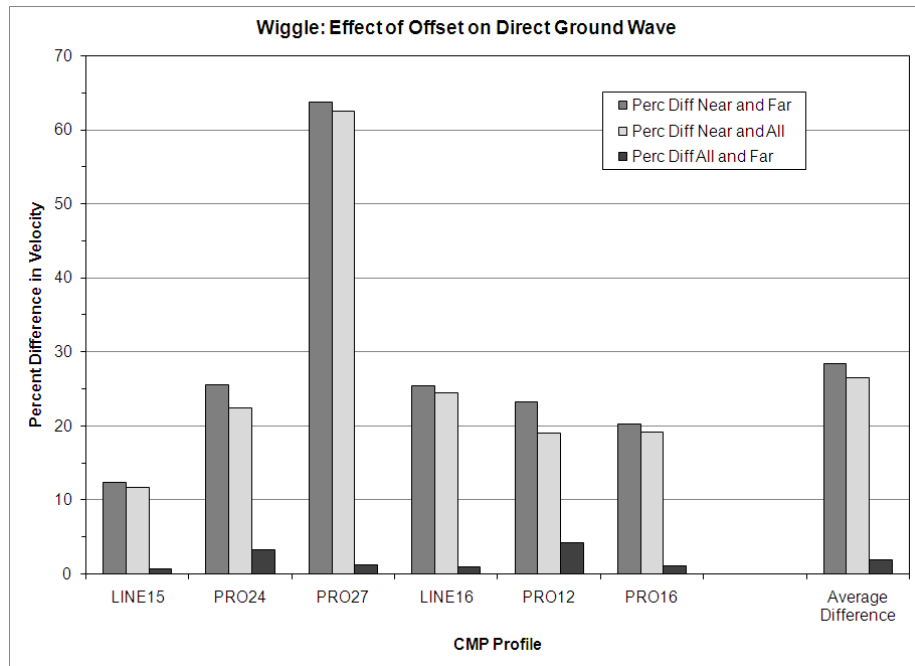
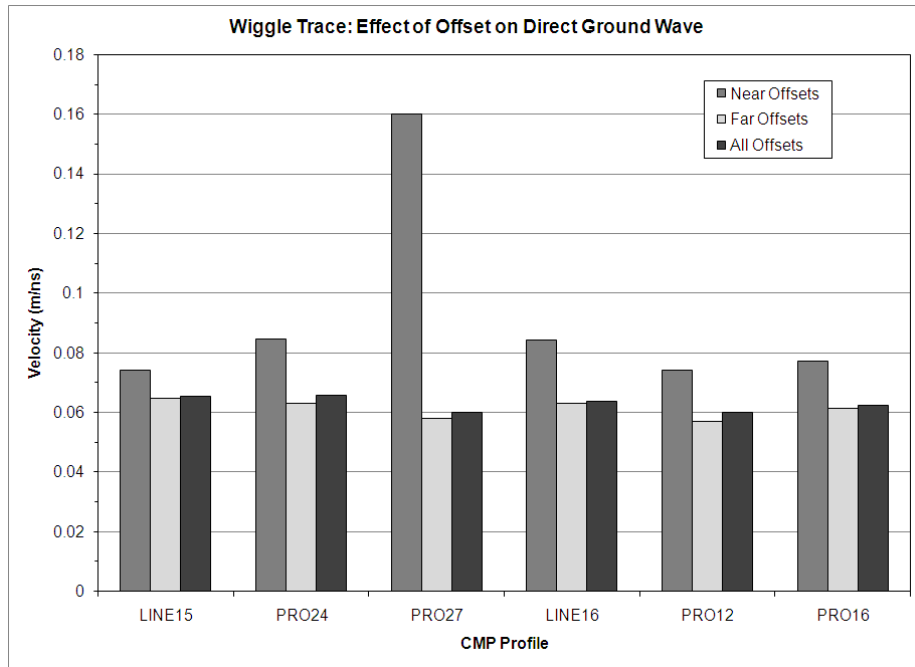


Figure 41: Effect of offset on direct ground wave velocities. Top: Effect of offset on direct ground wave velocities in wiggle trace images. Bottom: Percent difference in direct ground wave velocities depending on offset in wiggle trace images.

Such large variations in velocity based on offset have important implications for velocity analyses but also for survey design. For these particular CMP profiles, offsets of one meter and less were significantly impacted by near offset effects. If CMP surveys are not long enough, it will be impossible to detect these variations, and will cause confusion as to why the direct airwave velocities do not match the speed of light. Other factors contribute to the significant effect of offset, namely wow effects and attenuation of the wavelet with offset. These effects are illustrated in Figure 42. Wow affects the wavelet by elongating it and amplifying it, so that if a position 2 pick were made along near offset traces (as indicated), the resulting velocity ($1/V_1$) would be slower than corresponding picks from larger offsets (indicated in Figure 42 as $1/V_2$). These changes in velocity represent the effects of wow only and should not be confused with changes in velocity due to lithology or layering.

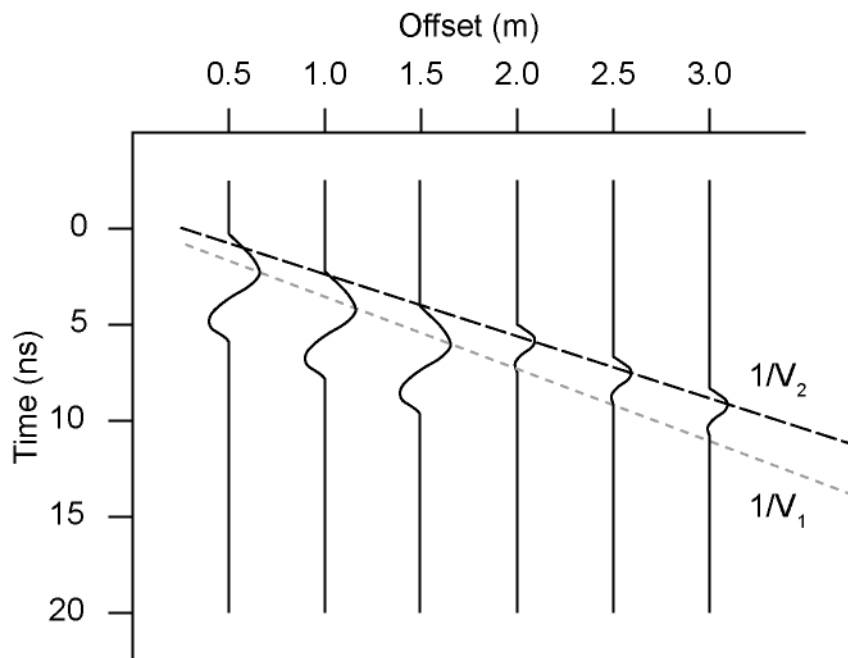


Figure 42: Effect of "wow" and attenuation with offset.

Offset had a similarly dramatic effect on the direct air and ground wave velocities in raster images as it did in wiggle trace images. For all six CMP profiles, direct airwave velocities for near offsets are significantly faster than both far offset and all offset velocities (Figure 43); direct airwave velocities were slower in wiggle trace images. Near offsets have an average velocity that is almost 0.10 m/ns faster than both far offset and all offset velocities; this difference is also double that found in wiggle trace images. Furthermore, near offset velocities are 50% faster than far offset velocities. In raster images, far offset and all offset velocities varied by as much as 14%. This is the largest percent difference found in the offset analyses. Direct ground wave velocities in raster images are again significantly slower than both far and all offsets (Figure 44), with comparable differences in velocity (about 0.030 m/ns). Velocities for far and all offsets are similar to one another, with only negligible differences between them; a similar result was seen in wiggle trace images.

Velocity variations due to offset are not only significant for all datasets collected at Los Naranjos, but they are also highly variable. The variability of these results is most likely related to the fact that these CMP profiles were collected at several different locations at the site. Since wow is also a result of the electrical properties of the ground, the variability might just represent differing physical properties at the site.

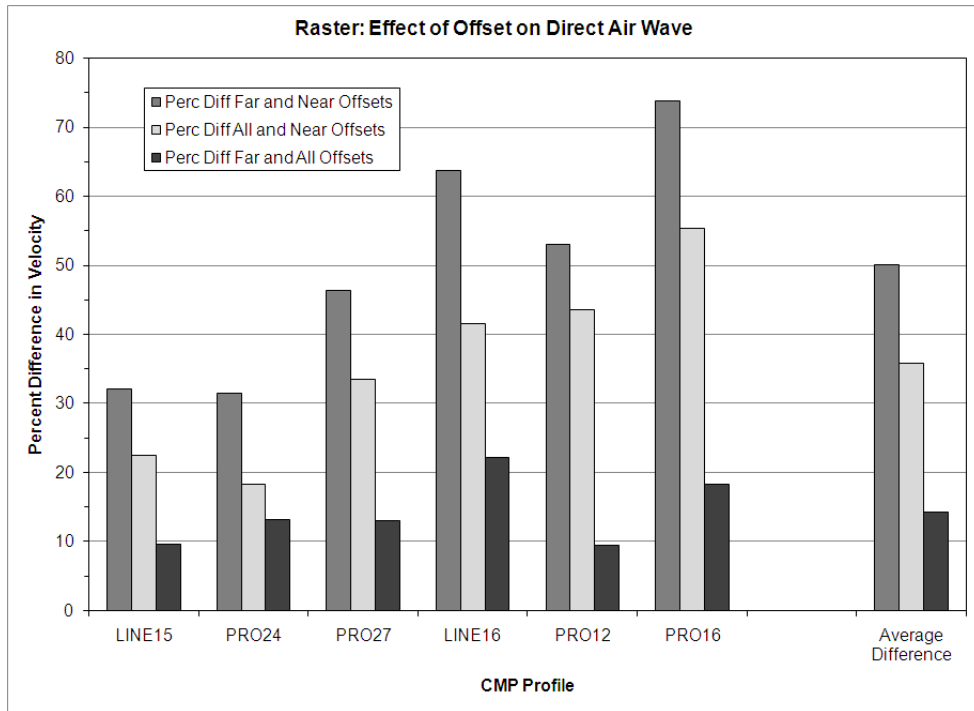
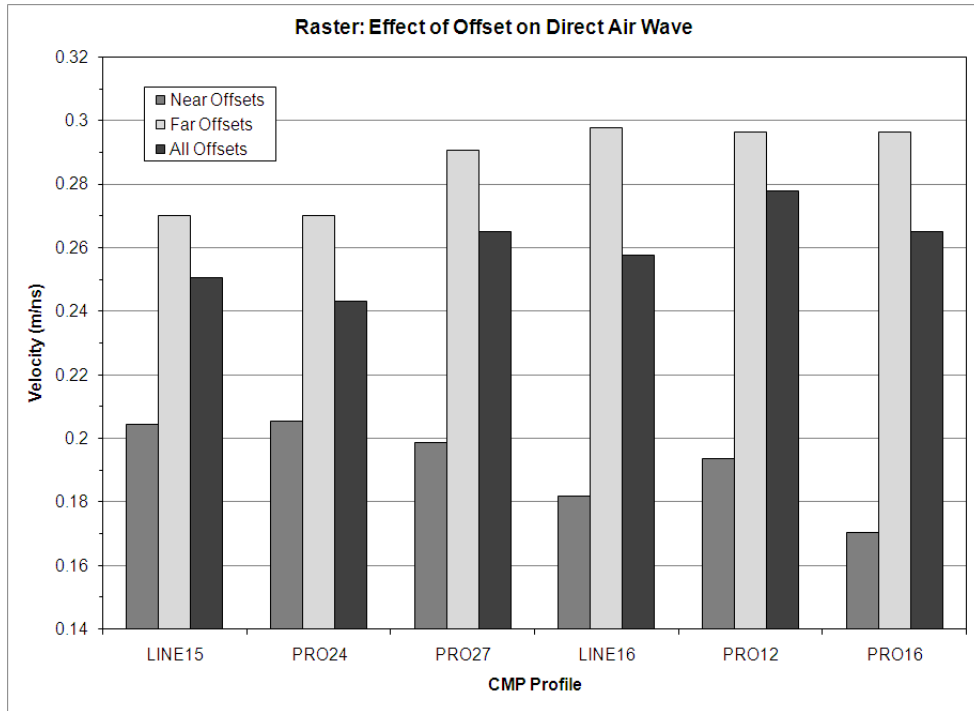


Figure 43: Effect of offset on direct airwave velocities in raster images. Top: Effect of offset on direct airwave velocities in raster images. Bottom: Percent difference in direct airwave velocities depending on offset in raster images.

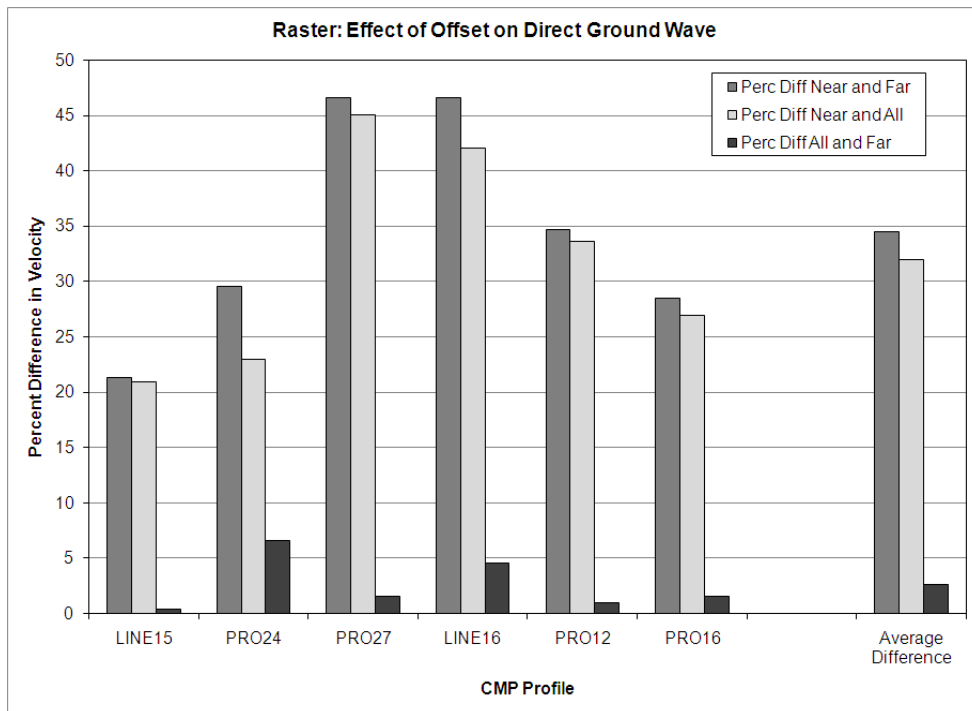
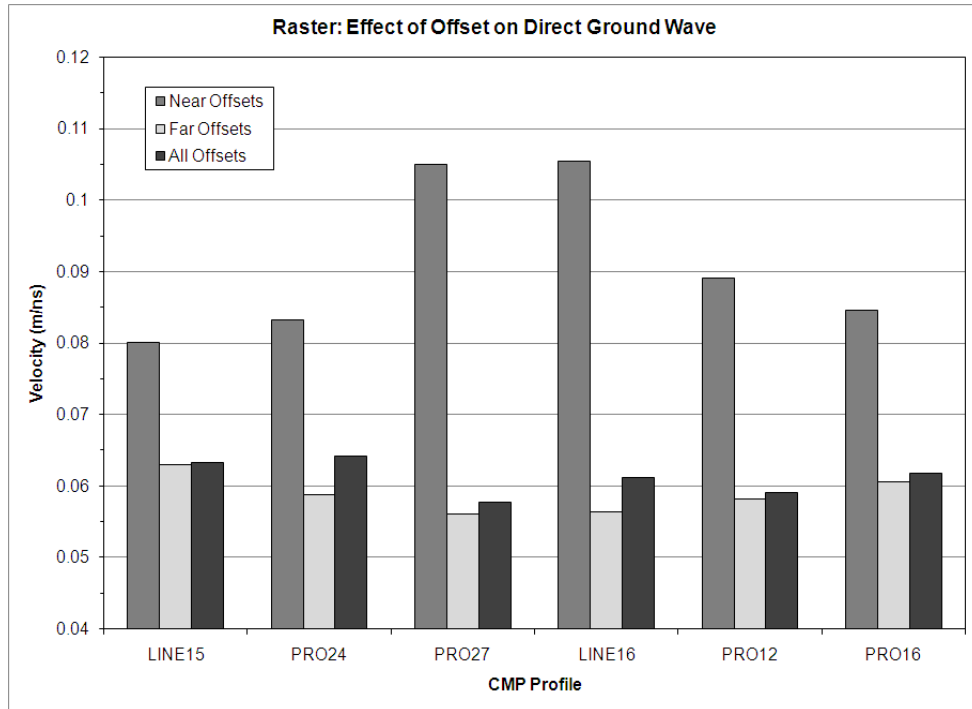


Figure 44: Effect of offset on direct ground wave velocities in raster images. Top: Effect of offset on direct ground wave velocities in raster images. Bottom: Percent difference in direct ground wave velocities depending on offset in raster images.

Effect of Picking Technique (Visual “Best Fit” Lines versus Formal Linear Regression)

Wiggle trace images were used to determine if specific picking techniques (visual line fits using display tools versus linear regression of individual arrival time picks) would produce significant variations in velocity. Best fit lines were created at the first break positions on traces of the direct air and direct ground waves. Picks were again guided by endpoints that allowed for the most linear section between them that fit through as many traces as possible, and traces that exhibited large static shifts were avoided. Green (1938, p. 297) noted that a single bad pick can have an adverse effect on velocity estimates, so he encouraged the use of multiple picks to minimize the effects of one bad one. Linear regression was accomplished by making multiple (first break position) picks along the direct air and ground waves. A computer-generated best fit line was then calculated for these points, and velocities were calculated by taking the reciprocal of the resulting slope of the best fit line.

These analyses show that visual line fits result in faster airwave velocities than linear regression in all six CMP profiles (Figure 45). Mostly, these differences are not dramatic, but significant differences were noted for PRO12 and PRO16. Similar results were noted for direct ground wave velocities (Figure 46), but the variations in velocity were more significant. The most likely explanation for the difference in velocity is that best fit lines are tied only to the endpoints, whereas linear regression analyses weigh individual traces so that slight variations, or static shifts in the data can affect the results.

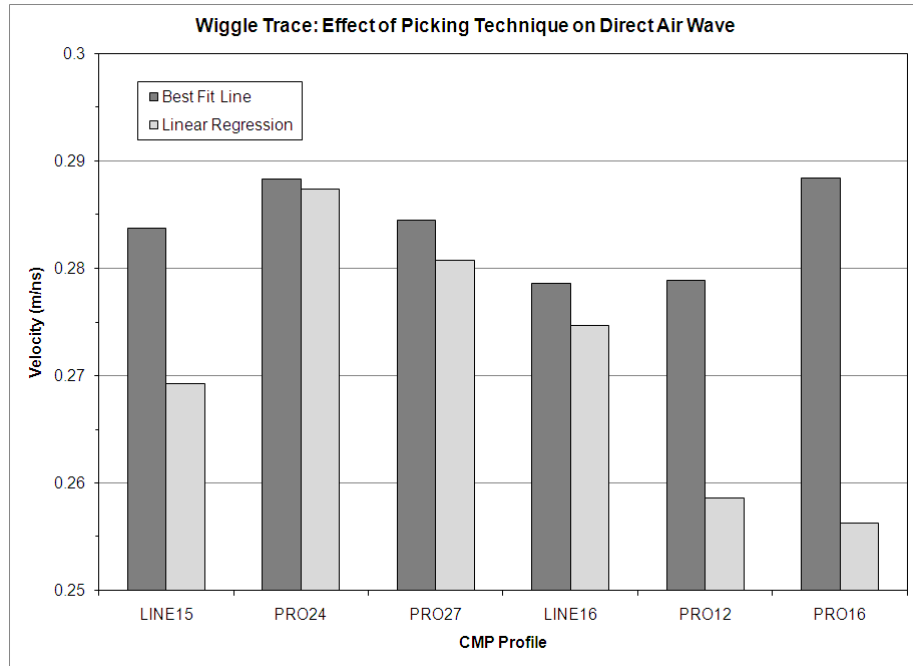


Figure 45: Effect of picking technique on direct airwave velocities in wiggle trace images.

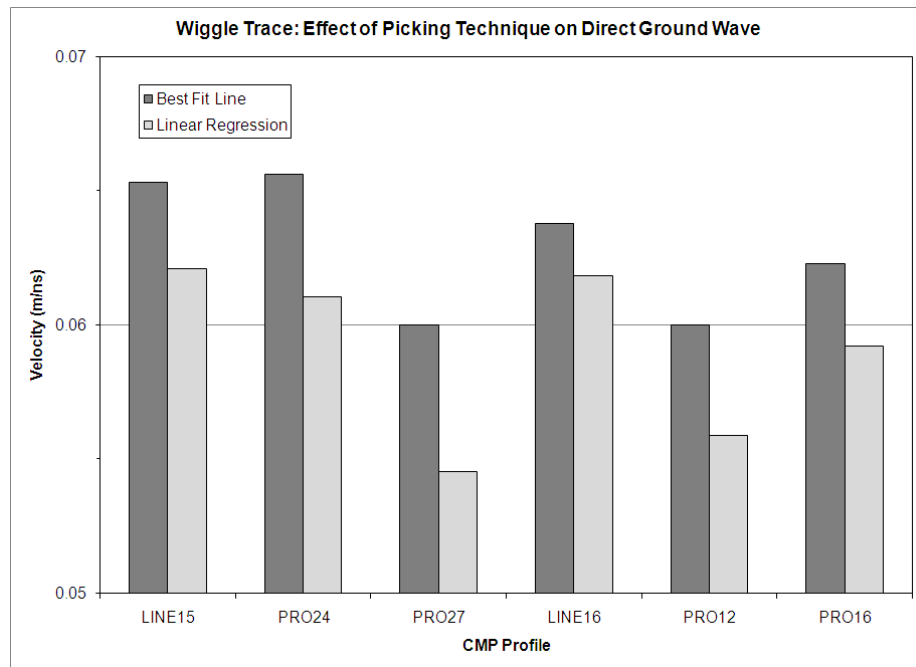


Figure 46: Effect of picking technique on direct ground wave velocities in wiggle trace images.

Velocity Spectra / Semblance Analysis

Numerous studies have documented the similarities between seismic and GPR data and the applicability of seismic processing algorithms to GPR data (Fisher *et al.*, 1992a; Fisher *et al.*, 1992b; Grasmueck, 1994). One method that is standard in seismic processing is the generation of velocity spectra or semblance analyses (Cook and Taner, 1969; Cunningham and Heffring, 1980; Dinstel, 1971; Taner and Koehler, 1969) that provide an independent means to calculate velocities for an entire CMP profile. In this approach, reflections are summed after removal of trial NMO corrections based on trial stacking velocities. When the correct velocity is used, the signals are aligned and the resulting sum is a maximum (Annan, 2005; Yilmaz, 2001). In Figure 47, six reflections are visible, which match fairly well with the reflections noted on the CMP profile. Although there is good correlation between the velocity spectra and the CMP profile, there are slight variations in the times of specific reflections. These variations are most likely caused by the imperfect shape of the reflections in the actual field data (one reflection may generate two maxima).

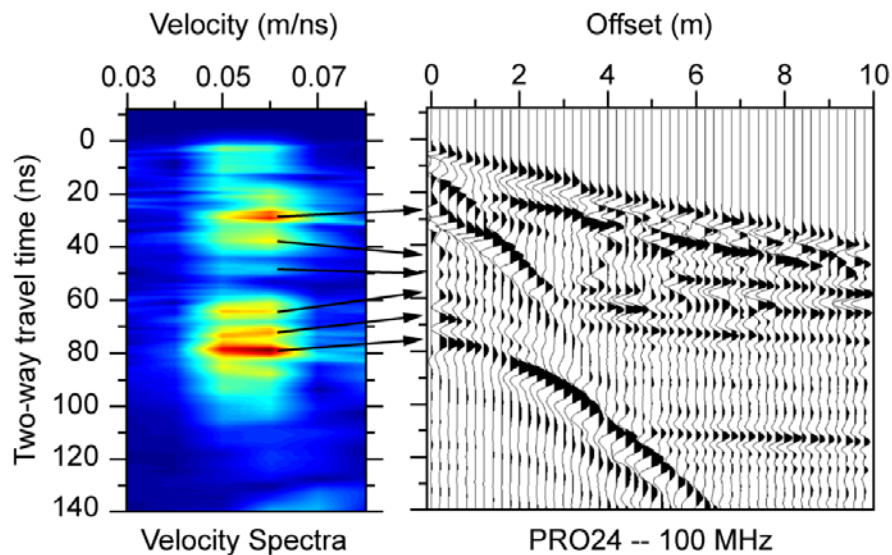


Figure 47: Velocity spectra for CMP PRO24, with 6 clear maxima representing corresponding reflections and the trial stacking velocities that result in their alignment.

Synthetic CMP Profiles

One final set of analyses involved generating synthetic CMP profiles as an independent check of the velocities calculated directly from the CMP profiles from Los Naranjos. Parameters specific to individual CMP profiles collected at Los Naranjos were used to make the comparisons as accurate as possible. In one instance, a 100 MHz synthetic was created in commercial seismic software with direct air and ground waves and one reflection (Figure 48). The synthetic reflection correlates with the strong reflection (Reflection 5) in CMP PRO 24, which is located at 70.2 nanoseconds. Reflection 5 was generated using an average velocity of 0.055 m/ns, which corresponds with the average velocity calculated for this reflection in CMP PRO24. Figure 48 shows the expected similarity between the synthetic and CMP PRO24.

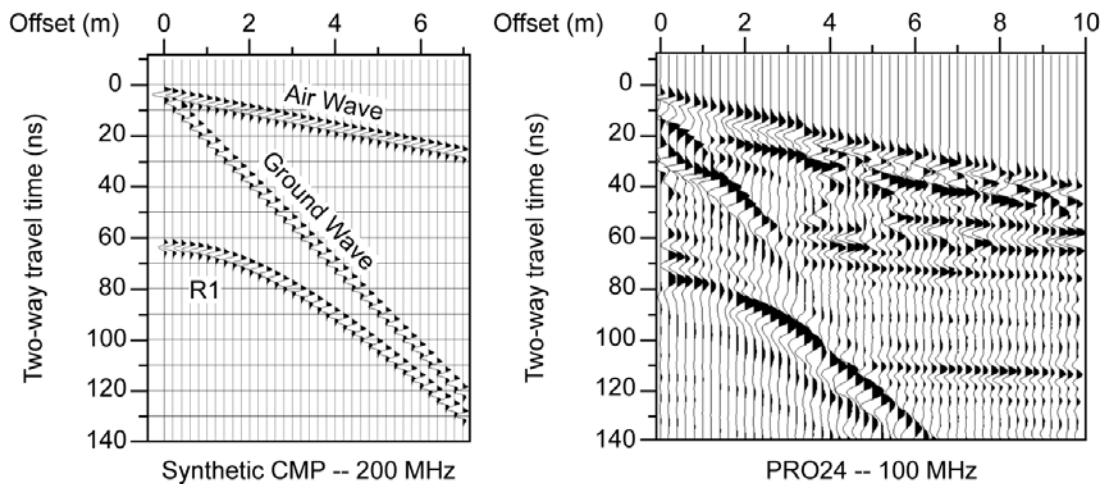


Figure 48: Comparison of a synthetic CMP with CMP PRO24.

The synthetic CMP discussed here represents an ideal data set, free of attenuation, noise, wow, and changes in the shape of the wavelet that are all present in the CMP data collected at Los Naranjos. Although this is a simplistic version of real-

world data, the synthetic was constructed this way specifically so that it could provide an ideal model in which picking error could be constrained. Ideally, linear regression analyses should produce an exact match to the specific velocities that were input into the synthetic; variations from these velocities indicate picking error. Table 2 contains the details of the velocities input into the synthetic and the corresponding velocities that were calculated using position 1, 2, and 5 picks. Under ideal conditions, picking position should not matter for either the direct air or ground wave, as all calculated velocities matched the input velocities. These results vary from those calculated from the Los Naranjos dataset. Velocities calculated for the reflection, however, match the Los Naranjos dataset more closely, with position 1 producing the fastest velocity and position 5 producing the slowest. The resulting position 1 reflection velocity is the only one that matches the velocity input into the synthetic. Variations in reflection velocity correspond to increases in the corresponding T_0 times and result in velocity estimates that differ by about 2 % and 5.5 %, respectively.

Table 2: Velocity estimates from the 100 MHz synthetic CMP profile.

	Synthetic Velocity (m/ns)	Position 1 (m/ns)	Position 2 (m/ns)	Position 5 (m/ns)
Direct Airwave	0.30	0.30	0.30	0.30
Direct Ground Wave	0.060	0.060	0.060	0.060
Reflection	0.055	0.055	0.054	0.052

Effect on Depth and Interval Velocity Estimates

As mentioned previously, an important reason for collecting CMP data is to use the calculated velocity estimates to convert GPR data from time into depth. Accurate velocity estimates are essential, especially if GPR data are to be correlated

with excavated materials. By undertaking analyses on successive reflections from a CMP profile, it is possible to determine the effect variations in average velocity has on depth estimates as well as corresponding interval velocities.

For this series of analyses, CMP PRO 24 was selected as the best example, because it has 5 clear reflections that range from about 40 nanoseconds to about 70 nanoseconds. Analyses similar to those performed on the direct airwave and direct ground wave were performed on reflections, including differences in position (positions 1, 2, and 5), image display, offset, and linear regression analyses. Additional reflection analyses involved the first-break time (T_0 , R_0 , and inferred T_0) of each reflection. For interval velocities, it is necessary to know T_0 , but this value corresponds to the instant the transmitting antenna first emitted its signal; this value is very difficult to know or determine (Annan, 2005). Fortunately, a proxy can be used, which is R_0 , or the time at which the receiving antenna first records a signal. R_0 is often substituted, as the difference between R_0 and T_0 is negligible. R_0 is related to T_0 by

$$R_0 = T_0 + \frac{s}{c} \quad (7)$$

where, s is the antennae separation, and c is the speed of light. In this paper, where the effects of negligible differences in average velocity are important, we tested to see if using R_0 would make a difference. R_0 is about 1.3 nanoseconds larger than T_0 . Finally, a third value of T_0 was used. This value, which can be inferred from $T^2 - X^2$ analyses, is the point at which the best-fit line crosses the y-axis and can be found in the equation

$$y = mx + b \quad (8)$$

where b is the T_0 value. This value of T_0 is the largest and is larger than R_0 by almost 1.5 nanoseconds.

As seen in Figure 49, these different analyses had significant effects on resulting interval velocities. For the most part, the general trends are the same, with the exception of the near offset analysis, which produced much higher velocities than the other methods. Variations in interval velocities within each layer range to more than 0.040 m/ns, which corresponds to a range of about -64 to +87 % of their mean.

The effect on depth estimates from the eight analyses of CMP PRO24 is portrayed in Figure 50. There is a great deal of variation among these methods, with the top of layer 1 ranging from about 0.90 meters to 1.1 meters. The thickness of this layer is also quite variable. The base of layer 4 varies by more than 20 centimeters. By selecting positions 2 or 5, the depth at which layer 1 occurs deepens, indicating these positions are not adequate in representing the appropriate depth at which it occurs.

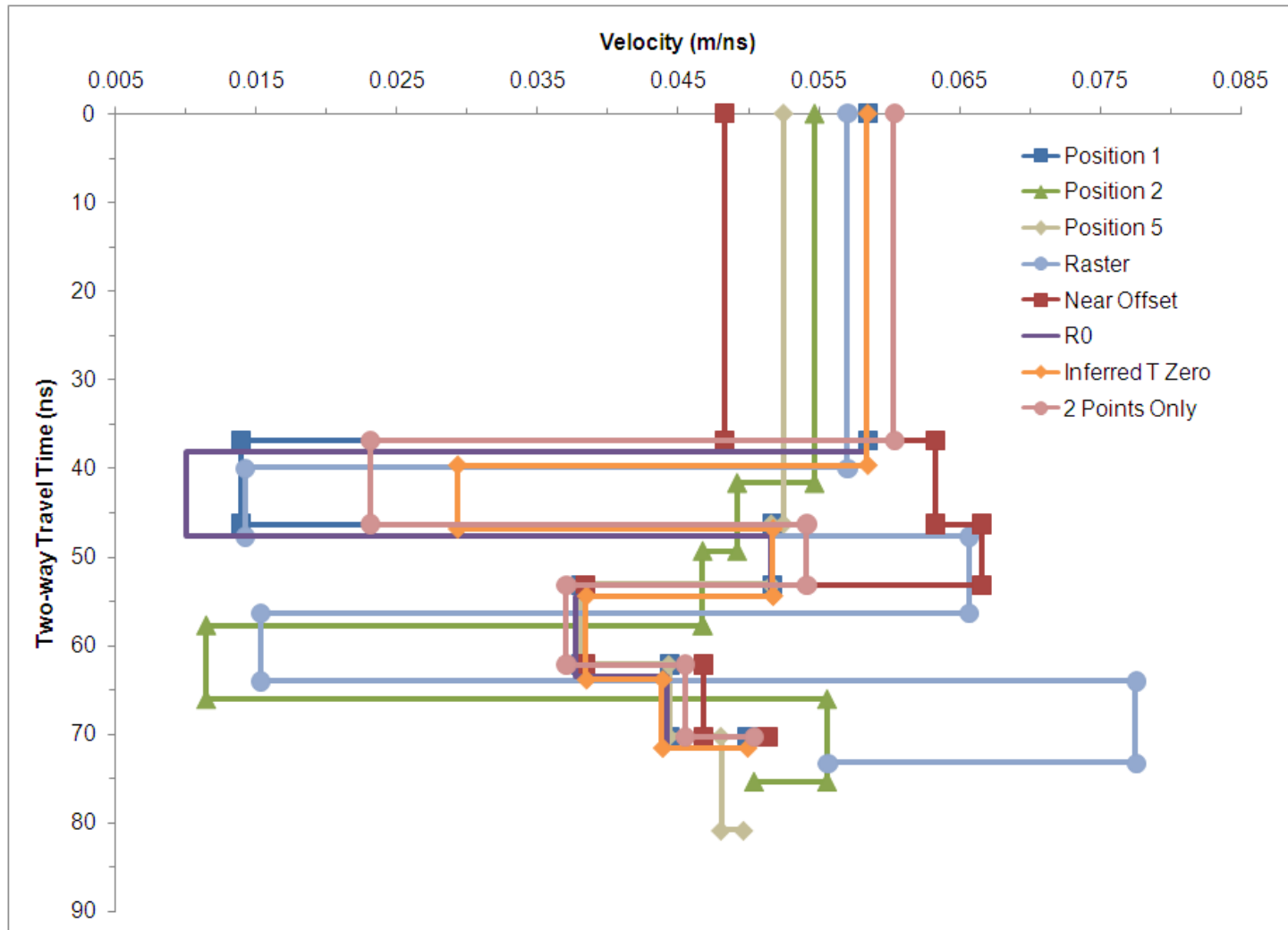


Figure 49: Interval velocities for CMP PRO24 based on all of the different picking strategies used in this paper.

CMP PRO 24

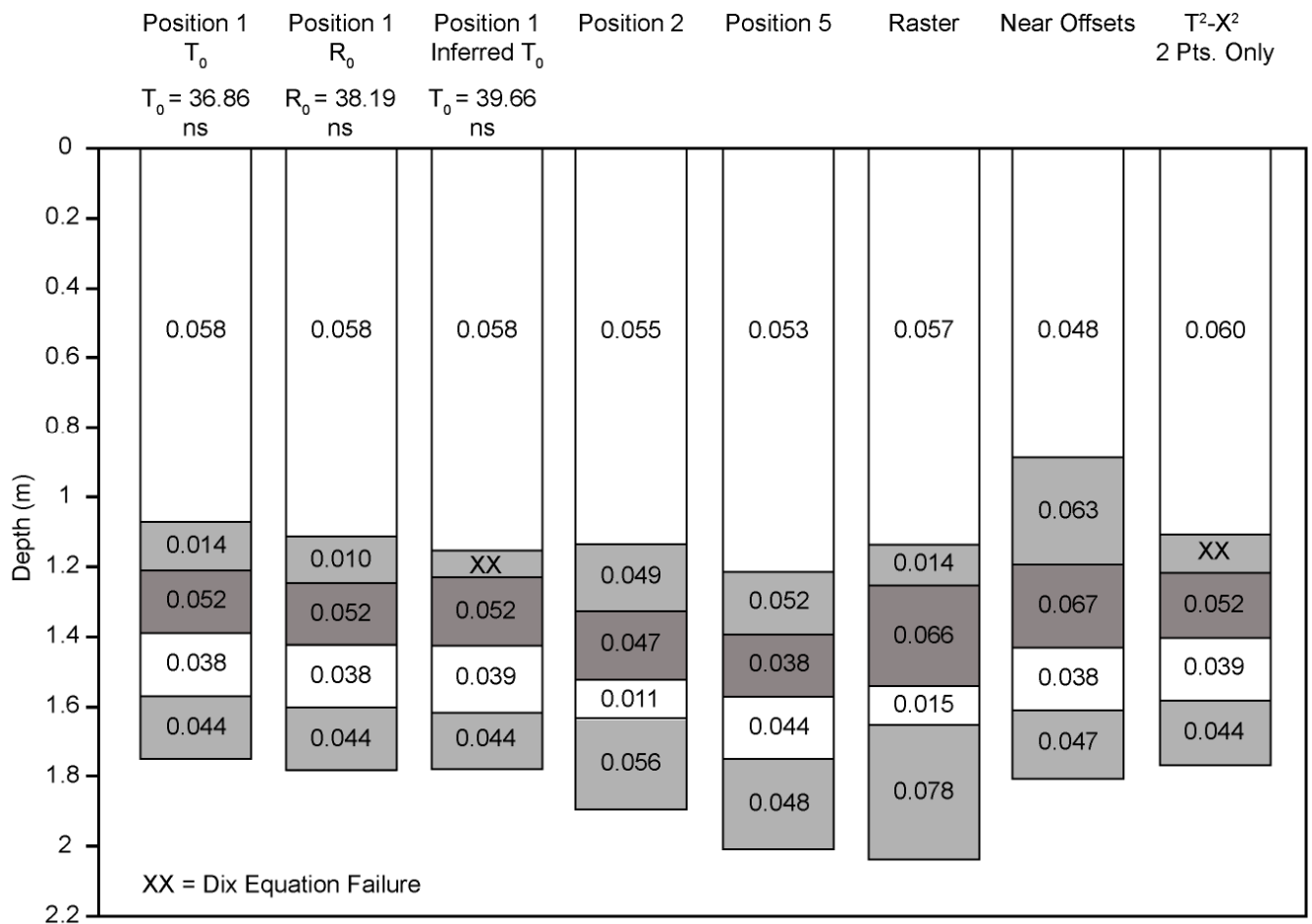


Figure 50: Depth sections for CMP PRO24, showing the effect of slight variations in velocity on corresponding depths. Numbers within boxes indicate interval velocities.

Near offsets affected interval velocities and depth estimates more than any other analysis. Although the effect of offset is significant, it is more than just the variation in waveform. It is also related to the non-hyperbolic behavior of reflections. Reflections are generally hyperbolic in shape, but they differ slightly from a true mathematical hyperbola (Yilmaz, 2001). This deviation is relatively small, but it is more significant for larger antenna separations (Annan, 2005, p. 432).

Conclusions

In all of the analyses presented here, noticeable to significant differences in velocity estimates resulted simply because of the specific picking criteria that were used. Yet, GPR articles that discuss the specific picking criteria used to calculate velocities are rare; those that discuss the robustness of their velocity calculations are even rarer. If we are to advance the science of CMP analyses, it is imperative to develop a standardized method for velocity analysis to be used by all GPR practitioners.

Slight errors in depth estimates can have a significant impact on the success of archaeo-geophysical studies, especially when GPR data are tied to excavations that extend only a meter or two in depth. Under ideal circumstances, all reflections generated in CMP profiles would be correlated directly with specific layers exposed in open excavation units, thereby highlighting (and quantifying) any resulting errors in depth estimates. If any errors were noted, several different velocity analyses could be performed on the CMP data to determine the technique that generated the most accurate depth estimates. At protected sites like Los Naranjos, where excavations are limited and invasive testing is discouraged, this is not immediately possible. Fortunately, we can use several proxies that allow for a direct comparison with what

should be, namely the synthetic CMP profile and the direct airwave which has a known velocity.

Based on the analyses performed in this paper, we have created several recommendations for best practice. First, to perform velocity analyses as consistently as possible, we recommend using wiggle trace images instead of raster images so that the same point along each trace can be picked consistently. Second, we recommend extending picks to offsets that are significant enough to correct for near-offset errors (in this paper, at least one meter). Third, based on strong correlations between calculated velocities with the synthetic CMP profiles and the expected direct airwave velocities, we recommend using position 1 for all velocity analyses. Position 2 (maximum peak) picks should be avoided, as they are affected by amplitude scaling and are also slower than expected values. Position 5 picks should also be avoided due to the discrepancy between these velocities and those expected from the direct airwave and the synthetic CMP velocities. Implied changes in T_0 will affect these analyses, resulting in what appears to be slower velocities that are due simply to different T_0 times. Although, under ideal conditions, picking position should not matter for either the direct air or direct ground wave, it does appear to have an effect on actual field data. Because we advocate being as consistent as possible, we recommend choosing position 1 for all picking. We also recommend using formal linear regression analyses that take into account each trace so that endpoint bias is not a significant factor. Finally, and most importantly, we advocate the dissemination of specific picking information in all papers that deal with CMP data so that a reader can determine the accuracy of such results.

Acknowledgments

CMP data discussed in this paper were collected during a joint Cornell University – University of California, Berkeley field program at Los Naranjos in 2003, directed by Professors John Henderson (Cornell) and Rosemary Joyce (Berkeley). This research is conducted under the auspices of the Instituto Hondureño de Antropología e Historia, and we greatly acknowledge their support of this research. We would also like to thank the students who participated in the Cornell-Berkeley program and helped collect these data. Sensor and Software's *EKKO_View Deluxe* was used for all of the initial data processing. All velocity analyses (i.e. picking) were performed in *ReflexW* (v. 4.5). Synthetic CMP profiles were generated in Landmark's *ProMax* software.

REFERENCES

- Al-Chalabi, M. (1974). An Analysis of Stacking, RMS, Average, and Interval Velocities Over a Horizontally Layered Ground. *Geophysical Prospecting*, 22: 458-475.
- Annan, A.P. (2005). Ground-Penetrating Radar. In: D.K. Butler (Editor), *Near-Surface Geophysics*. Society of Exploration Geophysicists, Tulsa, pp. 357-438.
- Annan, A.P. and Davis, J.L. (1976). Impulse radar soundings in permafrost. *Radio Science*, 11: 383-394.
- Baker, G.S., Jordan, T.E. and Pardy, J. (2007). An introduction to ground penetrating radar (GPR). In: G.S. Baker and H.M. Jol (Editors), *Stratigraphic Analyses Using GPR: Geological Society of America Special Paper 432*. Geological Society of America, pp. 1-18.
- Baudez, C.F. and Becquelin, P. (1973). *Archéologie de Los Naranjos. Mission Archéologique et Ethnologique Française au Mexique, Mexico*.
- Bristow, C.S. and Jol, H.M. (2003). An introduction to ground penetrating radar (GPR) in sediments. In: C.S. Bristow and H.M. Jol (Editors), *Ground Penetrating Radar in Sediments*. Geological Society, London, Special Publications, 211, pp. 1-7.

Clough, J.W. (1976). Electromagnetic Lateral Waves Observed by Earth-Sounding Radars. *Geophysics*, 41(NA6): 1126-1132.

Cook, E.E. and Taner, M.T. (1969). Velocity Spectra and Their Use in Stratigraphic and Lithologic Differentiation. *Geophysical Prospecting*, XVII(4): 433-448.

Cunningham, A.B. and Heffring, H.H. (1980). Interpretation of Velocity Spectra. *Geophysics*, 45(12): 1741-1752.

Daniels, D.J. (Editor), (2004). *Ground Penetrating Radar 2nd Edition*. IEE Radar, Sonar, Navigation and Avionics Series 15. The Institution of Electrical Engineers, London.

Dinstel, W.L. (1971). Velocity Spectra and Diffraction Patterns. *Geophysics*, 36(2): 415-417.

Dix, C.H. (1952). *Seismic Prospecting for Oil*. Harper and Brothers, New York.

Fisher, E., McMechan, G.A. and Annan, A.P. (1992a). Acquisition and Processing of Wide-Aperture Ground-Penetrating Radar Data. *Geophysics*, 57(3): 495-504.

Fisher, E., McMechan, G.A., Annan, A.P. and Cosway, S.W. (1992b). Examples of Reverse-Time Migration of Single-Channel, Ground-Penetrating Radar Profiles. *Geophysics*, 57(4): 577-586.

Franks, F. (1972). *Water, a comprehensive treatise*, 1. Plenum Press, New York.

- Gerlitz, K., Knoll, M.D., Cross, G.M., Luzitano, R.D. and Knight, R. (1993).
Processing Ground Penetrating Radar Data to Improve Resolution of Near-Surface Targets, Proceedings of the Symposium on the Application of Geophysics to Engineering and Environmental Problems, Edited by Ronald S. Bell and C. Melvin Lepper, pp.561-574, San Diego, CA.
- Grasmueck, M. (1994). Application of Seismic Processing Techniques to Discontinuity Mapping with Ground-penetrating Radar in Crystalline Rock of the Gotthard Massif, Switzerland, Proceedings of the Fifth International Conference on Ground Penetrating Radar, June 12-16, Kitchener, Ontario, Canada: 1135-1149., Waterloo Centre for Groundwater Research, Waterloo, Ontario, Canada.
- Greaves, R.J., Lesmes, D.P., Lee, J.M. and Toksöz, M.N. (1996). Velocity variations and water content estimated from multi-offset, ground-penetrating radar. *Geophysics*, 61(3): 683-695.
- Green, C.H. (1938). Velocity Determination by Means of Reflection Profiles. *Geophysics*, 3(4): 295-305.
- Jol, H.M. and Bristow, C.S. (2003). GPR in sediments: advice on data collection, basic processing and interpretation, a good practice guide. . In: C.S. Bristow and H.M. Jol (Editors), *Ground Penetrating Radar in Sediments*. Geological Society, London, Special Publications, 211, pp. 9-27.

- Joyce, R.A. (2004a). Unintended consequences? Monumentality as a novel experience in Formative Mesoamerica. *Journal of Archaeological Method and Theory*, 11(1): 5-29.
- Joyce, R.A. (2004b). Unprecedented Projects: The Birth of Mesoamerican Pyramids. *Expedition*, 46(2): 7-11.
- Joyce, R.A. and Henderson, J.S. (2002). La arqueología del periodo Formativo en Honduras: nuevos datos sobre el «estilo olmeca» en la zona maya. *Mayab*, 15: 5-17.
- Kearey, P., Brooks, M. and Hill, I. (2002). *An introduction to geophysical exploration*. Blackwell Scientific Publications, Oxford, England.
- Neal, A. (2004). Ground-penetrating radar and its use in sedimentology: principles, problems and progress. *Earth-Science Reviews*, 66(3-4): 261-330.
- Reynolds, J.M. (1997). *An Introduction to Applied and Environmental Geophysics*. John Wiley & Sons, Chichester.
- Schuster, A. (1909). *An introduction to the theory of optics*. E. Arnold, London.
- Sensors & Software Inc. (2003). *EKKO_View Enhanced & EKKO_View Deluxe*, Mississauga, ON.

- Sheriff, R.E. (1976). Inferring Stratigraphy from Seismic Data. The American Association of Petroleum Geologists Bulletin, 60(4): 528-542.
- Sheriff, R.E. and Geldart, L.P. (1995). Exploration seismology. Cambridge University Press, Cambridge; New York.
- Taner, M.T. and Koehler, F. (1969). Velocity Spectra - Digital Computer Derivation and Applications of Velocity Functions. Geophysics, 34(6): 859-881.
- Yelf, R. (2004). Where is true time zero?, Proceedings of the Tenth International Conference on Ground Penetrating Radar, 20-24 June, Delft, The Netherlands., Evert Slob, Alex Yarovoy and Jan Rhebergen (editors). Delft University of Technology, The Netherlands and the Institute of Electrical and Electronics Engineers, Inc., Piscataway, New Jersey: 279-282.
- Yilmaz, Ö. (2001). Seismic data analysis: processing, inversion, and interpretation of seismic data. Society of Exploration Geophysicists, Tulsa, OK.

CHAPTER 4

DISCRIMINATION OF BURIED ARTIFACTS AT LOS NARANJOS, HONDURAS USING THREE-DIMENSIONAL MIGRATION OF GROUND-PENETRATING RADAR (GPR) DATA AND MAGNETOMETRY DATA

Abstract

Three-dimensional migration, rarely applied to ground-penetrating radar (GPR) data at archaeological sites, has proven critical to the interpretation of GPR results from the early Mesoamerican archaeological site of Los Naranjos, Honduras. In one particular dataset, numerous diffraction hyperbolae dominate the GPR cross-sections, ranging in depth from about 0.30 to 1.20 meters. Although these diffractions vary in amplitude, discriminating among them on the unmigrated imagery is problematic at best. Two-dimensional migration suggests differences in diffractor shape, but only 3D migration provides the necessary detail to identify anomalous features. The most distinctive diffractor on the 3D migrated imagery corresponds with a prominent magnetic anomaly. The dimensions of this diffractor, as deduced from the 3D imagery, and its magnetic properties suggest that this feature may correspond to buried sculpture with a basaltic composition, rather than detrital rocks (limestone) or building blocks (sandstone) shed from nearby structures. We suggest that this feature marks a previously unrecognized sculpture similar to the distinctive Olmec-style columns and statuary that have already been recovered at the surface of Los Naranjos.

Introduction

The archaeological site of Los Naranjos is located on the northwestern shore of Lake Yojoa, within the present-day Department of Cortés in central Honduras (Figure

51). The site has attracted attention for more than seven decades (Stone, 1934; Strong *et al.*, 1938; Yde, 1936; Yde, 1938b), and the detailed site maps and descriptions of stratified sedimentary deposits produced by these early endeavors have proven invaluable for modern researchers. Recent excavations (Baudez and Becquelin, 1973; Henderson and Joyce, 2003; Henderson and Joyce, 2004; Joyce and Henderson, 2002) within a portion of the site known as the Principal Group documented a series of occupations that date continuously from the Early Formative to the Early Postclassic Periods (1100 B.C. – A.D. 1200), making Los Naranjos a very early Mesoamerican archaeological site. The Principal Group of Los Naranjos is an area of about 2 hectares that contains large earthen platform mounds, several low flat mounds, terraces, and plazas (Figure 52). Of special interest to this study is the small number of Olmec-style sculptures recovered at the surface of this site (Joyce and Henderson, 2002) because they possibly relate to a feature of interest that was generated in the geophysical data.

Researchers from Cornell University and the University of California, Berkeley initiated a joint archaeological field program at Los Naranjos in 2002. Excavations during the summers of 2003 and 2004 were somewhat limited in extent, but they documented the presence of Early and Middle Formative communities that lived adjacent to Structure IV (Figure 53) (Henderson and Joyce, 2003; Henderson and Joyce, 2004; Joyce and Henderson, 2002), which is the second largest platform mound within the Principal Group. As part of their research, they requested that non-invasive geophysical methods be used to map the presence and extent of these early communities.



Figure 51: Location of Los Naranjos, on the northwestern shore of Lake Yojoa. The site is located within the present-day Department of Cortés in Central Honduras.

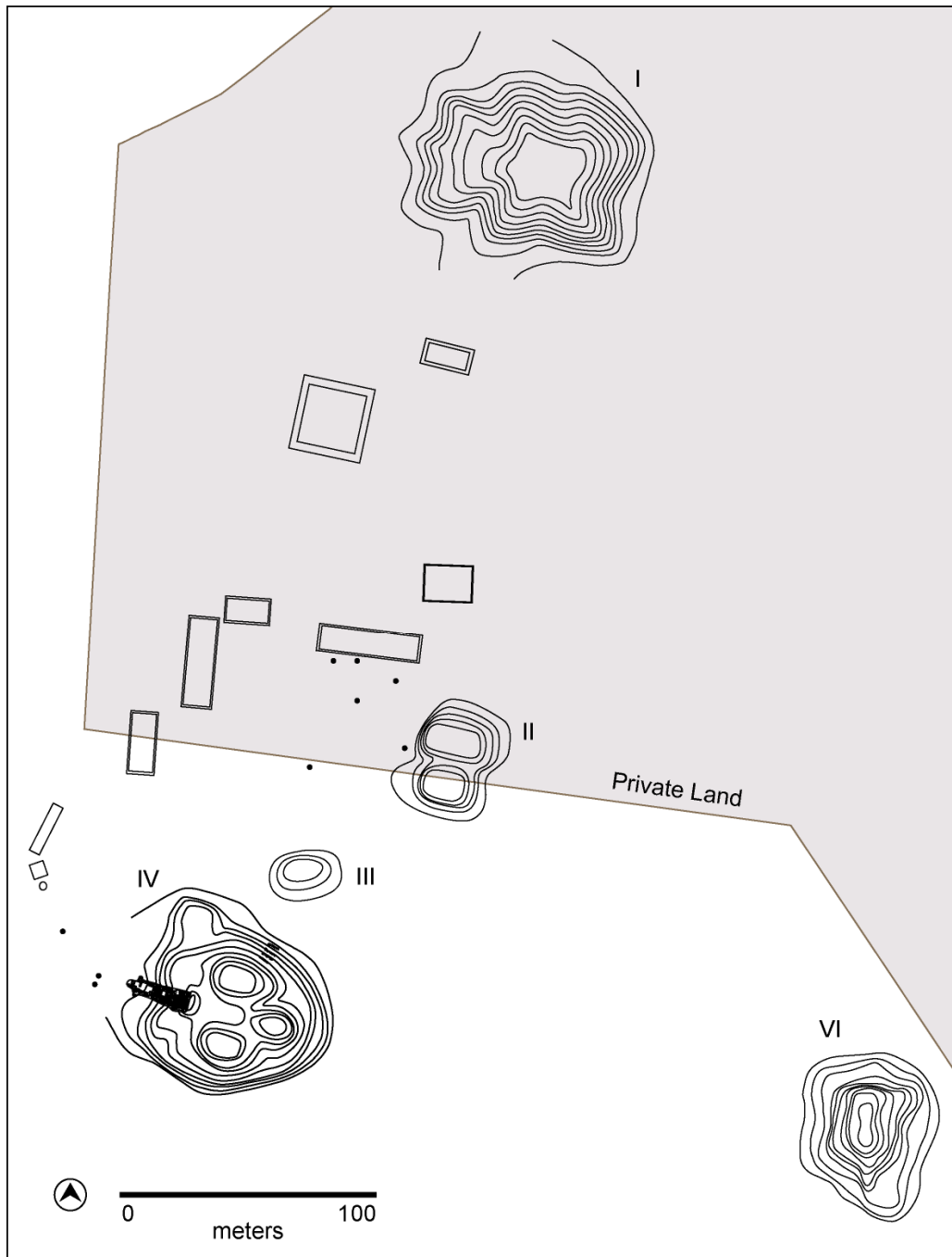


Figure 52: Principal Group of Los Naranjos. All geophysical research was conducted to the north of Structure IV. Small black dots indicate the approximate locations of sculpture previously located at the surface of the site. The basemap is modified from Baudez and Becquelin (1973), Cruz C. and Valles Pérez (2002), and Dixon *et al.* (2001).

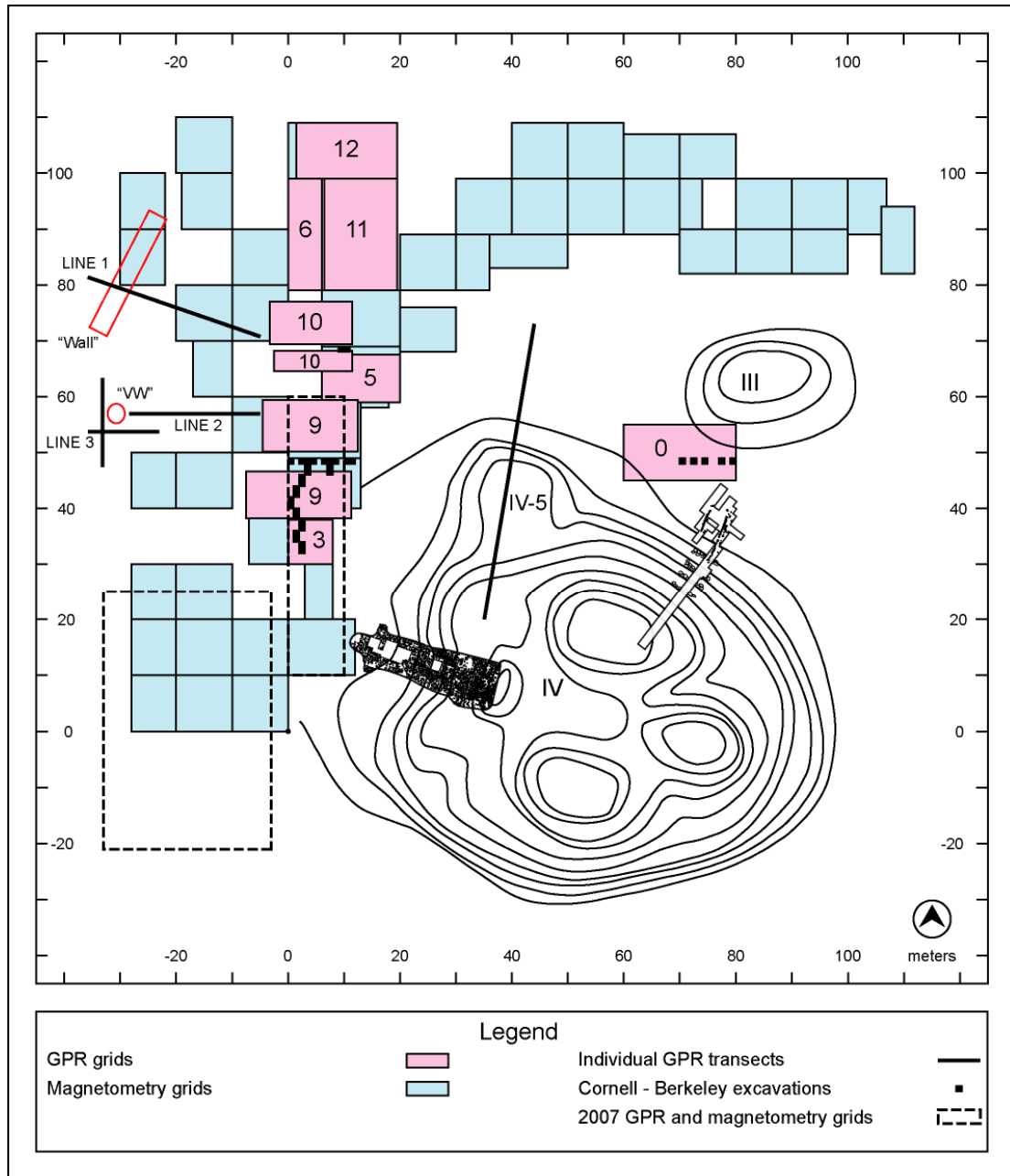


Figure 53: Location of all geophysical grids at Los Naranjos in relation to Structure IV. Note stone-lined ramp on west side of Structure IV.

Beyond the obvious pedagogical objectives, a goal of the geophysical data collection was to test the efficacy of these methods in delineating archaeological and geological subsurface features at this site, as they represented some of the first uses of

geophysical methods at archaeological sites in Honduras. Initially, it was hoped that the results of the geophysical surveys could be used to plan all of the archaeological excavations, but the logistics of the field program prevented all data from being analyzed prior to the establishment of test units. As a result, many of the features of interest imaged in the geophysical data were not excavated. Nevertheless, the results of these surveys helped to identify archaeological features in the subsurface, define 3D geometric relationships between features partially excavated, and establish geological context without excavations. The application of geophysical methods at Los Naranjos is particularly significant since a portion of the site is preserved as the *Parque Arqueológico – Ecológico Los Naranjos* (Navarro Tábora, 2004) and is protected from further destructive excavations (Cruz C. and Valles Pérez, 2002). In chapters 5 and 6 of this dissertation, the principal results from the GPR studies at Los Naranjos are reviewed. Here we focus on a specific subset of the GPR data wherein three-dimensional migration, combined with joint analyses of the magnetometry data, has proven particularly valuable in discriminating archeological features without excavation.

Prior to this research, geophysical methods had only been applied to a handful of research projects at archaeological sites in Honduras (Blaisdell-Sloan, 2006; Luke *et al.*, 1997; Luke and Brady, 1998; Pastor, 2003; Stierman, 2004; Stierman and Brady, 1999; Tchakirides, 2007; Tchakirides *et al.*, 2005). To date, there have only been geophysical surveys at about 20 archaeological sites throughout the rest of Mesoamerica (Aitken and Stewart, 2004; Breiner and Coe, 1972; Chávez *et al.*, 2001; Chavez *et al.*, 2009; Conyers, 1995; Fowler *et al.*, 2007; Hesse *et al.*, 1997; Karlberg and Sjöstedt, 2007; Lopez-Loera *et al.*, 2000; Morrison *et al.*, 1970a; Ovando-Shelley and Manzanilla, 1997; Sauck *et al.*, 1998; Sheets, 1985; Valdes and Kaplan, 2000; Welch, 2001). Thus, in this region the full potential of geophysical methods has not

been realized as it has at archaeological sites in other parts of the world (e.g. Conyers, 2004; Kvamme, 2003).

Platform Mounds and Sculpture

Structure IV is the southernmost large earthen platform mound within the Principal Group and measures about 100 meters by 90 meters (Figure 53). The main section of the platform mound is 7 meters tall, but 4 small structures on the top add another 3 meters in height. Baudez and Becquelin (1973) suggested that Structure IV became an expansive structure during the Middle Formative (Table 3), as presumed Jaral phase artifacts were recovered from the deepest levels. A re-analysis of their data and stratigraphic profiles suggests it was originally constructed during the Early Formative as a modest platform that might have been built as an extension of an existing household (John Henderson, personal communication), with major expansion and enlargement not occurring until the early part of the Middle Formative (Table 3).

Table 3: Mesoamerican time periods and associated date ranges (modified from Joyce, 2004a).

Period:	Date Range:
Postclassic	A.D. 1000 – 1521
Late Classic	A.D. 600 – 1000
Early Classic	A.D. 250 – 600
Late Formative	400 B.C. – A.D. 250
Middle Formative	900 – 400 B.C.
Early Formative	1600 – 900 B.C.
Archaic	8000 – 1600 B.C.

More recent excavations in the area adjacent to Structure IV uncovered evidence for Early Formative occupations, but none of Middle Formative occupations (Henderson and Joyce, 2004). The Middle Formative expansion of Structure IV reflects a significant change in the use of space and coincides with important social changes seen in many other parts of Mesoamerica at this time (Dixon *et al.*, 1994; Joesink-Mandeville, 1987). The west slope of Structure IV, lined with flat paving stones (Figure 53), provided the presumed point of access to the summit. If this structure was no longer an extension of an elite household, but the focus of a new kind of public space (i.e. monumental architecture), residential structures may no longer have been appropriate in the area that served as its main access. Middle Formative burials located within Structure IV revealed evidence of wealth and the creation of distinction in objects such as large jade ear spools (Baudez and Becquelin, 1973), indicating Structure IV had ceremonial significance during this time period.

Excavations on an extension added to the north side of Structure IV (labeled IV-5 in Figure 53) uncovered several rooms of a house that dates to the Late Formative (Baudez and Becquelin, 1973). Additional excavations on the northeastern face of Structure IV (Figure 53) aimed to locate house floors, burials, or other evidence of occupation (Baudez and Becquelin, 1973). These excavations uncovered a series of limestone blocks that had formed lower courses of walls. Some basalt blocks were found closest to Structure IV. The rocks were discovered beginning at depths of about 1.2-1.3 meters. It is not clear from these excavations if the walls represent a house foundation, but it seems unlikely that a house would have been built on the steep side of the platform mound (Baudez and Becquelin, 1973). If these walls do represent a structure, it is possible that the house originally extended to the north of Structure IV, an area that corresponds to GPR Grid 0 in our study (Figure 53).

Olmec-style sculptures are believed to have been associated with Structure IV. The earliest record of them appeared in the literature in 1934 when Doris Stone visited the site after learning of the presence of carved stone from a resident in the Ulúa Valley (Stone, 1934). She described four sculptures located within the Principal Group that had either traditional Olmec or Maya styles (Figure 54). Monuments 1 and 2 (Figure 54), a combination of a serpent/shark head and an anthropomorphic head, respectively, are similar in style to sculptures found at the Olmec site of La Venta (Joyce and Henderson, 2002). Monuments 3 and 4 (Figure 54), which Stone (1934) attributed to Maya forms standing in submission, more likely represent Olmec-style forms of an anthropomorphic figure and transformation figure, respectively (Joyce and Henderson, 2002). [Joyce and Henderson (2002) later designated monument numbers]. The original locations of these Olmec-style sculptures remain uncertain, but since early researchers found them within the Principal Group, including near Structure IV (Figure 52), their location in open spaces adjacent to platform mounds suggests they are likely public monuments or displays that delineated and segregated the space (Cyphers, 1999; Grove, 1999; Joyce and Grove, 1999; Love, 1999). Geophysical methods have successfully located sculpture at the Olmec site of La Venta (Breiner and Coe, 1972), and it was hoped that they would be similarly successful at Los Naranjos.



Figure 54: Olmec-style sculpture recovered previously at the surface of Los Naranjos. Monument 1: combination of a serpent / shark head ; Monument 2: anthropomorphic head ; Monument 3: anthropomorphic figure; Monument 4: transformation figure. Sculpture interpretations are from Joyce and Henderson (2002).

Geophysical Data Collection at Los Naranjos

Ground-penetrating radar is an active geophysical method that transmits electromagnetic energy into the ground and receives the resulting signals after they have reflected off subsurface features or interfaces (Conyers, 2004). Variations in the electrical properties of subsurface materials cause the transmitted signal to travel at a different velocity. A portion of the energy is reflected back to the surface at each change in velocity and is denoted the relative dielectric permittivity (RDP) or relative dielectric contrast (Annan, 2005). Reflection profiles provide a cross-sectional view of the subsurface and are useful for viewing stratigraphy and structure of subsurface materials. All cross-sectional images display data in two-way travel time measured in nanoseconds (1×10^{-9} seconds), as well as in corresponding depths computed using velocity information obtained *in situ* from common mid-point (CMP) data (Jol and Bristow, 2003; Tchakirides and Brown, in prep).

Magnetometry is a passive geophysical method that measures deviations in the Earth's magnetic field that can be caused by anthropogenic features that have a strong

magnetic susceptibility in contrast with the surrounding matrix. Examples of such features with a thermoremanent magnetization are hearths, kilns, or burned house floors (Kvamme, 2003). Features constructed from intrinsically magnetic materials, such as basalt, also generate strong magnetic anomalies due to the alignment of iron-rich minerals (Burger *et al.*, 2006).

As part of a joint Cornell University – University of California, Berkeley field program during the summer of 2003 (Figure 53), GPR data collection involved 50, 100, 200, and 250 megahertz (MHz) (1×10^6 Hz) antennae. Closely-spaced orthogonal lines that resulted in 3D grids comprise the majority of data collected (Figure 53). Several individual transects (Figure 53), also known as “wildcat surveys” because they are geared towards reconnaissance of features worthy of further study (Berg and Bruch, 1982), completed the 2003 data collection at Los Naranjos. During field testing, the 200 MHz and 250 MHz antennae provided an adequate depth of penetration while still maintaining sufficient resolution of features (Conyers, 2004) and were thus chosen as the primary data collection parameters. Magnetometry covered a much larger area than the GPR surveys (Figure 53). Additional higher frequency (400 MHz) 3D GPR data and magnetometry data collected in 2007 (Tchakirides, 2007) complete the geophysical suite (Figure 53).

The focus of this paper is on data collected within Grid 0, a 20 x 10 meter grid located between the northeastern edge of Structure IV and the southern edge of Structure III (Figure 53). Nineteen individual two-dimensional data profiles, collected in a bi-directional survey mode, comprise Grid 0. Data points were collected every 5 centimeters along each profile, and individual profiles were spaced 50 centimeters apart. A time window of 70 nanoseconds proved to correspond to an adequate depth of penetration within this portion of the site. Using an average velocity of 0.060 m/ns calculated from six common mid-point (CMP) profiles from Los Naranjos

(Tchakirides and Brown, in prep), this time window corresponds to a depth of about 2 meters.

Unmigrated GPR data from Grid 0 contain more than 400 diffraction hyperbolae, with apices ranging from 10 to 40 nanoseconds, or about 0.3 to 1.2 meters depth. Some, or perhaps many, are likely due to naturally accumulated rocks or building detritus from the construction or subsequent alteration of Structure IV. Archaeological excavations (Operation 1) within this grid (Figure 55) encountered evidence of construction activity, including packed surfaces and building debris (numerous stones and fragments of wattle and daub) (Henderson and Joyce, 2003). Given the Olmec-style sculptures that have been previously found at Los Naranjos, however, it is certainly plausible that some of these hyperbolic reflections may mark such sculpture, or fragments thereof, still in the ground in a region not excavated or below the shallow Cornell – Berkeley excavations.

Grid 0 is the focus of this paper not only because the numerous hyperbolic diffractions generated in the GPR profiles make an excellent test case for 3D migration, but also because these data differ from almost all other GPR data collected at the site. Relatively few diffraction hyperbolae were generated in other cross-sectional GPR profiles from Los Naranjos. Instead, the data are dominated by complex stratigraphy, several geological deposition sequences, and possible faulting (Figure 56). This difference in the types of features visible in reflection profiles suggests that very different activities may have been taking place within this particular region of the site.

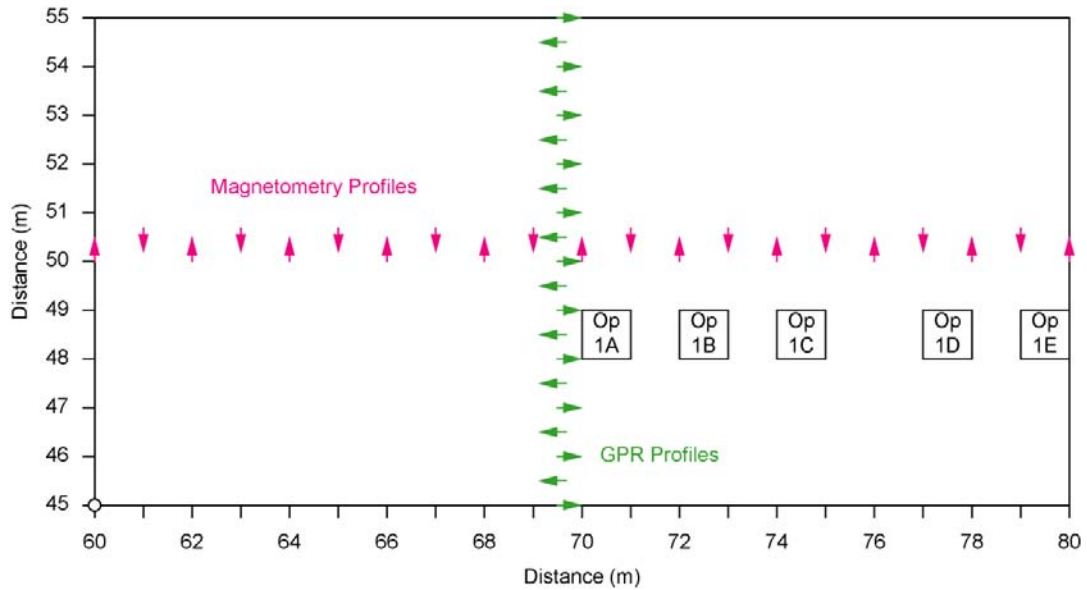


Figure 55: Location of Operation 1 (Op 1) excavation units within GPR Grid 0. Also noted are the locations and orientations of both the GPR and magnetometry data that were collected within this grid.

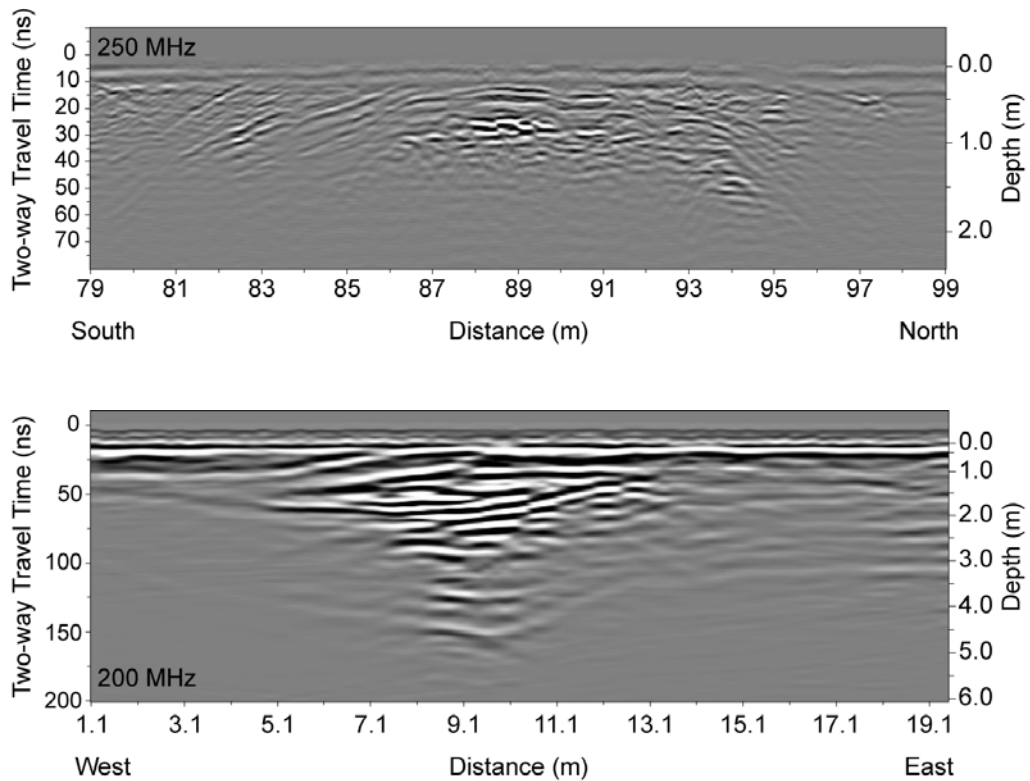


Figure 56: Examples of GPR data collected at Los Naranjos. Most other GPR data are dominated by complex stratigraphy, rather than numerous diffraction hyperbolae like that imaged in Grid 0. Vertical exaggeration = 2x.

When viewing unmigrated data, it is often difficult to determine the precise location of a diffracting body, as multiple diffractions from one small subsurface feature may appear on several parallel cross-sectional views. Pinpointing the true apex of the diffraction is important not just for locating specific features but also for calculating the velocity of the medium above the diffraction using hyperbolic curve-fitting analyses (Conyers, 1996). When calculating velocities using hyperbolic curve-fitting analyses, it is assumed that each diffraction was generated directly below the antennae, and not to the sides, thereby representing the apex of the diffracting body. Diffractions from the edges of an object will have a characteristically wider curvature, and therefore slower velocity than at its apex (Schilt *et al.*, 1981), so if a diffraction from the side of an object is misidentified as originating at its apex, the calculated velocity will be incorrect. Early attempts at quantifying the spatial distribution of these diffractions in unmigrated data were unsatisfactory (Tchakirides *et al.*, 2006a), mainly because it was not possible to discriminate sideswipe from inline diffraction energy. Three-dimensional migration has subsequently produced a more accurate view of the subsurface by repositioning energy to their correct subsurface source positions.

Migration

As the GPR system moves along the ground surface, electromagnetic energy radiates into the ground in a three-dimensional cone that is defined by the limits of the Fresnel zone (Lindsey, 1989). Thus, the GPR system images not just what is directly beneath the unit, but also in front, back, and to the sides (Meats, 1996). This type of energy pattern generates reflections from any point within the cone of transmission, but records them in a GPR profile as if they originated directly below the antennae (Kearey *et al.*, 2002; Neal, 2004; Yilmaz, 2001).

Fundamentally, the goals of migration are to correct GPR reflection data so that they accurately represent the subsurface (Neal, 2004) and to increase the resolution of features in reflection profiles (Hogan, 1988). There are many techniques for implementing migration. Here we use a form of Kirchhoff summation, in which energy is summed along an appropriate diffraction hyperbola, thus focusing reflected energy at its apex (Hogan, 1988; Schneider, 1978). Diffractions collapse back to their respective point sources. In general migration steepens and shortens reflections and moves them in the updip direction (Chun and Jacewitz, 1981) (Figure 57). When the correct parameters for migration are used, subsurface reflections will be relocated to the position corresponding to the physical location in the subsurface of the features that generated them. Thus migration is essential to correctly correlate specific features of interest in GPR data to geological or archaeological cross-sections.

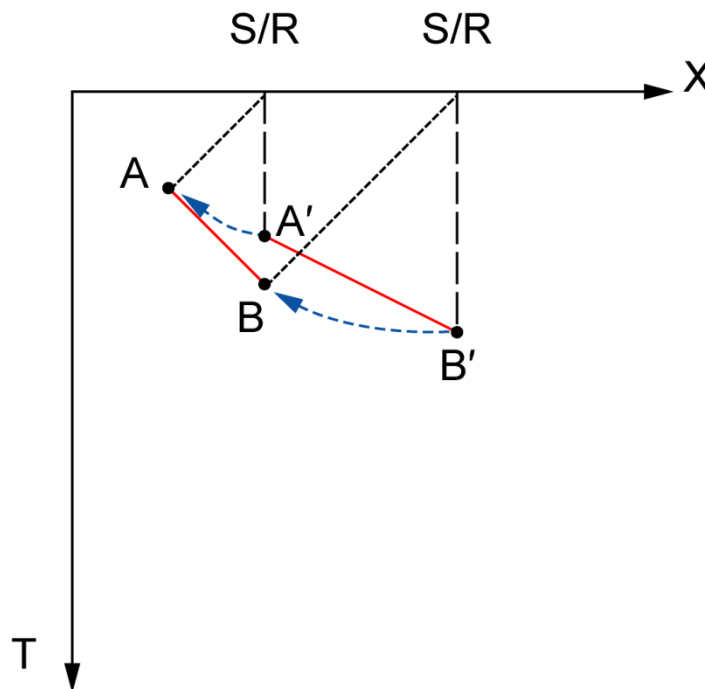


Figure 57: The process of migration. A'-B' is migrated to A-B, its correct location in the subsurface. Figure is modified from Chun and Jacewitz (1981).

Migration has been a standard processing technique in the seismic industry since it was used to process the first seismic data collected in the early 1920s (Bednar, 2005; Neal, 2004; Sheriff and Geldart, 1995), but its use has not been as widespread in GPR projects (Hogan, 1988). Recently, GPR practitioners began migrating data for sedimentological, geological, and geotechnical applications (Burke *et al.*, 2008; Fisher *et al.*, 1989; Fisher *et al.*, 1996; Lehmann and Green, 2000; Majjala, 1992; Neal, 2004). Although a few notable examples from the archaeological geophysics community have been published recently (Booth *et al.*, 2008; Leckebusch, 2000; Leckebusch and Peikert, 2001; Leucci, 2002; Leucci and Negri, 2006; Zhou and Sato, 2001), archaeological geophysicists have been slow to embrace this technique for a host of reasons, most likely related to the increased expense involved in collecting and processing three-dimensional data (Meats, 1996). The recent advances in some GPR data-processing programs means that migration is readily available on some standard data processing programs, including *EKKO Mapper 3* (Sensors & Software Inc., 2007), *ReflexW* (Sandmeier, 2006), and *GPR-Slice* (Goodman *et al.*, 1995), but some of these programs only allow for 2D migration.

In recent years, geophysicists, particularly those working at archaeological sites, have begun to collect true 3D GPR data (Booth *et al.*, 2008; Grasmueck *et al.*, 2004). These surveys differ from the standard pseudo-3D grids that are merely a collection of closely-spaced 2D profiles and usually employ a grid spacing of 0.1 to 0.2 meters in all directions. The results of their high-resolution research are promising, and many of the map and cross-sectional views show an improvement in the resolution of subsurface features. Unfortunately, it is still unrealistic for many GPR practitioners to collect such high-resolution data sets, given the increased cost of such time-consuming field projects.

In general, for three-dimensional migration to produce the most accurate results, a “true 3D” dataset is needed. A true 3D dataset is one in which data are sampled according to the Nyquist sampling theorem, which requires the distance between measurements not exceed one-quarter of a wavelength in all directions (Grasmueck *et al.*, 2004; Grasmueck *et al.*, 2005; Nyquist, 1928). In this survey, 250 MHz antennae were used, and an average velocity of about 0.060 m/ns was determined from *in situ* measurements (Tchakirides and Brown, in prep). Using these parameters, the resulting wavelength would be about 0.24 meters. Although the center frequency of this system is 250 MHz, the frequency of the transmitted signal for Grid 0 was only about 140 MHz (Figure 58). The actual wavelength, therefore, is about 0.43 meters. Given this wavelength, data would need to be collected approximately every 10 centimeters in both inline and cross-line directions to be considered unaliased (Nyquist, 1928). Although the inline spacing for Grid 0 (0.050 m) satisfies this requirement, the cross-line spacing of 0.50 meters considerably exceeds this criteria. Fortunately, aliasing is only a concern for steeply dipping reflectors that exceed angles of approximately 60 degrees (Grasmueck *et al.*, 2005). For this dataset (and the particular hyperbola of interest), most of the energy migrated occurs at angles of approximately 12 degrees (Figure 59), because that is where the majority of the energy is located. To calculate the wavelength accurately, the apparent velocity should be used, rather than the true velocity, as the apparent velocity is more important for reflections. Using a 0.50 meter transect spacing, a true velocity of 0.060 m/ns, and the actual transmitted frequency of 140 MHz, aliasing may be occurring when dip angles exceed 12.37 degrees (Figure 59). It is possible, therefore, that some aliasing of the GPR signal may occur, but we minimized this by selecting an appropriate aperture width (see below).

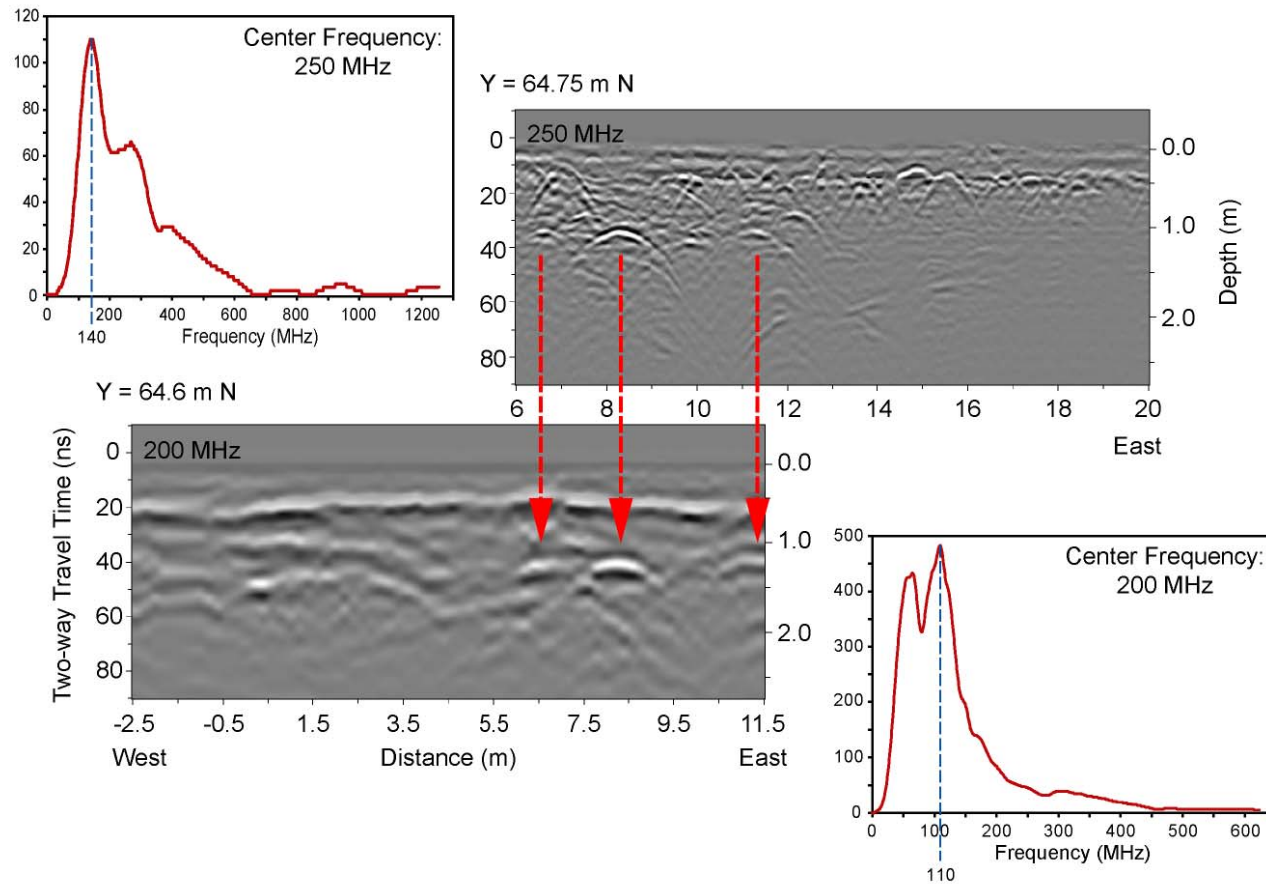


Figure 58: Comparison between the 250 MHz and 200 MHz data and corresponding frequency spectra. LINEX6475, collected in Grid 5, is the closest profile to LINEX646, collected within Grid 10. The three hyperbolae generated at about 35 nanoseconds are visible in both profiles, but the 250 MHz is able to resolve features better than its lower frequency counterpart. Corresponding frequency spectra show the ideal center frequency is not transmitted into the ground, but is downloaded by 44 % and 45 %, respectively.

Three-dimensional Migration

Prior to migration, the data were filtered with a high-pass “dewow” filter to remove signal saturation effects (low frequency “wow”) (Gerlitz *et al.*, 1993; Sensors & Software Inc., 2003). Wow can be introduced because of the electrical properties of the ground (Jol and Bristow, 2003) or when the transmitting and receiving antennae are too close to one another (Sensors & Software Inc., 2003). All cross-sectional reflection profiles shown in this paper have been dewowed.

The Kirchhoff method was selected for migration because it is a versatile and easily applicable migration algorithm (Bednar, 2005). Kirchhoff migration, also known as diffraction migration (Chun and Jacewitz, 1981), is governed by the principle that the radius of curvature of a diffraction hyperbola is directly related to the velocity of the medium in which it was generated and the time at which it occurs (Yilmaz, 2001). In a constant velocity medium, narrow diffraction hyperbolae have a slower velocity than diffractions that have a larger radius of curvature. In unmigrated data, hyperbolic diffractions are represented by:

$$t_D(X, x, z) = 2 \left[(t_0 / 2)^2 + ((x - X) / V)^2 \right]^{1/2} \quad (9)$$

where t , x , and z correspond to vertical positions within the earth, X represents horizontal position along a diffraction hyperbola, and V is the velocity of the subsurface feature (Hogan, 1988, p. 345).

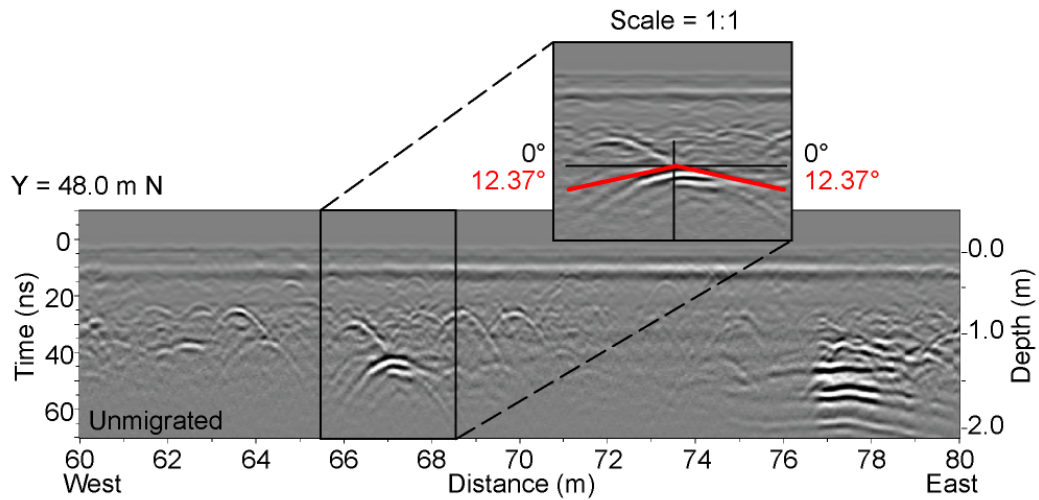


Figure 59: Dip angle affected by aliasing. Aliasing may occur when dip angles exceed 12.37 degrees. Vertical exaggeration of cross-sectional view is 2x. Scale of inset is 1:1.

A key parameter for Kirchhoff migration is aperture width (Yilmaz, 2001), which refers to the number of traces that are summed along each diffraction hyperbola. Aperture widths that are too small will result in poor lateral resolution, whereas large aperture widths can increase the chance of corruption by noise and lateral variations in subsurface velocity (Rastogi and Phadke, 2002). Selecting an aperture width that is appropriate for the data will result in focusing of energy along all diffractions without degrading the quality of the data in either the deep or shallow regions. In seismology, velocities may vary greatly with depth, thereby necessitating variable aperture widths based on specific time ranges. In this particular case, we found that GPR velocities do not vary significantly with depth (Tchakirides and Brown, in prep). Thus, use of a constant aperture width for migration of the Los Naranjos data was deemed adequate.

We determined an appropriate aperture width by trial and error, comparing results using 5, 15, 30, and 401 traces (the total number of traces in each profile)

(Figure 60). In the end, we selected a constant aperture width of 30 traces for 2D migration, as this aperture width adequately collapsed the diffraction hyperbolae of interest without introducing any discernable noise into the data. Given the in-line sampling of 0.050 m for all GPR data within Grid 0, the total summation width was 1.5 meters, comparable to the depth of interest. Three-dimensional migration needs to accommodate a much larger volume of data (Sandmeier, 2006), so it is not always possible to use a comparable aperture width. In our case, software limitations prohibited us from using an aperture width larger than 12 traces for this grid of data, so we used a constant aperture width of 12 traces for 3D migration.

A second key parameter for Kirchhoff migration is velocity (Yilmaz, 2001). For migration to work properly, velocity calculations should be accurate to within 10-20 %, or vary by no more than 0.010 – 0.020 m/ns from their actual value (Lehmann and Green, 2000, p. 836). Fortunately, we had available the results of detailed *in situ* velocity analyses at this site (Tchakirides and Brown, in prep), which indicated that a constant velocity of 0.60 m/ns was appropriate.

Y = 48.0 m N

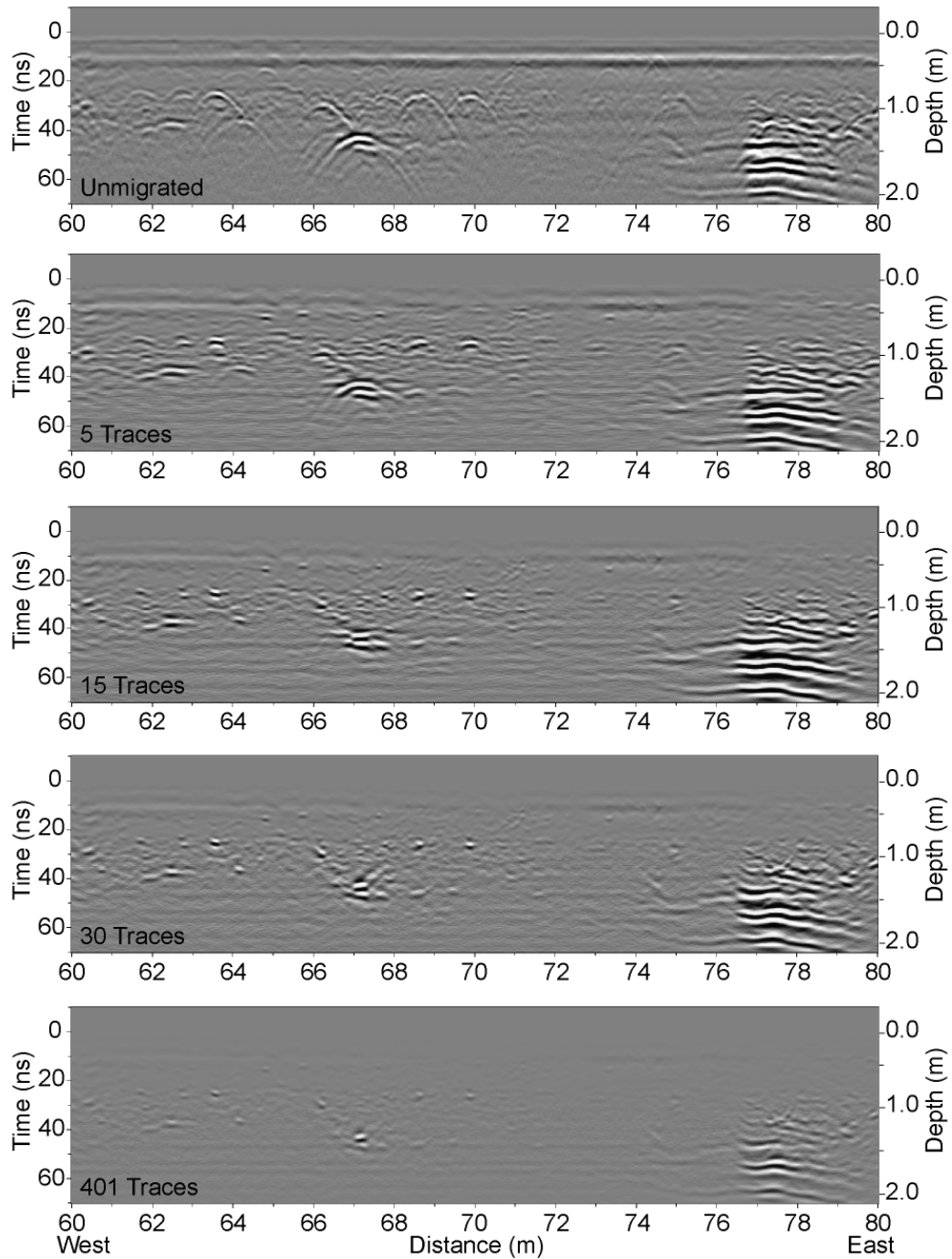


Figure 60: Comparison of aperture width for 2D Kirchhoff migration. Unmigrated data, aperture widths of 5 traces, 15 traces, 30 traces, and 401 traces (the total number of traces in each GPR profile) are shown. Vertical exaggeration = 2x.

The effect of three-dimensional migration is clear in Figure 61. In the unmigrated data from Grid 0 (Figure 61a), numerous subsurface features are suggested

by the many overlapping diffraction hyperbolae. While the diffraction hyperbolae are clearly visible, the details of the causative bodies are obscured the overlapping nature of the hyperbola tails as well as subtle variations in hyperbola curvature. Two-dimensional migration offers an improved representation of the subsurface (Figure 61b), with most major diffractions collapsed back to their apparent point sources. With the long diffraction tails gone, it is now easier to identify the specific locations of these features. These point sources are represented as small, high-amplitude features that are less than 50 centimeters in width.

The limitations of the 2D migration are only apparent when compared to the 3D results. In the 3D migrated image in Figure 61c, most of the individual point sources are much smaller in extent than their 2D migrated counterparts, evidence of the much greater resolution achieved. Moreover, approximately one-quarter of the point sources apparent on a given 2D images are no longer visible in the 3D migrated image (Figure 61b, c), presumably because they are due to out-of-plane features that had been mis-positioned along the 2D line.

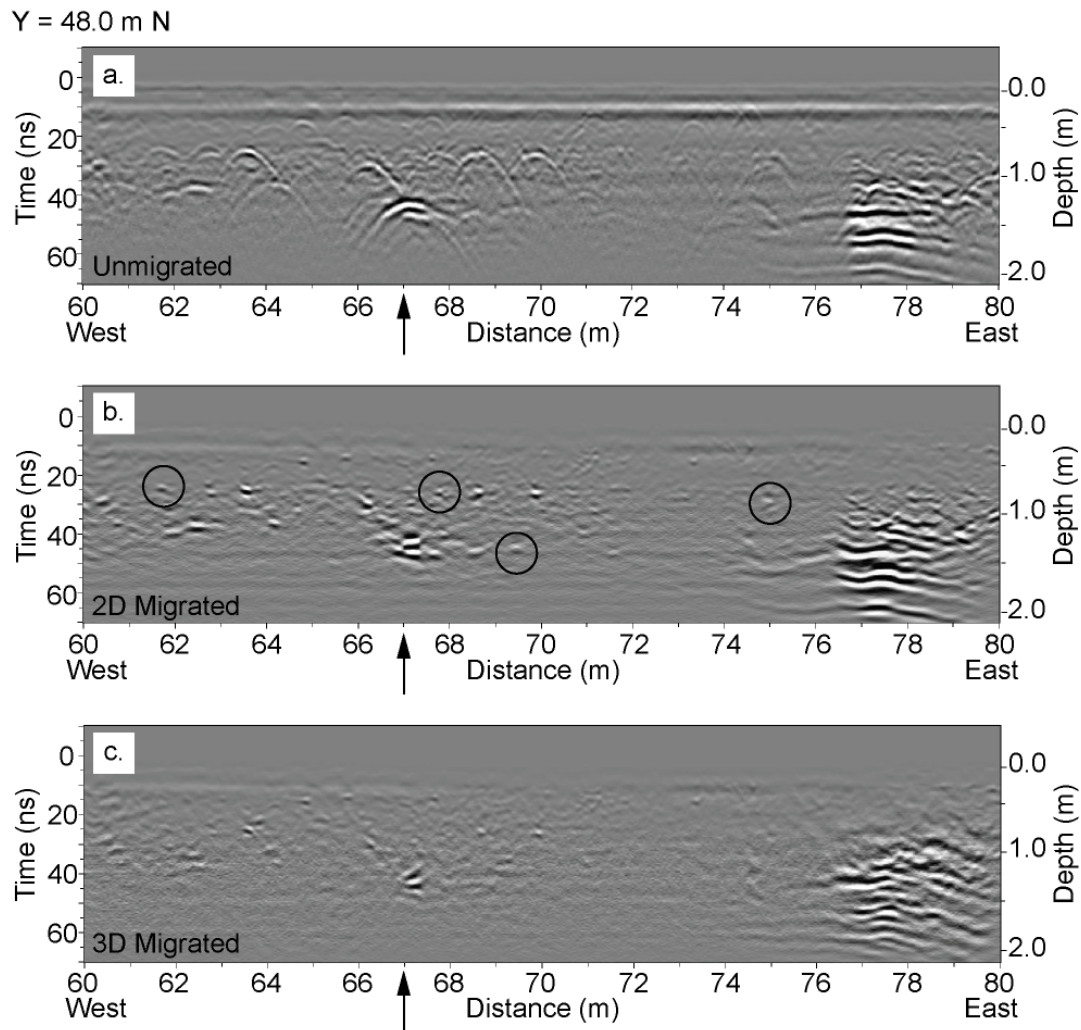


Figure 61: Comparison of unmigrated, 2D migrated, and 3D migrated views of GPR profile Y = 48.0 m N, located within GPR Grid 0. The high-amplitude feature discussed here is located at about 67 meters (indicated by black arrows). Black circles highlight several point sources that are no longer visible in 3D migrated data. Vertical exaggeration = 2x.

Discrimination of Diffractor Geometry

Hyperbolic diffractions in GPR data are usually interpreted as due to features that have dimensions that are smaller than one wavelength of the transmitted signal (Grasmueck and Weger, 2003 p. 1181). According to the estimated subsurface velocity and the actual frequency of the transmitted pulse, the effective wavelength is

about 43 centimeters. When the “envelope” (Sensors & Software Inc., 2003) of the 3D migrated cross-sectional views are plotted (Figure 62), it is possible to see that the dimensions of individual point sources are all approximately 40 centimeters or less. These point sources are roughly circular in shape and most are concentrated within the uppermost meter of the profile.

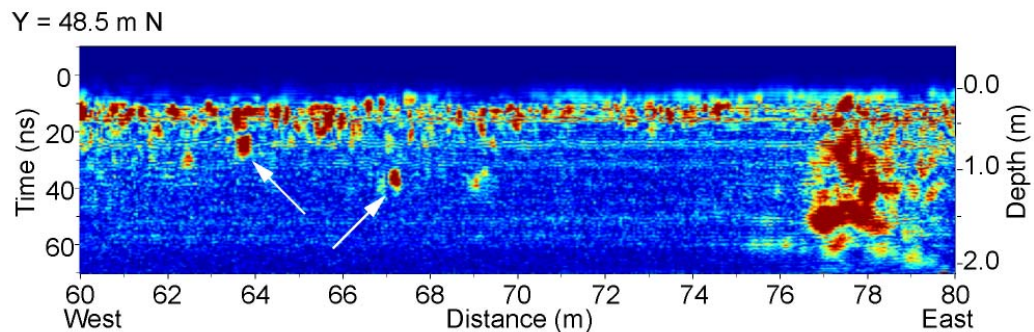


Figure 62: Envelope applied to a 3D migrated cross-sectional view from Grid 0. Individual point diffractors are visible as small red circular features, approximately 40 cm or less in diameter (white arrows highlight two of them). Note the feature at ~67 meters. Vertical exaggeration = 2x.

Most of the numerous point sources appear much like what we would expect from individual rocks in cross-sectional view. The limited shallow excavations within Grid 0 uncovered rocks that were similar in diameter to those imaged in the GPR data, suggesting we are mapping many more of these features than were excavated within Operation 1. Because of the sheer number of these point source features within this grid (and their lack within almost all other GPR grids), we suspect many may simply relate to rocks that once comprised the terrace walls that have since eroded down the slopes of Structure IV.

Among these numerous point sources, one feature stands out. The prominent diffraction hyperbola at 67 meters differs from the others in terms of its amplitude,

radius of curvature, depth (Figure 61), and 3D shape (Figure 63). This feature has the highest amplitude of any feature within Grid 0, the largest radius of curvature, and is located deeper than almost every other diffraction hyperbola. In unmigrated map view (Figure 63), this feature does not have a well-defined shape but has a maximum width of about 1 meter. In the 2D migrated image (Figure 63), the linearity of the feature is more pronounced. Comparison with the 3D migrated image suggests this feature is longer and narrower than that imaged with 2D migration, with a major axis that is about 1.5 meters long and about 0.5 meters wide (Figure 63).

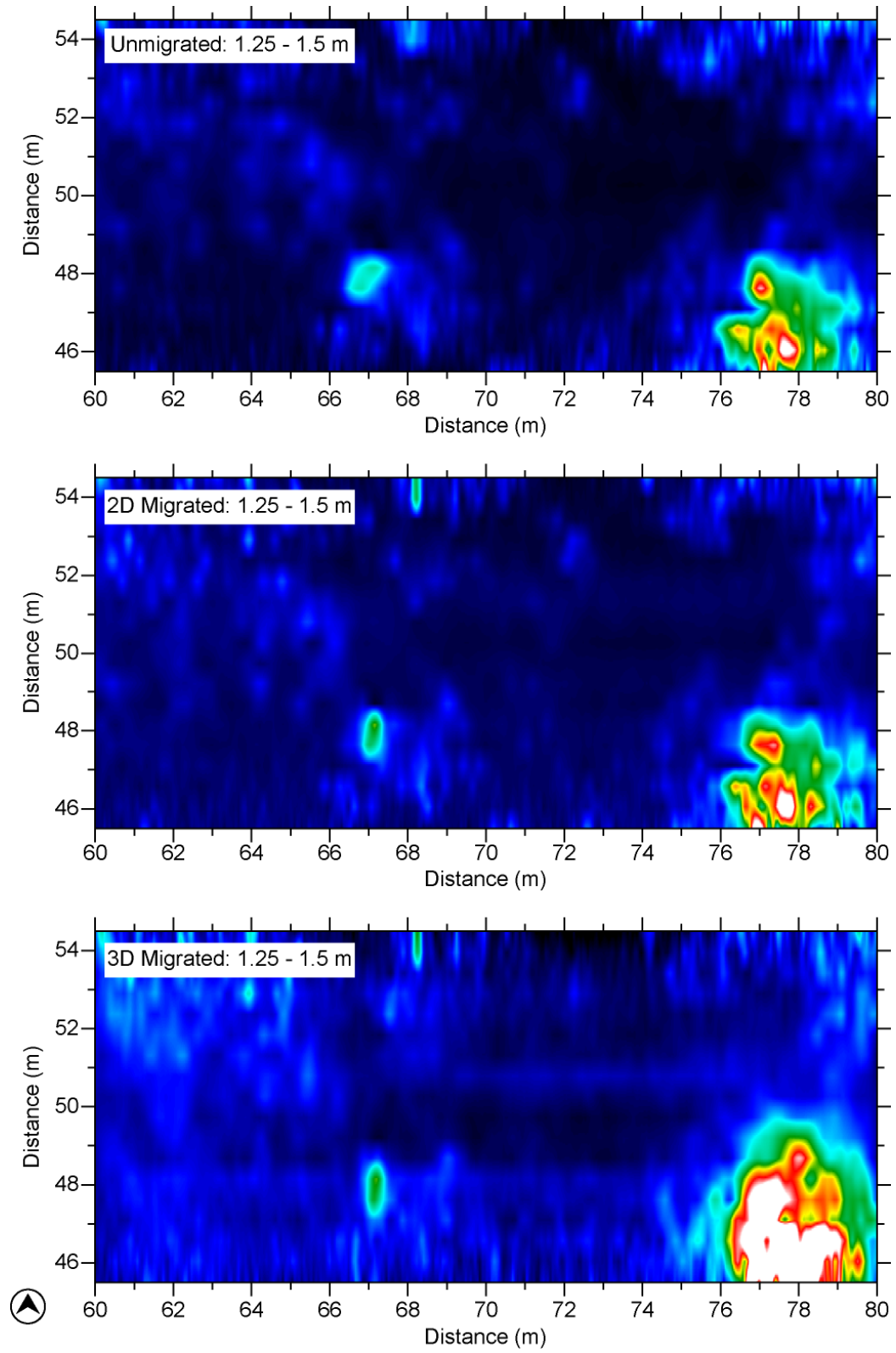


Figure 63: Comparison of unmigrated, 2D migrated, and 3D migrated plan view GPR images of the high-amplitude feature at $x = 67$ m from a depth of 1.25 – 1.5 meters.

Correlation with Magnetometry

Magnetometry data were collected in gradiometer mode, using two sensors that were oriented horizontally and spaced 1 meter apart. Because of this configuration, it is possible to view the data from the individual sensors as well as the horizontal gradients. Results of this survey are shown in Figure 64. The data from the left and right sensors are dominated by a large high-amplitude feature in the northeast corner of data (Figure 64), which correlates with the location of Structure III (Figure 53). Magnetometry data from the left sensor (Figure 64) and magnetic gradiometry data (Figure 64) from Grid 0 show a dipolar anomaly that overlies the GPR reflection feature of interest at $x = 67$ m, discussed above. Since magnetic objects are often located mid-way between the high- and low-amplitude portions of their resulting anomalies (Bevan, 2006), the source of this anomaly should lie at about 48 meters along profile $X = 67$. This corresponds well with the location of the high-amplitude diffraction in the GPR data. This same feature is not visible in the right sensor image (Figure 64), which implies that it is too localized to be imaged by that sensor given the configuration of the sensors during data collection. The higher amplitude of the magnetic anomaly of this particular feature compared with the signals from most of the other diffractor locations implies that its source consists of material with a higher magnetic susceptibility, for example basalt rather than non-magnetic limestone or sandstone.

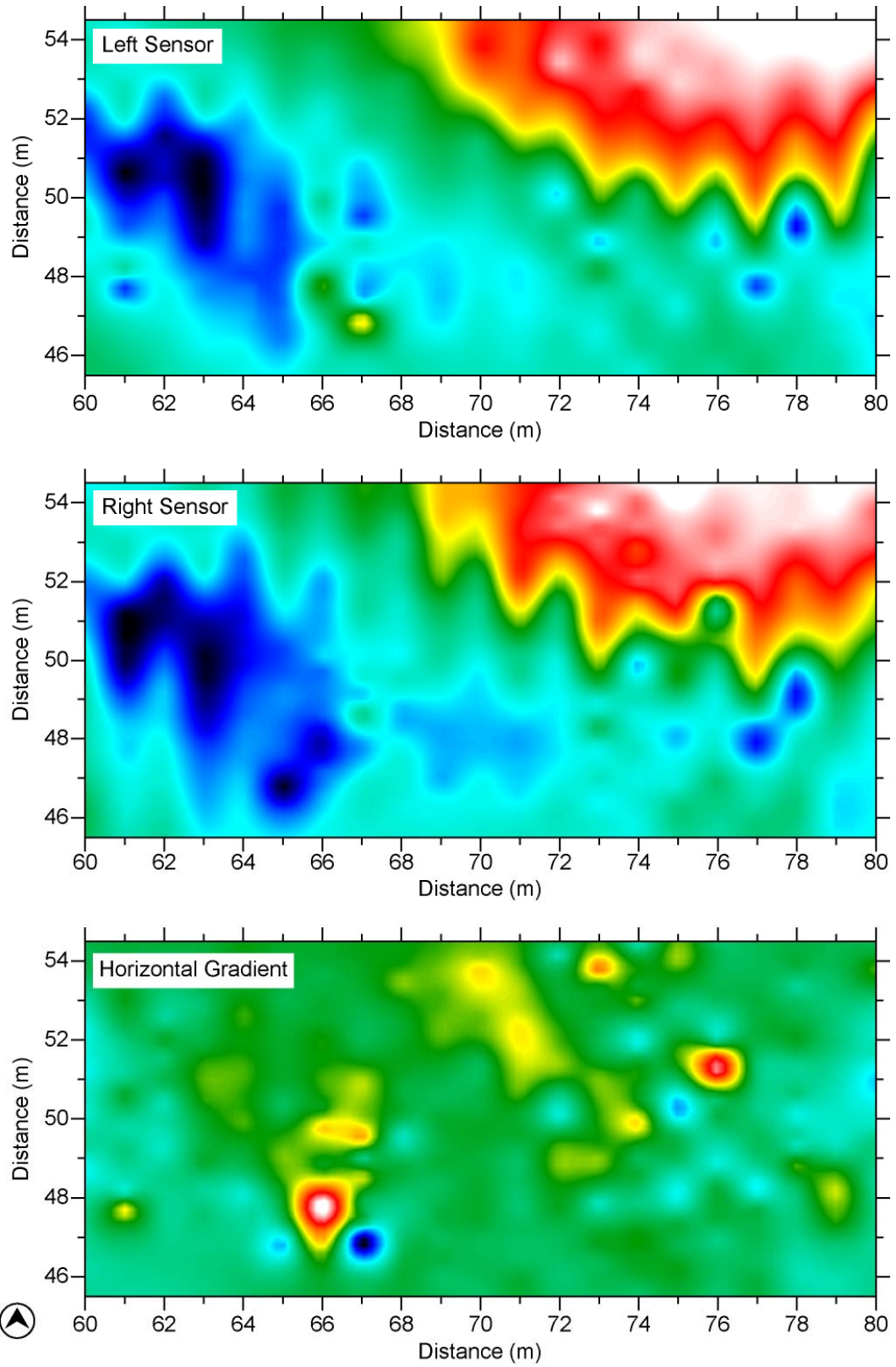


Figure 64: Comparison of magnetometry data collected within Grid 0.

To determine the likely lithology of this feature, we created a simple spherical model (e.g. Burger *et al.*, 2006, p. 468)

$$Z_A = \frac{\left(\frac{4}{3}\pi R^3 k F_E\right) \sin i}{\left(x^2 + z^2\right)^{\frac{3}{2}}} \left[\frac{3z^2}{\left(x^2 + z^2\right)} - \left(\frac{3xz}{\left(x^2 + z^2\right)} \cot i \right) - 1 \right] \quad (10)$$

where Z_A is the vertical induced magnetic field of the sphere; F_E is the Earth's magnetic field at the site (nT); k is the magnetic susceptibility of the feature (emu); i is the magnetic inclination of the site (degrees); R is the radius of the sphere (m); x is the horizontal position (m); and z is the depth to the center of the sphere (m).

The inclination of the Earth's magnetic field at Los Naranjos is 43.88°, and the total magnetic field was 39,087 nT on the day of data acquisition (NOAA, 2009). The sphere was assumed to lie with its center at the depth indicated by the GPR (i.e. 1.49 m), and its radius (0.25 m) was estimated from the wavelength of the GPR data. Magnetic susceptibility of 0.055 emu and 0.00003 emu were chosen to represent possible basalt and sandstone lithologies, respectively, (e.g. Telford, 1976, p. 121).

The anomalies computed from the spherical model assuming the feature is basalt are clearly a better fit to the observed anomaly than the sandstone alternative, even assuming the largest magnetic susceptibility value possible for a sandstone lithology (Telford, 1976). Limestone produced a similar result. The correlation between the basalt model and the data is not perfect (Figure 65), which may be attributed to a source geometry more complex than the simple sphere used to generate this model.

We propose here that this particular feature, based on its dimensions, material, and location, corresponds to a piece of buried sculpture, similar to the four Olmec-style basalt sculptures already documented on the surface of the site (Joyce and

Henderson, 2002). During our own field mapping within the Principal Group during the summer of 2006, we recognized previously unreported columns within the private property to the north of the site, to the west of Structure II (Figure 52). The presence of these columns suggests that additional columns or sculpture might still be located at the site, and possibly buried. If so, they would be expected to present a geophysical signature like that associated with the anomaly in Grid 0. We cannot rule out the possibility that this feature simply represents basalt detritus similar to the few stone blocks excavated at the base of Structure IV (Baudez and Becquelin, 1973). However, given the dimensions of this feature and the absence of other features of a similar size and amplitude in the immediate area, we suspect it represents a piece of buried sculpture instead.

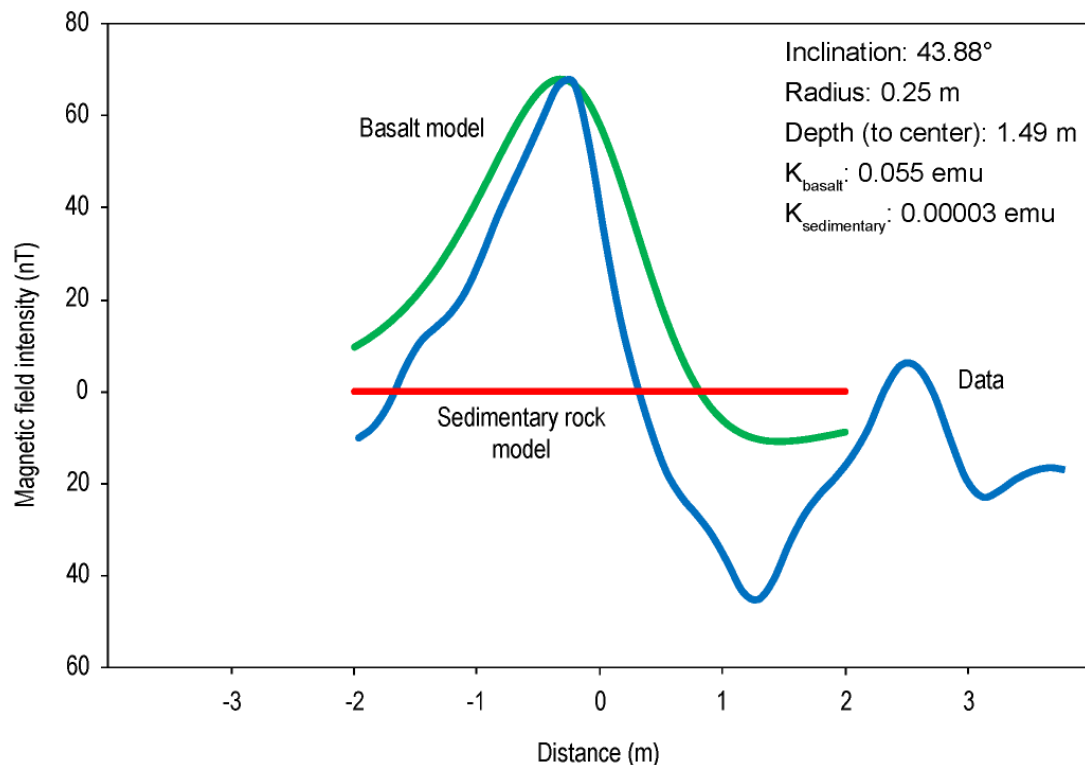


Figure 65: Comparison of basalt and sedimentary rock models with the actual magnetometry data collected over the high-amplitude feature generated in Grid 0. Values input into the model are noted in the top right. The basalt model matches well with the actual data, whereas the sedimentary rock model is not a good fit.

Conclusions

Diffraction hyperbolae are one of the most useful signatures for identifying small dimensional or cylindrical bodies on GPR data. Two-dimensional migration often obscures or diminishes the visibility of corresponding sources, which is one reason why migration is not as common in GPR studies as in seismic surveys. Here we provide a case study in which migration, especially 3D migration, provides essential geometrical constraints on the identity of a key buried archaeological artifact prior to excavation. When coupled with magnetometry to constrain composition, the 3D migrated GPR data provide a compelling case for an archeologically significant feature of interest that in other circumstances would be a modest footnote with excavation. Through these comparative analyses, we were able to determine that this feature is composed of a magnetic material most likely basalt. The shape, dimensions, and material are similar to examples of sculpture that have already been discovered at the surface of the site. If this feature is an additional sculpture, its placement in relation to Structure IV is intriguing, as such sculpture was often placed in relation to the platform mounds to denote their significance and the sacred nature of the space surrounding them (Grove, 1999).

Given the logistics of the archaeological field program at the site, it was not possible to excavate this feature at the time to determine its genesis. Restrictions imposed on excavations at Los Naranjos may prevent this feature from ever being excavated or even probed in the future, thereby necessitating the use of the complementary high-resolution geophysical methods like those used in this study to determine as much as possible about features buried within the shallow subsurface. Three-dimensional migration of GPR data and correlation with magnetometry data allowed us to determine the significance of a specific feature of interest that would have eluded us if these techniques were not employed.

Recent advances in 3D GPR survey design and implementation have documented the benefits of acquiring true 3D data, and studies such as this one demonstrate the benefits of processing data using 3D algorithms. Improvements in interpretation of subsurface features warrant the additional time and expenses associated with obtaining such a high level of detail. We argue for the continued and expanded use of 3D migration in archaeogeophysical studies to generate an accurate representation of the subsurface, whereby all features are located at the correct location and depth.

Acknowledgments

Special thanks to Professors John Henderson (Cornell) and Rosemary Joyce (Berkeley) for their assistance with this research. Their excavations at Los Naranjos during the summers of 2003 and 2004 added much to this paper. We also thank the students from Cornell and Berkeley who participated in these field seasons. Kira Blaisdell-Sloan directed the collection of the magnetic data. Professor Larry Brown, Joel Haenlein, and students from Cornell acquired the 2003 GPR data. Three-dimensional migration was performed using *ReflexW*, and Sensor's and Software Inc. *EKKO_Mapper 3* was used for initial processing and image display. Funding for this research was generously provided by an AAPG Grant-in Aid, a GSA Research Grant, and an SEG Scholarship.

REFERENCES

- Aitken, J.A. and Stewart, R.R. (2004). Investigations using Ground Penetrating Radar (GPR) at a Maya Plaza Complex in Belize, Central America., In Proceedings of the Tenth International Conference on Ground-Penetrating Radar: June 21-24, Delft, The Netherlands., Evert Slob, Alex Yarovoy and Jan Rhebergen (editors). Delft University of Technology, The Netherlands and the Institute of Electrical and Electronics Engineers, Inc., Piscataway, New Jersey, pp. 447-450.
- Annan, A.P. (2005). Ground-Penetrating Radar. In: D.K. Butler (Editor), Near-Surface Geophysics. Society of Exploration Geophysicists, Tulsa, pp. 357-438.
- Baudez, C.F. and Becquelin, P. (1973). Archéologie de Los Naranjos. Mission Archéologique et Ethnologique Française au Mexique, Mexico.
- Bednar, J.B. (2005). A brief history of seismic migration. *Geophysics*, 70(3): 3MJ-20MJ.
- Berg, F. and Bruch, H. (1982). Georadar: Archaeological interpretation of soil Radar data. *PACT News*, 7: 285-294.
- Bevan, B.W. (2006). Understand Magnetic Maps, pp. 1-30.
- Blaisdell-Sloan, K. (2006). An Archaeology of Place and Self: The Pueblo de Indios of Ticamaya, Honduras (1300-1800 AD), Unpublished Ph.D. Dissertation,

Department of Anthropology, University of California, Berkeley, Berkeley,
CA.

Booth, A.D., Linford, N.T., Clark, R.A. and Murray, T. (2008). Three-dimensional, multi-offset ground-penetrating radar imaging of archaeological targets. *Archaeological Prospection*, 15(2): 93-112.

Breiner, S. and Coe, M.D. (1972). Magnetic Exploration of the Olmec Civilization. *American Scientist*, 60(5): 566-575.

Burger, H.R., Sheehan, A.F. and Jones, C.H. (2006). *Introduction to Applied Geophysics: Exploring the Shallow Subsurface*. W.W. Norton & Company, New York.

Burke, M.J., Woodward, J., Russell, A.J., Fleisher, P.J. and Bailey, P.K. (2008). Controls on the sedimentary architecture of a single event englacial esker: Skeiðarárjökull, Iceland. *Quaternary Science Reviews*, 27(19-20): 1829-1847.

Chávez, R.E., Cámara, M.E., Tejero, A., Barba, L. and Manzanilla, L. (2001). Site characterization by geophysical methods in The Archaeological Zone of Teotihuacan, Mexico. *Journal of Archaeological Science*, 28(12): 1265-1276.

Chavez, R.E., Tejero, A., Argote, D.L. and Camara, M.E. (2009). Geophysical Study of a Pre-Hispanic Lakeshore Settlement, Chiconahuapan Lake, Mexico. *Archaeological Prospection*, early view.

Chun, J.H. and Jacewitz, C.A. (1981). *Fundamentals of Frequency-Domain Migration*.

Geophysics, 46(5): 717-733.

Conyers, L.B. (1995). The use of ground-penetrating radar to map the buried structures and landscape of the Ceren Site, El Salvador. *Geoarchaeology: An International Journal*, 10(4): 275-299.

Conyers, L.B. (1996). Velocity Analysis in Archaeological Ground-Penetrating Radar Studies. *Archaeological Prospection*, 3: 25-38.

Conyers, L.B. (2004). *Ground-Penetrating Radar for Archaeology. Geophysical Methods for Archaeology*. AltaMira Press, Walnut Creek, CA.

Cruz C., O.N. and Valles Pérez, E. (2002). Excavaciones en la Estructura IV del conjunto principal, Los Naranjos. *Yaxkin*, 21: 45-62.

Cyphers, A. (1999). From Stone to Symbols: Olmec Art in Social Context at San Lorenzo Tenochtitlán. In: D.C. Grove and R.A. Joyce (Editors), *Social Patterns in Pre-Classic Mesoamerica*. Dumbarton Oaks, Washington, DC, pp. 155-182.

Dixon, B. *et al.* (1994). Formative-Period Architecture at the Site of Yarumela, Central Honduras. *Latin American Antiquity*, 5(1): 70-87.

Dixon, B., Webb, R. and Hasemann, G. (2001). Arqueología y ecoturismo en el sitio de Los Naranjos, Honduras. *Yaxkin*, 20: 55-75.

- Fisher, E. *et al.* (1989). Determination of Bedrock Topography beneath the Greenland Ice-Sheet by 3-Dimensional Imaging of Radar Sounding Data. *Journal of Geophysical Research-Solid Earth and Planets*, 94(B3): 2874-2882.
- Fisher, S.C., Stewart, R.R. and Jol, H.M. (1996). Ground penetrating radar (GPR) data enhancement using seismic techniques. *Journal of Environmental & Engineering Geophysics*, 1(2): 89-96.
- Fowler, W.R., Estrada-Belli, F., Bales, J.R., Reynolds, M.D. and Kvamme, K.L. (2007). Landscape Archaeology and Remote Sensing of a Spanish-Conquest Town: Ciudad Vieja, El Salvador. In: J. Wiseman and F. El-Baz (Editors), *Remote Sensing in Archaeology*. Springer, New York, pp. 395-421.
- Gerlitz, K., Knoll, M.D., Cross, G.M., Luzitano, R.D. and Knight, R. (1993). Processing Ground Penetrating Radar Data to Improve Resolution of Near-Surface Targets, *Proceedings of the Symposium on the Application of Geophysics to Engineering and Environmental Problems*, Edited by Ronald S. Bell and C. Melvin Lepper, pp.561-574, San Diego, CA.
- Goodman, D., Nishimura, Y. and Rogers, J.D. (1995). GPR Time Slices in Archaeological Prospection. *Archaeological Prospection*, 2: 85-89.
- Grasmueck, M., Weger, R. and Horstmeyer, H. (2004). Three-dimensional ground-penetrating radar imaging of sedimentary structures, fractures, and archaeological features at submeter resolution. *Geology*, 32(11): 933-936.

- Grasmueck, M., Weger, R. and Horstmeyer, H. (2005). Full-resolution 3D GPR imaging. *Geophysics*, 70(1): K12-K19.
- Grove, D.C. (1999). Public Monuments and Sacred Mountains: Observations on Three Formative Period Social Landscapes. In: D.C. Grove and R.A. Joyce (Editors), *Social Patterns in Pre-Classic Mesoamerica*. Dumbarton Oaks, Washington, DC, pp. 255-300.
- Henderson, J.S. and Joyce, R.A. (2003). Informe Preliminar: Investigaciones Arqueológicas en Los Naranjos, Lago de Yojoa, Junio 2003. Manuscript on file at the Instituto Hondureño de Antropología e Historia, Tegucigalpa, Honduras.
- Henderson, J.S. and Joyce, R.A. (2004). Informe Preliminar: Investigaciones Arqueológicas en Los Naranjos, Lago de Yojoa, Junio 2004. Manuscript on file at the Instituto Hondureño de Antropología e Historia, Tegucigalpa, Honduras.
- Hesse, A., Barba, L., Link, K. and Ortiz, A. (1997). A Magnetic and Electrical Study of Archaeological Structures at Loma Alta, Michoacan, Mexico. *Archaeological Prospection*, 4: 53-67.
- Hogan, G. (1988). Migration of ground-penetrating radar data: A technique for locating subsurface targets, 59th Annual International Meeting of the Society of Exploration Geophysicists, pp. 345-347.

Joesink-Mandeville, L.R.V. (1987). Yarumela, Honduras: Formative Period Cultural Conservatism and Diffusion. In: E.J. Robinson (Editor), *Interaction on the Southeast Mesoamerican Frontier: Prehistoric and Historic Honduras and El Salvador*. BAR International Series., Oxford, pp. 196-214.

Jol, H.M. and Bristow, C.S. (2003). GPR in sediments: advice on data collection, basic processing and interpretation, a good practice guide. . In: C.S. Bristow and H.M. Jol (Editors), *Ground Penetrating Radar in Sediments*. Geological Society, London, Special Publications, 211, pp. 9-27.

Joyce, R.A. (2004). Mesoamerica: A Working Model for Archaeology. In: J.A. Hendon and R.A. Joyce (Editors), *Mesoamerican Archaeology: Theory and Practice*. Blackwell Studies in Global Archaeology. Blackwell, Malden, MA, pp. 1-42.

Joyce, R.A. and Grove, D.C. (1999). Asking New Questions about the Mesoamerican Pre-Classic. In Grove, D. C., and Joyce, R. A. (eds.), *Social Patterns in Pre-Classic Mesoamerica*, Dumbarton Oaks, Washington, DC, pp. 1-14.

Joyce, R.A. and Henderson, J.S. (2002). La arqueología del periodo Formativo en Honduras: nuevos datos sobre el «estilo olmeca» en la zona maya. *Mayab*, 15: 5-17.

- Karlberg, T. and Sjöstedt, D. (2007). Archaeological Exploration in Nicaragua using Ground Penetrating Radar: A Minor Field Study, Unpublished Master's Thesis, Department of Chemical Engineering and Geosciences, Division of Applied Geophysics, Luleå University of Technology, Luleå, Sweden.
- Kearey, P., Brooks, M. and Hill, I. (2002). An introduction to geophysical exploration. Blackwell Scientific Publications, Oxford, England.
- Kvamme, K.L. (2003). Geophysical surveys as landscape archaeology. *American Antiquity*, 68(3): 435-457.
- Leckebusch, J. (2000). Two- and Three-dimensional Ground-penetrating Radar Surveys Across a Medieval Choir: a Case Study in Archaeology. *Archaeological Prospection*, 7: 189-200.
- Leckebusch, J. and Peikert, R. (2001). Investigating the True Resolution and Three-dimensional Capabilities of Ground-penetrating Radar Data in Archaeological Surveys: Measurements in a Sand Box. *Archaeological Prospection*, 8: 29-40.
- Lehmann, F. and Green, A.G. (2000). Topographic migration of georadar data: Implications for acquisition and processing. *Geophysics*, 65(3): 836-848.
- Leucci, G. (2002). Ground-penetrating Radar Survey to Map the Location of Buried Structures under Two Churches. *Archaeological Prospection*, 9: 217-228.

- Leucci, G. and Negri, S. (2006). Use of ground penetrating radar to map subsurface archaeological features in an urban area. *Journal of Archaeological Science*, 33(4): 502-512.
- Lindsey, J.P. (1989). The Fresnel zone and its interpretive significance. *Geophysics: The Leading Edge of Exploration*, 18: 33-39.
- Lopez-Loera, H. *et al.* (2000). Magnetic study of archaeological structures in La Campana, Colima, western Mesoamerica. *Journal of Applied Geophysics*, 43(1): 101-116.
- Love, M.W. (1999). Ideology, material culture, and daily practice in Pre-Classic Mesoamerica: A Pacific Coast perspective. In Grove, D. C., and Joyce, R. A. (eds.), *Social Patterns in Pre-Classic Mesoamerica*, Dumbarton Oaks, Washington, DC, pp. 127–153.
- Luke, B.A., Begley, C.T., Chase, D.S., Ross, A.J. and Brady, J.E. (1997). Rapid-Response Geophysical Site Investigations at a Pre-Columbian Settlement in Honduras., *Proceedings, Symposium on the Application of Geophysics to Engineering and Environmental Problems.*, Compiled by R.S. Bell, Reno, Nevada, 23-26 Mar 1997. Wheat Ridge, CO: Environmental and Engineering Geophysical Society, 2: 983-992.
- Luke, B.A. and Brady, J.E. (1998). Application of Seismic Surface Waves at a Pre-Columbian Settlement in Honduras. *Archaeological Prospection*, 5: 139-157.

Majjala, P. (1992). Application of some seismic data processing methods to ground penetrating radar data, Fourth International Conference on Ground Penetrating Radar: June 8-13, Rovaniemi, Finland., Pauli Hanninen and Sini Autio (editors). Geological Survey of Finland, Special Paper 16: 103-110.

Meats, C. (1996). An Appraisal of the Problems Involved in Three-Dimensional Ground Penetrating Radar Imaging of Archaeological Features. *Archaeometry*, 38(2): 359-379.

Morrison, F., Benavent, J., Clewlow, C.W. and Heizer, R.F. (1970). Magnetometer Evidence of a Structure within La Venta Pyramid. *Science*, 167(3924): 1488-1490.

Navarro Tábora, S.C. (2004). Parque Eco-Arqueológico Los Naranjos: Guía Interpretativa, Tegucigalpa, Honduras.

Neal, A. (2004). Ground-penetrating radar and its use in sedimentology: principles, problems and progress. *Earth-Science Reviews*, 66(3-4): 261-330.

NOAA (2009). NOAA's Geophysical Data Center -- Geomagnetic Online Calculator.

Nyquist, H. (1928). Certain Topics in Telegraph Transmission Theory. *Transactions A.I.E.E.*, February 1928: 617-644.

- Ovando-Shelley, E. and Manzanilla, L. (1997). An archaeological interpretation of geotechnical soundings under the Metropolitan Cathedral, Mexico City. *Archaeometry*, 39: 221-235.
- Pastor, L. (2003). Segundo Reporte Sobre Prospección Geofísica en Copán (Honduras). In: R. Viel (Editor), *El Paleopaisaje de Copán: Cuatro Mil Anos de Transformaciones del Paisaje en el Valle de Copán (CD-ROM)*, Copán Ruinas, pp. 1-12.
- Rastogi, R. and Phadke, S. (2002). Optimal aperture width selection and parallel implementation of Kirchhoff migration algorithm, SPG 4th Conference & Exposition on Petroleum Geophysics, Mumbai, India, pp. 1-7.
- Sandmeier, K.J. (2006). ReflexW Version 4.0, Karlsruhe, Germany.
- Sauck, W.A., Desmond, L.G. and Chavez, R.E. (1998). Preliminary GPR Results from Four Maya Sites, Yucatan, Mexico, In Proceedings of the Seventh International Conference on Ground-Penetrating Radar, May 27-30, 1998., University of Kansas, Lawrence, Kansas, USA. Radar Systems and Remote Sensing Laboratory, University of Kansas, pp. 101-114.
- Schilt, F.S., Kaufman, S. and Long, G.H. (1981). A 3-Dimensional Study of Seismic Diffraction Patterns from Deep Basement Sources. *Geophysics*, 46(12): 1673-1683.

- Schneider, W.A. (1978). Integral Formulation for Migration in 2 and 3 Dimensions. *Geophysics*, 43(1): 49-76.
- Sensors & Software Inc. (2003). EKKO_View Enhanced & EKKO_View Deluxe, Mississauga, ON.
- Sensors & Software Inc. (2007). EKKO_Mapper User's Guide, Mississauga, ON, 1-76 pp.
- Sheets, P.D. (1985). Geophysical Exploration for Ancient Maya Housing at Cerén, El Salvador. *National Geographic Society Research Reports*, 20: 645-656.
- Sheriff, R.E. and Geldart, L.P. (1995). *Exploration seismology*. Cambridge University Press, Cambridge; New York.
- Stierman, D.J. (2004). Sobre métodos geofísicos en Talgua, Memoria VII Seminario de Antropología de Honduras "Dr. George Hasemann". Instituto Hondureño de Antropología e Historia, Tegucigalpa, pp. 303-322.
- Stierman, D.J. and Brady, J.E. (1999). Electrical Resistivity Mapping of Landscape Modifications at the Talgua Site, Olancho, Honduras. *Geoarchaeology: An International Journal*, 14(6): 495-510.
- Stone, D.Z. (1934). A new southernmost Maya city (Los Naranjos on Lake Yojoa, Honduras). *Maya Research*, 1(2): 125-128.

- Strong, W.D., Kidder, A. and Paul, A.J.D. (1938). Preliminary Report on the Smithsonian Institution - Harvard University Archaeological Expedition to Northwestern Honduras, 1936, Washington.
- Tchakirides, T.F. (2007). Preliminary Informe: Geophysical Data Collection at Los Naranjos and Puerto Escondido, Honduras. Manuscript on file at the Instituto Hondureño de Antropología e Historia, Tegucigalpa, Honduras.
- Tchakirides, T.F. and Brown, L.D. (in prep). Effect of Reflection Picking Criteria on In Situ Velocity Estimates from Ground-penetrating Radar Common Mid-point Data from the Archaeological Site of Los Naranjos, Honduras.
- Tchakirides, T.F., Brown, L.D. and Henderson, J.S. (2005). GPR Experience at Mesoamerican Archaeological Sites in Honduras: Puerto Escondido and Copán, Eos. Trans. AGU, 86(18), Jt. Assem. Suppl., Abstract NS41A-03.
- Tchakirides, T.F., Brown, L.D. and Henderson, J.S. (2006). Estimation of Diffractor Morphology from Analysis of Amplitude and Travel Time Curvature at the Maya Archaeological Site of Los Naranjos, Honduras., In Proceedings of the 11th International Conference on Ground Penetrating Radar: June 19-22, Columbus, Ohio, p. 1-8.
- Telford, W.M. (1976). Applied geophysics. Cambridge University Press, London ; New York, xvii, 860 pp.

- Valdes, J.A. and Kaplan, J. (2000). Ground-penetrating radar at the Maya site of Kaminaljuyu, Guatemala. *Journal of Field Archaeology*, 27(3): 329-342.
- Welch, D. (2001). The Chacalapan Geophysical Survey, Veracruz, Mexico. Reports submitted to FAMSI, <http://www.famsi.org>, Accessed August 18, 2006.
- Yde, J. (1936). A Preliminary Report of the Tulane University-Danish National Museum Expedition to Central America 1935. *Maya Research*, 3(1): 24-37.
- Yde, J. (1938). A Reconnaissance of Northwestern Honduras. A Report of the Work of the Tulane University-Danish National Museum Expedition to Central America 1935. *Acta Archaeologica*, 9: 1-99.
- Yilmaz, Ö. (2001). Seismic data analysis: processing, inversion, and interpretation of seismic data. Society of Exploration Geophysicists, Tulsa, OK.
- Zhou, H. and Sato, M. (2001). Archaeological Investigation in Sendai Castle using Ground-Penetrating Radar. *Archaeological Prospection*, 8: 1-11.

CHAPTER 5
THREE-DIMENSIONAL GEOPHYSICAL IMAGING OF SUBSURFACE
GEOLOGICAL AND ANTHROPOGENIC FEATURES AT LOS NARANJOS,
HONDURAS WITH GROUND-PENETRATING RADAR AND
MAGNETOMETRY*

Abstract

Three-dimensional ground-penetrating radar (GPR) data and magnetic gradiometry data were acquired at the archaeological site of Los Naranjos, Honduras during the summer of 2003 and the spring of 2007 in order to map geological strata and the areal extent of features excavated during limited archaeological excavations. GPR proved especially effective at delineating Quaternary stratigraphy and identifying localized buried features such as pop-up structures and basins. Depth of imaging was generally in excess of 5 meters. Complex layering, strata onlaps, unconformities, and faults provide evidence of geological and tectonic activity at the site. Correlation between magnetic anomalies and GPR-imaged features provides a means of distinguishing a range of lithologies and artifact compositions. Anomalous, high-amplitude GPR diffraction hyperbolae suggest that sculpture may still be buried at the site. The GPR results have been useful for distinguishing between natural and anthropogenic features and are consistent with a clay interior of the large earthen platform mounds. Although GPR surveys at other sites in Honduras have had limited success, the Los Naranjos results show considerable potential for this technology in defining geological setting and mapping buried anthropogenic structures. Most importantly, geophysical methods have proven especially effective for probing this protected site in a non-invasive and non-destructive manner.

* Submitted to *Yaxkin*.

Introduction

Los Naranjos is a multi-component (multi-occupation) site located on the northwestern shore of Lake Yojoa within the present-day Department of Cortés in central Honduras (Figure 66). Initial settlement of Los Naranjos predates the Classic Period constructions of Copán by more than 1,000 years. It has been said that “fuera de Copán, Los Naranjos es el sitio arqueológico más importante de Honduras” (Cruz C. and Valles Pérez, 2002, p. 46). Its early-age, large earthen monumental architecture, and statues in Olmec style have attracted attention for more than seven decades (Baudez and Becquelin, 1973; Henderson and Joyce, 2004; Stone, 1934; Strong *et al.*, 1938; Yde, 1938a).

The wealth of information obtained during these earlier studies encouraged the Instituto Hondureño de Antropología e Historia (IHAH) to designate a portion of the site within the Principal Group as the Parque Eco-Arqueológico Los Naranjos to be preserved and protected (Cruz C. and Valles Pérez, 2002; Dixon *et al.*, 2001; Navarro Tábora, 2004). With this designation, IHAH requested that no further extensive excavations occur at the site. This situation makes the application of non-invasive shallow geophysical methods particularly attractive, because they make it possible to study features from the site in three dimensions without excavation, thus protecting it for future study.

Geophysical methods have only been applied to a handful of archaeological studies in Honduras (Lisman *et al.*, 2005; Luke and Brady, 1998; Pastor, 2003; Stierman, 2004; Stierman and Brady, 1999; Tchakirides *et al.*, 2005). For that matter, the number of such surveys throughout Mesoamerica is relatively limited (Aitken and Stewart, 2004; Breiner and Coe, 1972; Chávez *et al.*, 2001; Conyers, 1995; Hesse *et al.*, 1997; Lopez-Loera *et al.*, 2000; Morrison *et al.*, 1970a; Ovando-Shelley and Manzanilla, 1997; Sauck *et al.*, 1998; Sheets, 1985; Valdes and Kaplan, 2000). Thus,

in this region the full potential of geophysical methods has not been realized as it has at archaeological sites in other parts of the world (e.g. Conyers, 2004; Kvamme, 2003).

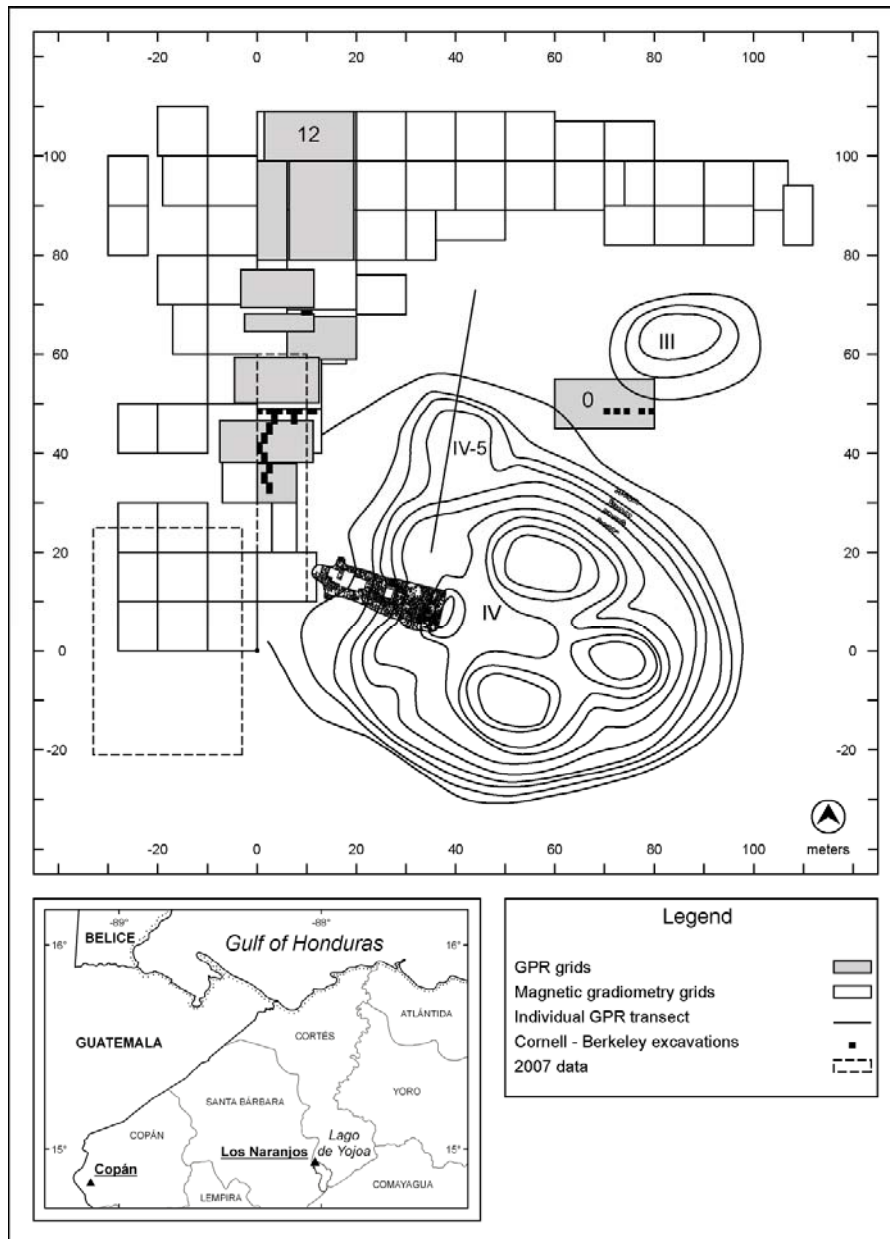


Figure 66: Site map of a portion of the Principal Group at Los Naranjos, showing all geophysical data collected in relation to Structure IV. Grids 0 and 12 are discussed in the text. Basemap is modified from Baudez and Becquelin (1973) and Cruz C. and Valles Pérez (2002).

By employing geophysical methods, it is possible to obtain a relatively expansive subsurface view of a site, which can rarely, if ever, be achieved from limited archaeological excavations alone (Conyers, 2004). At sites with stratigraphy as complex as Los Naranjos, it would take years to excavate through successive occupation layers in order to obtain as complete a picture of site usage. Although GPR can provide a broadscale view of a site, it cannot provide information regarding specific ages or lengths of occupations. Geophysical methods such as those used in this study can probe large areas without disturbance, thus providing a context for maximizing the benefits from future excavations while minimizing their disruption of the site.

Los Naranjos

Los Naranjos is situated within the tectonic region known as the Yojoa Valley, which is a Quaternary-aged graben at the north end of Lake Yojoa (Manton, 1987). The site is located at an elevation of about 630 meters and is flanked by low limestone hills to the west and east. Bedrock of Cretaceous limestone (Yojoa Group) is overlain by Quaternary basaltic lava flows (Williams and McBirney, 1969), that provided raw materials for building and carving stone in antiquity.

The main area of archaeological interest at Los Naranjos is the Principal Group, which is defined by a cluster of almost 20 large earthen platform mounds arranged in a regular plan with several open plazas. The earliest known features from within the Principal Group date to the latter half of the Early Formative, making Los Naranjos one of the earliest archaeological sites in Mesoamerica. Previous excavations uncovered wattle and daub structures within the plaza (Henderson and Joyce, 2004), evidence of social ranking provided by a burial interred within Structure IV (Baudez and Becquelin, 1973), as well as “one of the most wonderful collections of

polychrome pottery ever produced by a single site within the Maya area” (Yde, 1938a, p. 29).

A small portion of the Principal Group, approximately one hectare in size immediately to the north of Structure IV, is the focus of this paper (Figure 66). This region of the Principal Group was selected for study in an effort to understand the Early and Middle Formative communities that lived adjacent to the platform mounds, especially Structure IV (Henderson and Joyce, 2003; Henderson and Joyce, 2004; Joyce and Henderson, 2002). The construction of the basal platform of Structure IV most likely began as an extension of a house in the Early Formative Period that was later enlarged and expanded during the Middle Formative to accommodate an elite residence (Joyce, 2004b).

Ground-penetrating Radar and Magnetometry

Two shallow geophysical techniques were employed at Los Naranjos. Ground-penetrating radar is an active geophysical method that transmits electromagnetic energy into the ground and receives the resulting signals after they have reflected off subsurface features or interfaces (Conyers, 2004). Variations in the electrical properties of subsurface materials cause the transmitted signal to travel at a different velocity. A portion of the energy is reflected back to the surface at each change in velocity (relative dielectric permittivity). Reflection profiles provide a cross-sectional view of the subsurface and are useful for viewing stratigraphy and structure of subsurface materials. All cross-sectional images display data in two-way travel time measured in nanoseconds (1×10^{-9} seconds), as well as in corresponding depths computed using velocity information obtained *in situ* from common mid-point data (Jol and Bristow, 2003; Tchakirides and Brown, in prep).

Magnetometry is a passive geophysical method that measures deviations in the Earth's magnetic field that can be caused by anthropogenic features, such as hearths, kilns, or burned house floors that have a strong magnetic susceptibility in contrast with the surrounding matrix (Kvamme, 2003). Walls constructed from magnetic rocks such as basalt also generate magnetic anomalies as the magnetic minerals in these rocks orient themselves with the Earth's magnetic field (Clark, 1990). Plan view images of GPR and magnetic gradiometry show variations in relative amplitude of reflected waves and variations in magnetic field strength, respectively.

Methods

As part of a joint Cornell University – University of California, Berkeley field program during the summer of 2003 (Figure 66), GPR data collection involved the Sensors and Software, Inc. pulseEKKO 100 with 50, 100, and 200 megahertz (MHz) (1×10^6 Hz) antennae and the Noggin-250 with 250 MHz antennae. Closely-spaced (0.40 meters or 0.50 meters) orthogonal lines that resulted in 3D grids of data comprise the majority of data collected, but several individual transects augment these grids. During field testing, the 200 MHz and 250 MHz antennae provided an adequate depth of penetration while still maintaining sufficient resolution of features (Clark, 1990, p. 119) and served as the primary data collection tools. Magnetic gradiometry data, acquired with the Geometrics, Inc. G-858 system, covered a much larger area than the GPR surveys (Figure 66). Kira Blaisdell-Sloan, then a graduate student at Berkeley, directed the magnetic gradiometry data collection and provided the data for this project. Additional higher frequency (400 MHz) 3D GPR data and magnetic gradiometry data (Figure 66) collected in 2007 (Tchakirides, 2007) complete the geophysical suite collected.

Results

Faults

Shallow faulting is indicated on a number of the GPR cross-sections, especially within Grid 12, and stratal offsets are common within the uppermost 4 meters of this grid (Figure 67). The dominant type of fault seems to be reverse (Figure 67), indicating east-west compression. A linear “pop-up structure,” a feature compressed and pushed upwards, appears to core the portion of the plaza within the central portion of Grid 12 (Figure 67). This fault-bounded structure is evident as a distinct southwest to northeast trending feature in map view, with sharp contrasts in amplitude visible on either side but especially along its eastern boundary (Figure 67). We suggest that this faulting may represent direct evidence of earthquake activity in the region.

Earthquakes within Honduras are not unexpected, given the plate tectonic setting, and seismic events have been documented from both recent and prehistoric data (Ambraseys, 1995; Ambraseys and Adams, 1996; Carr and Stoiber, 1977; Güendel and Bungum, 1995; Kovach, 2004; Osiecki, 1981; White and Harlow, 1993). To our knowledge, however, these results are the first paleoseismic indications visible within specific strata from the Lake Yojoa area. One goal of future research would be to date these faults to determine if there is a correlation between earthquake activity and specific occupations within the site.

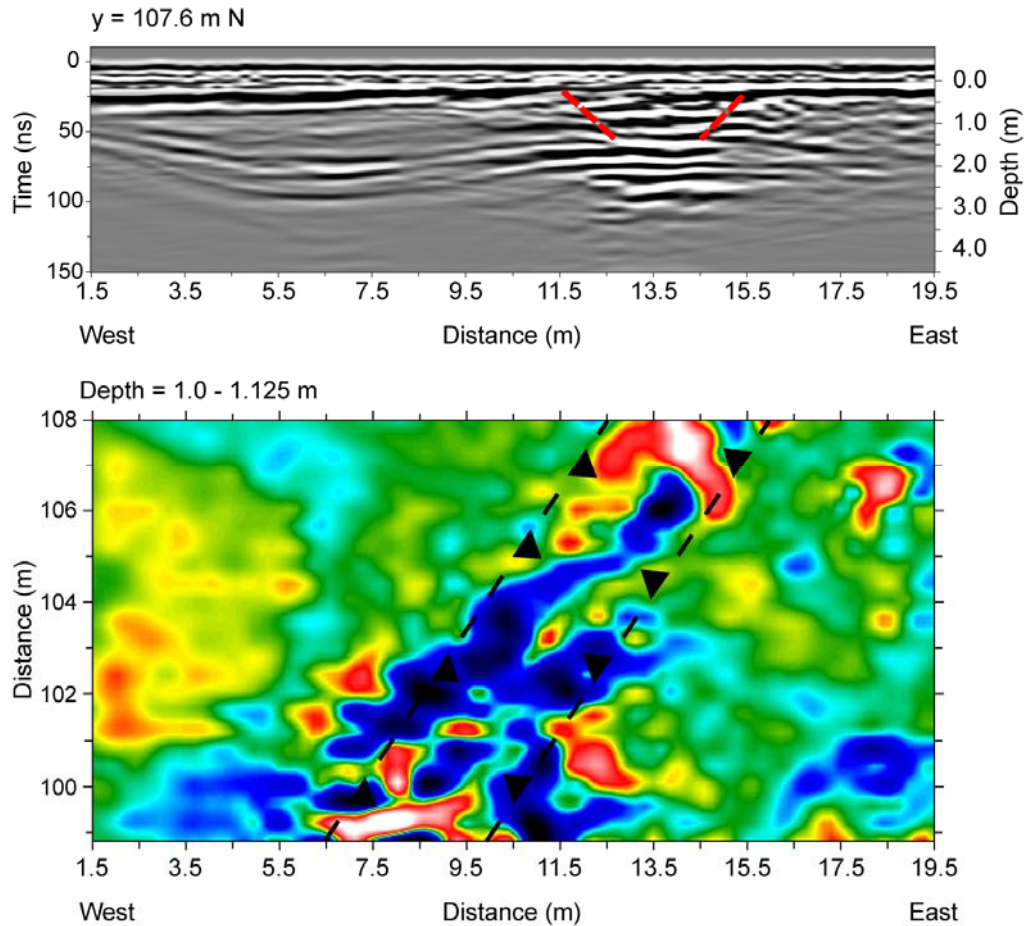


Figure 67: “Pop-up” structure imaged within the plaza at Los Naranjos. Top: Cross-sectional view of GPR data from Grid 12, with an example of reverse faulting located between 11.5 and 15.5 meters (indicated in red). Stratal offsets extend to almost 4 meters depth in some of the cross-sectional views. Bottom: Map view of GPR data from Grid 12 showing the fault-bounded pop-up structure that trends southwest to northeast.

Minor Basins

Intriguing aspects of the stratigraphy imaged by GPR are the depocenters (areas where sediment is deposited) that underlie the plaza. The deepest depocenter is defined by a series of concave strata at a basal depth of about 2.5 meters (Figure 68), which seems to be disrupted along its eastern edge by the “pop-up structure” described above. This deeper unit is in turn overlain by a much thinner (about 1 meter thick) depositional sequence that onlaps it from the west (Figure 68).

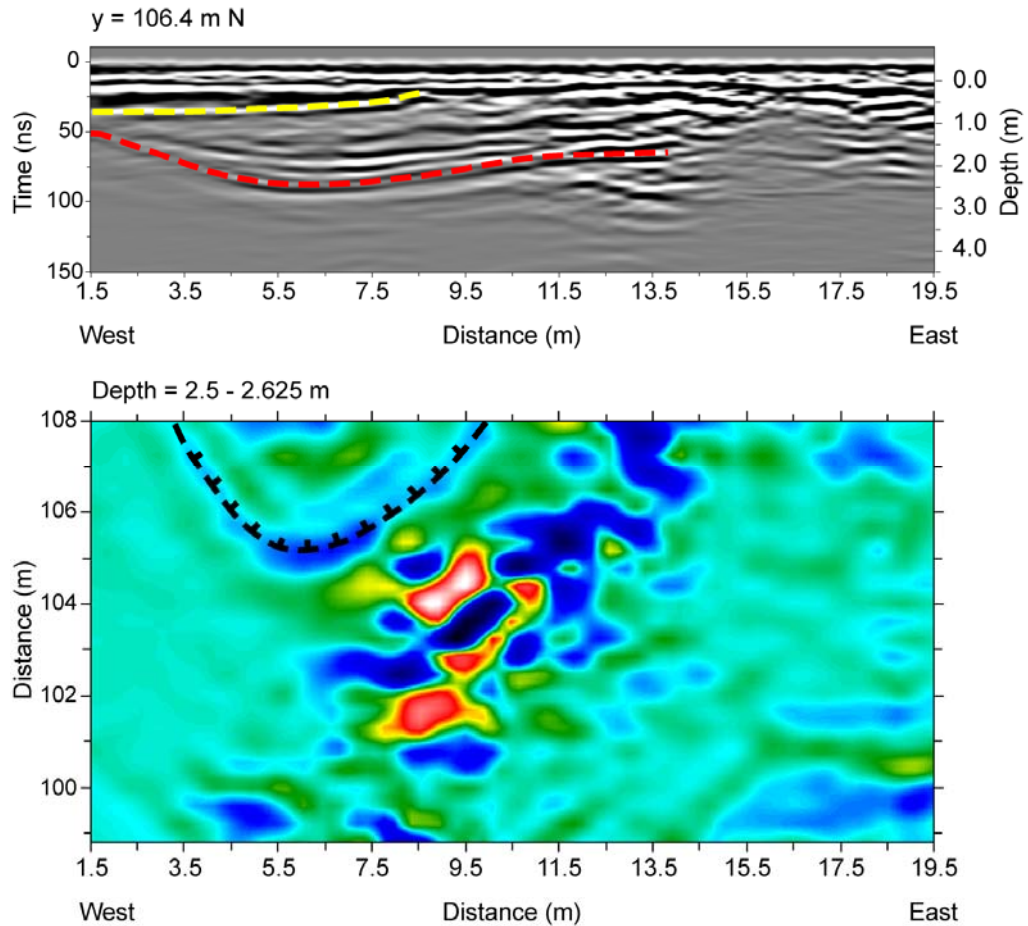


Figure 68: Small depocenters imaged by GPR. Top: Cross-sectional view of GPR data from Grid 12 showing two of the depocenters noted in Grid 12. Onlap is indicated in yellow, and a basin is indicated in red. Bottom: Map view of GPR data from Grid 12 showing contours of pronounced layering from the basin. One contour is noted in black.

The shallower unit might correspond to relatively recent overflow deposits from the drainage canal dug from the northern shore of Lake Yojoa (Cruz C. and Valles Pérez, 2002) that is located about 200 meters to the west. The deeper, thicker unit, on the other hand, could have archaeological significance, as its base lies at a depth similar to Early Formative occupations encountered about 50 meters to the south during the Cornell – Berkeley excavations (Henderson and Joyce, 2004). Its depth, dimensions, and location within the plaza would suggest it might have ceremonial

significance as a constructed basin, as similar ponds have been noted in plazas at other Mesoamerican sites. For example, at the Olmec site of San Lorenzo Tenochtitlán, Cyphers (1999, p. 159-165), noted specific monuments located in relation to “lagunas” visible at the surface, but suggested the latter might be much more recent than proposed originally by Krotser (1973). Understanding the complete geometry, age, and composition of these shallow layers should be a priority for future coring or excavations at Los Naranjos.

Buried Sculpture?

Each geophysical method measures a specific physical property of the ground. Therefore, complementary results are often produced when multiple methods are employed at the same site (Clay, 2001; Kvamme, 2003). In this study, we found that ground-penetrating radar and magnetic gradiometry used together provided an effective means of determining the depth, dimensions, and lithology of specific features of interest. This is apparent especially in Grid 0, which is located between Structures III and IV (Figure 66).

Grid 0 contained scores of diffraction hyperbolae, with apices ranging from 10 to 40 nanoseconds (about 0.3 to 1.2 meters depth). Each apex corresponds to the top of a buried object. Many of these may have been generated by reflections from rocks, perhaps detritus fallen from the slope of Structure IV, which is only about 5 meters to the south of Grid 0. However, one feature stands out from the rest. The prominent diffraction hyperbola at 67 meters along the transect differs from the others in terms of its amplitude and shape (Figure 69a), as it has a much higher amplitude and a larger radius than the other hyperbolae generated within this grid. Both peak amplitude and diffraction curvature are expected to be dependent upon the object’s morphology, specifically its size (Tchakirides *et al.*, 2006a).

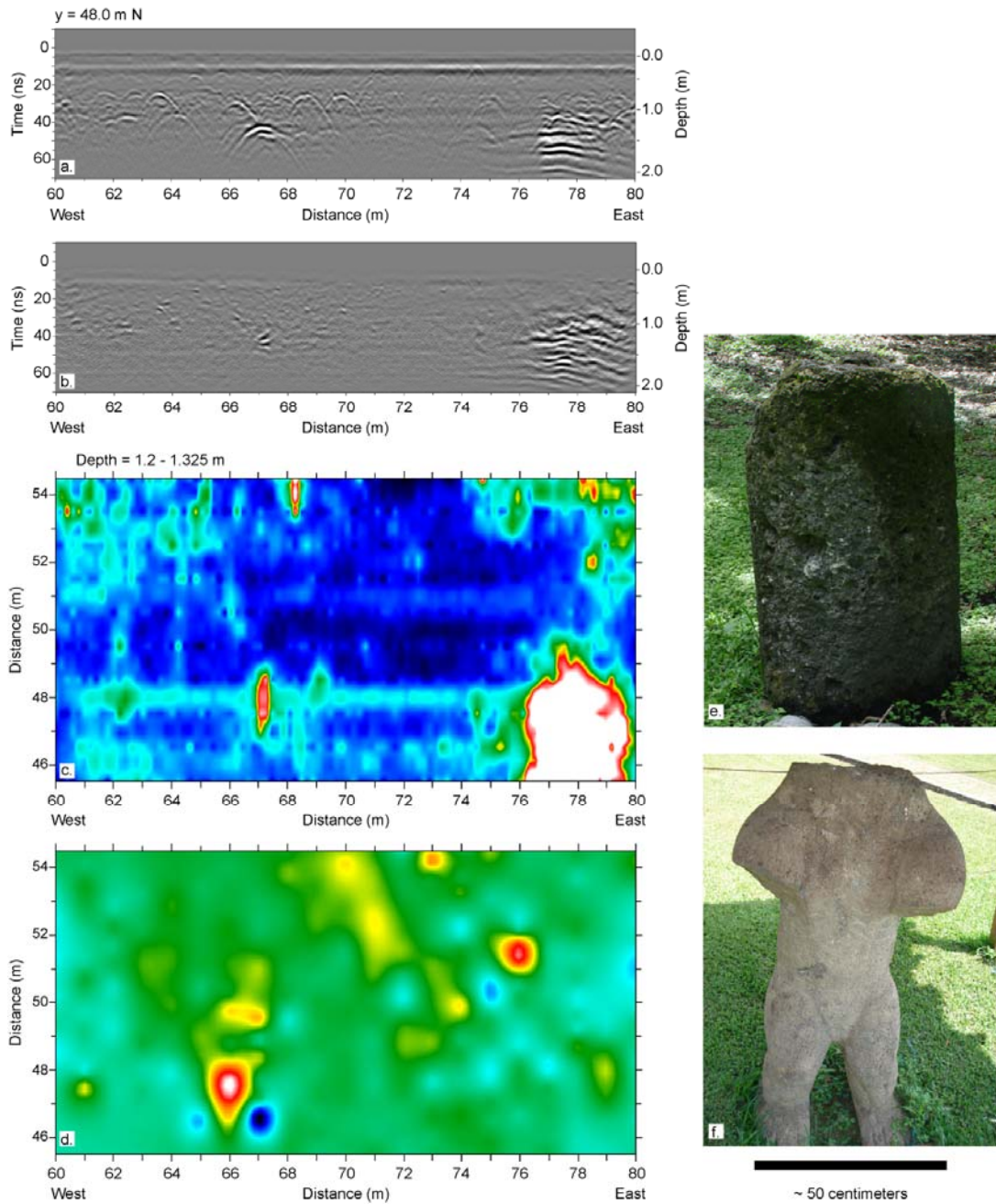


Figure 69: Possible buried sculpture at Los Naranjos. (a.) Unmigrated cross-sectional GPR transect showing the high-amplitude diffraction hyperbola at 67 m; (b.) 3D migrated view of the same data; (c.) Map view of 3D migrated GPR data; (d.) Magnetic gradiometry data. The high-amplitude feature at about 67 meters could represent a buried column or piece of sculpture, like those already discovered at Los Naranjos (e. and f.).

In 3D migrated images, diffraction hyperbolae generated by small rocks should collapse to simple point sources. The feature at 67 meters, however, does not collapse to a point like the other diffractions within the grid (Figure 69b), suggesting it is much larger. When plotted in map view, this high-amplitude feature appears elongate with a major axis that is about 2 meters long and less than 0.50 meters wide (Figure 69c).

Furthermore, magnetic gradiometry data indicate that this feature is composed of more magnetic material than the other diffractors, perhaps reflecting rock mineralogy, for example basalt rather than non-magnetic limestone. Magnetic gradiometry data from Grid 0 show a dipolar anomaly that overlies the GPR reflection feature (Figure 69d). Note that magnetic objects are often located mid-way between the high- and low-amplitude signals (Bevan, 2006), which would place the magnetic object at about 67 meters. This corresponds well with the location of the high-amplitude diffraction in the GPR data.

One possible interpretation for this particular feature, based on its dimensions, material, and location is that it could be a piece of buried sculpture, similar to the four Olmec-style basalt sculptures already documented on the surface at the site (Figure 69e, f) (Joyce and Henderson, 2002). The original location of these sculptures in open spaces adjacent to platform mounds suggests they are likely public monuments or displays, which served to delineate and segregate the space (Grove, 1999). During our own field mapping within the Principal Group during the summer of 2006, we recognized previously unreported columns within the private property to the north of the site. The presence of these columns suggests that additional columns or sculpture might still be located at the site, and possibly buried. If so, they would be expected to present a geophysical signature like that associated with the anomaly in Grid 0.

Inside Structure IV

Ground-penetrating radar probed inside a portion of Structure IV (Figure 66) in one transect collected with the 100 MHz antennae. The lower frequency antennae imaged to greater depths than the 200MHz antennae used for most of the surveys discussed thus far. This transect began on the flat ground north of Structure IV, continued across the base of the mound and its northwestern extension (Structure IV-5), and ended at the summit at an elevation of almost 7 meters (Figure 70). The deep (6 m) penetration characteristic of the plaza floor north of Structure IV ends abruptly at the edge of the mound. Previous excavations within the mound (Baudez and Becquelin, 1973) found its core to be comprised of clay, which is often a very absorptive medium for GPR due to its conductive properties (Conyers, 2004). The lack of radar penetration is consistent with a clay core and certainly indicates that the platform mound material is different from the plaza matrix that is well-imaged by the GPR surveys north of the mound.

Excavations from Baudez and Becquelin's 1967-69 fieldwork (Baudez and Becquelin, 1973) provide information regarding specific reflections within this transect. Diffraction hyperbolae along the slope between the base of the mound and the extension of Structure IV (labeled Structure IV-5) (from 20 to 24 meters in Figure 70) may correspond to a stone terrace wall uncovered during their work. Also imaged within this transect is evidence of their excavations in Structure IV-5, visible from about 30 to 37 meters (Figure 70). In this portion, excavations revealed several rooms of a residence, dating to the Late Formative Period (Baudez and Becquelin, 1973, p. 42-43).

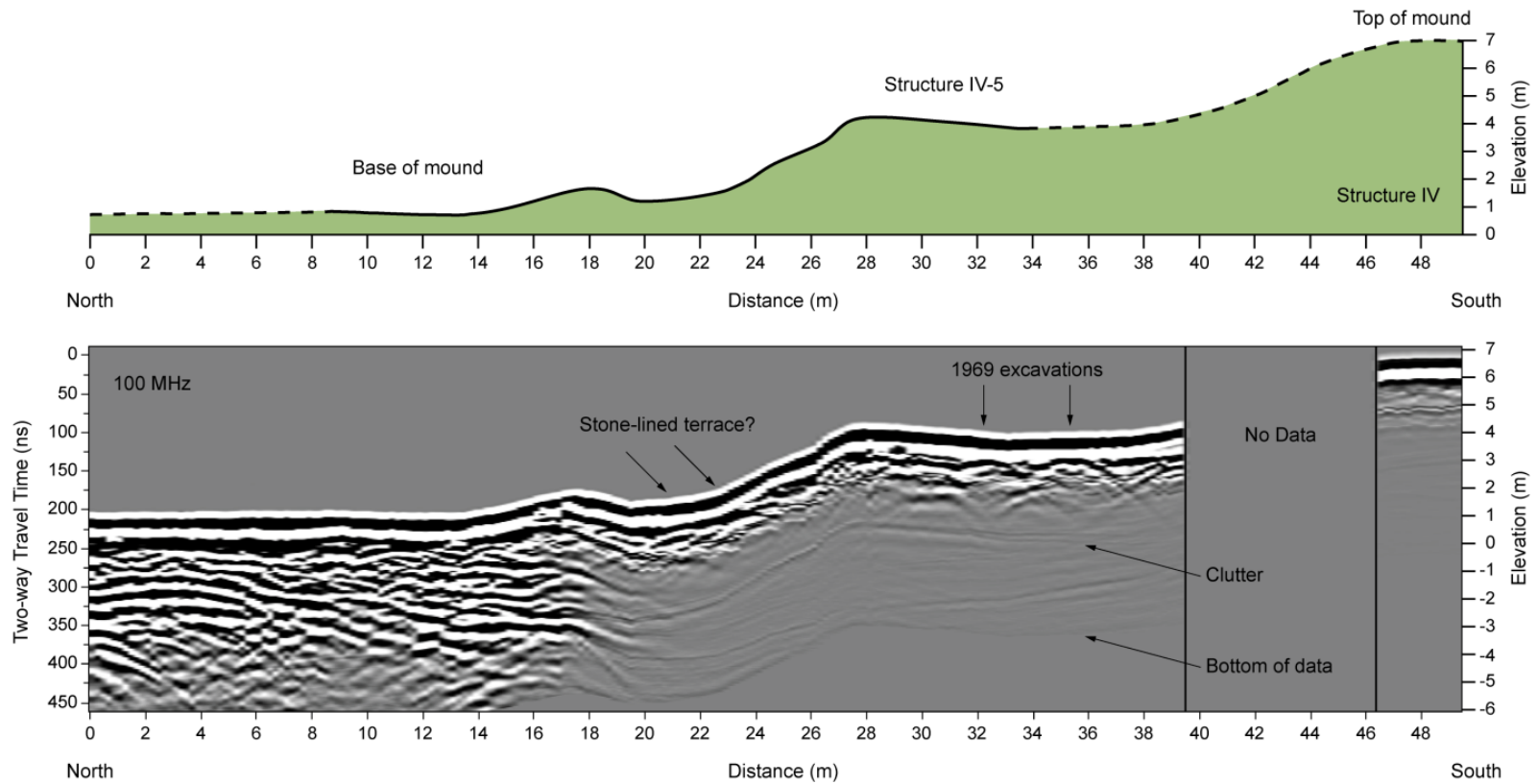


Figure 70: Topographically corrected GPR cross-sectional view across Structure IV. Top: Topography along GPR transect. Bottom: GPR transect over Structure IV. Note the limited signal penetration within the platform mound. No data were collected between about 40 to 47 meters. Vertical exaggeration = 2x.

Conclusions

GPR surveys at Los Naranjos have revealed that the stratigraphy of the area NW of Structure IV is dominated by approximately 6 meters of sub-horizontal strata that is disrupted in places by what appears to be a fault-bounded structure. These strata are overlain locally by thin, overlapping units that suggest small depositional centers. In places, the strata contain numerous diffraction hyperbolae that suggest small-scale objects that may correspond to natural rock detritus, material lost from the platform mound facings, or possibly sculpture in at least one case. The combined use of GPR and magnetic gradiometry proved effective in identifying the lithology of certain buried features.

Due to site-specific conditions, shallow geophysical techniques are not always effective in addressing archaeological issues (Conyers, 2004). Our own GPR and magnetic gradiometry surveys at other Honduran sites have proven challenging given the sedimentary matrix (Tchakirides, 2007; Tchakirides *et al.*, 2005). However, the Los Naranjos results clearly demonstrate that geophysical data can provide high-resolution images of subsurface stratigraphy, structure, and features of archaeological interest. We again emphasize that such geophysical observations provide a means of assessing key site relationships in 3D over large areas in relatively rapid fashion and in a non-intrusive, non-destructive manner.

Acknowledgments

The authors would like to thank the Instituto Hondureño de Antropología e Historia, especially Dr. Dario Euraque, Msc. Eva Martinez, Lic. Aldo Zelaya, and the late Juan Alberto Durón for support and encouragement during this project. We would also like to thank Msc. Eva Martinez and Dr. Jennifer von Schwerin for the opportunity to present this research at the 3D Archaeology Workshop at Copán in

April 2009. Prof. John Henderson (Cornell University) and Prof. Rosemary Joyce (UC Berkeley) have provided invaluable assistance, and we greatly acknowledge their participation in this research. Finally, we would like to thank the students who participated in the 2003 archaeological excavations and geophysical data collection and the 2004 excavations. Their efforts are greatly appreciated.

REFERENCES

- Aitken, J.A. and Stewart, R.R. (2004). Investigations using Ground Penetrating Radar (GPR) at a Maya Plaza Complex in Belize, Central America., In Proceedings of the Tenth International Conference on Ground-Penetrating Radar: June 21-24, Delft, The Netherlands., Evert Slob, Alex Yarovoy and Jan Rhebergen (editors). Delft University of Technology, The Netherlands and the Institute of Electrical and Electronics Engineers, Inc., Piscataway, New Jersey, pp. 447-450.
- Ambraseys, N.N. (1995). Magnitudes of Central-American Earthquakes 1898-1930. *Geophysical Journal International*, 121(2): 545-556.
- Ambraseys, N.N. and Adams, R.D. (1996). Large-magnitude Central American earthquakes, 1898-1994. *Geophysical Journal International*, 127(3): 665-692.
- Baudez, C.F. and Becquelin, P. (1973). *Archéologie de Los Naranjos. Mission Archéologique et Ethnologique Française au Mexique, Mexico.*
- Bevan, B.W. (2006). Understand Magnetic Maps, pp. 1-30.
- Breiner, S. and Coe, M.D. (1972). Magnetic Exploration of the Olmec Civilization. *American Scientist*, 60(5): 566-575.

- Carr, M.J. and Stoiber, R.E. (1977). Geologic Setting of Some Destructive Earthquakes in Central-America. *Geological Society of America Bulletin*, 88(1): 151-156.
- Chávez, R.E., Cámara, M.E., Tejero, A., Barba, L. and Manzanilla, L. (2001). Site characterization by geophysical methods in The Archaeological Zone of Teotihuacan, Mexico. *Journal of Archaeological Science*, 28(12): 1265-1276.
- Clark, A. (1990). *Seeing Beneath the Soil: Prospecting Methods in Archaeology*. Routledge, New York, NY.
- Clay, R.B. (2001). Complementary Geophysical Survey Techniques: Why Two Ways are Always Better Than One. *Southeastern Archaeology*, 20(1): 31-43.
- Conyers, L.B. (1995). The use of ground-penetrating radar to map the buried structures and landscape of the Ceren Site, El Salvador. *Geoarchaeology: An International Journal*, 10(4): 275-299.
- Conyers, L.B. (2004). *Ground-Penetrating Radar for Archaeology. Geophysical Methods for Archaeology*. AltaMira Press, Walnut Creek, CA.
- Cruz C., O.N. and Valles Pérez, E. (2002). Excavaciones en la Estructura IV del conjunto principal, Los Naranjos. *Yaxkin*, 21: 45-62.

- Cyphers, A. (1999). From Stone to Symbols: Olmec Art in Social Context at San Lorenzo Tenochtitlán. In: D.C. Grove and R.A. Joyce (Editors), *Social Patterns in Pre-Classic Mesoamerica*. Dumbarton Oaks, Washington, DC, pp. 155-182.
- Dixon, B., Webb, R. and Hasemann, G. (2001). Arqueología y ecoturismo en el sitio de Los Naranjos, Honduras. *Yaxkin*, 20: 55-75.
- Grove, D.C. (1999). Public Monuments and Sacred Mountains: Observations on Three Formative Period Social Landscapes. In: D.C. Grove and R.A. Joyce (Editors), *Social Patterns in Pre-Classic Mesoamerica*. Dumbarton Oaks, Washington, DC, pp. 255-300.
- Güendel, F. and Bungum, H. (1995). Earthquakes and Seismic Hazards in Central America. *Seismological Research Letters*, 66(5): 19-25.
- Henderson, J.S. and Joyce, R.A. (2003). Informe Preliminar: Investigaciones Arqueológicas en Los Naranjos, Lago de Yojoa, Junio 2003. Manuscript on file at the Instituto Hondureño de Antropología e Historia, Tegucigalpa, Honduras.
- Henderson, J.S. and Joyce, R.A. (2004). Informe Preliminar: Investigaciones Arqueológicas en Los Naranjos, Lago de Yojoa, Junio 2004. Manuscript on file at the Instituto Hondureño de Antropología e Historia, Tegucigalpa, Honduras.

- Hesse, A., Barba, L., Link, K. and Ortiz, A. (1997). A Magnetic and Electrical Study of Archaeological Structures at Loma Alta, Michoacan, Mexico. *Archaeological Prospection*, 4: 53-67.
- Jol, H.M. and Bristow, C.S. (2003). GPR in sediments: advice on data collection, basic processing and interpretation, a good practice guide. . In: C.S. Bristow and H.M. Jol (Editors), *Ground Penetrating Radar in Sediments*. Geological Society, London, Special Publications, 211, pp. 9-27.
- Joyce, R.A. (2004). Unintended consequences? Monumentality as a novel experience in Formative Mesoamerica. *Journal of Archaeological Method and Theory*, 11(1): 5-29.
- Joyce, R.A. and Henderson, J.S. (2002). La arqueología del periodo Formativo en Honduras: nuevos datos sobre el «estilo olmeca» en la zona maya. *Mayab*, 15: 5-17.
- Kovach, R.L. (2004). *Early earthquakes of the Americas*. Cambridge University Press, Cambridge.
- Krotser, R. (1973). El agua ceremonial de los olmecas. *Boletín, Instituto Nacional de Antropología e Historia, México*, 2: 43-48.
- Kvamme, K.L. (2003). Geophysical surveys as landscape archaeology. *American Antiquity*, 68(3): 435-457.

- Lisman, T., Tchakirides, T.F., Brown, L.D. and Henderson, J.S. (2005). GPR Surveys at Los Naranjos, an Early Formative Mesoamerican Site in Central Honduras, *Eos. Trans. AGU*, 86(18), Jt. Assem. Suppl., Abstract NS41A-04.
- Lopez-Loera, H. *et al.* (2000). Magnetic study of archaeological structures in La Campana, Colima, western Mesoamerica. *Journal of Applied Geophysics*, 43(1): 101-116.
- Luke, B.A. and Brady, J.E. (1998). Application of Seismic Surface Waves at a Pre-Columbian Settlement in Honduras. *Archaeological Prospection*, 5: 139-157.
- Manton, W.I. (1987). Tectonic Interpretation of the Morphology of Honduras. *Tectonics*, 6(5): 633-651.
- Morrison, F., Benavent, J., Clewlow, C.W. and Heizer, R.F. (1970). Magnetometer Evidence of a Structure within La Venta Pyramid. *Science*, 167(3924): 1488-1490.
- Navarro Tábora, S.C. (2004). Parque Eco-Arqueológico Los Naranjos: Guía Interpretativa, Tegucigalpa, Honduras.
- Osiecki, P.S. (1981). Estimated Intensities and Probable Tectonic Sources of Historic (Pre-1898) Honduran Earthquakes. *Bulletin of the Seismological Society of America*, 71(3): 865-881.

- Ovando-Shelley, E. and Manzanilla, L. (1997). An archaeological interpretation of geotechnical soundings under the Metropolitan Cathedral, Mexico City. *Archaeometry*, 39: 221-235.
- Pastor, L. (2003). Segundo Reporte Sobre Prospección Geofísica en Copán (Honduras). In: R. Viel (Editor), *El Paleopaisaje de Copán: Cuatro Mil Anos de Transformaciones del Paisaje en el Valle de Copán (CD-ROM)*, Copán Ruinas, pp. 1-12.
- Sauck, W.A., Desmond, L.G. and Chavez, R.E. (1998). Preliminary GPR Results from Four Maya Sites, Yucatan, Mexico, In *Proceedings of the Seventh International Conference on Ground-Penetrating Radar, May 27-30, 1998.*, University of Kansas, Lawrence, Kansas, USA. Radar Systems and Remote Sensing Laboratory, University of Kansas, pp. 101-114.
- Sheets, P.D. (1985). Geophysical Exploration for Ancient Maya Housing at Cerén, El Salvador. *National Geographic Society Research Reports*, 20: 645-656.
- Stierman, D.J. (2004). Sobre métodos geofísicos en Talgua, Memoria VII Seminario de Antropología de Honduras "Dr. George Hasemann". Instituto Hondureño de Antropología e Historia, Tegucigalpa, pp. 303-322.
- Stierman, D.J. and Brady, J.E. (1999). Electrical Resistivity Mapping of Landscape Modifications at the Talgua Site, Olancho, Honduras. *Geoarchaeology: An International Journal*, 14(6): 495-510.

- Stone, D.Z. (1934). A new southernmost Maya city (Los Naranjos on Lake Yojoa, Honduras). *Maya Research*, 1(2): 125-128.
- Strong, W.D., Kidder, A. and Paul, A.J.D. (1938). Preliminary Report on the Smithsonian Institution - Harvard University Archaeological Expedition to Northwestern Honduras, 1936, Washington.
- Tchakirides, T.F. (2007). Preliminary Informe: Geophysical Data Collection at Los Naranjos and Puerto Escondido, Honduras. Manuscript on file at the Instituto Hondureño de Antropología e Historia, Tegucigalpa, Honduras.
- Tchakirides, T.F. and Brown, L.D. (in prep). Effect of Reflection Picking Criteria on In Situ Velocity Estimates from Ground-penetrating Radar Common Mid-point Data from the Archaeological Site of Los Naranjos, Honduras.
- Tchakirides, T.F., Brown, L.D. and Henderson, J.S. (2005). GPR Experience at Mesoamerican Archaeological Sites in Honduras: Puerto Escondido and Copán, *Eos. Trans. AGU*, 86(18), Jt. Assem. Suppl., Abstract NS41A-03.
- Tchakirides, T.F., Brown, L.D. and Henderson, J.S. (2006). Estimation of Diffractor Morphology from Analysis of Amplitude and Travel Time Curvature at the Maya Archaeological Site of Los Naranjos, Honduras., In Proceedings of the 11th International Conference on Ground Penetrating Radar: June 19-22, Columbus, Ohio, p. 1-8.

- Valdes, J.A. and Kaplan, J. (2000). Ground-penetrating radar at the Maya site of Kaminaljuyu, Guatemala. *Journal of Field Archaeology*, 27(3): 329-342.
- White, R.A. and Harlow, D.H. (1993). Destructive Upper-Crustal Earthquakes of Central-America since 1900. *Bulletin of the Seismological Society of America*, 83(4): 1115-1142.
- Williams, H. and McBirney, A.R. (1969). *Volcanic History of Honduras*. University of California Publications in Geological Sciences, 85: 1-101.
- Yde, J. (1938). *An archaeological reconnaissance of northwestern Honduras; a report of the work of the Tulane university-Danish national museum expedition to Central America, 1935*. Levin & Munksgaard, Copenhagen.

CHAPTER 6
IDENTIFYING ARCHAEOLOGICAL AND GEOLOGICAL FEATURES IN
THREE-DIMENSIONAL GROUND-PENETRATING RADAR AND
MAGNETOMETRY DATA FROM LOS NARANJOS, HONDURAS

Abstract

Three-dimensional ground-penetrating radar (GPR) data and magnetometry data augmented limited archaeological excavations of a Cornell University – University of California, Berkeley field program at the site of Los Naranjos in 2003 by mapping geological strata and the areal extent of partially excavated features. Additional higher frequency GPR data and magnetometry data were collected during the spring of 2007 in an effort to provide higher resolution images of a specific portion of Los Naranjos west of the large earthen platform mound designated Structure IV. Ground-penetrating radar delineated Quaternary stratigraphy to depths ranging from 2 to 6 meters at the site. Key features revealed by the GPR data include a previously unrecognized buried structure, small depocenters (basins), buried sculpture (possibly Olmec in nature?), a stone-lined path, faults, and a possible volcanic marker horizon. Correlation of the GPR data with magnetometry data helped identify a basaltic lithology for the buried sculpture and a highly magnetic material for the buried structure. The GPR results have also been useful at probing the interior of Structure IV as well as determining a geological origin for an exposed rock “wall” within the plaza and an anthropogenic origin for a large basalt boulder known informally as the “Volkswagen.” The results obtained at Los Naranjos show considerable potential for this technology in defining geological setting and mapping buried anthropogenic structures. Most importantly, these geophysical methods have proven especially effective for probing this protected site in a non-invasive and non-destructive manner.

Introduction

In the past four decades, archaeologists have gone from dreaming about “an instrument that would allow them to ‘see’ beneath the surface of the ground even before excavation” (Breiner and Coe, 1972, p. 566) to regularly employing such sophisticated methods in research endeavors throughout the world (Conyers, 2004; Doolittle and Miller, 1991; Weymouth, 1986b). Archaeologists have realized the potential contribution of geophysical methods because of the numerous examples where surveys have been undertaken successfully. Geophysical surveys can benefit archaeological projects by targeting specific areas to excavate (Bevan and Kenyon, 1975; Kenyon, 1977; Stierman and Brady, 1999), non-invasively studying a protected site where excavations are prohibited (Wood *et al.*, 1984), or documenting a site prior to its impending development or destruction (Valdes and Kaplan, 2000).

Although the use of geophysical methods to answer archaeologically significant questions has increased in recent years, these techniques are still used primarily as a “pre-excavation strategy” (Roskams, 2001, p. 51-54), whereby interesting features are identified and are then targeted for future excavation. In this scenario, only preliminary interpretations of the data are necessary, as these hypotheses can then be “ground truthed” by actual excavations to determine the genesis of specific features. When regulations at an archaeological site prohibit large-scale or even minimal excavations, the luxury of simply pinpointing interesting features to excavate no longer exists. Instead, interpretations of each dataset must be robust, and it becomes necessary to glean as much useful information from them as possible. Through careful and thorough processing of the data, an expansive subsurface view of a site can emerge; such a view is rarely, if ever, achieved from limited archaeological excavations alone (Conyers, 2004).

The geophysical data presented here were collected during an archaeological field program at the site of Los Naranjos, Honduras that was co-sponsored by Cornell University and the University of California, Berkeley. Los Naranjos is a multi-component (multi-occupation) archaeological site located on the northwestern shore of Lake Yojoa, within the present-day Department of Cortés in central Honduras (Figure 71). At sites with stratigraphy as complex as Los Naranjos, it would take years to excavate through successive occupation layers in order to obtain a complete picture of site usage. Although geophysical techniques can provide a broad-scale view of a site, they cannot provide information regarding specific ages or lengths of occupations. They can, however, probe large areas without disturbance, thus providing a context for maximizing the benefits from any future excavations while minimizing their disruption of the site.

The portion of Los Naranjos where these data were acquired is known as the Principal Group, which is an area of about 2 hectares that is characterized by numerous large earthen platform mounds, several low flat mounds, terraces, and open plazas (Figure 72). The site itself is extensive, measuring more than 6,400 x 800 meters; other mounds known to exist (Yde, 1936), but not yet mapped, along the western shore of Lake Yojoa may relate to the site as well. A portion of the site is preserved by the Instituto Hondureño de Antropología e Historia (IHAH) as the Parque Arqueológico – Ecológico Los Naranjos. With this designation, IHAH requested that no further extensive excavations occur at the site (Cruz C. and Valles Pérez, 2002). This situation makes the application of non-invasive shallow geophysical methods particularly attractive, because they make it possible to study features from the site in three dimensions without excavation, thus protecting it for future study. The Principal Group, partially located within this property, contains the largest earthen platform mounds, the tallest of which measures more than 10 meters in

total height. All of the geophysical research undertaken at Los Naranjos has occurred within the Principal Group.



Figure 71: Location of Los Naranjos, on the northwestern shore of Lake Yojoa. The site is located within the present-day Department of Cortés in Central Honduras.

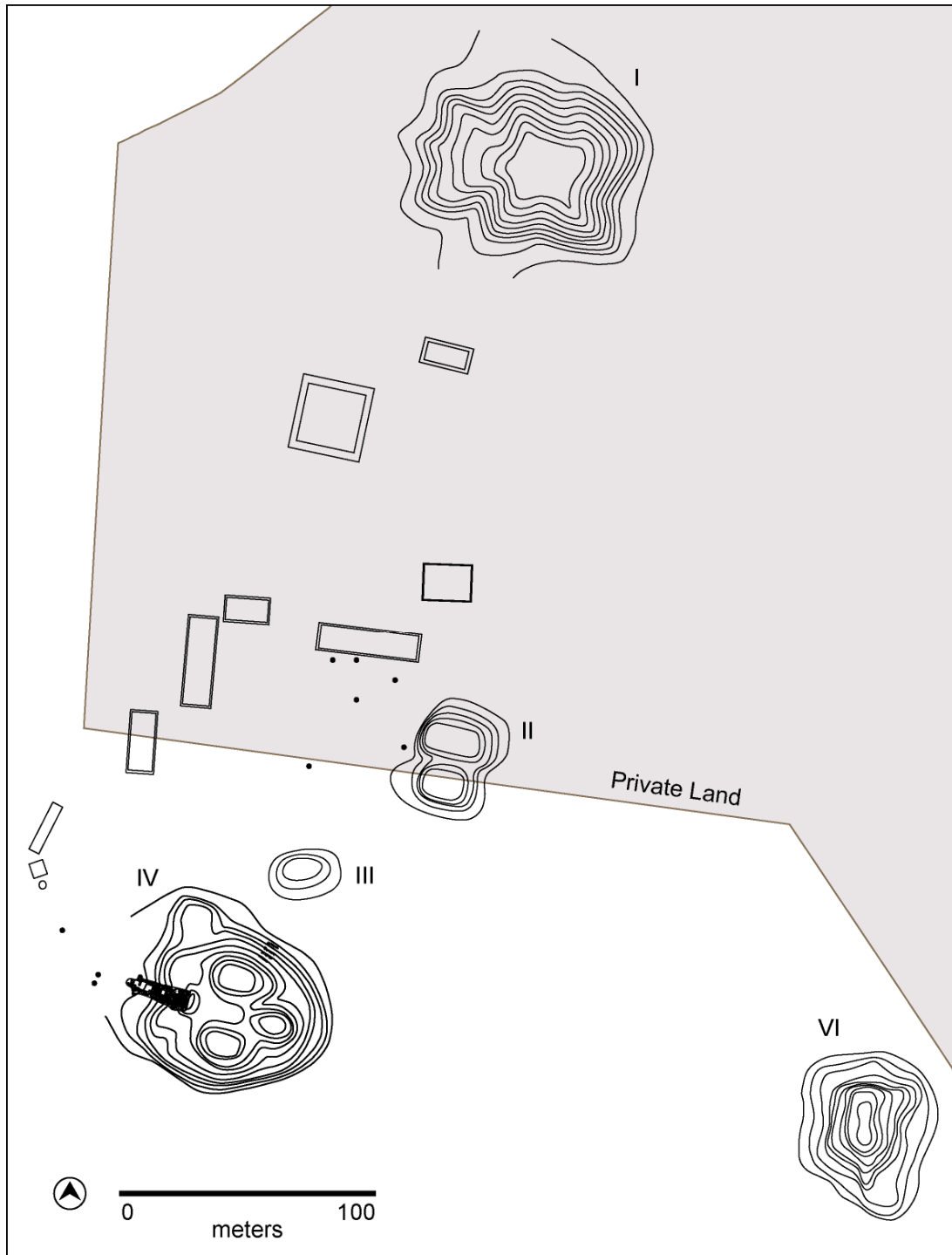


Figure 72: Principal Group of Los Naranjos. All geophysical research was conducted to the north of Structure IV. Small black dots indicate the approximate locations of sculpture previously located at the surface of the site. The basemap is modified from Baudez and Becquelin (1973), Cruz C. and Valles Pérez (2002), and Dixon *et al.* (2001).

Tectonic and Geologic Environment of Los Naranjos

Honduras is located on the Chortis Block of the Caribbean Plate in Central America (Figure 73). The Chortis Block is comprised of continental crust that is pre-Mesozoic in age (Elming *et al.*, 2001, p. 294). To the west of Honduras, the Cocos Plate subducts beneath the Caribbean Plate in a northeasterly direction along the portion known as the Middle America Trench (Figure 73). Central America is a tectonically-active region (Isacks *et al.*, 1968; Molnar and Sykes, 1969), and the locations of earthquakes have helped to define the plate boundaries in this region. The numerous earthquakes along the Middle America Trench produce the diagnostic signature of a subduction zone, whereby the down-going slab is identified by progressively deeper earthquakes (Figure 74). Numerous earthquakes occur each year (Figure 75), and in late May, 2009, a M_w 7.3 earthquake struck the northern coast of Honduras (Figure 75), causing widespread destruction.

Los Naranjos is situated within the tectonic region known as the Yojoa Valley, which is a Quaternary-aged graben at the north end of Lake Yojoa (Manton, 1987). The site is located at an elevation of about 630 meters and is flanked by low limestone hills to the west and east. Bedrock of Cretaceous limestone (Yojoa Group) is overlain by Quaternary basaltic lava flows (Williams and McBirney, 1969) (Figure 76), both of which appear to have provided raw materials for building structures and statuary.

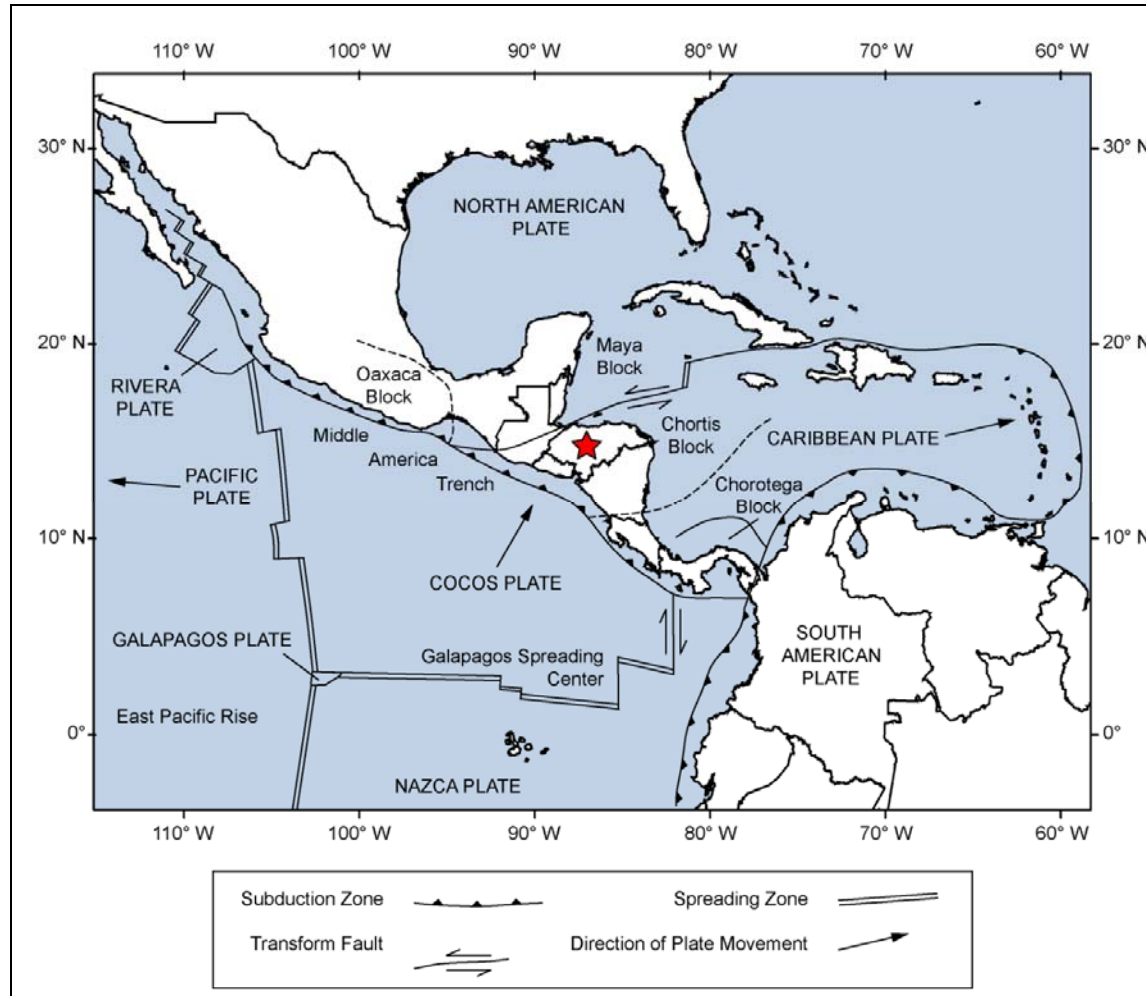


Figure 73: Tectonic map of Central America. Honduras is located on the Chortis Block of the Caribbean Plate. The Cocos Plate is being subducted beneath the Caribbean Plate.

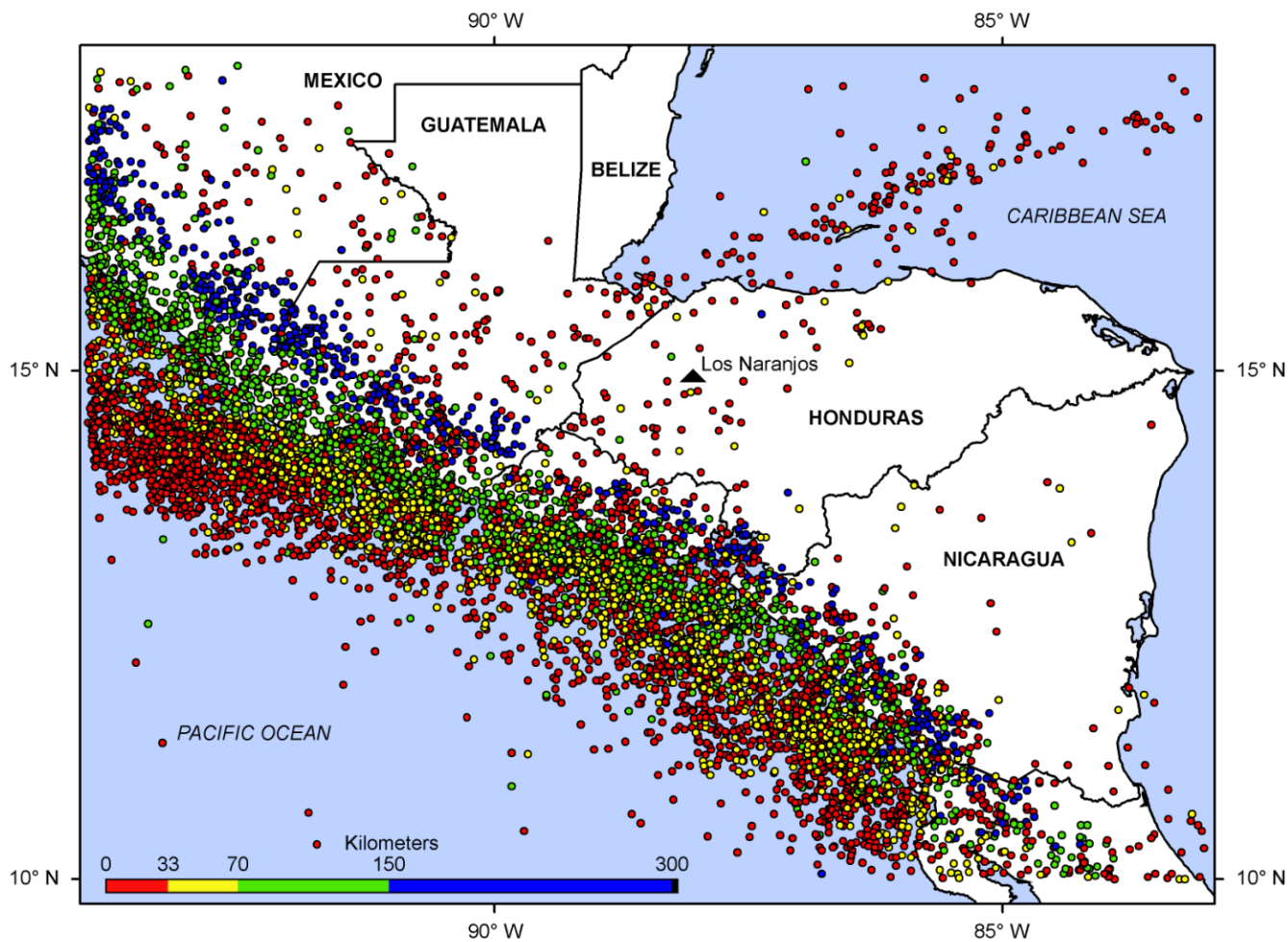


Figure 74: Locations of all of the NEIC earthquakes from the years 1973 - 2009. The earthquake locations indicate the subduction of the Cocos Plate beneath the Caribbean Plate. Earthquakes to the north of Honduras lie along the Motagua Fault.

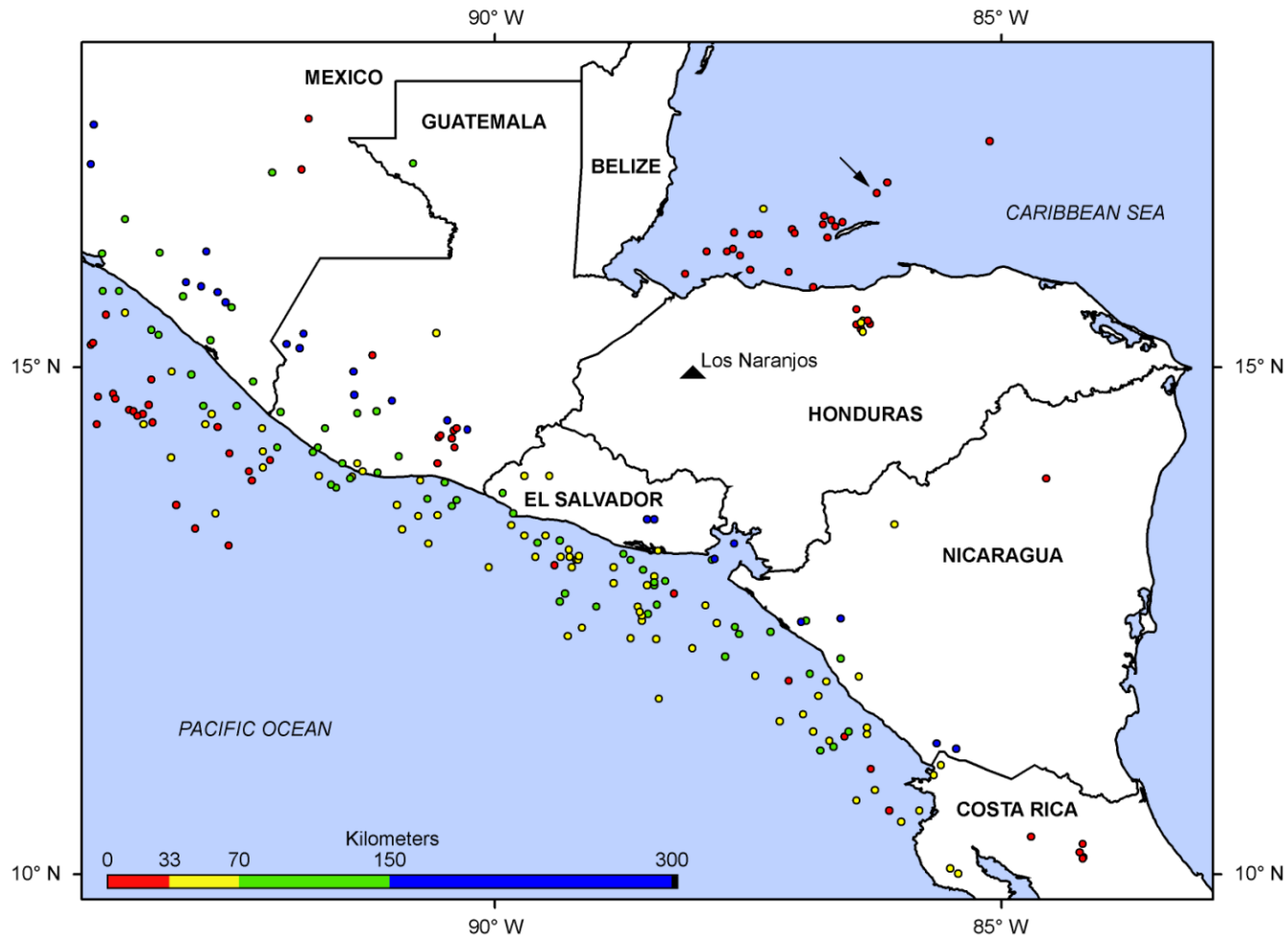


Figure 75: Locations of all of the 2009 earthquakes from the NEIC catalog. The numerous earthquakes indicate Central America is a tectonically active region. The black arrow indicates the M_w 7.3 earthquake (10 km depth) that occurred in late May, 2009, causing extensive damage in Honduras.

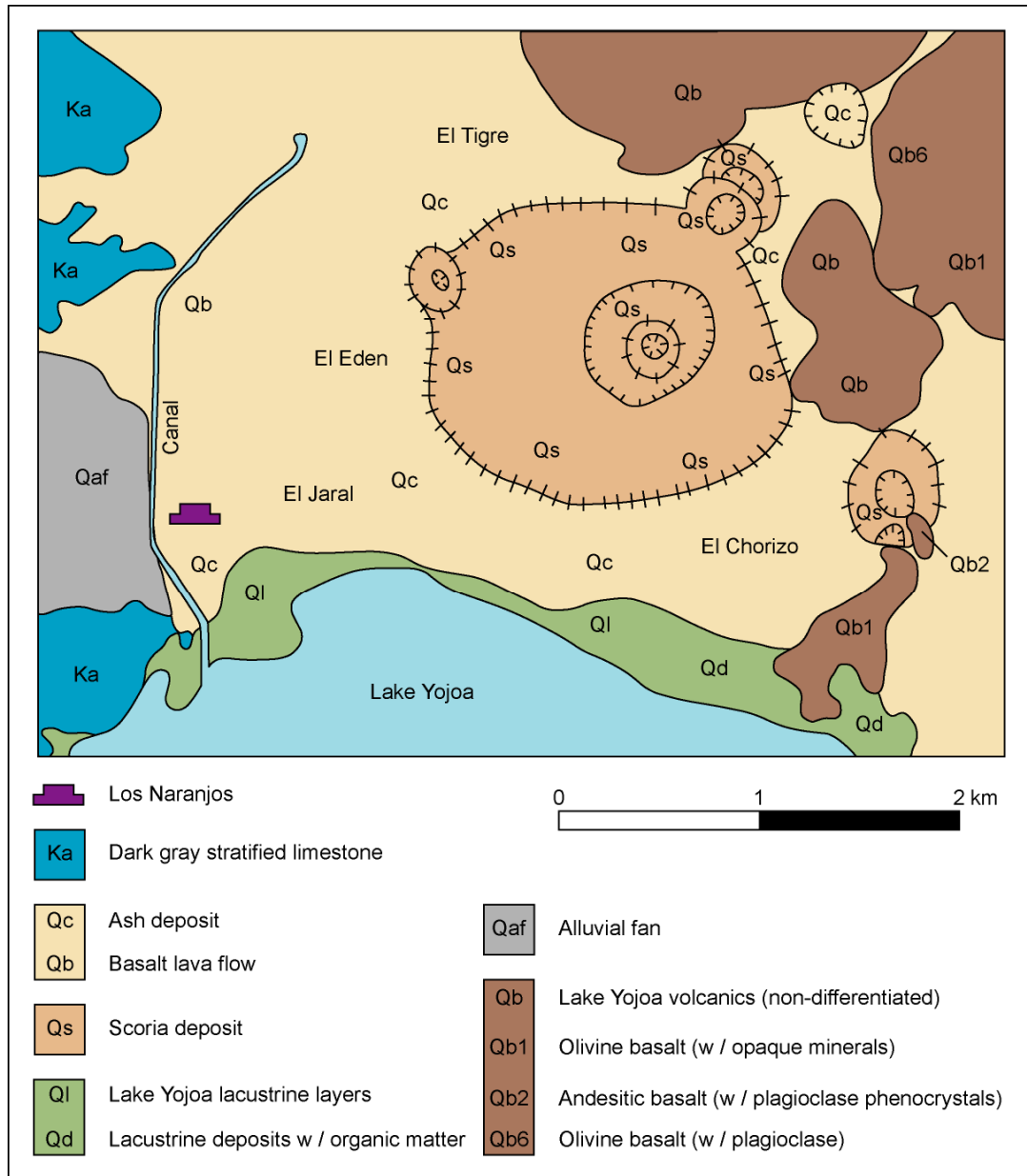


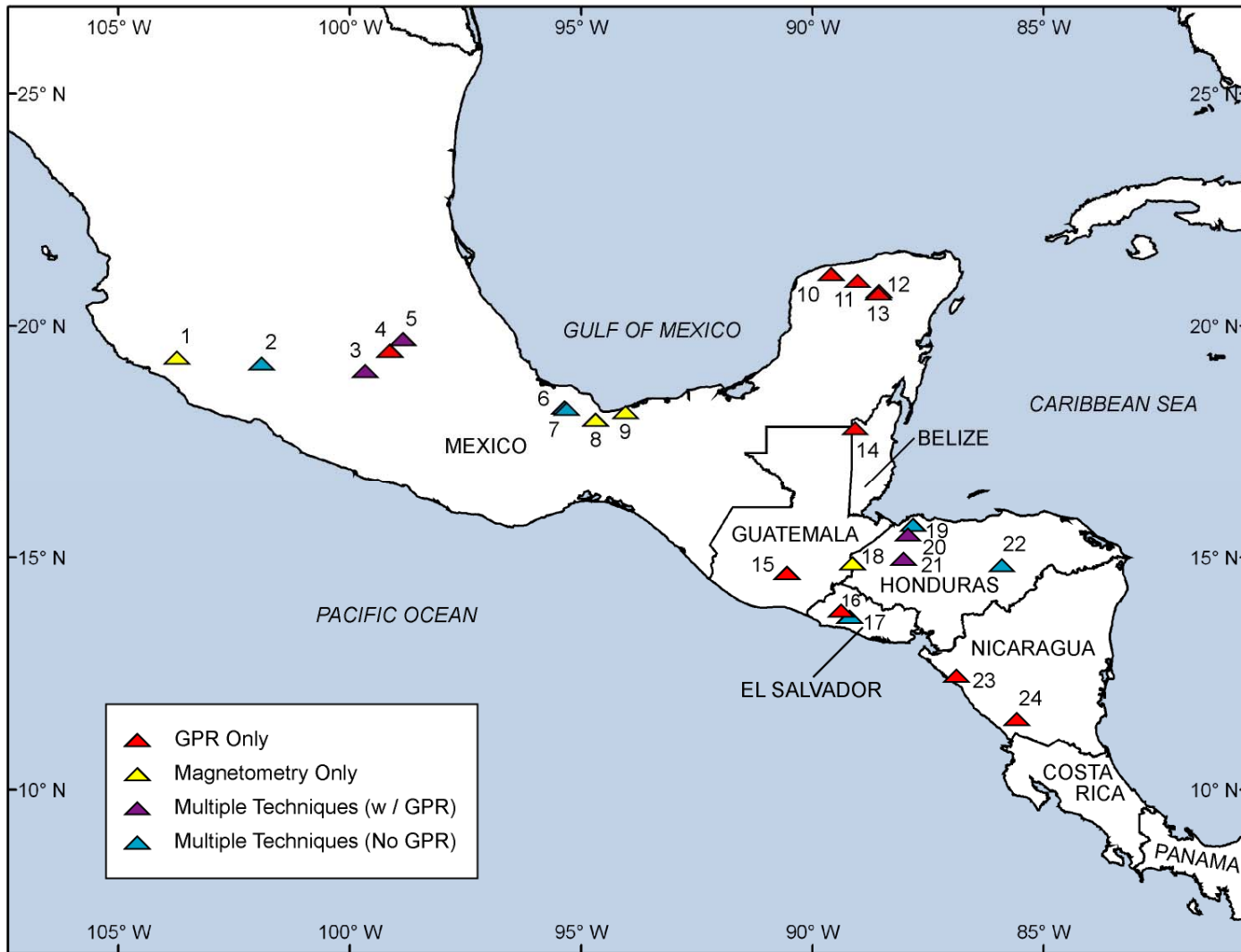
Figure 76: Geologic map of Los Naranjos, Honduras and surrounding area. Map is modified from Instituto Geográfico Nacional (1973).

Previous Geophysical Research in Mesoamerica

Aside from the present study at Los Naranjos, geophysical methods have only been applied to a handful of archaeological studies in Honduras (e.g. Blaisdell-Sloan,

2006; Luke *et al.*, 1997; Luke and Brady, 1998; Pastor, 2003; Stierman, 2004; Stierman and Brady, 1999; Tchakirides, 2007; Tchakirides *et al.*, 2005) (Figure 77). Their use at archaeological sites throughout Mesoamerica is growing, although these applications are still relatively limited. Of the hundreds, or even thousands, of archaeological sites in Mesoamerica, geophysical studies have only been conducted at twenty-four of them (Aitken and Stewart, 2004; Breiner and Coe, 1972; Chávez *et al.*, 2001; Chavez *et al.*, 2009; Conyers, 1995; Fowler *et al.*, 2007; Hesse *et al.*, 1997; Karlberg and Sjöstedt, 2007; Lopez-Loera *et al.*, 2000; Morrison *et al.*, 1970a; Ovando-Shelley and Manzanilla, 1997; Sauck *et al.*, 1998; Sheets, 1985; Valdes and Kaplan, 2000; Welch, 2001) (Figure 77). Thus, in this region the full potential of geophysical methods has not been realized as it has at archaeological sites in other parts of the world (Conyers, 2004; Kvamme, 2003), such as the United States (e.g. Dalan, 1991; Kvamme and Ahler, 2007; Weymouth, 1986a; Weymouth, 1986b), Japan (e.g. Goodman and Nishimura, 1993; Goodman *et al.*, 1994), or Brazil (e.g. Bevan and Roosevelt, 2003; Roosevelt, 2007). We hope that the results of this study will showcase the possibility of obtaining useful results from other archaeological sites in the tropical environments of Mesoamerica.

Figure 77: Locations of the 24 geophysical surveys conducted at Mesoamerican archaeological sites, discussed in text. **1:** La Campana (Lopez-Loera *et al.*, 2000); **2:** Loma Alta (Hesse *et al.*, 1997); **3:** Chiconahuapan Lake (Chavez *et al.*, 2009); **4:** Mexico City (Ovando-Shelley and Manzanilla, 1997); **5:** Teotihuacan (Chávez *et al.*, 2001); **6:** El Tecolote (Welch, 2001); **7:** Cinco Cerros (Welch, 2001); **8:** San Lorenzo (Breiner and Coe, 1972); **9:** La Venta (Morrison *et al.*, 1970a; Morrison *et al.*, 1970b); **10:** Dzibilchaltun (Sauck *et al.*, 1998); **11:** Izamal (Sauck *et al.*, 1998); **12:** Chichen Itza (Sauck *et al.*, 1998); **13:** Balankanche (Sauck *et al.*, 1998); **14:** Ma'ax Na (Aitken and Stewart, 2004); **15:** Kaminaljuyu (Valdes and Kaplan, 2000); **16:** Ceren (Conyers, 1995; Sheets, 1985); **17:** Ciudad Vieja (Fowler *et al.*, 2007); **18:** Copan (Pastor, 2003); **19:** Ticamaya (Blaisdell-Sloan, 2006); **20:** Puerto Escondido (Tchakirides *et al.*, 2005); **21:** Los Naranjos (Tchakirides *et al.*, 2006b); **22:** Talgua (Luke *et al.*, 1997; Luke and Brady, 1998; Stierman, 2004; Stierman and Brady, 1999); **23:** Leon Viejo (Karlberg and Sjöstedt, 2007); **24:** Isla de Ometepe (Karlberg and Sjöstedt, 2007).



Previous Research at Los Naranjos

Los Naranjos first appeared in the literature in 1934 when Doris Stone visited the site after learning of the presence of carved stone from a resident in the Ulúa Valley (Stone, 1934). She described four sculptures located within the Principal Group that had either traditional Olmec or Maya styles. Monuments 1 and 2 (Figure 78), a combination of a serpent/shark head and an anthropomorphic head, respectively, are similar in style to sculptures found at the Olmec site of La Venta (Joyce and Henderson, 2002). Monuments 3 and 4 (Figure 78), which Stone (1934) attributed to Maya forms standing in submission, more likely represent Olmec-style forms of an anthropomorphic figure and transformation figure, respectively (Joyce and Henderson, 2002). [Joyce and Henderson (2002) later designated monument numbers]. During our own field mapping within the Principal Group during the summer of 2006, we recognized previously unreported columns within the private property to the north of the site, in the area south of Structure I and west of Structure II (Figure 72). These columns demonstrate that such statuary was an integral part of the site.



Figure 78: Olmec-style sculpture recovered previously at the surface of Los Naranjos. Monument 1: combination of a serpent / shark head ; Monument 2: anthropomorphic head; Monument 3: anthropomorphic figure; Monument 4: transformation figure. Sculpture interpretations are from Joyce and Henderson (2002).

The first excavations at Los Naranjos occurred in 1935 when Tulane University and the Danish National Museum sent an expedition to Honduras, partly to investigate Stone's report of Los Naranjos. Goals of this expedition were twofold: to delineate archaeological sites suitable for future excavations and to collect "archaeological specimens" for curation in Copenhagen (Yde, 1936; Yde, 1938b). This research at Los Naranjos, which focused mainly on the area near Structure I (Figure 72), was limited in nature, yet it "yielded one of the most wonderful collections of polychrome pottery ever produced by a single site within the Maya area" (Yde, 1936, p. 29).

More expansive, but still limited, excavations by William Duncan Strong, Alfred Kidder, and A.J. Drexel Paul in 1936 delineated the remains of several house platforms as well as clearly-defined stratigraphic horizons about 100 meters north of Structure I (Strong *et al.*, 1938). One horizon of note was sterile yellow clay that was deposited on top of early occupations. A unit similar to this in color and lack of artifact count was excavated to the west of Structure IV by the Cornell-Berkeley group in 2004. These units are potentially correlative; if so, this yellow clay might represent a period of no occupation (due to flooding or some other natural disaster) or may have been brought in intentionally to cover Early Formative (Table 4) occupations as part of later construction phases.

More than 30 years passed before the next stage of excavations. During the years 1967-69, a French team, led by Claude Baudez and Pierre Becquelin, excavated several locations within the site, but most notably within Structure IV. Baudez and Becquelin (1973) suggested that Structure IV began initially as an expansive structure during the Middle Formative (Table 4), as presumed Jaral phase artifacts were recovered from the deepest levels. Stratigraphic profiles from Baudez and Becquelin seem to suggest several construction phases, though they only identify one. A more

plausible explanation is that it was originally constructed during the Early Formative as a modest platform that might have been built as an extension of an existing household, with major expansion and enlargement not occurring until the early part of the Middle Formative. Support for this hypothesis comes from the Cornell – Berkeley excavations to the west of Structure IV during the summer of 2004; they uncovered only Early Formative artifacts and none of the Middle Formative (Henderson and Joyce, 2004).

Table 4: Mesoamerican time periods and associated date ranges (modified from Joyce, 2004a).

Period:	Date Range:
Postclassic	A.D. 1000 – 1521
Late Classic	A.D. 600 – 1000
Early Classic	A.D. 250 – 600
Late Formative	400 B.C. – A.D. 250
Middle Formative	900 – 400 B.C.
Early Formative	1600 – 900 B.C.
Archaic	8000 – 1600 B.C.

The Middle Formative expansion of Structure IV reflects a significant change in the use of space and coincides with important social changes seen in many other parts of Mesoamerica at this time (Dixon *et al.*, 1994; Joesink-Mandeville, 1987). The west slope of Structure IV, lined with flat paving stones (Figure 79), provided the presumed point of access to the summit. Middle Formative burials located within Structure IV revealed evidence of wealth and the creation of distinction in objects such as large jade ear spools (Baudez and Becquelin, 1973). This suggests the coincident

emergence of ranking or stratification, for which there is no evidence during the preceding periods (Marcus and Adams, 2005; Powis, 2005).

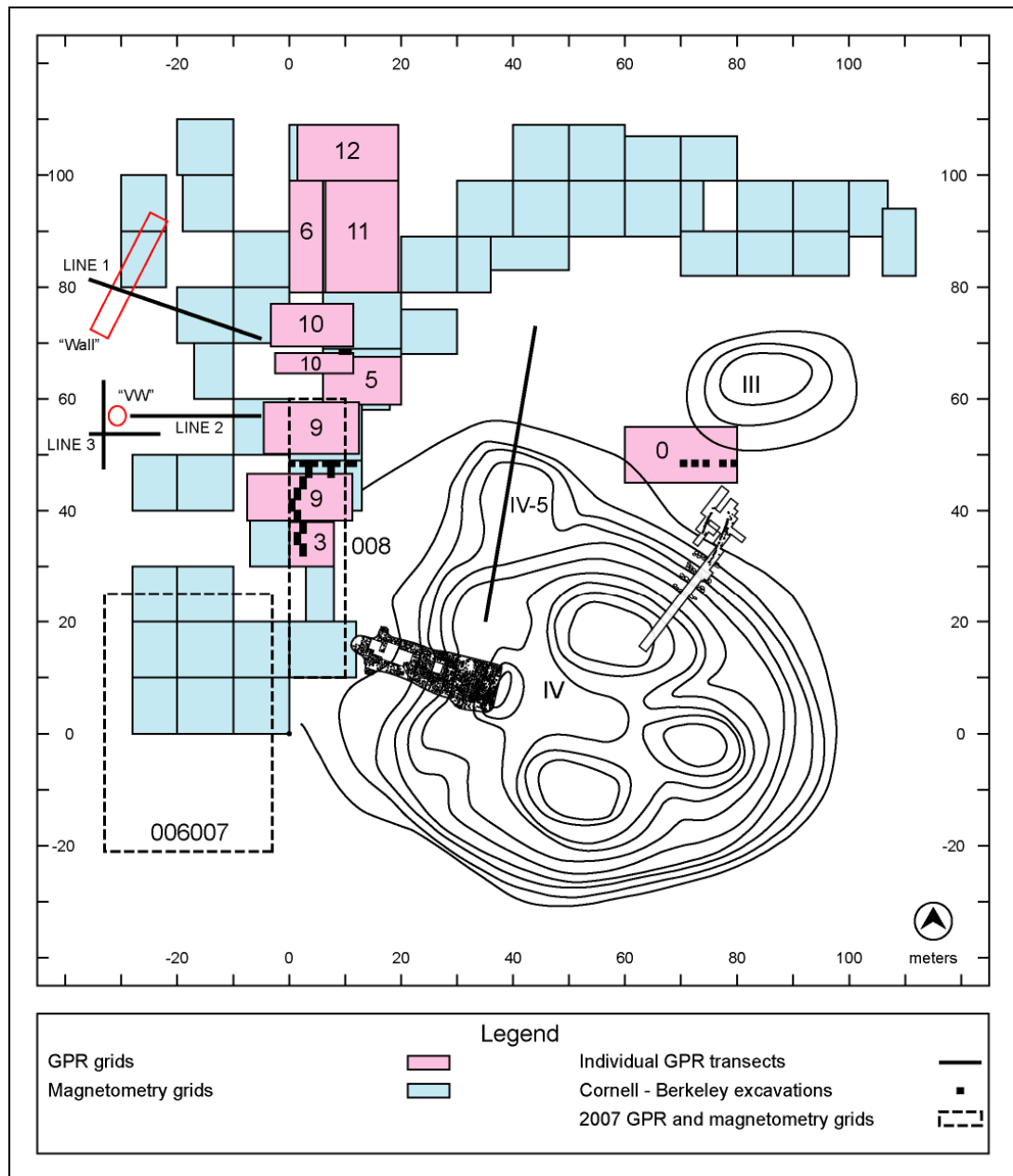


Figure 79: Location of all geophysical grids at Los Naranjos in relation to Structure IV. Numbers within grids refer to GPR grids. Note stone-lined ramp on west side of Structure IV.

Occupations appear to have shifted more than once during the Formative Period. Excavations on an extension added to the north side of Structure IV (labeled IV-5 in Figure 79) uncovered several rooms of a house that dates to the Late Formative (Table 4) (Baudez and Becquelin, 1973). If Middle Formative occupations were not located within the vicinity of Structure IV, the presence of housing complexes from the Late Formative suggest that what had been a different kind of public space had changed again, and could once more accommodate elite residence. Determining whether Middle Formative occupations were actually located adjacent to Structure IV, but just not in the area previously excavated, would help to determine whether these occupations really shifted, and if so, will help to clarify their significance in relation to the platform mounds.

The wealth of information obtained during these earlier studies caught the attention of the Instituto Hondureño de Antropología e Historia (IHAAH). Proyecto Arqueológico Cuenca del Lago de Yojoa (PACLY) began in 1995 as an effort to preserve a portion of the site as an ecological and archaeological park. This effort culminated in 2001 with the designation of the *Parque Eco-Arqueológico Los Naranjos* (Dixon *et al.*, 2001; Navarro Tábora, 2004).

Since the designation of park status, only minimal excavations have been permitted. In 2001, Oscar Neil Cruz and Erick Valles Pérez (2002) reconstructed the access ramp on Structure IV and exposed a portion of the terrace on the northeastern slope of Structure IV in hopes of making the site more easily interpretable to visitors. The last excavations to occur were undertaken by a joint Cornell University – University of California, Berkeley project (Figure 79), led by Professors John Henderson and Rosemary Joyce in 2003 and 2004 (Henderson and Joyce, 2003; Henderson and Joyce, 2004; Joyce, 2004b). The primary objectives of their study were to locate and document Early Formative Period occupations in the vicinity of

Structure IV. As part of their research, they requested that non-invasive geophysical methods be used to map the presence and extent of these early communities.

Beyond the obvious pedagogical objectives, a goal of the geophysical data collection was to test the efficacy of these methods in delineating archaeological and geological subsurface features at this site, as they represented some of the first uses of geophysical methods at archaeological sites in Honduras. Initially, it was hoped that the results of the geophysical surveys could be used to plan all of the archaeological excavations, but the logistics of the field program prevented all data from being analyzed prior to the establishment of test units. As a result, many of the features of interest imaged in the geophysical data were not excavated. Nevertheless, the results of these surveys helped to identify archaeological features in the subsurface, define 3D geometric relationships between features partially excavated, and establish geological context without excavations. Ground-penetrating radar data were acquired by Professor Larry Brown and students from Cornell. Kira Blaisdell-Sloan, then a graduate student at Berkeley, collected the magnetometry data. Additional GPR and magnetometry data were collected adjacent to Structure IV during the spring of 2007 (Tchakirides, 2007).

Ground-penetrating Radar

Basic Principles

Ground-penetrating radar is an active geophysical method that transmits electromagnetic energy into the ground and receives the resulting signals after they have reflected off subsurface features or interfaces (Conyers, 2004; Daniels, 2004; Neal, 2004; Reynolds, 1997). Variations in the electrical properties of subsurface materials cause the transmitted signal to travel at a different velocity. A portion of the energy is reflected back to the surface at each change in velocity and is denoted the

relative dielectric permittivity (RDP) or relative dielectric contrast (Annan, 2005). Reflection profiles (Figure 80) provide a cross-sectional view of the subsurface and are useful for viewing stratigraphy and structure of subsurface materials. All cross-sectional images display data in two-way travel time measured in nanoseconds (1×10^{-9} seconds), as well as in corresponding depths computed using velocity information obtained *in situ* from common mid-point (CMP) data (Jol and Bristow, 2003; Tchakirides and Brown, in prep).

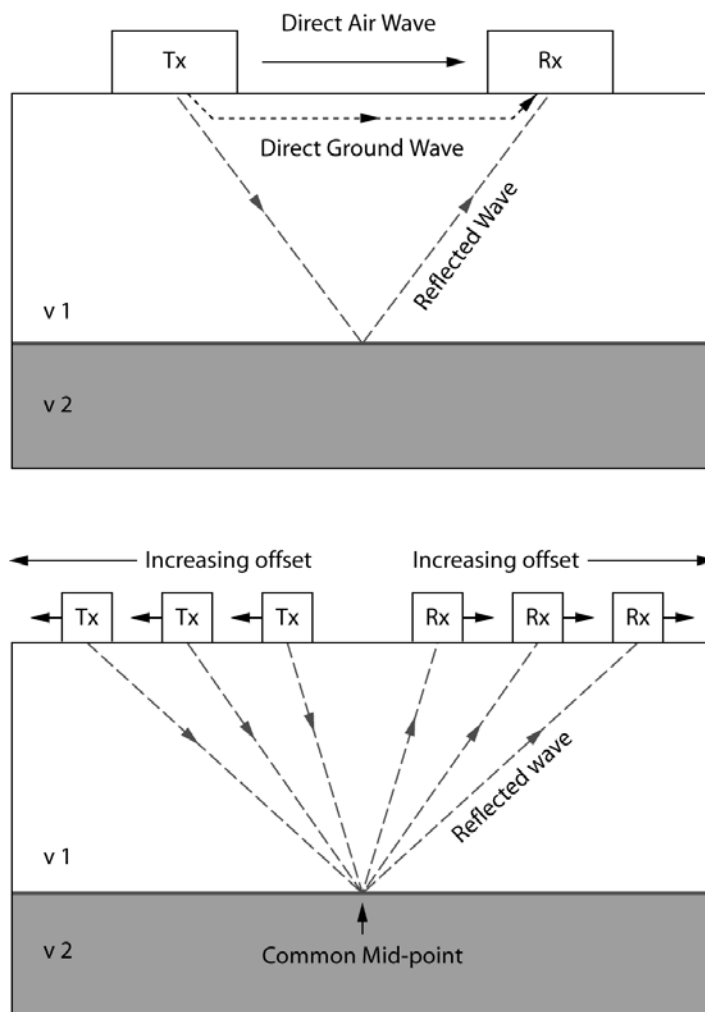


Figure 80: GPR data collection strategies. Top: Common offset method, showing the travel paths of the direct air and ground waves and the reflected wave generated by the surface of Layer 1 and Layer 2. $v_1 > v_2$. Bottom: Common midpoint (CMP) method.

In the CMP method, the transmitting and receiving antennae are moved apart from a fixed point (mid-point) at a set interval (Figure 80). For constant velocity media, the travel time for both the air and direct ground arrivals is a linear function of source-receiver offset, whereas reflected arrivals are hyperbolic functions of offset (Annan and Davis, 1976; Reynolds, 1997). Velocities for the direct arrivals are usually estimated from the travel time versus offset plots by measuring the reciprocal of the resulting slope. Average velocity from the surface to a reflecting interface can be obtained either by fitting hyperbolic functions using trial velocities or plotting the square of the travel time versus the square of the offset, in which case the velocity is represented by the square root of the reciprocal of the slope (Reynolds, 1997).

GPR Data Acquisition at Los Naranjos

In the 2003 field work, a Sensors and Software, Inc. Noggin 250 cart-mounted system, with 250 MHz antennae (Figure 81), was used to acquire some of the data at Los Naranjos. In addition, a Sensors and Software, Inc. pulseEKKO 100 bistatic system (Figure 81), equipped with 50, 100, and 200 MHz antennae, was employed to provide deeper penetration profiles, additional 3D coverage, and common mid-point (CMP) data. The Noggin 250 system, selected initially to collect the majority of the GPR data at the site, failed due to heat problems during the surveying of Grid 6; therefore, all subsequent surveys were undertaken using the pulseEKKO 100, with most data acquired with the 200 MHz antennae. For grids collected with the pulseEKKO system (Grids 9, 10, 11, and 12) (Figure 79), a step size of 20 centimeters was used, and individual transects within each grid were spaced 40 centimeters apart (Table 5). A transect spacing of 0.25 or 0.5 meters was used in the Noggin grids (Grids 0, 2, 3, 5, and 6) (Figure 79 and Table 5). A bi-directional survey mode was used for all of the grids (Figure 82), and the starting point was always located in the

bottom left corner (SW) (Figure 82). The only exception to this was Grid 0, which had its original data collection starting point in the upper left corner (NW), with LINEX0 being the northernmost profile. The profiles were later flipped so that LINEX0 became the southernmost profile. All geophysical grids are co-registered to the Cornell – Berkeley archaeological site grid that was established at the beginning of the 2003 field season. Coordinates of all grids and individual profiles, therefore, reflect the locations within this larger site grid.



Figure 81: Geophysical equipment used during the 2003 and 2007 field seasons. (a.) pulseEKKO GPR, with 200 MHz antennae. (b.) Noggin 250 MHz GPR. (c.) SIR-3000 GPR, with 400 MHz antennae. (d.) Geometrics G-858 magnetometer.

Table 5: 2003 GPR data collection parameters.

Grid #	System	Center Frequency (MHz)	Profile Direction	Grid Size (m)	Profile Separation (m)	In-line Spacing (m)
0	Noggin	250	X (W – E)	20 x 10	0.5	0.05
2	Noggin	250	Y (S – N)	8 x 8	0.25	0.05
3	Noggin	250	X (W – E)	8 x 8	0.25	0.05
5	Noggin	250	X (W – E)	14 x 8.5	0.25	0.05
6	Noggin	250	Y (S – N)	6 x 20	0.25	0.05
9N	pulseEKKO	200	X (W – E)	17 x 9.25	0.4	0.2
9S	pulseEKKO	200	X (W – E)	19.5 x 8	0.4	0.2
10N	pulseEKKO	200	X (W – E)	15 x 8	0.4	0.2
10S	pulseEKKO	200	X (W – E)	14 x 3.6	0.4	0.2
11	pulseEKKO	200	X (W – E)	13.5 x 20	0.4	0.2
12	pulseEKKO	200	X (W – E)	12.5 x 10	0.4	0.2

Higher frequency GPR data were acquired at Los Naranjos in the spring of 2007 (Table 6) (Tchakirides, 2007), immediately to the west of Structure IV (Figure 79). This time, a GSSI SIR-3000 system with 400 MHz antennae (Figure 81) was used to collect the GPR data. The higher frequency GPR unit was selected in the hopes of producing a higher resolution image of the subsurface, as the 2003 GPR data from this area are characterized by limited penetration and poor resolution of features.

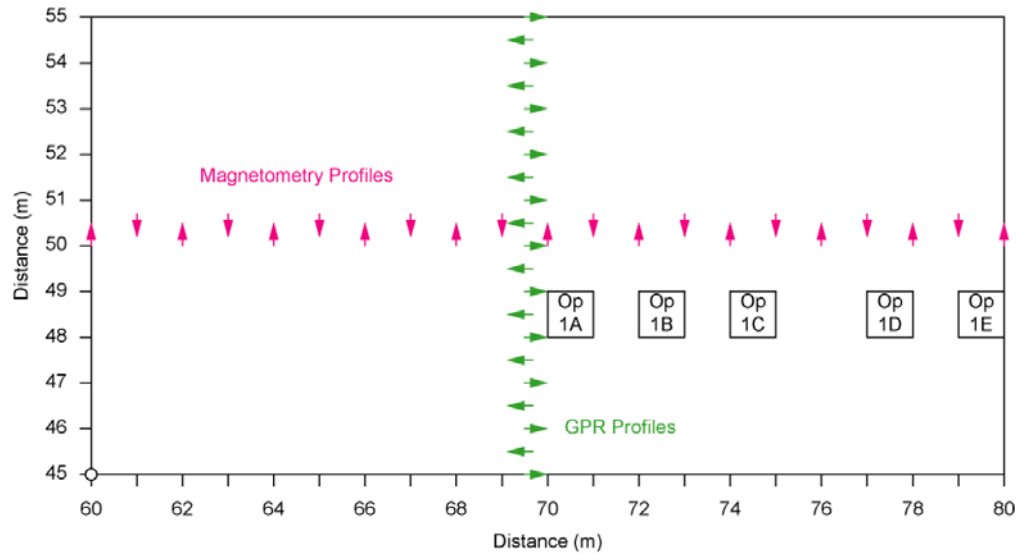


Figure 82: Bi-directional GPR and magnetometry data collection scheme in Grid 0. Also shown are the five Cornell – Berkeley excavation units from Operation 1 (Op 1).

Table 6: 2007 GPR data collection parameters.

Grid #	System	Center	Profile	Grid	Profile	In-line
		Frequency (MHz)	Direction		Size (m)	
006007	SIR-3000	400	Y (S – N)	21 x 34	0.5	0.02
008	SIR-3000	400	Y (S – N)	13 x 50	0.5	0.02

Data Processing

A substantial effort was invested in “cleaning up” and processing the GPR data to extract as much useful information from them as possible. The first step in data cleanup involved renaming all of the GPR files so that they were labeled according to the site grid, such as LINEX470 (47.0 m N) or LINEY300 (3.0 m E). Next, alternate profiles within each grid were reversed so that they were all oriented in the same direction, either west to east or south to north. The data collection starting point for all

grids was the southwest corner, so all of the odd-numbered profiles were reversed (the first line collected was labeled LINEX0 or LINEY0). For all of the GPR data collected with the Noggin 250 MHz system, it was necessary to reset the starting coordinate of alternating profiles so that each profile aligned properly. This step was necessary because of slight variations in line length due to slippage of the survey wheel. Similarly, the data files were chopped so that each profile had the same number of traces. This created grids of uniform size, which was necessary for migration to work correctly (Sandmeier, 2006).

Obviously bad traces were zeroed then replaced by a new trace derived from interpolating traces on either side of the suspect trace. All profiles were examined for trace polarity reversals that might have resulted from inadvertent flipping of the orientation of the transmitting and receiving antennae during data collection. Polarity was then corrected for consistency among all of the profiles. This was an issue for the pulseEKKO data only, since the Noggin and GSSI antennae are fixed. Next, all GPR data were filtered with a high-pass “dewow” filter to remove signal saturation effects (Gerlitz *et al.*, 1993; Sensors & Software Inc., 2003). Wow can be introduced because of the electrical properties of the ground (Jol and Bristow, 2003) or when the transmitting and receiving antennae are too close to one another (Sensors & Software Inc., 2003). All cross-sectional reflection profiles shown in this paper have been dewowed. Time zero corrections were then performed using the “Datum Timezero” option built into *Ekko_View Deluxe* (Sensors & Software Inc., 2003) so that the time zero was reset to the first break point (See Chapter 3) of each trace.

For the 2007 GPR data, some additional steps were necessary, as these data were collected slightly differently than the 2003 data. For instance, the 2007 data were collected using an amplitude gain in the field to enhance initial viewing of the data. Because I wanted to work with the raw data for processing, this original header

gain was removed, then the data were dewowed. The 2007 data were also collected using a small time shift, so the time zero of each data file was manually reset using the first break point of the first trace in each file.

A Hilbert transform was used to calculate the “envelope” of each trace (Figure 83) prior to generating GPR time slices, which involved a fast Fourier transform to shift negative frequencies by 90 degrees then an inverse Fourier transform (Goodman *et al.*, 1995; Sensors & Software Inc., 2003; White, 1991). Time-slice images derived from the envelope are often more easily interpreted.

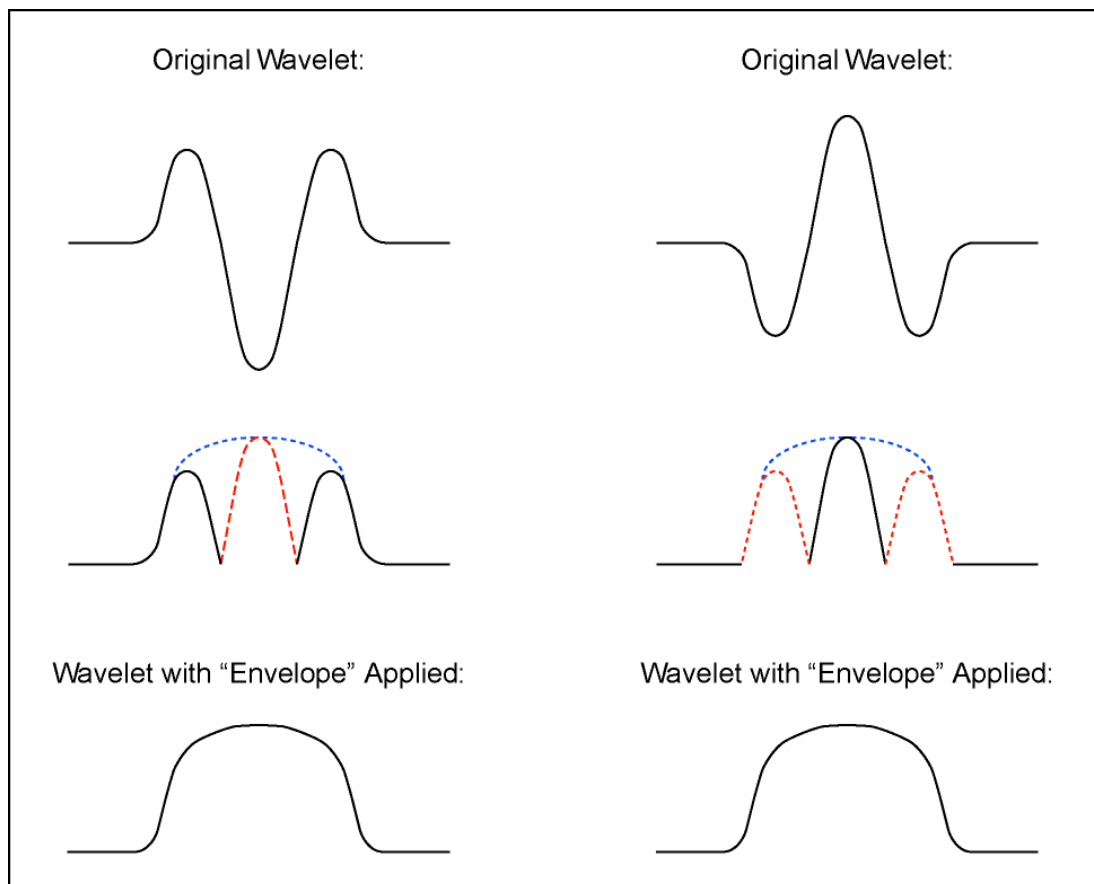


Figure 83: Schematic of a wavelet before, during, and after the "envelope" is applied. Modified from Sensors & Software, Inc. (2003, p. 92; Figure 8-15).

Frequency Dependence

In GPR surveys, a trade-off exists between the depth of penetration of the GPR signal and the resulting resolution of features, with lower frequencies penetrating to greater depths, but higher frequencies resolving features better. In this study, the 400 MHz antennae penetrated to depths of only about 50 centimeters, whereas the 100 MHz penetrated to depths of almost six meters. The 250 MHz antennae are thought to provide the best trade-off between depth of penetration and resolution of features in archaeological contexts (Clark, 1990).

A less well-known aspect of GPR frequencies is that the characteristic frequency of GPR antennae is the center frequency of the signal emitted in air. However, the frequency of the signal that is coupled into the ground can range anywhere from one-half to two times this “ideal” frequency. There is no easy way to predict the amount at which the transmitted frequency will vary, but it usually is reduced about 10 to 50 %, depending on the ground conditions (Greg Johnston, personal communication). This is referred to generally as “frequency pull-down” (Figure 84), but there is no standard definition (Greg Johnston, personal communication). In this example, the 250 MHz shifted to 140 MHz, which is a loss of 44%. The 200 MHz shifted down to 110 MHz, which is a loss of 45%.

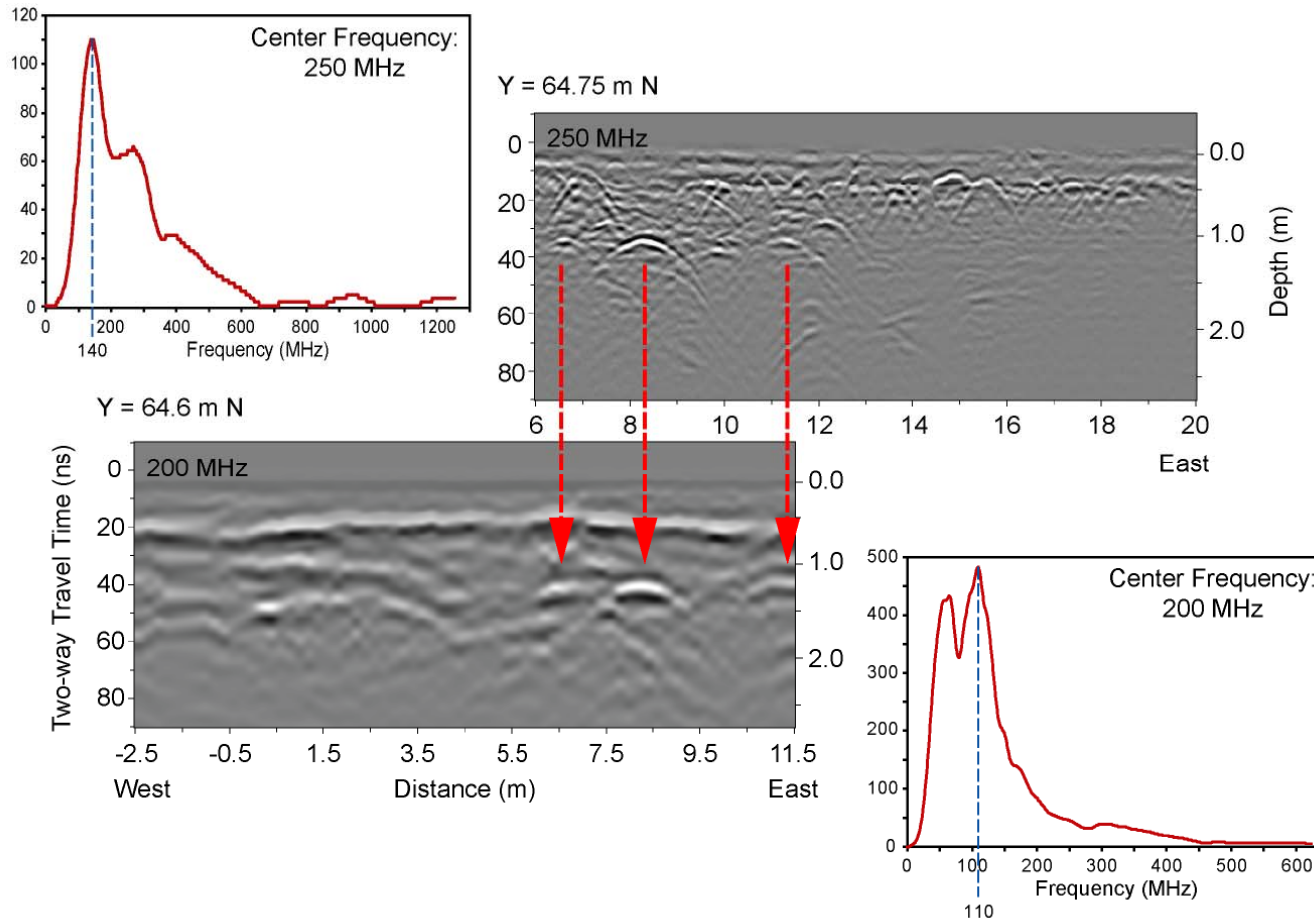


Figure 84: Comparison between the 250 MHz and 200 MHz antennae. LINEX6475, collected in Grid 5, is the closest profile to LINEX646, collected within Grid 10. The three hyperbolae generated at about 35 nanoseconds are visible in both profiles, but the 250 MHz is able to resolve features better than its lower frequency counterpart. Corresponding frequency spectra show the ideal center frequency is not transmitted into the ground, but is downloaded by 44 % and 45 %, respectively.

Velocity Estimation

Six CMP profiles (Figure 85) were included as part of the geophysical data collection at Los Naranjos to provide estimates of *in situ* GPR velocities. The CMP technique (see above) is a commonly used method for estimating subsurface velocities from both seismic and GPR data (Bristow and Jol, 2003; Sheriff and Geldart, 1995), and the estimates extracted are generally considered to be robust (Jol and Bristow, 2003). Any variation caused by display mode or limitations in screen resolution was thought to vary by 1 to 2 % at most (Annan and Davis, 1976). While conducting initial analyses of the CMP profiles from Los Naranjos, we noticed that velocities varied much more than 1 to 2 % depending on the particulars of the technique used to estimate velocity. For example, for CMP PRO 27 we obtained a ground wave velocity of 0.060 m/ns when visually fitting a line between 2 points, but we obtained an estimate of 0.055 m/ns with linear regression analyses using points picked from all the traces, a difference of 8.3 %. This led us to perform a systematic study of several common picking strategies, display modes, and analytic techniques to evaluate the impact of these various “picking” criteria on the resulting velocity estimates (Tchakirides and Brown, in prep). The results of these analyses proved invaluable for comparisons with the archaeological excavation data, as accurate velocities are needed to convert GPR data from travel time into depth.

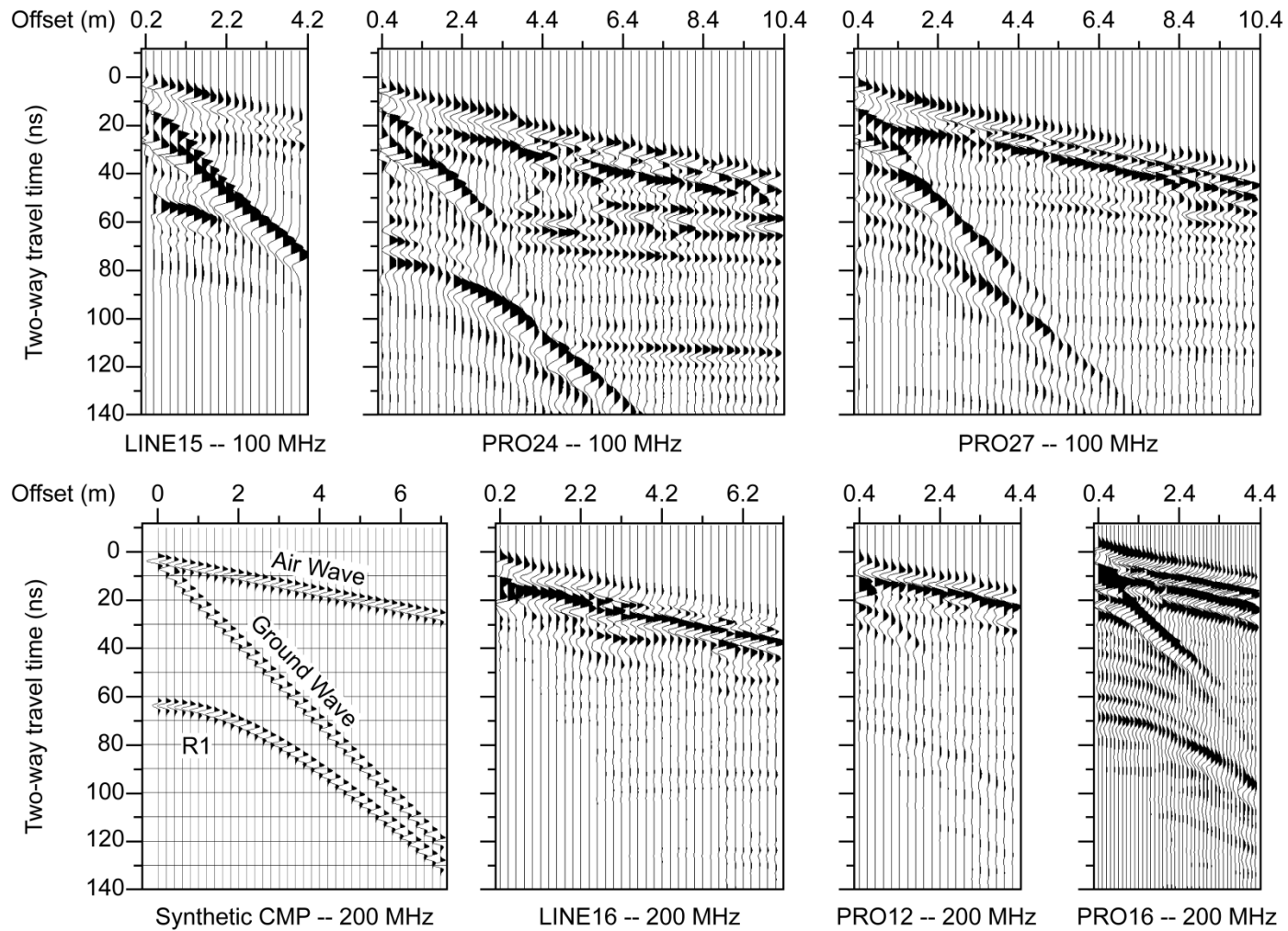


Figure 85: Wiggle trace images of the six CMP profiles collected at Los Naranjos. A synthetic CMP is shown in the bottom left, with direct air and ground waves, and one reflection. Vertical exaggeration = 2x.

Three-dimensional Migration

As the GPR system moves along the ground surface, electromagnetic energy radiates into the ground in a three-dimensional cone that is defined by the limits of the Fresnel zone (Lindsey, 1989). Thus, the GPR system images not just what is directly beneath the unit, but also in front, back, and to the sides (Meats, 1996). This type of energy pattern generates reflections from any point within the cone of transmission, but records them in a GPR profile as if they originated directly below the antennae (Kearey *et al.*, 2002; Neal, 2004; Yilmaz, 2001).

Fundamentally, the goals of migration are to correct GPR reflection data so that they accurately represent the subsurface (Neal, 2004) and to increase the resolution of features in reflection profiles (Hogan, 1988). There are many techniques for implementing migration. Here we use a form of Kirchhoff summation, in which energy is summed along an appropriate diffraction hyperbola, thus focusing reflected energy at its apex (Hogan, 1988; Schneider, 1978). Kirchhoff migration, also known as diffraction migration (Chun and Jacewitz, 1981), is governed by the principle that the radius of curvature of a diffraction hyperbola is directly related to the velocity of the medium in which it was generated and the time at which it occurs (Yilmaz, 2001). In a constant velocity medium, narrow diffraction hyperbolae have a slower velocity than diffractions that have a larger radius of curvature. When the correct parameters for migration are used, subsurface reflections will be relocated to the position corresponding to the physical location in the subsurface of the features that generated them. In general migration steepens and shortens reflections and moves them in the updip direction (Chun and Jacewitz, 1981) (Figure 86). Thus migration is essential to correctly correlate specific features of interest in GPR data to geological or archaeological cross-sections.

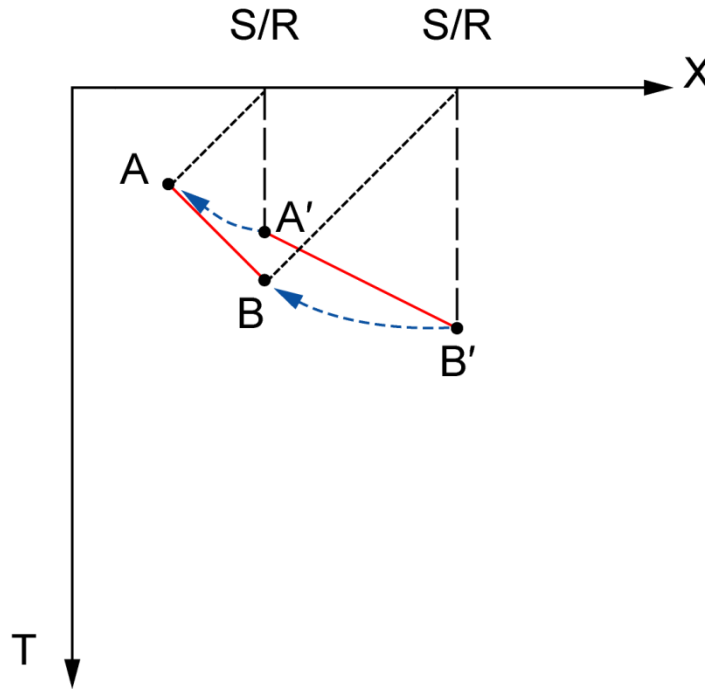


Figure 86: The process of migration. A'-B' is migrated to A-B, its correct location in the subsurface. Figure is modified from Chun and Jacewitz (1981).

Magnetometry

Magnetometry is a passive geophysical method that measures deviations in the Earth's magnetic field that can be caused by anthropogenic features that have a strong magnetic susceptibility in contrast with the surrounding matrix. Examples of such features with a thermoremanent magnetization are hearths, kilns, or burned house floors (Kvamme, 2003). Features constructed from intrinsically magnetic materials, such as basalt, also generate strong magnetic anomalies due to the alignment of iron-rich minerals (Burger *et al.*, 2006). Plan view images of magnetometry data show variations in magnetic field strength.

Acquisition of Magnetic Data

A Geometrics G-858 cesium vapor magnetometer was used to acquire data at Los Naranjos in 2003, with all surveys occurring within the Principal Group. Data

were acquired in 58 grids, which overlapped much of the same areas as GPR and significantly expanded subsurface geophysical coverage (Figure 79). Similar to the GPR surveys, magnetometry data (Figure 87) were collected in a bi-directional mode, with all transects oriented south to north. Individual transects were spaced 1 meter apart (Figure 88). Two additional grids of magnetometry data were collected in 2007 (Figure 79), but for these data, both the sensor spacing and transect spacing were decreased in order to produce higher resolution datasets (Figure 88). The magnetometry data collected at Los Naranjos are used here to corroborate the GPR findings when appropriate.

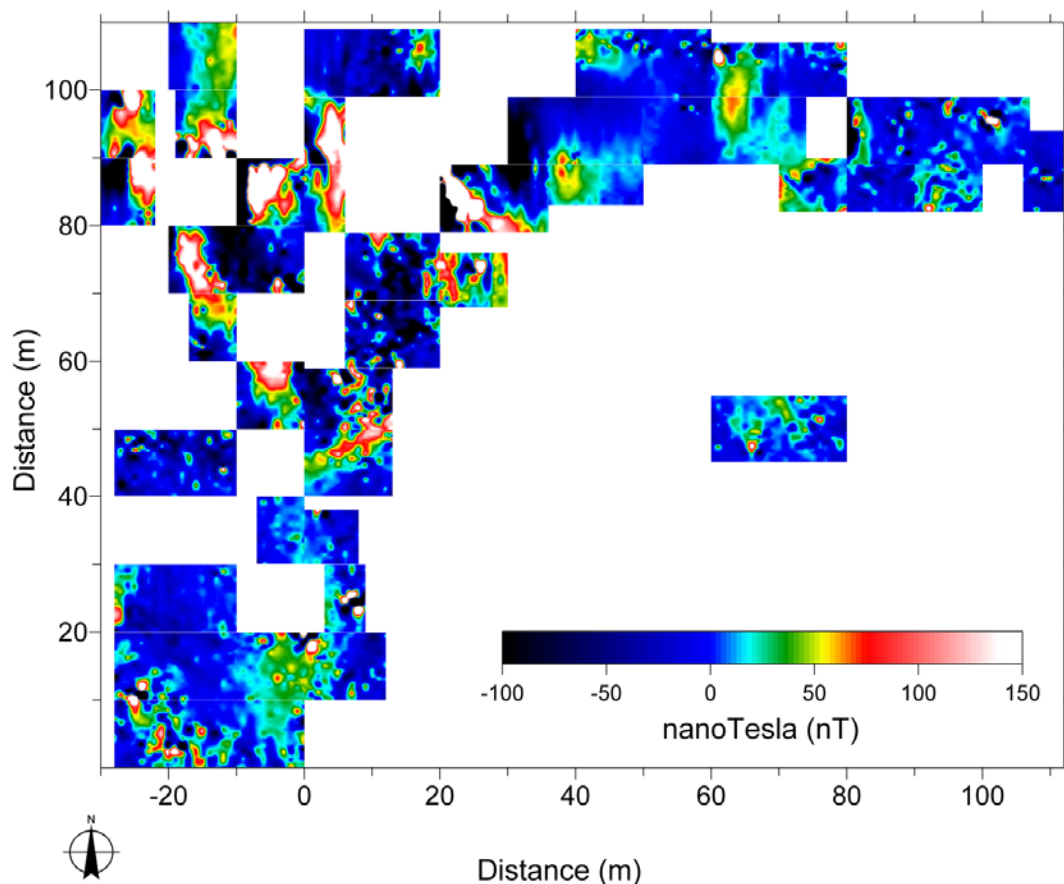


Figure 87: Map view of the 2003 horizontal gradient magnetometry data from Los Naranjos.

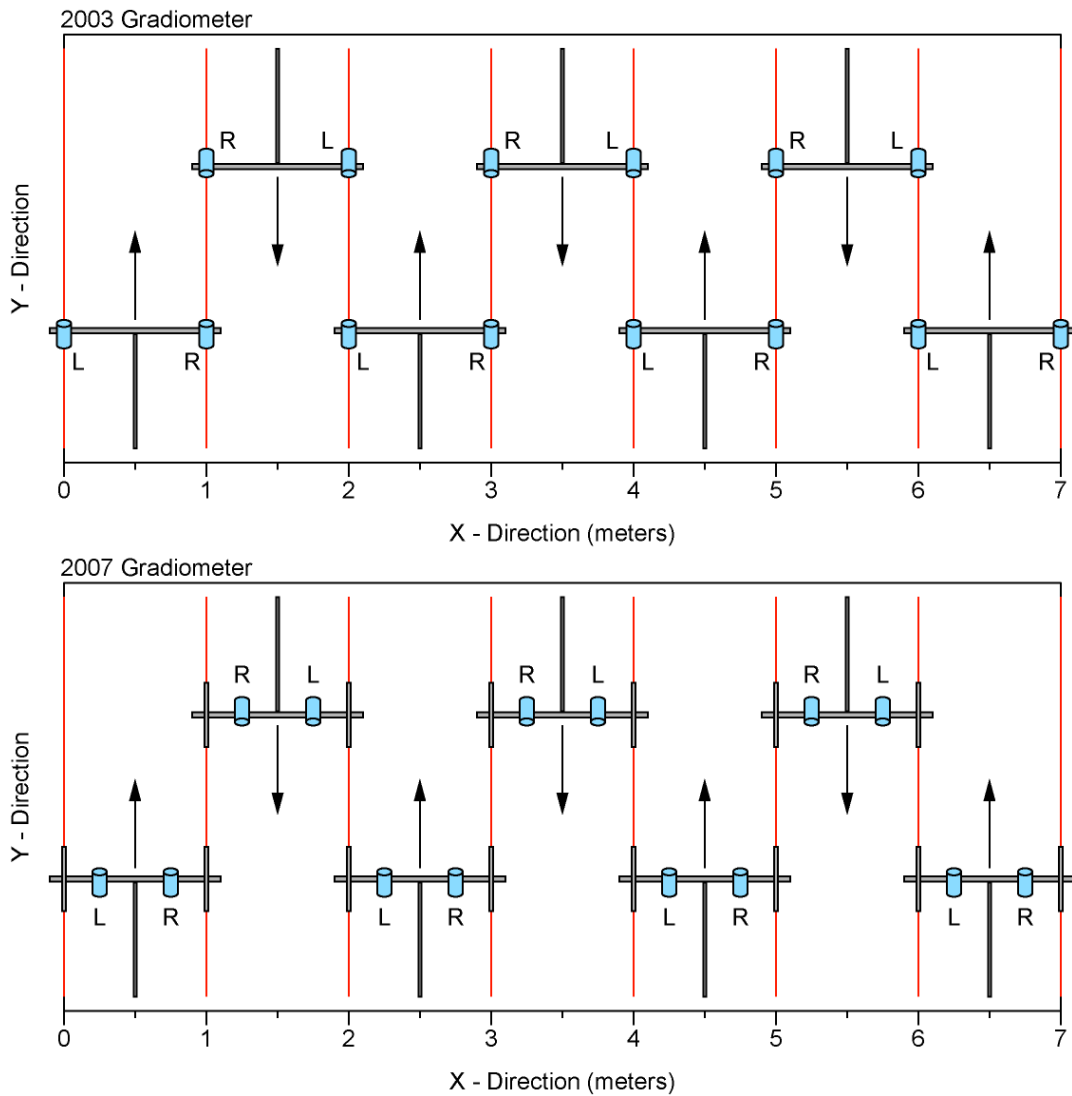


Figure 88: Comparison of the 2003 and 2007 magnetometry data collection. In the 2003 data collection, the unit was carried along the ground, and the sensors were spaced 1 meter apart in-line but overlapped in the cross-line profiles. In the 2007 data collection scheme, the sensors were attached to the pole with wheels, and there was a consistent 50-centimeter spacing between sensors (in-line and cross-line). Red lines indicate location of tape measures on the ground. Teal cylinders represent sensors (L: left and R: right), and the gray objects represent the unit (without wheels in 2003 and with wheels in 2007). Arrows indicate direction of movement.

Geophysical Results

Buried Sculpture?

Each geophysical method measures a specific physical property of the ground. Therefore, complementary results are often produced when multiple methods are employed at the same site (Clay, 2001; Kvamme, 2003). In this study, we found that ground-penetrating radar and magnetometry used together provided an effective means of determining the depth, dimensions, and lithology of several specific subsurface features. One example from Grid 0, located between Structures III and IV (Figure 79), highlights this.

Grid 0 contained scores of diffraction hyperbolae, with apices ranging from 10 to 40 nanoseconds, or about 0.3 to 1.2 meters depth, with each apex corresponding to the top of a buried object. Many of these may have been generated by reflections from rocks, perhaps detritus fallen from the slope of Structure IV, which is only about 5 meters to the south of Grid 0 (Figure 79). One feature, however, stands out from the rest in terms of its amplitude and shape (Figure 89a). The prominent diffraction hyperbola at 67 meters has a much higher amplitude and a larger radius than the other hyperbolae within this grid. Both peak amplitude and diffraction curvature are expected to be dependent upon the object's morphology, specifically its size (Tchakirides *et al.*, 2006a).

In 3D migrated images, diffraction hyperbolae generated by small rocks should collapse to simple point sources. The feature within Grid 0 at 67 meters, however, does not collapse to a point like the other diffractions within the grid (Figure 89b), suggesting it is much larger in size. When plotted in map view, this high-amplitude feature appears elongate with a major axis that is about 1.5 meters long and approximately 0.5 meters wide (Figure 89c).

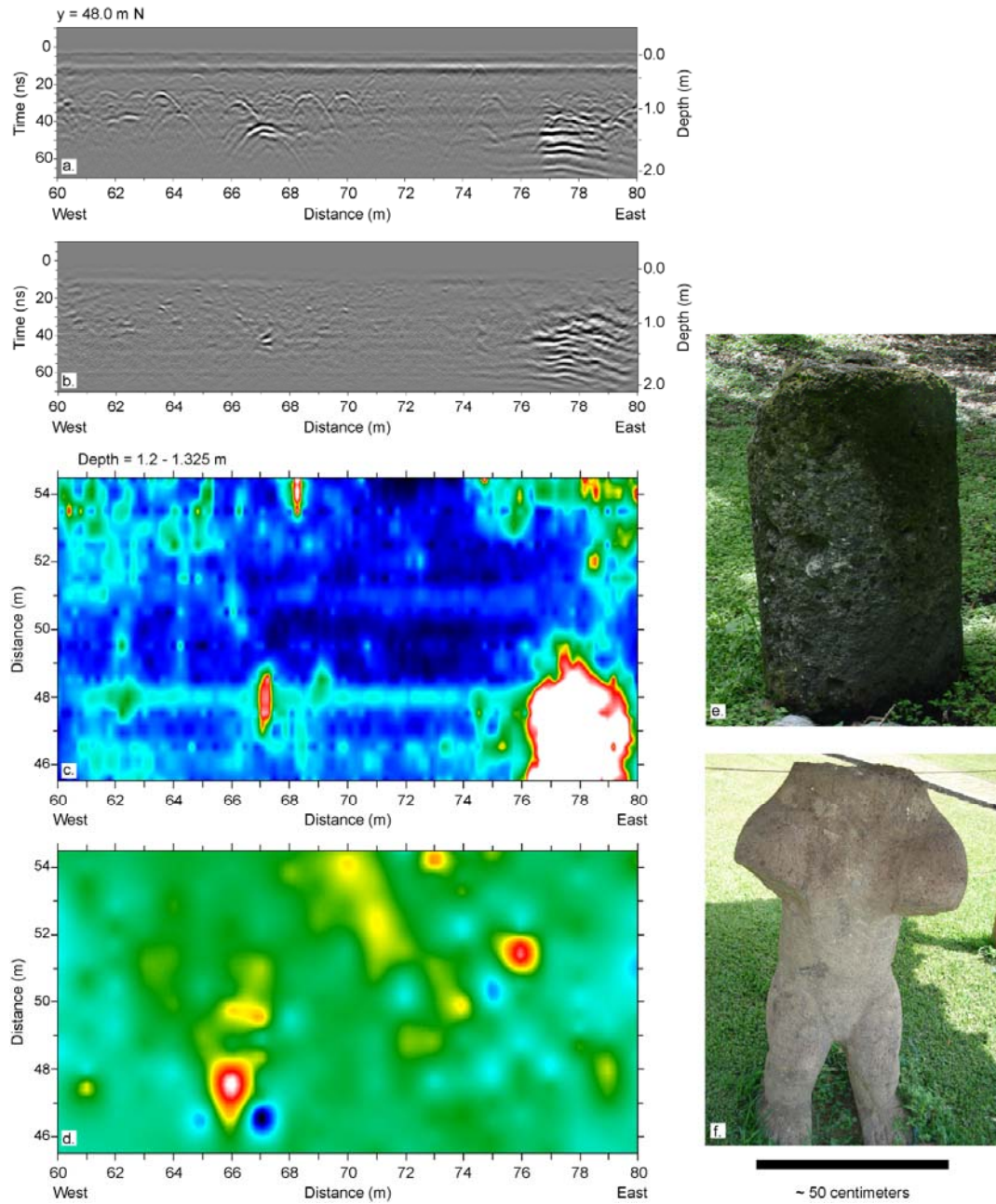


Figure 89: Possible buried sculpture at Los Naranjos. (a.) Unmigrated cross-sectional GPR transect showing the high-amplitude diffraction hyperbola at 67 m; (b.) 3D migrated view of the same data; (c.) Map view of 3D migrated GPR data; (d.) Magnetic gradiometry data. The high-amplitude feature at about 67 meters could represent a buried column or piece of sculpture, like those already discovered at Los Naranjos (e. and f.).

Furthermore, horizontal gradient magnetometry data indicate that this feature is composed of more magnetic material than the other diffractors, perhaps reflecting rock mineralogy, for example basalt rather than non-magnetic limestone.

Magnetometry data from Grid 0 show a dipolar anomaly that overlies the GPR reflection feature (Figure 89d). Note that magnetic objects are often located mid-way between the high- and low-amplitude signals (Bevan, 2006), which would place the magnetic object at about 67 meters. This corresponds well with the location of the high-amplitude diffraction in the GPR data.

One possible interpretation for this particular feature, based on its dimensions, material, and location is that it could be a piece of buried sculpture, similar to the four Olmec-style basalt sculptures already documented on the surface at the site (Joyce and Henderson, 2002) (Figure 78 and Figure 89 e, f). The original locations of these Olmec-style sculptures remain uncertain, but since early researchers found them within the Principal Group, including near Structure IV (Figure 72), their location in open spaces adjacent to platform mounds suggests they are likely public monuments or displays that delineated and segregated the space (Cyphers, 1999; Grove, 1999; Joyce and Grove, 1999; Love, 1999). During our own field mapping within the Principal Group during the summer of 2006, we recognized previously unreported columns within the private property to the north of the site. The presence of these columns suggests that additional columns or sculpture might still be located at the site, and possibly buried. If so, they would be expected to present a geophysical signature like that associated with the anomaly in Grid 0.

Faulting and Paleoseismology

Shallow faulting is indicated on a number of the GPR cross-sections, especially within Grid 12 (Figure 90). Stratal offsets are common within the

uppermost 4 meters of this grid. The dominant type of fault seems to be reverse (Figure 90), indicating east-west compression. The subsurface geometry of it suggests a linear “pop-up” structure, a feature compressed and pushed upwards, at the core of the plaza within the central portion of Grid 12 (Figure 90). This fault-bounded structure is evident as a distinct southwest to northeast trending feature in map view, with sharp contrasts in amplitude visible on either side but especially along its eastern boundary (Figure 90). We suggest that this faulting may be direct evidence of earthquake activity in the region.

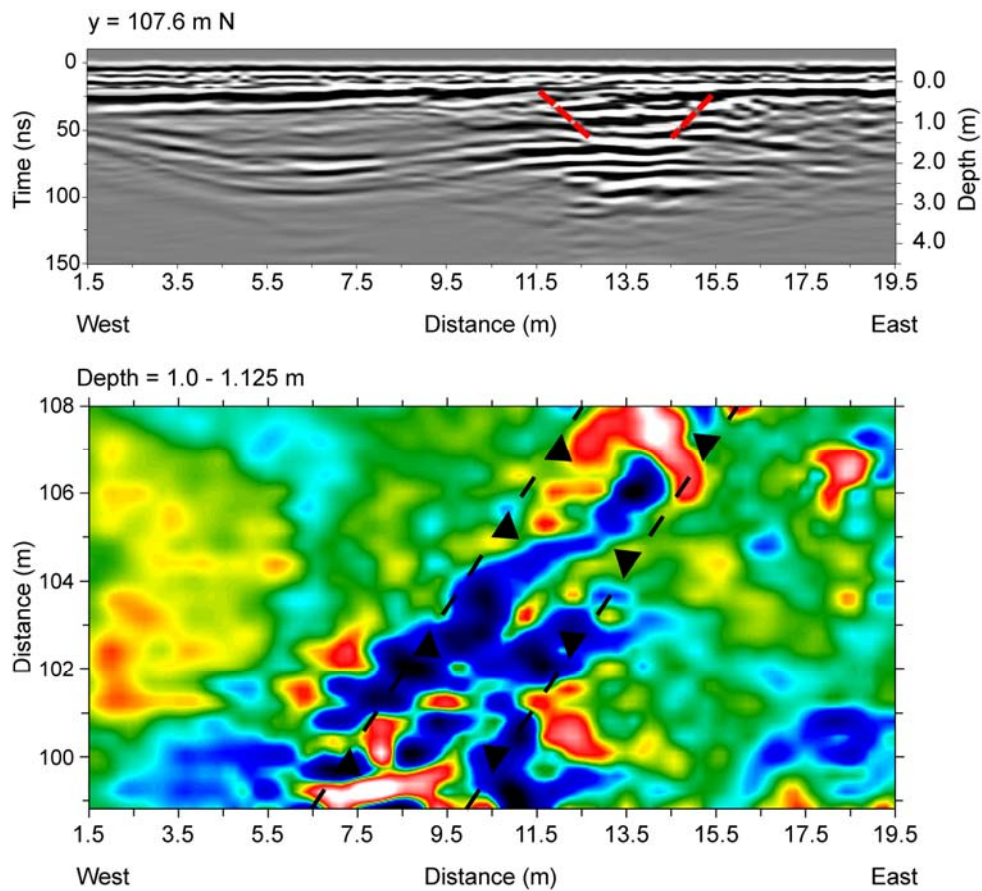


Figure 90: “Pop-up” structure imaged within the plaza at Los Naranjos. Top: Cross-sectional view of GPR data from Grid 12, with an example of reverse faulting located between 11.5 and 15.5 meters (indicated in red). Stratal offsets extend to almost 4 meters depth in some of the cross-sectional views. Bottom: Map view of GPR data from Grid 12 showing the fault-bounded pop-up structure that trends southwest to northeast.

Earthquakes within Honduras are consistent with the plate tectonic setting (see above), and seismic events have been documented from both recent and prehistoric data (Ambraseys, 1995; Ambraseys and Adams, 1996; Carr and Stoiber, 1977; Güendel and Bungum, 1995; Kovach, 2004; Osiecki, 1981; White and Harlow, 1993). To our knowledge, however, these results are the first paleoseismic indications visible within specific strata from the Lake Yojoa area. One goal of future research would be to date these faults to determine if there is a correlation between earthquake activity and specific occupations within the site.

Small Depocenters

Perhaps the most intriguing aspect of the stratigraphy evident in the GPR data are apparent localized depocenters within the plaza. The deepest depocenter is defined by a series of concave strata at a basal depth of about 2.5 meters (Figure 91), which seems to be disrupted along its eastern edge by the pop-up structure described above. This deeper unit is in turn overlain by a much thinner (about 1 meter thick) depositional sequence that onlaps it from the west (Figure 91).

The shallower unit might correspond to relatively recent overflow deposits from the drainage canal dug from Lake Yojoa (Cruz C. and Valles Pérez, 2002) that is located about 200 meters to the west. The deeper, thicker unit, on the other hand, could have archaeological significance, as its base lies at a depth similar to Early Formative occupations encountered about 50 meters to the south during the Cornell – Berkeley excavations (Henderson and Joyce, 2004). Its depth, dimensions, and location within the plaza would suggest it might have ceremonial significance as a constructed basin, as similar ponds have been noted in plazas at other Mesoamerican sites. For example, at the Olmec site of San Lorenzo Tenochtitlán, Cyphers (1999, p. 159-165), noted specific monuments located in relation to *lagunas* visible at the

surface, but suggested the latter might be much more recent than proposed originally by Krotser (1973).

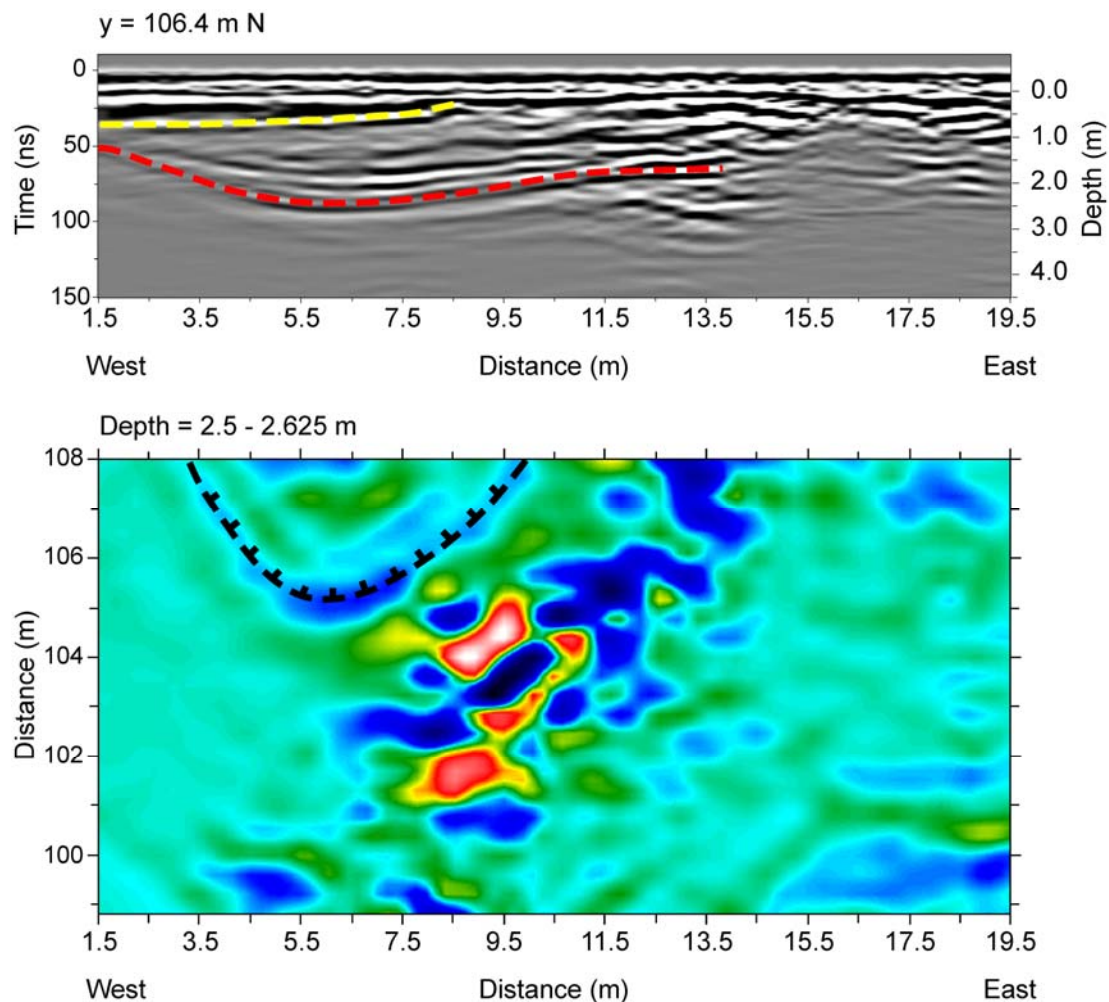


Figure 91: Small depocenters imaged by GPR. Top: Cross-sectional view of GPR data from Grid 12 showing two of the depocenters noted in Grid 12. Onlap is indicated in yellow, and a basin is indicated in red. Bottom: Map view of GPR data from Grid 12 showing contours of pronounced layering from the basin. One contour is noted in black.

In cross-sectional view, the GPR signal is attenuated below the deeper stratigraphic unit, and only subtle reflections are visible below it (Figure 91). One possible reason for the lack of deeper penetration is that the basin is lined with clay,

which would attenuate the GPR signal. If the lining is clay, determining whether it was intentionally lined to form an impermeable layer at the base would help to establish whether the genesis of this feature is anthropogenic or geological. Understanding the complete geometry, age, and composition of these shallow layers should be a priority for future coring or excavations at Los Naranjos.

Inside Structure IV

Ground-penetrating radar probed Structure IV (Figure 79) in a series of transects collected with the 100 MHz antennae that began on the flat ground north of Structure IV, continued across the base of the mound and its northwestern extension (Structure IV-5), and ended at the summit at an elevation of almost 7 meters (Figure 92). The individual profiles were pieced together to create this composite image that was then corrected for topography using elevations measured during the summer of 2006 fieldwork. The lower frequency antennae were selected specifically to image to greater depths than the 200MHz or 250 MHz antennae used for most of the surveys discussed thus far. This transect The deep (6 m) penetration characteristic of the plaza floor north of Structure IV ends abruptly at the edge of the mound (at about 18 meters on Figure 92). Previous excavations within the mound (Baudez and Becquelin, 1973) found its core to be comprised of clay, which is often a very absorptive medium for GPR due to its conductive properties (Conyers, 2004). The lack of radar penetration is consistent with a clay core and clearly indicates that the platform mound material is different from the plaza matrix that is well-imaged by the GPR surveys north of the mound. It is not possible to determine if this different matrix represents material brought in to construct Structure IV or if it represents the pre-existing topography of the site, but it is clear that the material is different than the surrounding matrix.

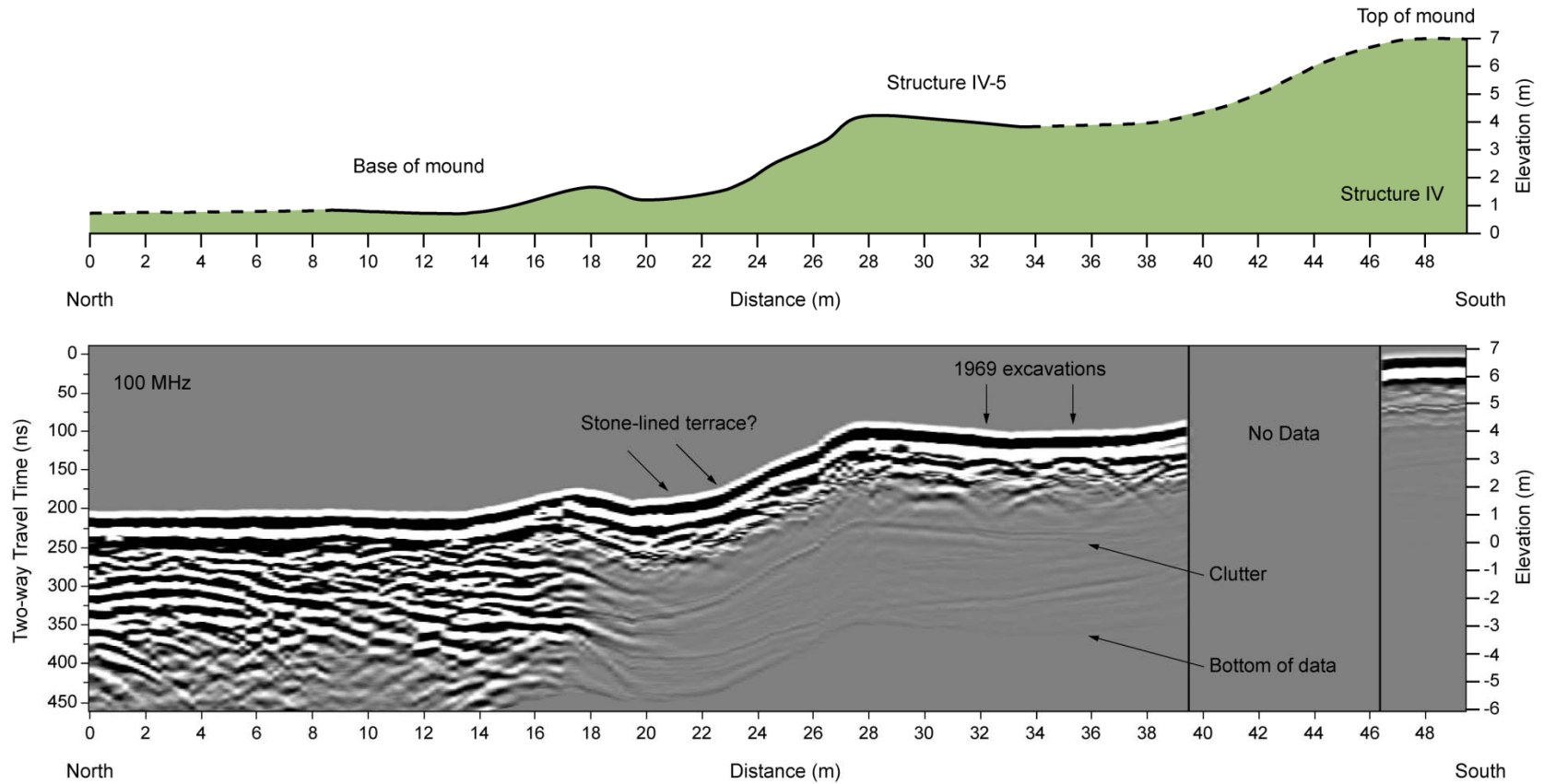


Figure 92: Topographically corrected GPR cross-sectional view across Structure IV. Top: Topography along GPR transect. Bottom: GPR transect over Structure IV. Note the limited signal penetration within the platform mound. No data were collected between about 40 to 47 meters. Vertical exaggeration = 2x.

Excavations from Baudez and Becquelin's 1967-69 fieldwork (Baudez and Becquelin, 1973) provide information regarding specific reflections within this transect. Diffraction hyperbolae along the slope between the base of the mound and the extension of Structure IV (labeled Structure IV-5) (from 20 to 24 meters in Figure 92) may correspond to a stone terrace wall uncovered during their work. Also imaged within this transect is evidence of their excavations in Structure IV-5, visible from about 30 to 37 meters (Figure 92). In this portion, excavations revealed several rooms of a residence, dating to the Late Formative Period (Baudez and Becquelin, 1973, p. 42-43). Additional features are visible in Figure 92, but they correspond to clutter (sideswipe) from the tree canopy and a visible bottom of the data, which is an artifact of the topographic correction.

Zone of Limited GPR Penetration

Although GPR penetration was excellent throughout most of Los Naranjos (2-6 meters), data collected in the southern portion of the plaza to the west of Structure IV are characterized by a depth of penetration less than about 60 to 70 centimeters. This low penetration zone is visible in GPR data collected in Grids 2 and 3 and the southern portion of Grid 9 (Figure 79). Grids 2 and 3 cover the same area, but profiles in Grid 2 were oriented South to North, whereas profiles in Grid 3 were oriented West to East (Table 5). Few reflections are visible in any of the cross-sectional views from these grids, and only a handful of diffraction hyperbolae were generated in these data.

We interpret the limited penetration in these datasets to result from a yellowish-brown clay layer that was encountered in Operation 4 during the 2004 Cornell – Berkeley excavations. Examination of one of the GPR cross-sectional views collected within Grid 3 (Figure 79) demonstrates this limited penetration and its possible relationship to excavated features (Figure 93). In profile LINEX3600 [3.60

m N], there are virtually no reflections deeper than about 70 centimeters (Figure 93). Operation 4G, excavated between 36 and 38 meters North and 2 to 3 meters within this profile, provides some clues about the possible reasons for such poor penetration within this region. A stratigraphic wall profile from the southernmost wall [36.0 m N] shows the numerous clay layers that were encountered. One layer in particular seems especially problematic: the yellowish-brown clay. This sterile layer (no artifacts) was described as “sticky” and “nasty” during excavations and was especially difficult to excavate. The basal depths of this yellow clay occurred from about 55 to about 70 centimeters in Operation 4, which coincides with the basal reflection in the GPR data. A similar yellowish-brown clay layer was also noted during the 1936 excavations to the north of Structure I (Strong *et al.*, 1938), and this layer was also sterile. Early Formative occupations were located immediately below the yellow clay layer in both cases.

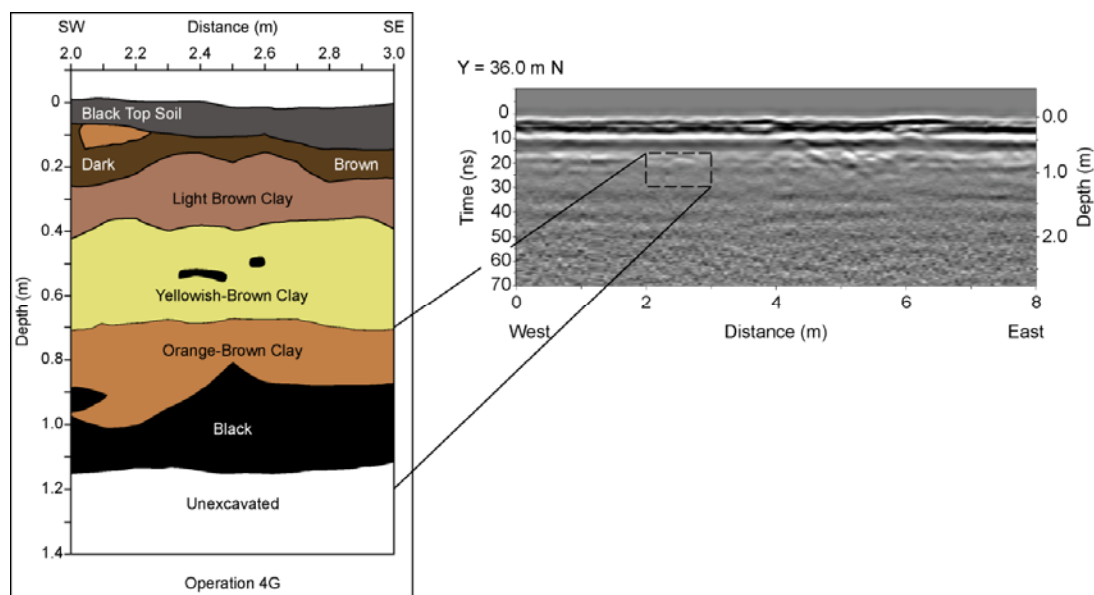


Figure 93: Limited GPR penetration in Grid 3 and comparison with an excavation wall profile. Excavation wall profile is from the CU-UCB excavation field program from Operation 4G, located at 36.0 m N. Corresponding GPR profile, LINEX3600 [36.0 m N], shows the lack of penetration at about 70 centimeters. This corresponds to the base of the yellowish-brown clay. GPR cross-sectional view = 1:1.

Signals from below this layer were not recorded, indicating the yellow clay layer is attenuating the GPR signal and masking reflections from all deeper layers. The yellow clay layer is especially interesting because it was only found in the vicinity of the Early Formative occupations (Operations 2 and 4). If this yellow clay layer results in limited GPR penetration, it may be possible to use this lack of penetration to identify additional early occupations. The only area of Los Naranjos to date to have such poor penetration is that found to the immediate west of Structure IV. Although this may only be a coincidence, the GPR data seem to suggest that this yellow clay layer is the culprit for limited penetration.

We decided, therefore, to return to Los Naranjos in the late spring of 2007 to collect additional GPR data using 400 MHz antennae in the hopes of achieving a higher resolution dataset. In portions of GPR Grid 008 (Figure 79), the 400 MHz antennae penetrated to depths of only about 40 centimeters, which was even less than the 250 MHz dataset. For the most part, however, the maximum depth of penetration was equivalent to the 250 MHz datasets, but the 400 MHz antennae provided a higher-resolution dataset that included visible reflections and diffraction hyperbolae throughout many of the profiles (Figure 94). In all three geophysical datasets, the maximum depth of penetration was about 70 centimeters.

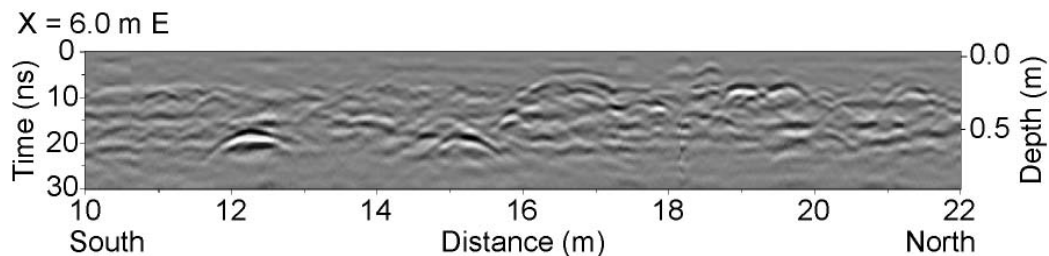


Figure 94: A portion of unmigrated 400 MHz LINEY60 [6.0 m E] from GPR Grid 008. Note the limited penetration deeper than about 70 centimeters. Vertical exaggeration = 2x.

A Previously Unrecognized Buried Structure?

Ground-penetrating radar Grid 6 is located atop the low topographic ridge that trends south to north through a portion of the main plaza at Los Naranjos (Figure 79). Unmigrated GPR data from Grid 6 contain prominent diffraction hyperbolae that are concentrated within the center of each of the profiles. These diffractions form a cluster between 86 and 95 meters North and range in depth from about 70 centimeters to 1.4 meters (Figure 95). Multiple continuous reflectors drape over the top of these diffractions, indicating burial by natural depositional processes (Figure 95). Strata in the southern portion of the grid dip steeply and are truncated just below the present ground surface (Figure 95), whereas strata north of the diffraction cluster have a shallower dip and are overlain by an additional set of diffraction hyperbolae between about 95 and 98 meters (Figure 95). The continuous reflections visible in Figure 95 are not intact throughout all of Grid 6, but are absent north of about 88 meters in the central (from W – E) portion of the grid where diffraction hyperbolae are present as shallow as 40 centimeters (Figure 96). In the eastern profiles of Grid 6, the reflections appear continuous again from south to north, but they no longer dip as steeply in the south as they did in the western portion of the grid (Figure 97). These patterns suggest the structure is shallowest in the central portion of the grid ($x = \sim 4$ m) and dips down on both sides (Figure 98).

Three-dimensional migrated profiles transform the cluster of diffraction hyperbolae into a sequence of sub-horizontal “steps” (from 86 to 92 meters), ranging in depth from about 50 centimeters to almost 1 meter (Figure 99). Unmigrated GPR map views of the Grid 6 data indicate that this buried structure is quasi-rectangular in shape and oriented southwest to northeast (Figure 100). This rectangular shape is visible from about 85 to 91 meters, at a depth of about 45 to 50 centimeters. Higher-amplitude anomalies within this rectangle cluster to form a possible smaller central

feature, and a high-amplitude circular feature is visible at the northeastern edge of the large rectangle (Figure 100). Furthermore, a linear high-amplitude anomaly was generated at about 82 meters (Figure 100).

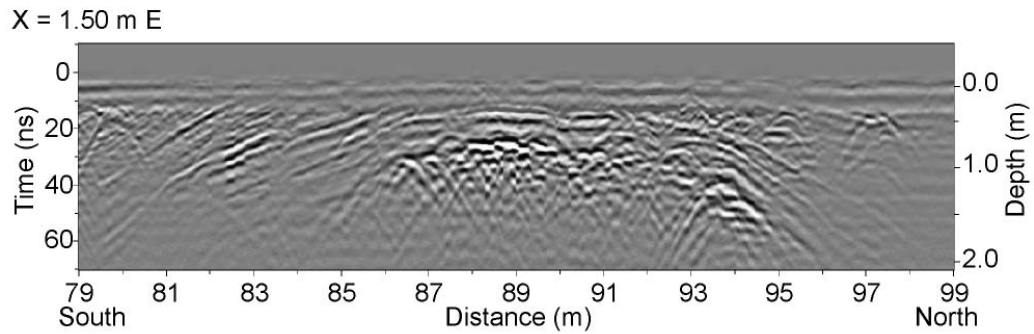


Figure 95: Draping sediments and clusters of diffraction hyperbolae in an unmigrated GPR cross-sectional view from Grid 6 (LINEY150). Diffraction hyperbolae are clustered between 86 and 95 meters and range in depth from about 70 centimeters to 1.4 meters. Note the continuous reflections that drape over these diffractions; their tops are truncated partially, especially in the south. Vertical exaggeration = 2x.

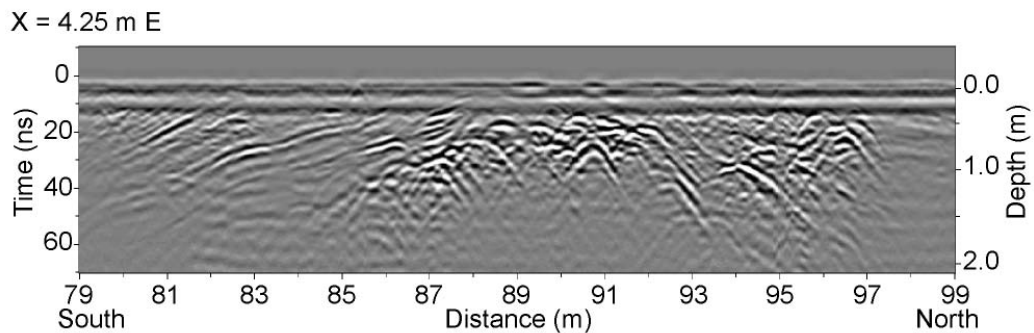


Figure 96: Truncated sediments in GPR Grid 6. Unmigrated GPR data (LINEY425). The draping sediments seem to be truncated at 88 meters (and north), possibly indicating disturbance of these sediments. Vertical exaggeration = 2x.

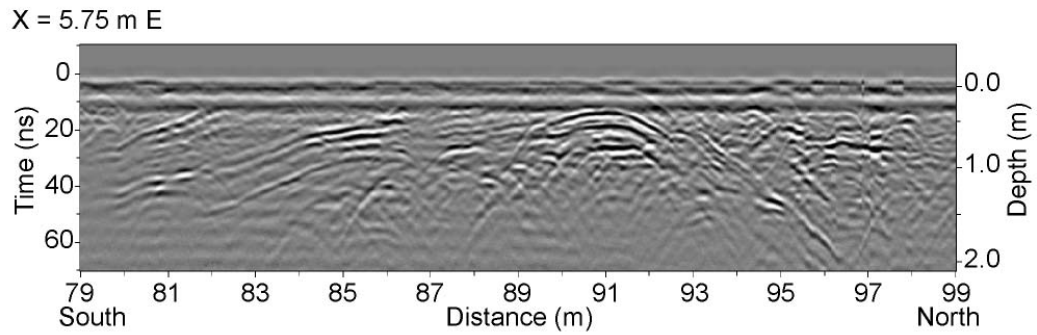


Figure 97: Shallow dipping sediments in GPR Grid 6. Unmigrated GPR data (LINEY575). The sediments that drape over the hyperbolae in the center of the profile appear to separate the center hyperbolae from those at the north end of the profile. Note that the dip of the draping reflections is not as steep as it was in profiles in the western portion of the grid. Vertical exaggeration = 2x.

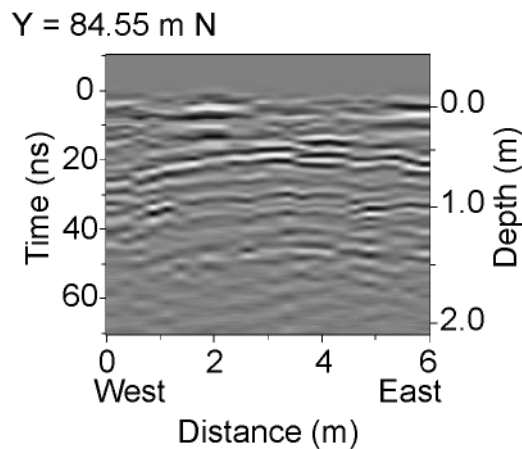


Figure 98: Cross-sectional view constructed perpendicular to GPR data collected within Grid 6, located at 84.55 m N. Note the draping reflections, with an apex at about 60 cm (located at $x \sim 3$ m). Vertical exaggeration = 2x.

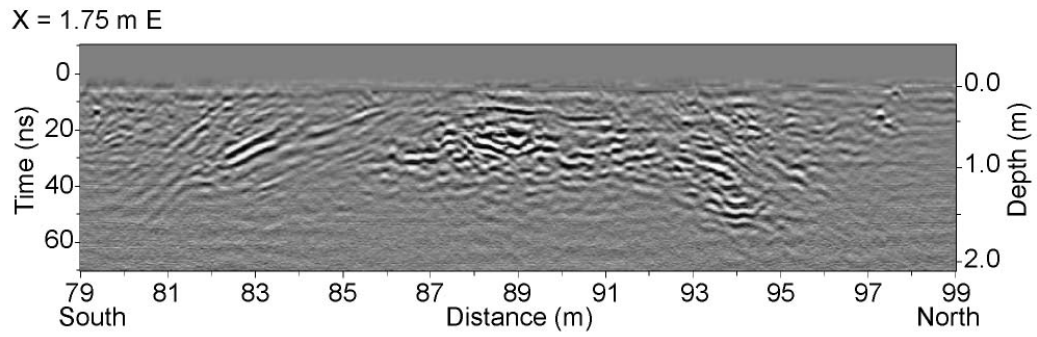


Figure 99: Sub-horizontal layers in GPR Grid 6. Three-dimensional migrated view of LINEY175 (3Dm_Y175). Note the sub-horizontal reflection between 86 and 90 meters, at a depth of about 80 centimeters. Vertical exaggeration = 2x.

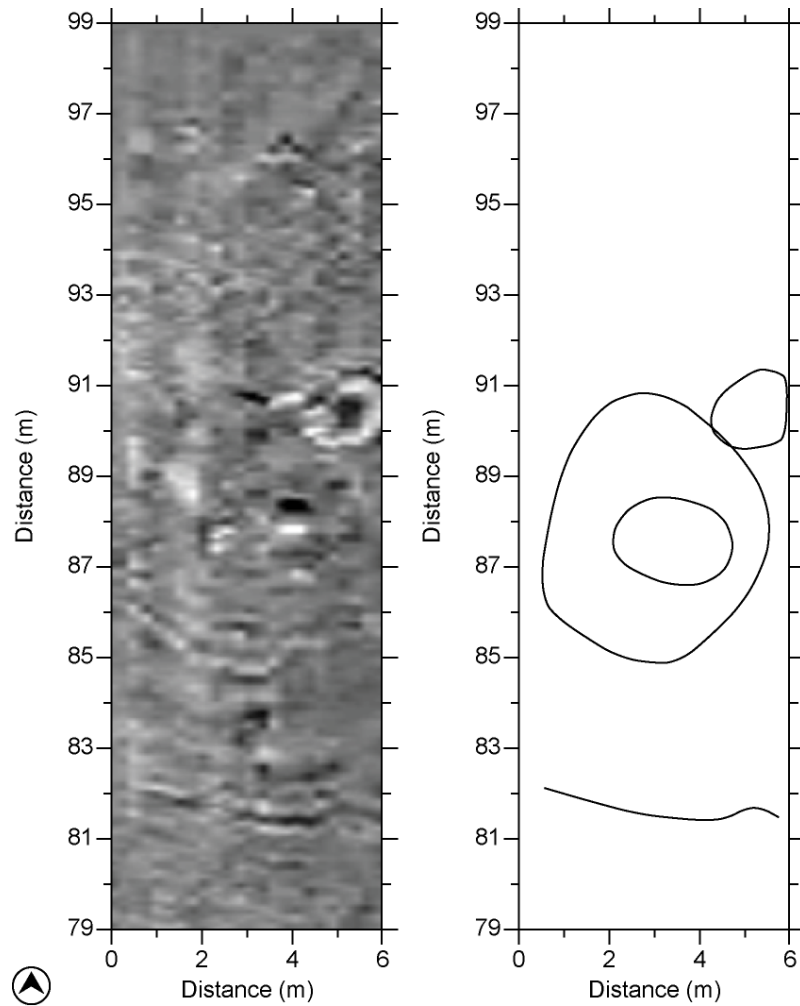


Figure 100: Possible buried structure in GPR Grid 6. Unmigrated map view of Grid 6 data, from 0.45 to 0.5 meters depth (left). Interpretation of the Grid 6 features (right).

Magnetic data acquired over GPR Grid 6 are highly magnetic, especially as compared to data acquired immediately to the north and east of this grid (Figure 101). The horizontal gradient magnetometry data acquired within GPR Grid 6 indicate a very high-amplitude linear anomaly that trends south to north the length of the grid (Figure 101). The highest magnetic field intensities were recorded in the eastern half of the grid, with the values increasing steadily from west to east (Figure 102). The highest amplitudes were generated in the northern half of the grid, which coincides with the high-amplitude domal reflection (Figure 103) and missing sedimentary cover within the central portion of the grid, as seen in Figure 96.

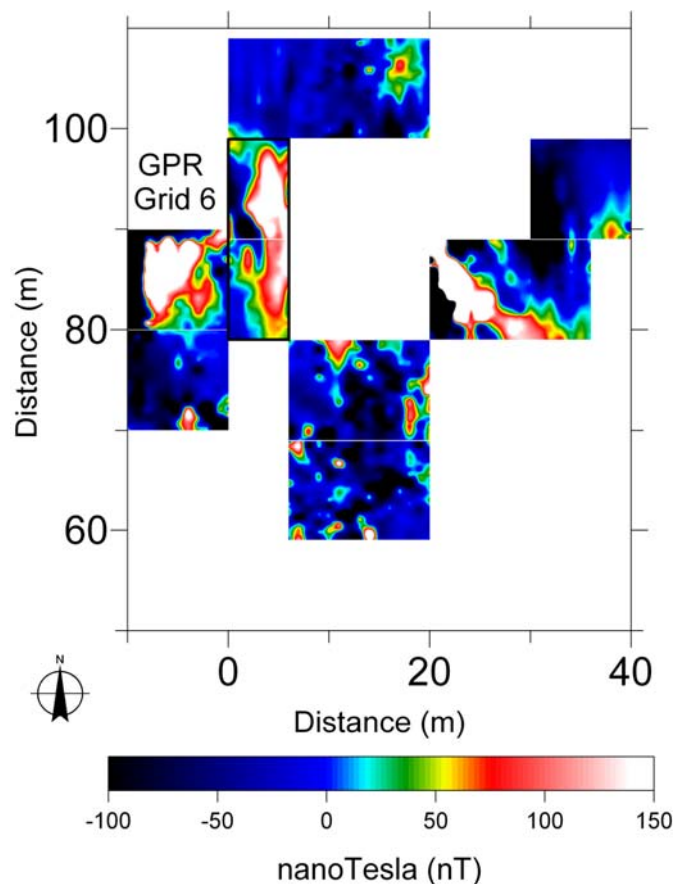


Figure 101: Horizontal gradient magnetometry data highlighting the buried structure imaged in Grid 6. The possible structure imaged in GPR Grid 6 is also a strong magnetic anomaly, indicating this feature (if archaeological) may have been burnt prior to burial or it may be comprised of magnetic materials, such as basalt rocks.

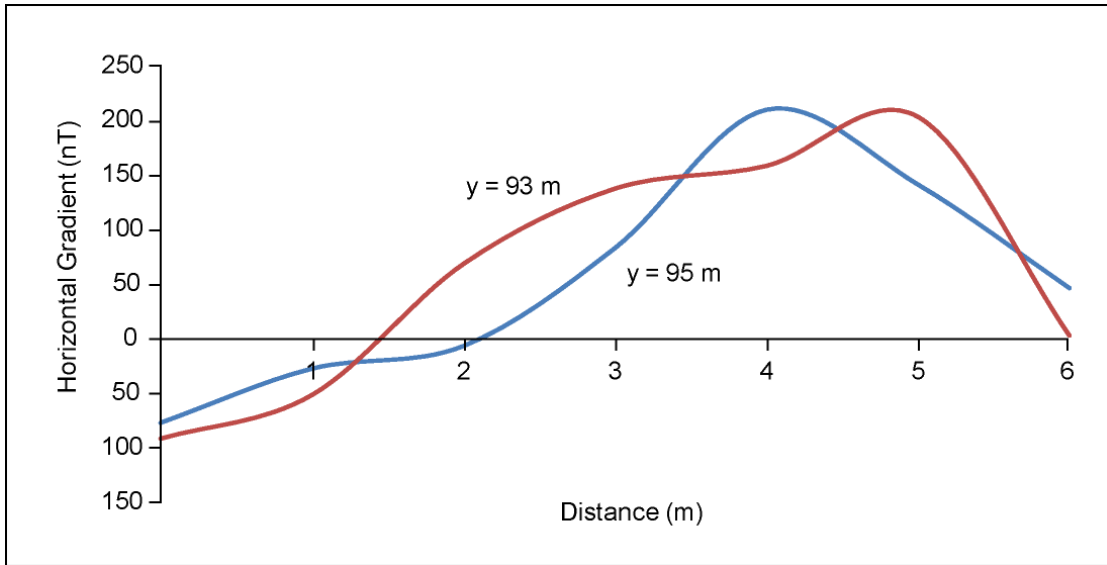


Figure 102: Horizontal gradient magnetometry profiles (transverse to direction of data collection) over the strong magnetic anomaly within Grid 6. The two profiles are located at $y = 93$ m N and $y = 95$ m N. Both profiles indicate an increase in magnetic field intensity from west ($x = 0$ m) to east ($x = 6$ m).

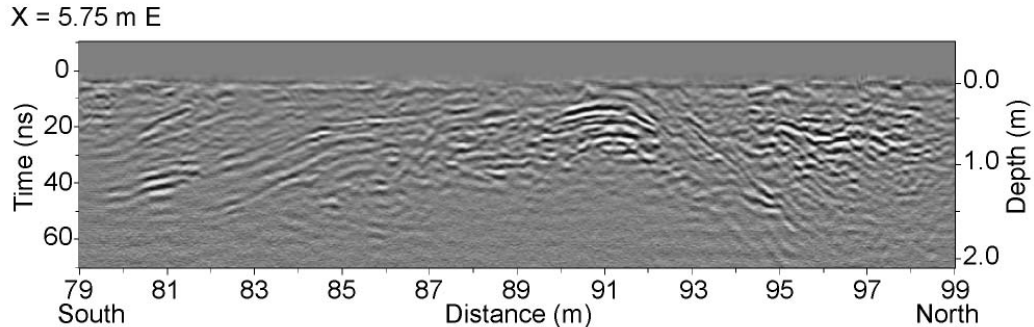


Figure 103: Domal reflection visible in GPR Grid 6. Three-dimensional migrated view of LINEY575 (3Dm_Y575). Note the high-amplitude domal reflection between 90 and 92 meters. Strata in the south appear intact (and geological), whereas the strata in the north appear disturbed. The reflections in the north correspond to the high-amplitude magnetic anomaly. Vertical exaggeration = $2x$.

The geometries within Grid 6 are complex, which may indicate several episodes of archaeological construction or perhaps collapse of some structure. We suggest the feature within the center of the grid represents a structure that may have

collapsed or was demolished intentionally. The sub-horizontal layering visible in the 3D migrated data at a depth of about 80 centimeters might indicate the floor of this original structure (Figure 99). The zone of higher-amplitude anomalies within this larger feature and the small high-amplitude circular feature might represent additions to this main structure, or the main structure might have served as a platform for these later smaller structures. If this feature does represent the remains of a former structure, it may have been demolished to form the platform of a later structure prior to the large deposition of sediment, indicated by the continuous reflections that drape over this feature. The high-amplitude magnetic anomaly might indicate the structure was built from magnetic material or was altered (burned?) prior to destruction and later burial. A similar succession of events was noted during the excavations of an Early Formative residence in Operation 2, located to the south in GPR Grid 9 (Figure 79) (Henderson and Joyce, 2003).

Natural Features versus Anthropogenic?

The GPR activities during the summer of 2003 included several isolated transects within the open plaza adjacent to Structure IV at Los Naranjos (Figure 79). The purpose of these surveys was to determine whether certain prominent features visible at the surface of the site were natural or anthropogenic. The two features discussed here include a low stone wall and a large boulder.

A low stone “wall” is visible in the western portion of the plaza, just to the west of the topographic ridge that runs north to south through this region. Existing maps of the Principal Group indicate the wall as a small rectilinear low mound that trends roughly southwest to northeast (Dixon *et al.*, 2001) (Figure 79). This mound is less than about 0.5 meter in height, and it is comprised of numerous large stones. Initial interpretations of this feature suggested it was either part of an exposed stone

wall that was mostly buried or that it was possibly a relict terrace wall of a low platform mound. Both interpretations indicated an anthropogenic origin. Ground-penetrating radar transect LINE1 was collected at an oblique angle across the plaza (Figure 79) to access the geometry of this feature by mapping the stratigraphy to either side. LINE1 began about 20 meters east of the wall, continued over the center of it, and ended about 8 meters to its west. The wall was located between positions -20 to -26 meters within LINE1.

In the GPR cross-sectional view of LINE1, the wall is associated with high-amplitude, sub-horizontal reflections extending from the surface to a depth of about 3 meters (Figure 104). The high amplitudes generated from the wall decrease sharply immediately to its west. Although the amplitudes in this western section are weaker than the rest of the profile, it is still possible to trace strata that appear to extend from within the wall westward (Figure 104). Reflections dip eastward from near the surface at the wall to depths of 3 meters at the east end of the profile.

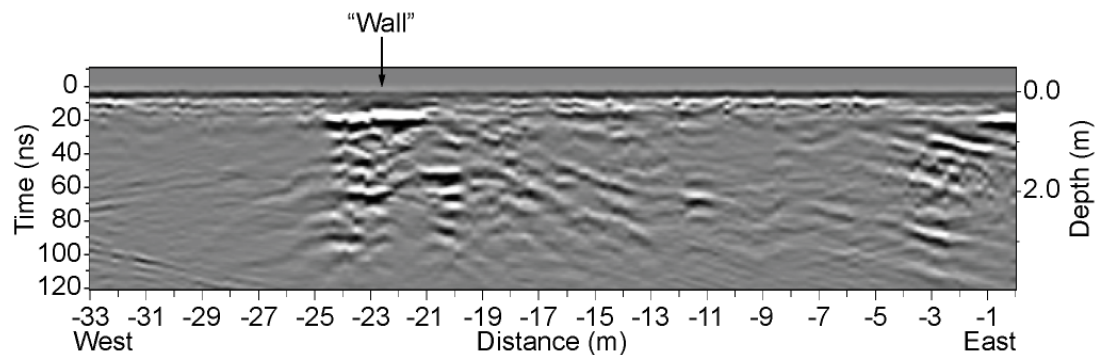


Figure 104: Unmigrated GPR transect LINE1 across the “wall.” The wall is located between -25 and -20 meters. Negative numbers indicate grid positions west of the site datum (0,0). Vertical exaggeration = 2x.

If this feature were an anthropogenic stone wall, we would expect strata to extend continuously beneath its surface expression, but reflections would not be

expected to be continuous through it. If this feature were a terrace wall of a low mound, strata would most likely shallow as they approached it, as if they were draping up to it. This is similar to what is imaged immediately to the east of the wall in LINE1 (Figure 104). The strong reflections on the eastern portion of the cross-section are dipping at the same angle as those adjacent to the wall, most likely indicating deposition on the flank of a pre-existing feature. We suggest this is a natural outcropping of igneous rock that could possibly indicate igneous rock that is overlapped by later sedimentary units. Bedrock at Los Naranjos is comprised of Cretaceous limestone (Yojoa Group) that is overlain by Quaternary basaltic lava flows (Williams and McBirney, 1969), adding support for our hypothesis.

Three additional transects were collected about 15 meters to the south of the wall (Figure 79) to determine the setting of several large basalt boulders, known informally as the Volkswagen (VW). The VW measures about 1.5 meters in height and about 3 meters in total length (Figure 105). Its large size and haphazard placement within the plaza initially suggested this feature was part of a natural bedrock outcrop. Ground-penetrating radar transect LINE2 was established immediately to the east of the VW (Figure 79), and transects LINE 3 and LINE5 were collected to the south and west, respectively (Figure 79).

In LINE2, high-amplitude reflections are visible in the western half of the GPR cross-sectional view (Figure 106), from a depth of about 1.5 meters to more than 4 meters. Several reflections are visible above these, but they are much weaker in amplitude. High-amplitude sub-parallel reflections were generated in LINE3 from a depth of about 2.0 to 3.5 meters (Figure 107) and in LINE5 from about 1.5 to 4.0 meters. In none of these profiles are there dipping (onlapping) reflections that suggest the VW is part of the local bedrock. Instead, the strata below it are continuous and undisturbed (Figure 107), suggesting the VW is allochthonous.



Figure 105: Large basalt boulder, known informally as the Volkswagen. View is towards the east.

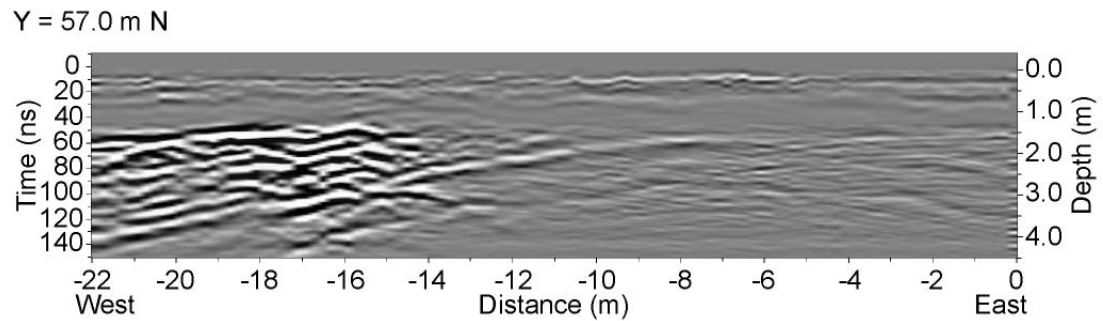


Figure 106: Unmigrated GPR transect LINE2, east of the VW. This transect approaches the VW, but does not intersect it. Strata appear continuous and undisturbed by the VW. Vertical scale is 1:1.

Y = 54.0 m N

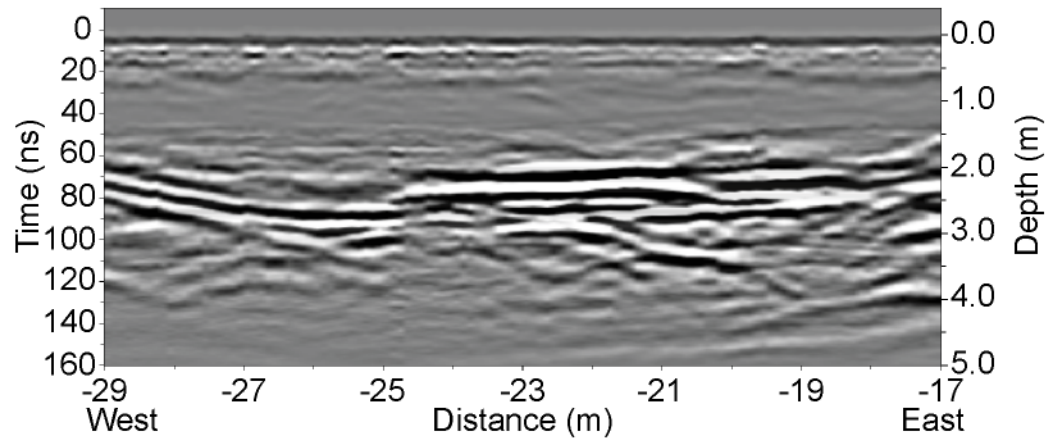


Figure 107: Unmigrated GPR transect LINE3, south of the VW. Strata appear continuous and undisturbed by the VW. Vertical scale is 1:1.

Small hand samples collected from the VW during the summer of 2006 were identified as andesitic basalt (Christopher Andronicos, personal communication), which is consistent with the lithology of the Lake Yojoa Volcanic Field (Instituto Geográfico Nacional, 1973) located about 6 km to the northeast of the site. While it is conceivable that such a large block was transported as part of a landfall, its isolated nature suggests that it may have been purposefully transported by the occupants of Los Naranjos to have ready access to raw materials for stone facings of platform mounds or to carve sculpture. It is not clear why they would have been deposited in the southern portion of the plaza, as this space was usually left open for public activities and events.

Volcanic Marker Horizon?

Ground-penetrating radar data from Grid 0 contain a high-amplitude feature in the southeastern corner of the grid. In cross-sectional views, this feature is represented by high-amplitude sub-parallel reflections between 77 and 79 meters, ranging in depth

from about 1.3 to 2.2 meters (Figure 108). Several of the unmigrated cross-sectional views from within this grid suggest some of the layers are continuous throughout a portion of Grid 0 possibly extending as far west as about 71 meters. In some profiles, this layering appears to be masked by diffractors that are immediately above it, but the 3D migrated versions indicate a continuity of reflections.

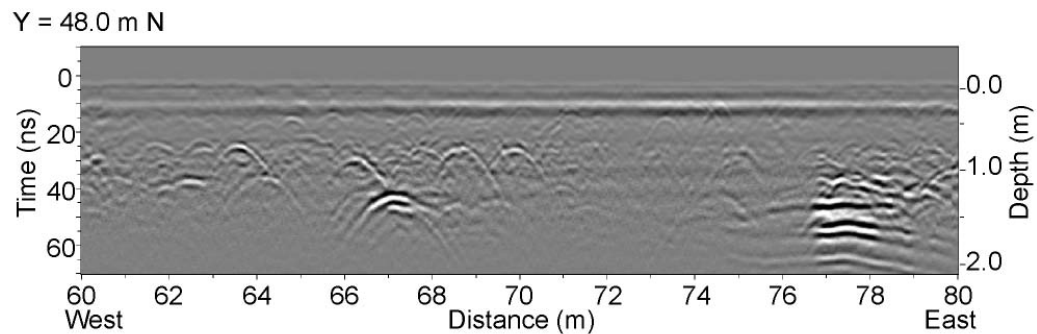


Figure 108: Unmigrated LINEX480 showing the high-amplitude, sub-horizontal reflections generated between 77 to 79 meters, ranging in depth from about 1.3 to 2.2 meters. Vertical exaggeration = 2x.

Map views indicate that this “bright spot” is roughly circular in shape and measures about 4 meters in length (NS) and 3.5 meters in width (EW) (Figure 109). Although its appearance is slightly mottled, it is a very prominent feature within this grid, and it exists over a substantial depth range. Corresponding magnetometry data within Grid 0 do not exhibit any anomaly, indicating that magnetic materials are not involved.

This feature is interesting not only because of its high amplitude, but because of its proximity to the 1960s excavations of Baudez and Becquelin (1973). Their excavations on the northeastern slope of Structure IV uncovered stones that formed the lower courses of parallel walls (Figure 109) thought to represent a house about 4 x 3 meters in size buried at a depth of about 50 centimeters (Baudez and Becquelin,

1973, p. 24-26). These walls do not extend into Grid 0, but earlier occupations were noted below the northern end of the easternmost wall (near area marked T14 on Figure 109), suggesting this GPR-imaged feature might be a remnant of an earlier occupation zone. Most interesting, perhaps, is that sterile soil, which was comprised mainly of volcanic ash, was encountered at a depth of about 1.3 meters (Baudez and Becquelin, 1973, p. 24) (Figure 110). This is the same depth at which these high-amplitude reflections begin. Perhaps the high-amplitude reflectivity corresponds to alteration of pre-existing layers due to drainage induced by Baudez and Becquelin's excavations. The difference in compaction of their backfilled materials as compared with the undisturbed sediment might have allowed for water to seep in and pool on these intact layers, thereby causing the high amplitudes.

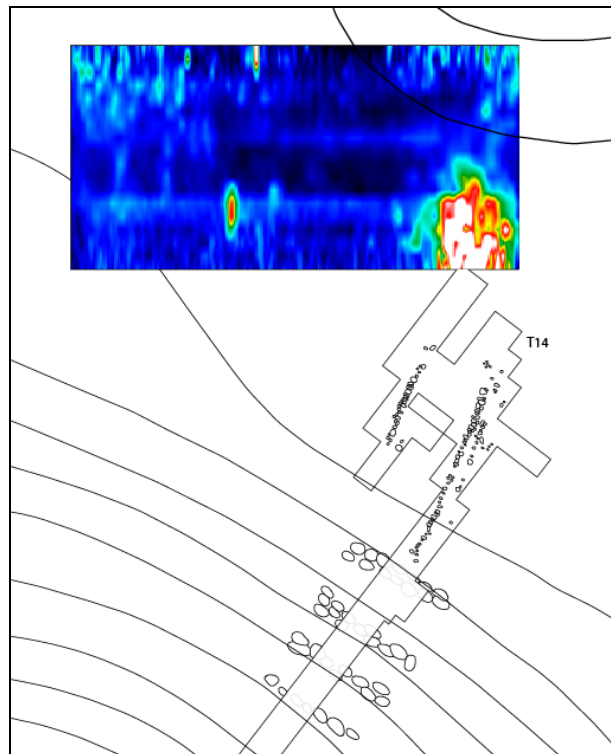


Figure 109: High-amplitude reflections in the southeastern corner of GPR Grid 0 in relation to the excavations of Baudez and Becquelin. This 3D migrated plan view image is from a depth of 1.25 to 1.325 meters. Basemap is modified from Baudez and Becquelin (1973, Figure 11).

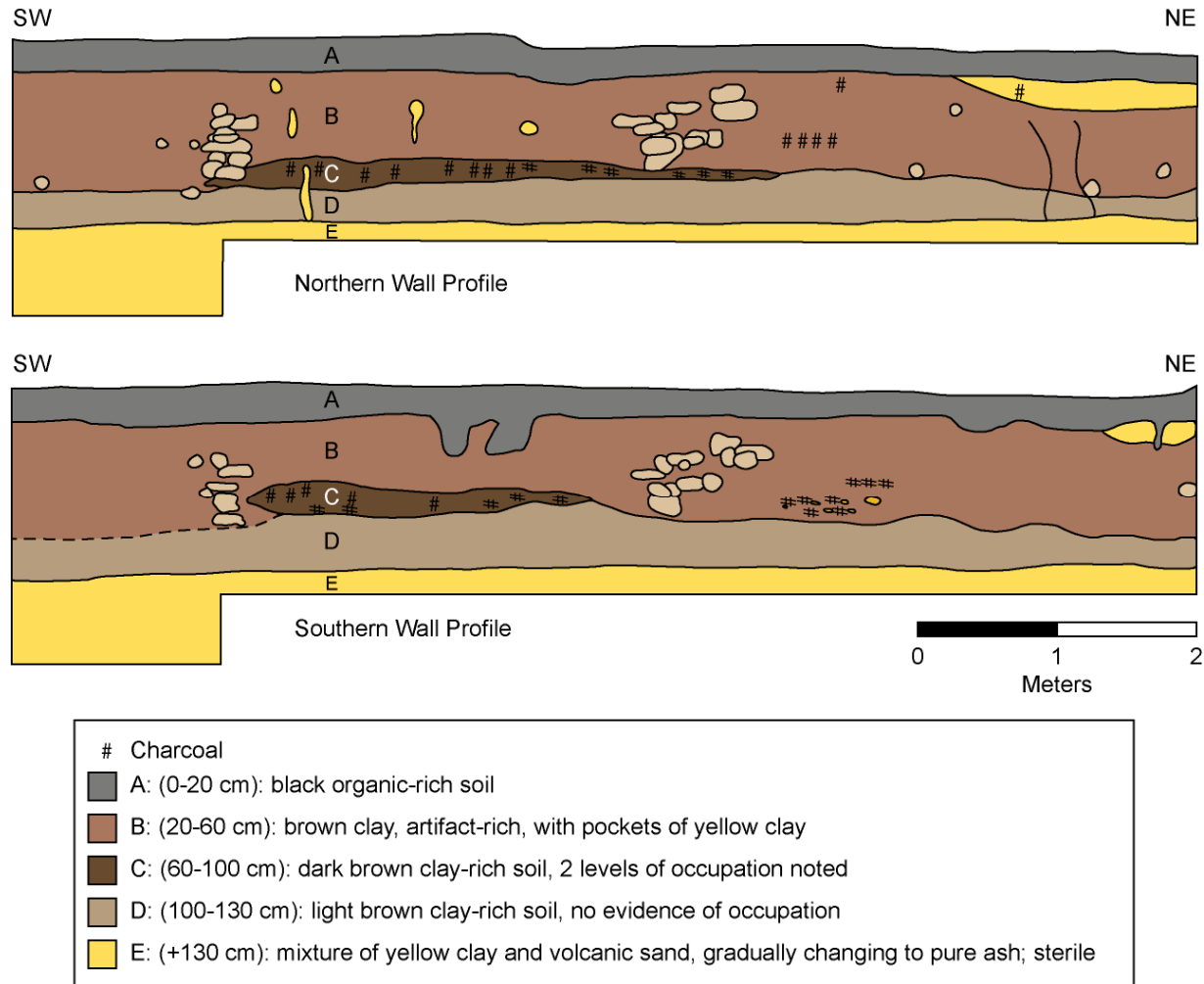


Figure 110: Stratigraphic wall profiles from Baudez and Becquelin's excavations on the northeastern slope of Structure IV. Note sterile yellow clay / ash layer. Modified from Baudez and Becquelin (1973, Figure 12).

In addition, we note that a sediment core from the northeastern side of Lake Yojoa recovered silicic volcanic ash known as the Tierra Blanca Joven (TBJ) from the eruption of El Salvador's Ilopango Volcano. The TBJ occurred at a depth of about 1.6 meters in the lake core and had a calibrated age of A.D. 130-385 (Mehring *et al.*, 2005), which corresponds to the Late Formative Period. The sterile ash unit uncovered during Baudez and Becquelin's excavations might be correlative to the Lake Yojoa TBJ, as they thought this portion of excavations dated to the Eden Phase, which corresponds to the Late Formative Period (Baudez and Becquelin, 1973, p. 29) as well. We speculate, therefore, that these high-amplitude reflections in the southeastern portion of Grid 0 correspond to the ash deposit encountered at depth during the excavations by Baudez and Becquelin (1973). The TBJ layer from the Ilopango Volcano was also excavated at the archaeological site of Cerén, El Salvador, where corresponding GPR surveys noted a similarly strong reflectivity (Conyers, 1995).

Stone-lined Path?

Our initial analyses of the Grid 0 GPR data sought to determine the significance of the spatial distribution of diffraction hyperbolae generated within this grid (Tchakirides *et al.*, 2006a). In that analysis, the coordinates of all diffraction apices on the unmigrated profiles were plotted. No obvious patterning was discerned. The 3D migrated results, however, suggest that systematic arrangements are present. For example, in the profile located at 46.5 meters N, numerous diffraction hyperbolae are visible between about 50 centimeters and 1 meter. Twelve of them occur at a relatively regular spacing at a depth of about 73 centimeters (Figure 111). In the western half of the profile, the diffractions are spaced about 1 meter apart but appear with a spacing of 2 meters in the eastern portion of the profile (Figure 111).

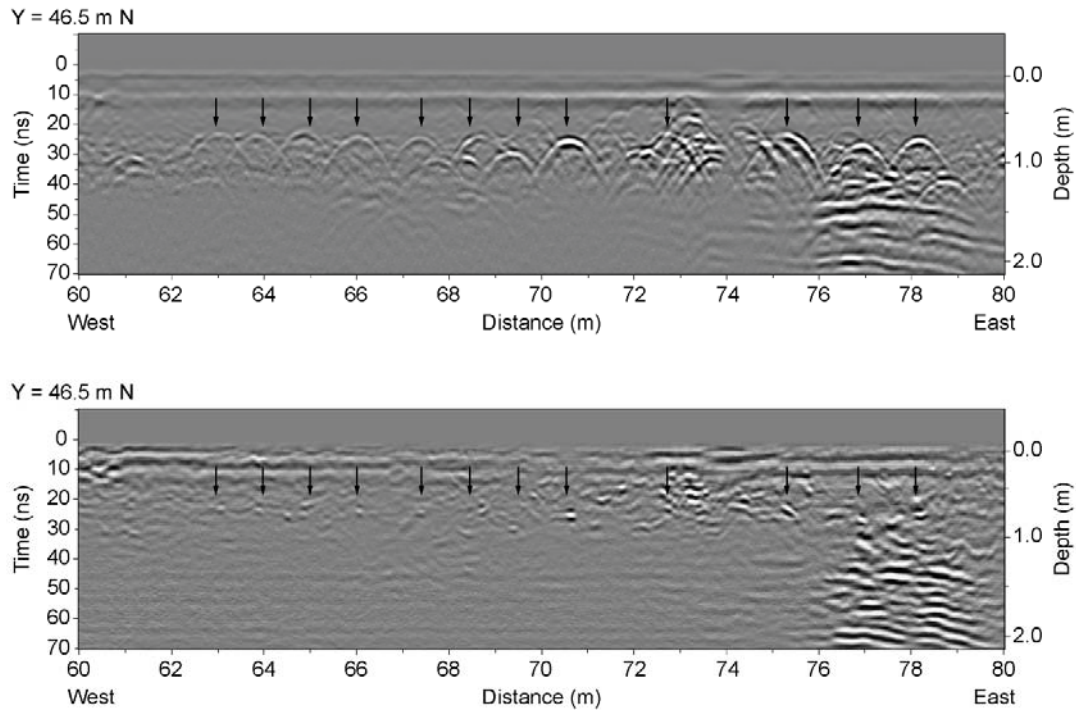


Figure 111: Possible stone-lined path imaged in GPR Grid 0. Top: Unmigrated LINEX465 cross-sectional view. There is a regular spacing of diffractions that seems to indicate a “path” at a depth of about 75 centimeters within GPR Grid 0. Bottom: 3D migrated LINEX465 cross-sectional view. The diffractions have collapsed to point sources with a regular spacing. Vertical exaggeration = 2x.

Three-dimensional migration collapses these diffractions to point sources with similar spacing (Figure 111). Their regular distribution is more easily discernable in the western portion of the grid in map view, as it was in cross-sectional view, because they appear unobstructed by other features (Figure 112). This pattern is more difficult to identify east of 75.5 meters (Figure 112). We suggest that this spacing is too regular for natural deposition, and may instead represent purposeful placement. Unfortunately, Operation 1 excavations, located within Grid 0 (Figure 82), did not extend this deep, so confirmation by direct observation is still lacking. We suggest these diffractions represent individual stones that may have been placed specifically to form a path, thereby defining an ancient living surface. Their significance might be related to early constructions located immediately to the north of Structure IV, as

Baudez and Becquelin (1973, p.24) recognized two occupation levels between 60 centimeters and 1 meter depth.

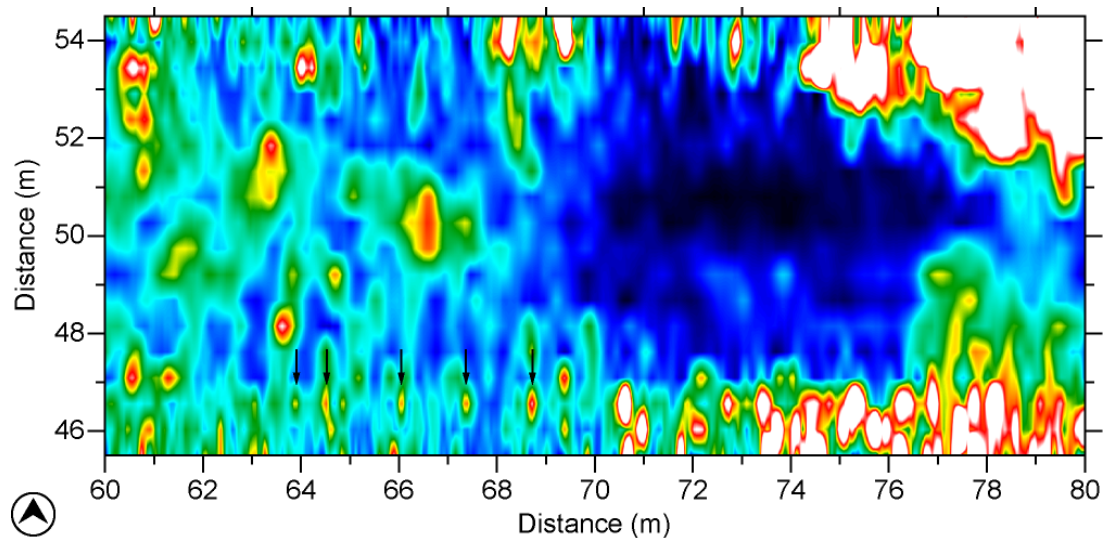


Figure 112: Map view of 3D migrated GPR Grid 0 data, from a depth of 70 to 80 centimeters. Note the regularly spaced line of high-amplitude features along 46.5 meters (indicated by black arrows) that most likely represents a stone-lined path.

Conclusions

GPR surveys at Los Naranjos have revealed both geological and archaeological features within the uppermost 6 meters of the site within the plaza of the Principal Group. Small basins that may have ceremonial significance, a previously unrecognized buried structure, and a possible buried sculpture to the north of Structure IV provide new insight into the use of space and occupation history of the site. A stone-lined path may be related to features excavated on the northeastern slope of Structure IV, and a possible volcanic marker horizon might serve to date some or all of these specific features. Geological stratigraphy was also imaged by GPR in the area NW of Structure IV. Sub-horizontal strata that are disrupted in places by what appears to be a fault-bounded structure highlight the potential for paleoseismology at this and other archaeological sites in the region.

The combined use of GPR and magnetometry proved effective in identifying a basaltic lithology of the buried sculpture imaged within Grid 0. Sophisticated GPR data processing steps such as three-dimensional migration have helped to produce a more accurate representation of the shallow subsurface at Los Naranjos, whereas extensive velocity analyses on CMP data have made it possible to correlate specific reflections generated in the GPR data with features excavated during the archaeological field school.

Due to site-specific conditions, shallow geophysical techniques are not always effective in addressing archaeological issues (Conyers, 2004). Our own GPR and magnetometry surveys at other Honduran sites have proven challenging given the sedimentary matrix (Tchakirides, 2007; Tchakirides *et al.*, 2005). However, the Los Naranjos results clearly demonstrate that geophysical data can provide high-resolution images of subsurface stratigraphy, structure, and features of archaeological interest. We again emphasize that such geophysical observations provide a means of assessing key site relationships in 3D over large areas in relatively rapid fashion and in a non-intrusive, non-destructive manner.

Acknowledgments

Special thanks to Professors John Henderson (Cornell) and Rosemary Joyce (Berkeley) for their assistance with this research. Their excavations at Los Naranjos during the summers of 2003 and 2004 added much to this paper. We also thank the students from Cornell and Berkeley who participated in these field seasons. Kira Blaisdell-Sloan directed the collection of the magnetic data, whereas Joel Haenlein and students from Cornell acquired the 2003 GPR data. Three-dimensional migration was performed using *ReflexW*, and Sensor's and Software Inc. *EKKO_Mapper 3* was used for initial processing and image display. Funding for this research was

generously provided by an AAPG Grant-in Aid, a GSA Research Grant, and an SEG Scholarship. We also would like to thank IHAH, students and field workers from 2003 and 2007, and Bill Perks for use of his Noggin system.

REFERENCES

- Aitken, J.A. and Stewart, R.R. (2004). Investigations using Ground Penetrating Radar (GPR) at a Maya Plaza Complex in Belize, Central America., In Proceedings of the Tenth International Conference on Ground-Penetrating Radar: June 21-24, Delft, The Netherlands., Evert Slob, Alex Yarovoy and Jan Rhebergen (editors). Delft University of Technology, The Netherlands and the Institute of Electrical and Electronics Engineers, Inc., Piscataway, New Jersey, pp. 447-450.
- Ambraseys, N.N. (1995). Magnitudes of Central-American Earthquakes 1898-1930. *Geophysical Journal International*, 121(2): 545-556.
- Ambraseys, N.N. and Adams, R.D. (1996). Large-magnitude Central American earthquakes, 1898-1994. *Geophysical Journal International*, 127(3): 665-692.
- Annan, A.P. (2005). Ground-Penetrating Radar. In: D.K. Butler (Editor), *Near-Surface Geophysics*. Society of Exploration Geophysicists, Tulsa, pp. 357-438.
- Annan, A.P. and Davis, J.L. (1976). Impulse radar soundings in permafrost. *Radio Science*, 11: 383-394.
- Baudez, C.F. and Becquelin, P. (1973). *Archéologie de Los Naranjos*. Mission Archéologique et Ethnologique Française au Mexique, Mexico.

- Bevan, B. and Kenyon, J. (1975). Ground-Penetrating Radar for Historical Archaeology. *MASCA Newsletter*, 11(2): 2-7.
- Bevan, B.W. (2006). Understand Magnetic Maps, pp. 1-30.
- Bevan, B.W. and Roosevelt, A.C. (2003). Geophysical exploration of Guajara, a prehistoric earth mound in Brazil. *Geoarchaeology-an International Journal*, 18(3): 287-331.
- Blaisdell-Sloan, K. (2006). An Archaeology of Place and Self: The Pueblo de Indios of Ticamaya, Honduras (1300-1800 AD), Unpublished Ph.D. Dissertation, Department of Anthropology, University of California, Berkeley, Berkeley, CA.
- Breiner, S. and Coe, M.D. (1972). Magnetic Exploration of the Olmec Civilization. *American Scientist*, 60(5): 566-575.
- Bristow, C.S. and Jol, H.M. (2003). An introduction to ground penetrating radar (GPR) in sediments. In: C.S. Bristow and H.M. Jol (Editors), *Ground Penetrating Radar in Sediments*. Geological Society, London, Special Publications, 211, pp. 1-7.
- Burger, H.R., Sheehan, A.F. and Jones, C.H. (2006). *Introduction to Applied Geophysics: Exploring the Shallow Subsurface*. W.W. Norton & Company, New York.

- Carr, M.J. and Stoiber, R.E. (1977). Geologic Setting of Some Destructive Earthquakes in Central-America. *Geological Society of America Bulletin*, 88(1): 151-156.
- Chávez, R.E., Cámara, M.E., Tejero, A., Barba, L. and Manzanilla, L. (2001). Site characterization by geophysical methods in The Archaeological Zone of Teotihuacan, Mexico. *Journal of Archaeological Science*, 28(12): 1265-1276.
- Chavez, R.E., Tejero, A., Argote, D.L. and Camara, M.E. (2009). Geophysical Study of a Pre-Hispanic Lakeshore Settlement, Chiconahuapan Lake, Mexico. *Archaeological Prospection*, early view.
- Chun, J.H. and Jacewitz, C.A. (1981). *Fundamentals of Frequency-Domain Migration. Geophysics*, 46(5): 717-733.
- Clark, A. (1990). *Seeing Beneath the Soil: Prospecting Methods in Archaeology*. Routledge, New York, NY.
- Clay, R.B. (2001). Complementary Geophysical Survey Techniques: Why Two Ways are Always Better Than One. *Southeastern Archaeology*, 20(1): 31-43.
- Conyers, L.B. (1995). The use of ground-penetrating radar to map the buried structures and landscape of the Ceren Site, El Salvador. *Geoarchaeology: An International Journal*, 10(4): 275-299.

- Conyers, L.B. (2004). Ground-Penetrating Radar for Archaeology. Geophysical Methods for Archaeology. AltaMira Press, Walnut Creek, CA.
- Cruz C., O.N. and Valles Pérez, E. (2002). Excavaciones en la Estructura IV del conjunto principal, Los Naranjos. *Yaxkin*, 21: 45-62.
- Cyphers, A. (1999). From Stone to Symbols: Olmec Art in Social Context at San Lorenzo Tenochtitlán. In: D.C. Grove and R.A. Joyce (Editors), *Social Patterns in Pre-Classic Mesoamerica*. Dumbarton Oaks, Washington, DC, pp. 155-182.
- Dalan, R.A. (1991). Defining Archaeological Features with Electromagnetic Surveys at the Cahokia Mounds State Historic Site. *Geophysics*, 56(8): 1280-1287.
- Daniels, D.J. (Editor), (2004). *Ground Penetrating Radar 2nd Edition*. IEE Radar, Sonar, Navigation and Avionics Series 15. The Institution of Electrical Engineers, London.
- Dixon, B. *et al.* (1994). Formative-Period Architecture at the Site of Yarumela, Central Honduras. *Latin American Antiquity*, 5(1): 70-87.
- Dixon, B., Webb, R. and Hasemann, G. (2001). Arqueología y ecoturismo en el sitio de Los Naranjos, Honduras. *Yaxkin*, 20: 55-75.
- Doolittle, J.A. and Miller, W.F. (1991). Use of Ground-Penetrating Radar Techniques in Archaeological Investigations., *Applications of Space-Age Technology in*

Anthropology Conference Proceedings, Second Edition., NASA Science and Technology Laboratory, Stennis Space Center, Mississippi: pp. 81-93.

Elming, S.A., Layer, P. and Ubieta, K. (2001). A palaeomagnetic study and age determinations of Tertiary rocks in Nicaragua, Central America. *Geophysical Journal International*, 147(2): 294-309.

Fowler, W.R., Estrada-Belli, F., Bales, J.R., Reynolds, M.D. and Kvamme, K.L. (2007). Landscape Archaeology and Remote Sensing of a Spanish-Conquest Town: Ciudad Vieja, El Salvador. In: J. Wiseman and F. El-Baz (Editors), *Remote Sensing in Archaeology*. Springer, New York, pp. 395-421.

Gerlitz, K., Knoll, M.D., Cross, G.M., Luzitano, R.D. and Knight, R. (1993). Processing Ground Penetrating Radar Data to Improve Resolution of Near-Surface Targets, Proceedings of the Symposium on the Application of Geophysics to Engineering and Environmental Problems, Edited by Ronald S. Bell and C. Melvin Lepper, pp.561-574, San Diego, CA.

Goodman, D. and Nishimura, Y. (1993). A Ground-Radar View of Japanese Burial Mounds. *Antiquity*, 67(255): 349-354.

Goodman, D., Nishimura, Y. and Rogers, J.D. (1995). GPR Time Slices in Archaeological Prospection. *Archaeological Prospection*, 2: 85-89.

- Goodman, D., Nishimura, Y., Uno, T. and Yamamoto, T. (1994). A Ground Radar Survey of Medieval Kiln Sites in Suzu City, Western Japan. *Archaeometry*, 36(2): 317-326.
- Grove, D.C. (1999). Public Monuments and Sacred Mountains: Observations on Three Formative Period Social Landscapes. In: D.C. Grove and R.A. Joyce (Editors), *Social Patterns in Pre-Classic Mesoamerica*. Dumbarton Oaks, Washington, DC, pp. 255-300.
- Güendel, F. and Bungum, H. (1995). Earthquakes and Seismic Hazards in Central America. *Seismological Research Letters*, 66(5): 19-25.
- Henderson, J.S. and Joyce, R.A. (2003). Informe Preliminar: Investigaciones Arqueológicas en Los Naranjos, Lago de Yojoa, Junio 2003. Manuscript on file at the Instituto Hondureño de Antropología e Historia, Tegucigalpa, Honduras.
- Henderson, J.S. and Joyce, R.A. (2004). Informe Preliminar: Investigaciones Arqueológicas en Los Naranjos, Lago de Yojoa, Junio 2004. Manuscript on file at the Instituto Hondureño de Antropología e Historia, Tegucigalpa, Honduras.
- Hesse, A., Barba, L., Link, K. and Ortiz, A. (1997). A Magnetic and Electrical Study of Archaeological Structures at Loma Alta, Michoacan, Mexico. *Archaeological Prospection*, 4: 53-67.

Hogan, G. (1988). Migration of ground-penetrating radar data: A technique for locating subsurface targets, 59th Annual International Meeting of the Society of Exploration Geophysicists, pp. 345-347.

Instituto Geográfico Nacional (1973). Mapa Geológico de Honduras, Escala 1:50,000.

Isacks, B., Oliver, J. and Sykes, L.R. (1968). Seismology and New Global Tectonics. *Journal of Geophysical Research*, 73(18): 5855-5899.

Joesink-Mandeville, L.R.V. (1987). Yarumela, Honduras: Formative Period Cultural Conservatism and Diffusion. In: E.J. Robinson (Editor), *Interaction on the Southeast Mesoamerican Frontier: Prehistoric and Historic Honduras and El Salvador*. BAR International Series., Oxford, pp. 196-214.

Jol, H.M. and Bristow, C.S. (2003). GPR in sediments: advice on data collection, basic processing and interpretation, a good practice guide. . In: C.S. Bristow and H.M. Jol (Editors), *Ground Penetrating Radar in Sediments*. Geological Society, London, Special Publications, 211, pp. 9-27.

Joyce, R.A. (2004a). Mesoamerica: A Working Model for Archaeology. In: J.A. Hendon and R.A. Joyce (Editors), *Mesoamerican Archaeology: Theory and Practice*. Blackwell Studies in Global Archaeology. Blackwell, Malden, MA, pp. 1-42.

- Joyce, R.A. (2004b). Unintended consequences? Monumentality as a novel experience in Formative Mesoamerica. *Journal of Archaeological Method and Theory*, 11(1): 5-29.
- Joyce, R.A. and Grove, D.C. (1999). Asking New Questions about the Mesoamerican Pre-Classic. In Grove, D. C., and Joyce, R. A. (eds.), *Social Patterns in Pre-Classic Mesoamerica*, Dumbarton Oaks, Washington, DC, pp. 1-14.
- Joyce, R.A. and Henderson, J.S. (2002). La arqueología del periodo Formativo en Honduras: nuevos datos sobre el «estilo olmeca» en la zona maya. *Mayab*, 15: 5-17.
- Karlberg, T. and Sjöstedt, D. (2007). *Archaeological Exploration in Nicaragua using Ground Penetrating Radar: A Minor Field Study*, Unpublished Master's Thesis, Department of Chemical Engineering and Geosciences, Division of Applied Geophysics, Luleå University of Technology, Luleå, Sweden.
- Kearey, P., Brooks, M. and Hill, I. (2002). *An introduction to geophysical exploration*. Blackwell Scientific Publications, Oxford, England.
- Kenyon, J.L. (1977). Ground-Penetrating Radar and Its Application to a Historical Archaeological Site. *Historical Archaeology*, 11: 48-55.
- Kovach, R.L. (2004). *Early earthquakes of the Americas*. Cambridge University Press, Cambridge.

- Krotser, R. (1973). El agua ceremonial de los olmecas. *Boletín, Instituto Nacional de Antropología e Historia, México*, 2: 43-48.
- Kvamme, K.L. (2003). Geophysical surveys as landscape archaeology. *American Antiquity*, 68(3): 435-457.
- Kvamme, K.L. and Ahler, S.A. (2007). Integrated Remote Sensing and Excavation at Double Ditch State Historic Site, North Dakota. *American Antiquity*, 72(3): 539-561.
- Lindsey, J.P. (1989). The Fresnel zone and its interpretive significance. *Geophysics: The Leading Edge of Exploration*, 18: 33-39.
- Lopez-Loera, H. *et al.* (2000). Magnetic study of archaeological structures in La Campana, Colima, western Mesoamerica. *Journal of Applied Geophysics*, 43(1): 101-116.
- Love, M.W. (1999). Ideology, material culture, and daily practice in Pre-Classic Mesoamerica: A Pacific Coast perspective. In Grove, D. C., and Joyce, R. A. (eds.), *Social Patterns in Pre-Classic Mesoamerica*, Dumbarton Oaks, Washington, DC, pp. 127–153.
- Luke, B.A., Begley, C.T., Chase, D.S., Ross, A.J. and Brady, J.E. (1997). Rapid-Response Geophysical Site Investigations at a Pre-Columbian Settlement in Honduras., *Proceedings, Symposium on the Application of Geophysics to Engineering and Environmental Problems.*, Compiled by R.S. Bell, Reno,

Nevada, 23-26 Mar 1997. Wheat Ridge, CO: Environmental and Engineering Geophysical Society, 2: 983-992.

Luke, B.A. and Brady, J.E. (1998). Application of Seismic Surface Waves at a Pre-Columbian Settlement in Honduras. *Archaeological Prospection*, 5: 139-157.

Manton, W.I. (1987). Tectonic Interpretation of the Morphology of Honduras. *Tectonics*, 6(5): 633-651.

Marcus, J. and Adams, R.E.W. (2005). The Formative Period in Mesoamerica: An Overview. In: T.G. Powis (Editor), *New Perspectives on Formative Mesoamerican Cultures*. BAR International Series 1377, pp. 203-211.

Meats, C. (1996). An Appraisal of the Problems Involved in Three-Dimensional Ground Penetrating Radar Imaging of Archaeological Features. *Archaeometry*, 38(2): 359-379.

Mehring, P.J., Sarna-Wojcicki, A.M., Wollwage, L.K. and Sheets, P. (2005). Age and extent of the Ilopango TBJ tephra inferred from a Holocene chronostratigraphic reference section, Lago de Yojoa, Honduras. *Quaternary Research*, 63(2): 199-205.

Molnar, P. and Sykes, L.R. (1969). Tectonics Caribbean and Middle America Regions from Focal Mechanisms and Seismicity. *Geological Society of America Bulletin*, 80(9): 1639-1684.

- Morrison, F., Benavent, J., Clewlow, C.W. and Heizer, R.F. (1970a). Magnetometer Evidence of a Structure within La Venta Pyramid. *Science*, 167(3924): 1488-1490.
- Morrison, F., Clewlow, C.W. and Heizer, R.F. (1970b). Magnetometer Survey of the La Venta Pyramid, 1969. *Contributions of the University of California Archaeological Research Facility*, 8: 1-20.
- Navarro Tábora, S.C. (2004). *Parque Eco-Arqueológico Los Naranjos: Guia Interpretativa*, Tegucigalpa, Honduras.
- Neal, A. (2004). Ground-penetrating radar and its use in sedimentology: principles, problems and progress. *Earth-Science Reviews*, 66(3-4): 261-330.
- Osiecki, P.S. (1981). Estimated Intensities and Probable Tectonic Sources of Historic (Pre-1898) Honduran Earthquakes. *Bulletin of the Seismological Society of America*, 71(3): 865-881.
- Ovando-Shelley, E. and Manzanilla, L. (1997). An archaeological interpretation of geotechnical soundings under the Metropolitan Cathedral, Mexico City. *Archaeometry*, 39: 221-235.
- Pastor, L. (2003). Segundo Reporte Sobre Prospección Geofísica en Copán (Honduras). In: R. Viel (Editor), *El Paleopaisaje de Copán: Cuatro Mil Anos de Transformaciones del Paisaje en el Valle de Copán (CD-ROM)*, Copán Ruinas, pp. 1-12.

- Powis, T.G. (2005). Formative Mesoamerican Cultures: An Introduction. In: T.G. Powis (Editor), *New Perspectives on Formative Mesoamerican Cultures*. BAR International Series 1377, pp. 1-14.
- Reynolds, J.M. (1997). *An Introduction to Applied and Environmental Geophysics*. John Wiley & Sons, Chichester.
- Roosevelt, A.C. (2007). Geophysical Archaeology in the Lower Amazon: A Research Strategy. In: J. Wiseman and F. El-Baz (Editors), *Remote Sensing in Archaeology*. Springer, New York, pp. 443-475.
- Roskams, S. (2001). *Excavation*. Cambridge University Press, Cambridge.
- Sandmeier, K.J. (2006). ReflexW Version 4.0, Karlsruhe, Germany.
- Sauck, W.A., Desmond, L.G. and Chavez, R.E. (1998). Preliminary GPR Results from Four Maya Sites, Yucatan, Mexico, In *Proceedings of the Seventh International Conference on Ground-Penetrating Radar, May 27-30, 1998.*, University of Kansas, Lawrence, Kansas, USA. Radar Systems and Remote Sensing Laboratory, University of Kansas, pp. 101-114.
- Schneider, W.A. (1978). Integral Formulation for Migration in 2 and 3 Dimensions. *Geophysics*, 43(1): 49-76.
- Sensors & Software Inc. (2003). *EKKO_View Enhanced & EKKO_View Deluxe*, Mississauga, ON.

- Sheets, P.D. (1985). Geophysical Exploration for Ancient Maya Housing at Cerén, El Salvador. *National Geographic Society Research Reports*, 20: 645-656.
- Sheriff, R.E. and Geldart, L.P. (1995). *Exploration seismology*. Cambridge University Press, Cambridge; New York.
- Stierman, D.J. (2004). Sobre métodos geofísicos en Talgua, Memoria VII Seminario de Antropología de Honduras "Dr. George Hasemann". Instituto Hondureño de Antropología e Historia, Tegucigalpa, pp. 303-322.
- Stierman, D.J. and Brady, J.E. (1999). Electrical Resistivity Mapping of Landscape Modifications at the Talgua Site, Olancho, Honduras. *Geoarchaeology: An International Journal*, 14(6): 495-510.
- Stone, D.Z. (1934). A new southernmost Maya city (Los Naranjos on Lake Yojoa, Honduras). *Maya Research*, 1(2): 125-128.
- Strong, W.D., Kidder, A. and Paul, A.J.D. (1938). *Preliminary Report on the Smithsonian Institution - Harvard University Archaeological Expedition to Northwestern Honduras, 1936*, Washington.
- Tchakirides, T.F. (2007). *Preliminary Informe: Geophysical Data Collection at Los Naranjos and Puerto Escondido, Honduras*. Manuscript on file at the Instituto Hondureño de Antropología e Historia, Tegucigalpa, Honduras.

- Tchakirides, T.F. and Brown, L.D. (in prep). Effect of Reflection Picking Criteria on In Situ Velocity Estimates from Ground-penetrating Radar Common Mid-point Data from the Archaeological Site of Los Naranjos, Honduras.
- Tchakirides, T.F., Brown, L.D. and Henderson, J.S. (2005). GPR Experience at Mesoamerican Archaeological Sites in Honduras: Puerto Escondido and Copán, *Eos. Trans. AGU*, 86(18), Jt. Assem. Suppl., Abstract NS41A-03.
- Tchakirides, T.F., Brown, L.D. and Henderson, J.S. (2006a). Estimation of Diffractor Morphology from Analysis of Amplitude and Travel Time Curvature at the Maya Archaeological Site of Los Naranjos, Honduras., In Proceedings of the 11th International Conference on Ground Penetrating Radar: June 19-22, Columbus, Ohio, p. 1-8.
- Tchakirides, T.F., Brown, L.D., Henderson, J.S. and Blaisdell-Sloan, K. (2006b). Integration, Correlation, and Interpretation of Geophysical Data at Los Naranjos, Honduras, In Proceedings of the Symposium on the Application of Geophysics to Engineering and Environmental Problems: April 2-6, 2006, Seattle, WA, p. 1400-1429.
- Valdes, J.A. and Kaplan, J. (2000). Ground-penetrating radar at the Maya site of Kaminaljuyu, Guatemala. *Journal of Field Archaeology*, 27(3): 329-342.
- Welch, D. (2001). The Chacalapan Geophysical Survey, Veracruz, Mexico. Reports submitted to FAMSI, <http://www.famsi.org>, Accessed August 18, 2006.

- Weymouth, J.W. (1986a). Archaeological Site Surveying Program at the University-of-Nebraska. *Geophysics*, 51(3): 538-552.
- Weymouth, J.W. (1986b). Geophysical Methods of Archaeological Site Surveying, *Advances in Archaeological Method and Theory*, vol. 9. Academic Press, pp. 311-395.
- White, R.A. and Harlow, D.H. (1993). Destructive Upper-Crustal Earthquakes of Central-America since 1900. *Bulletin of the Seismological Society of America*, 83(4): 1115-1142.
- White, R.E. (1991). Properties of instantaneous seismic attributes. *The Leading Edge*, 10(7): 26-32.
- Williams, H. and McBirney, A.R. (1969). Volcanic History of Honduras. *University of California Publications in Geological Sciences*, 85: 1-101.
- Yde, J. (1936). A Preliminary Report of the Tulane University-Danish National Museum Expedition to Central America 1935. *Maya Research*, 3(1): 24-37.
- Yde, J. (1938). A Reconnaissance of Northwestern Honduras. A Report of the Work of the Tulane University-Danish National Museum Expedition to Central America 1935. *Acta Archaeologica*, 9: 1-99.
- Yilmaz, Ö. (2001). Seismic data analysis: processing, inversion, and interpretation of seismic data. Society of Exploration Geophysicists, Tulsa, OK.